Dissertation zur Erlangung des Doktorgrades

der Fakultät für Chemie und Pharmazie

der Ludwig-Maximilians-Universität München

Organocatalyzed Morita-Baylis-Hillman Reaction:

Mechanism and Catalysis

Von

Yinghao Liu

Aus

Yantai, China

München, 2011

<u>Erklärung</u>

Diese Dissertation wurde im Sinne von § 13 Abs. 3 der Promotionsordnung vom 29. Januar 1998 von Herrn Prof. Dr. Hendrik Zipse betreut.

<u>Ehrenwörtliche Versicherung</u>

Diese Dissertation wurde selbständig, ohne unerlaubte Hilfe erarbeitet.

München, am 15. 12. 2010

Yinghao Liu

Dissertation eingereicht am 20. 12. 2010

1. Gutachter: Prof. Dr. Hendrik Zipse

2. Gutachter: Prof. Dr. Herbert Mayr

Mündliche Prüfung am 11.01.2011

To **GongGong** and **YangYang**

To 龚龚 和 秧秧

This work was carried out from 10. 2007 to 10. 2010 under the guidance of Prof. Dr. Hendrik Zipse at Department Chemie, Ludwig-Maximilians-Universität München.

my nice lab-neighbor **Raman Tandon**, and all my friends in Germany. It was you people who made my stay in Germany a great time. Vielen Dank, guys!

I acknowledge the China Scholarship Council and Ludwig-Maximilians-Universität München for financial support, and the international office of LMU for their kind help since my first arrival to Munich.

Most importantly I would like to thank my parents for their support, help and encouragement during my life.

The last and special thank goes to my wife for her love, support and company in these times. Thank you so much!

Yinghao Liu

25. 11. 2010

致　谢

同学对我过去学习生活的帮助.

感谢所有我的朋友们给予我的帮助。

最后，我要深深感谢多年来我的父母、爱人以及我所有善良的亲人们对我学业一贯的鼓励和支持，你们一直是支持我向前的动力，陪我走过每一段难忘的时光，我的每一点进步都饱含着你们的心血；尤其是龚龚，感谢你多年来的爱与陪伴、牺牲和支持，谢谢! Vielen Dank！

刘英豪

2010 年 11 月

于慕尼黑大学

ABBREVIATIONS

Ac	acetyl	m	multiplet
AN	acceptor number	Me	methyl
Ar	aryl	min	minute
BINOL	1,1'-Bi-2-naphthol	mol	mole
Bn	benzyl	MS	mass spectrometry
Boc	tert-butoxycarbonyl	MVK	methyl vinyl ketone
br	broad	NMR	nuclear magnetic resonance
Bu	butyl	o	ortho
calcd.	Calculated	p	para
conv.	conversion	pent	pentyl
d	doublet	Ph	phenyl
DABCO	1,4-Diazabicyclo[2.2.2] octane	Piv	pivaloyl
DCM	dichloromethane	PNP	*para*-nitrophenol
DBU	1,8-Diazabicyclo[5.4.0] undec-7-ene	PPY	4-pyrrolidinopyridine
DMAP	dimethylaminopyridine	*i*-Pr	isopropyl
DMF	dimethylformamide	q	quartet
DMSO	dimethyl sulfoxide	rt	room temperature
equiv.	equivalent	s	singlet
EI	electron-impact	t	triplet
ESI	Electron Spray Ionization	t-Bu	*tert*-butyl
GC	gas chromatography	TEMPO	2,2,6,6-Tetramethylpiperidine-1-oxyl
h	hour	TFA	trifluoroacetic acid
HRMS	high resolution mass spectroscopy	THF	tetrahydrofuran
IR	infra-red	Ts	4-toluenesulfonyl
HSQC	Heteronuclear Single Quantum Correlation	LUMO	lowest unoccupied molecular orbital
J	coupling constant (NMR)	HMBC	Heteromuclear Multiple Bond Correlation

1 INTRODUCTION

1.1 Organocatalysis

1.1.1 General aspects

During the past decade, there has been a remarkable increase in interest in the field of "Organocatalysis".[1] This term ORGANOCATALYSIS was introduced by MacMillan in 2000[2] and is used to describe a research area, which was driven by the desire to develop environmentally friendly methods that obviate the need for potentially toxic metal-based catalysts. Scheme 1 shows a selection of some typical organocatalysts.[3]
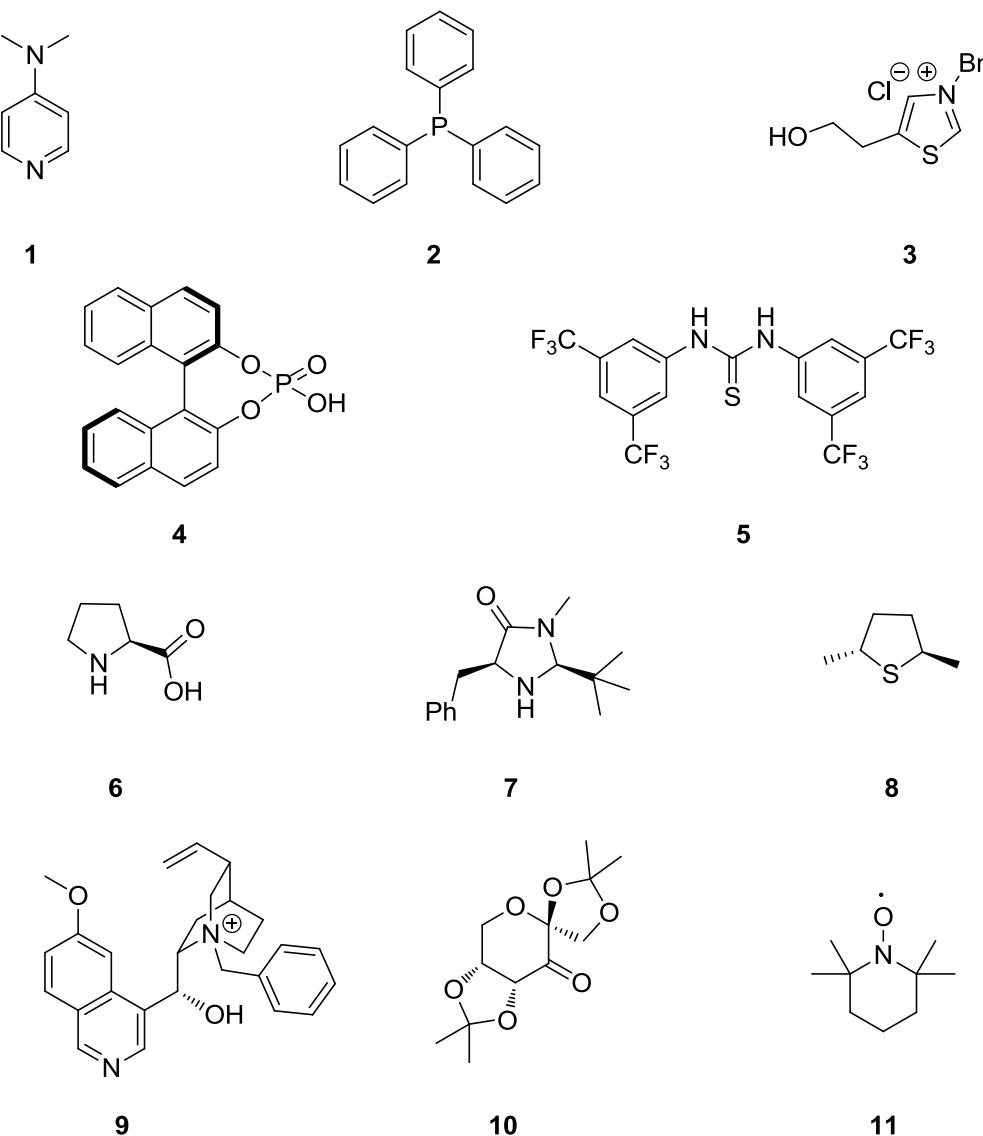
Scheme 1. Some selected typical organocatalysts.

While the attention of synthetic chemists was previously largely attracted to metal-containing or enzyme catalysis, it is obvious that the advent of organocatalysts brought the prospect of a complementary mode of catalysis, presenting some potential advantages.[4]

1) Generally, organic molecules are not so sensitive to oxygen and moisture in the atmosphere, so there is no need for demanding reaction conditions like inert gas atmosphere, special reaction vessels, or ultra-dry reagents and solvents.

2) A wide variety of organic compounds – such as amino acids, carbohydrates and hydroxy acids – are naturally available from the "chiral pool" as single enantiomers. Simple organocatalysts are therefore usually cheap to prepare and readily accessible in a range of quantities, suitable for small to industrial-scale reactions.

3) Small organic molecules are often non-toxic and environmentally friendly, increasing the safety of catalysis in both biological and chemical research across all research settings.

Although chemical transformations that use organic catalysts, have been documented sporadically over the past century, it was not until the 1990s, that the field of organocatalysis was 'born', coalescing around a small number of articles that inspired an explosion of research.[1,4]
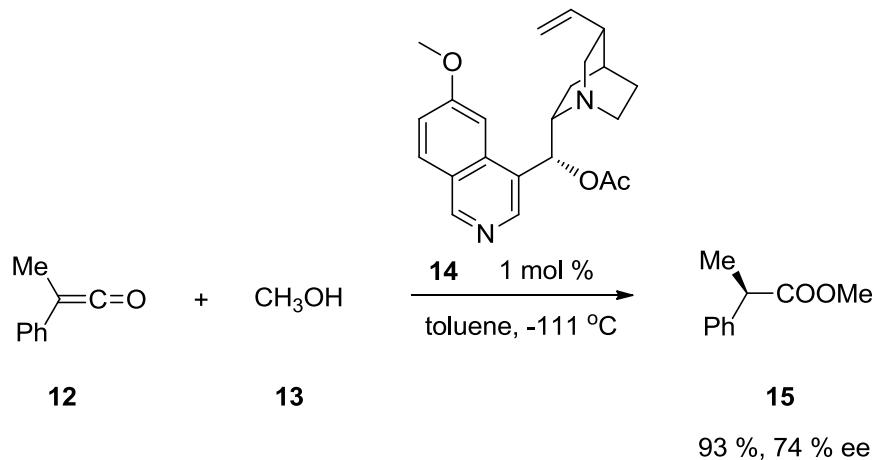
Scheme 2. The asymmetric organocatalytic synthesis of α-phenyl propionic acid esters reported by Pracejus in 1960.

Between 1960 and 1997, some important, non-enantioselective catalysts were developed such as DMAP (**1**), for acyl transfer reactions[5] and TEMPO (**11**), for

alcohol oxidation,[6] but there were still only few reports on the use of small organic molecules as catalysts for asymmetric reactions. In 1960, Pracejus reported the use of optically active amines like acetylquinine **14** as catalysts for the reaction of phenylmethyl ketene **12** with alcohols or amines (Scheme 2), which is the first reported example of an asymmetric organocatalytic process.[7]

16 **17** **18**
71 %, 99 % ee
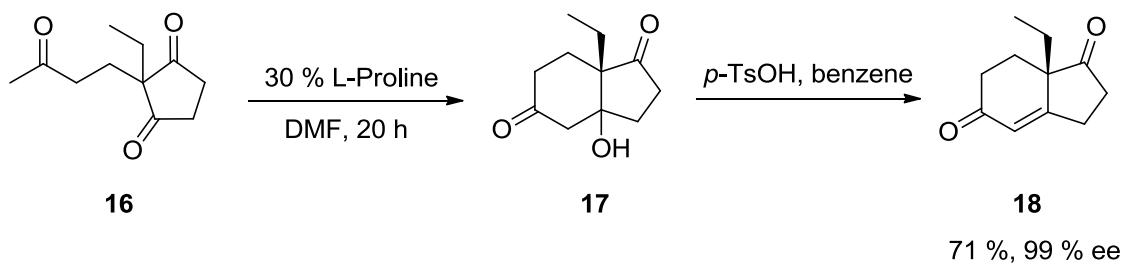
Scheme 3. L-Proline-promoted Hajos-Parrish-Eder-Sauer-Wiechert reaction.

The remarkable properties of proline as organocatalyst were explored for the first time in the intramolecular aldol reaction by Hajos and Parrish at Hoffmann-La Roche,[8] and the group of Eder, Sauer and Wiechert at Schering[9] in the early seventies (Scheme 3). The Hajos-Parrish-Eder-Sauer-Wiechert reaction was probably the most famous small organic molecule-catalyzed asymmetric reaction until the early 1990s. In these early reports, there was no emphasis on the potential benefits of using organocatalysts or on the demonstration of new organocatalytic concepts. Instead, these publications focused mostly on the individual chemical transformations that had been accomplished.[4]

19 **20**
81 %, 88 % ee
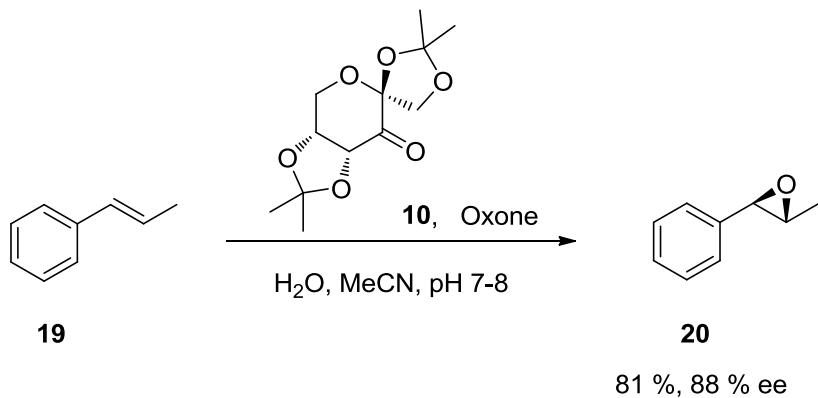
Scheme 4. Shi epoxidation of alkenes.

It was not until the late 1990s, that it was demonstrated for the first time that small organocatalysts could be used to solve important problems in chemical synthesis. For example Yian Shi,[10] Scott Denmark,[11] Dan Yang,[12] and their co-workers reported that enantioselective epoxidations of simple alkenes could be achieved with chiral ketones as catalysts (Scheme 4); shortly afterwards, Eric Jacobsen[13] and Elias J. Corey[14] described the first example of hydrogen-bonding catalysis, in an asymmetric Strecker reaction.[4]

21   +   **22** $\xrightarrow[\text{DMSO, rt}]{\textbf{6,} \text{ 30 mol \%}}$ **23**

97 %, 96 % ee
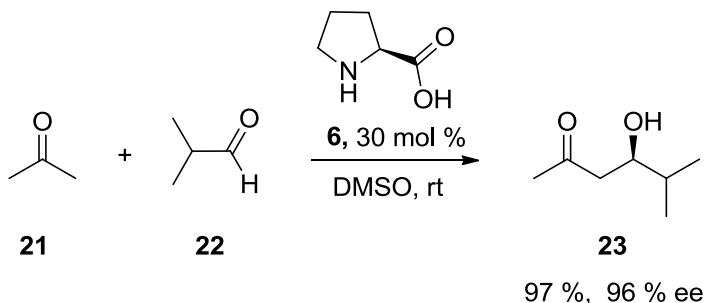
Scheme 5. L-Proline catalyzed intermolecular aldol reaction reported by Barbas, Lerner and List.

It was in 2000, that the field of organocatalysis was effectively launched by two publications, which appeared almost simultaneously: one from List, Lerner, and Barbas[15] on enamine catalysis of intermolecular aldol reactions (Scheme 5); and the other from the MacMillan group,[2] on iminium catalysis of enantioselective Diels-Alder reactions (Scheme 6). These studies introduced the term organocatalysis and showed a broader applicability of those transformations, which substantially raised the scientific interest in this area of research.

24   +   **25** $\xrightarrow{\textbf{7,} \text{ 5 mol \%}}$ **26**

82 %, 94 % ee
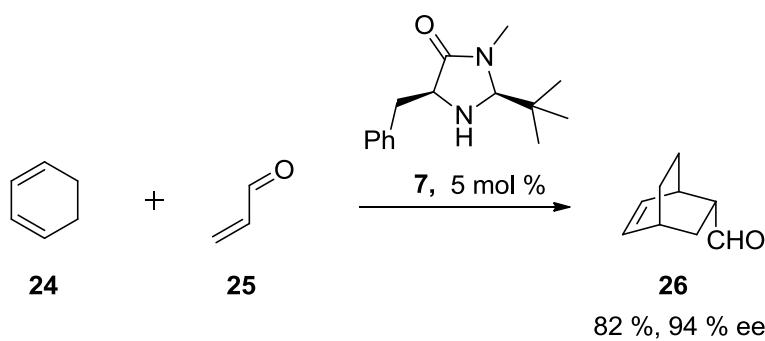
Scheme 6. Organocatalyzed Diels-Alders reaction reported by MacMillan.

Very crucial to the success of organocatalysis in the past decade was the invention or identification of generic modes of catalyst activation, induction and

reactivity.[4] A generic activation mode describes a reactive species that can participate in many reactions with consistent reactivity. Based on the activation modes, the great number of organocatalytic reactions can be categorized into four families:[3c] Lewis base and Lewis acid catalysis, Brønsted base and Brønsted acid catalysis. There are still some limitations of this classification such that not all organocatalytic processes can be simply described with these general activation modes, such as the alcohol oxidation with TEMPO. Also sometimes one organocatalyst could promote reactions in several joint activation modes. Therefore, in this manuscript, multifunctional catalysis is also included and described briefly.

1.1.2 Lewis base catalysis

The general mechanism of Lewis base catalysis is shown in Scheme 7. Lewis base catalyst B: first initiates the catalytical cycle, via nucleophilic addition, to convert substrates S into activated nucleophiles B^+-S^-, which could also be converted into electrophiles via elimination of a leaving group. B^+-S^- undergoes chemical transformation to intermediates B^+-P^-, then catalyst B: is regenerated with released product P. The majority of organocatalysts are N-, C-, O-, P-, and S-based Lewis bases B:, which transfer substrates into typical reactive intermediates such as iminium ions, enamines, acyl ammonium ions, ammonium enolates, etc. (Scheme 8).[3c]
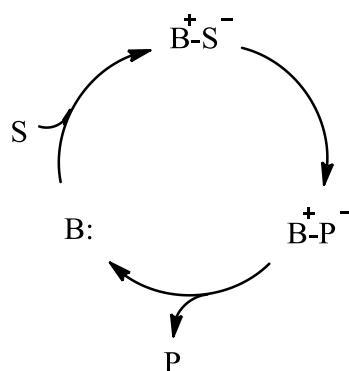
Scheme 7. Simplified general mechanism of Lewis base catalysis.

A typical case of enamine catalysis is shown in Scheme 9. The active species is an enamine intermediate **27** formed by the reversible reaction of proline with acetone. This then undergoes aldol-type addition with aldehyde to give product **23**.

The asymmetric enamine catalysis concept has been extended to Mannich reactions, [16] Michael addition, [17] Baylis-Hillman reaction, [18] and the α-functionalizations of aldehydes and ketones (aminations, [19] hydroxylations, [20] alkylation, [21] halogenation, [22]) etc.
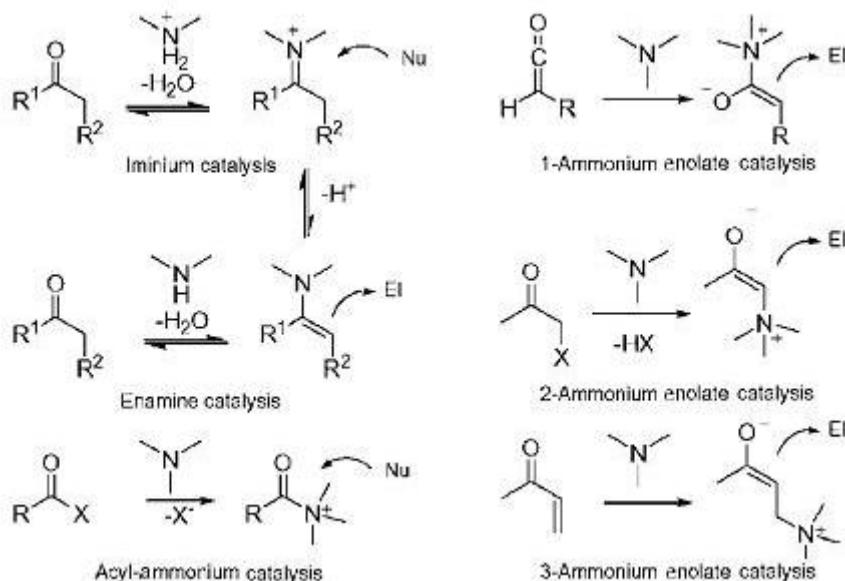
Scheme 8. Selected examples of Lewis base catalysis.

In the first iminium catalysis reaction reported by MacMillan,[2] the intermediate iminium **28** with lower LUMO energy represented higher reactivity compared to its precursor unsaturated aldehyde **25**. The Diels-Alder cycloaddition with diene proceeds smoothly to give product **26** with good enantioselectivity (Scheme 10). This concept of activating unsaturated aldehydes into more reactive intermediate iminium ions, has been used in more than 50 highly enantioselective protocols,[23] such as [3+2]-cycloaddition reactions,[24] Friedel-Crafts reactions,[25] etc.

21   **6**   **27**   **23**
97 %, 96 % ee
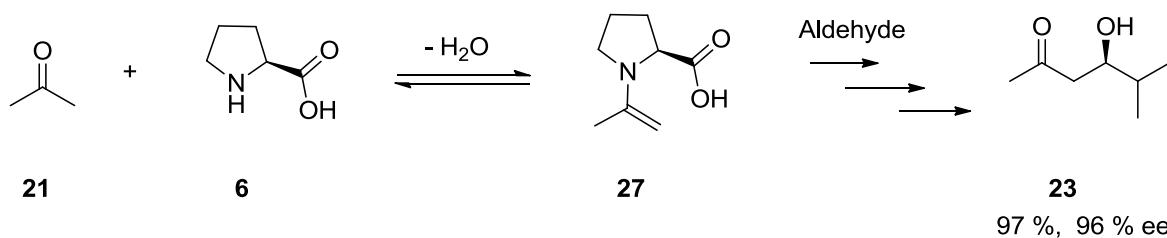
Scheme 9. Enamine catalysis in the L-Proline-catalyzed aldol reaction.
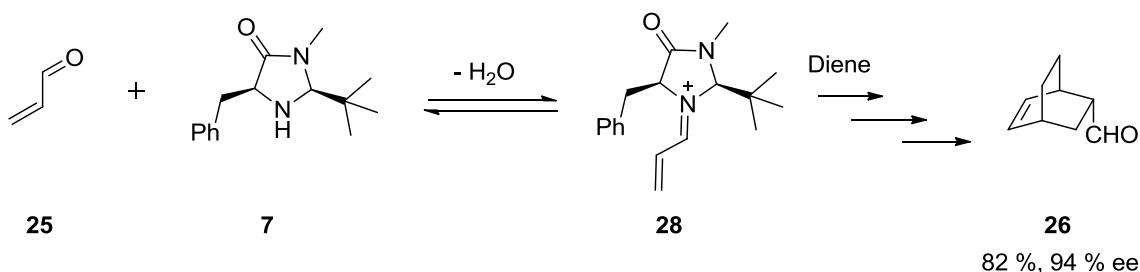
Scheme 10. The iminium catalysis in Diels-Alder reaction.

One important example for acyl-ammonium catalysis is the DMAP-catalyzed acylation of alcohols, which proceeds through an activated acylpyridinium intermediate (Scheme 11).[26] Based on the notion of acyl-ammonium catalysis, a series of chiral and reactive Lewis base organocatalysts were designed and tested in the kinetic resolution of alcohols[26a] and protonations of ketenes,[27] also in cycoladdition reactions,[28] halogenation reactions[29] and Michael addition reactions.[30]
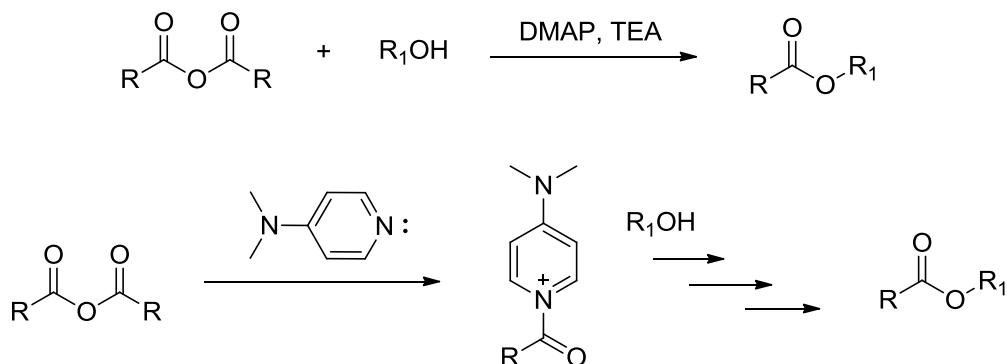
Scheme 11. The acyl-ammonium catalysis in DMAP catalyzed esterification.

Ammonium enolate catalysis involves a catalytically generated ammonium enolate intermediate that is formed via addition of Lewis base catalysts to electrophilic substrates and that further reacts with various electrophiles.[3c] The Morita-Baylis-Hillman reaction discussed in detail in this thesis in chapter 1.2 can also be classified into the category of 3-ammonium enolate catalysis.

1.1.3 Lewis acid catalysis

The general mechanism of Lewis acid catalysis is shown in Scheme 12. Lewis acid catalysis works in a quite similar manner as Lewis base catalysis: Lewis acid catalyst A activates electrophilic substrates S: to form the intermediate $A^{-}\text{-}S^{+}$,

which would further react or transfer into intermediate A$^-$-P$^+$. Catalyst A is then regenerated through elimination of product P.[3c]
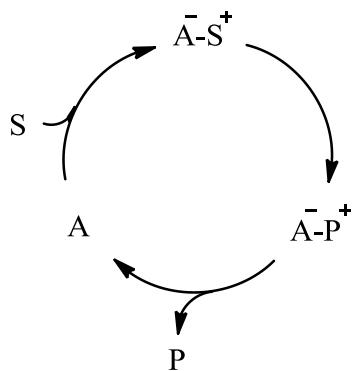
Scheme 12. Simplified general mechanism of Lewis acid catalysis.

Generally metal containing catalysts are a large and important family of Lewis acid catalyst. In the organocatalysis field there are also some important classes, such as phase transfer catalysts, which could catalyze effectively alkylation, Michael addition, aldol reaction, Mannich reaction, epoxidation, etc.[31] Another excellent class of Lewis acid catalysts are chiral ketone catalysts, which promote the enantioselective epoxidation of olefins via the formation of intermediate dioxiranes *in situ* generated from ketones and oxone.[10]

1.1.4 Brønsted base catalysis

The general mechanism of Brønsted base catalysis is shown in Scheme 13. The catalytic cycle is similar to Lewis type catalysis except the initiation with a (partial) deprotonation of substrate S-H by Brønsted base catalyst B.[3c]
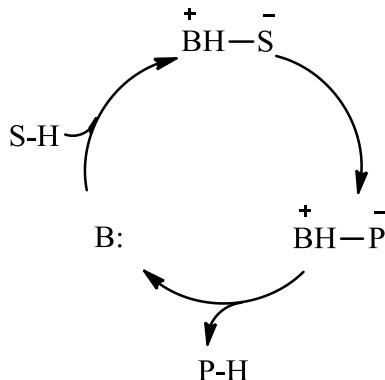
Scheme 13. Simplified general mechanism of Brønsted base catalysis.

One example of Brønsted base catalysis is the Diels-Alder reaction of anthrone **29** and various dienophiles, which follows a concerted mechanism via an intermediate oxyanion **30** *in situ* generated by deprotonation to give adduct **31** (Scheme 14).[32]

29   **30**   **31**

100 %
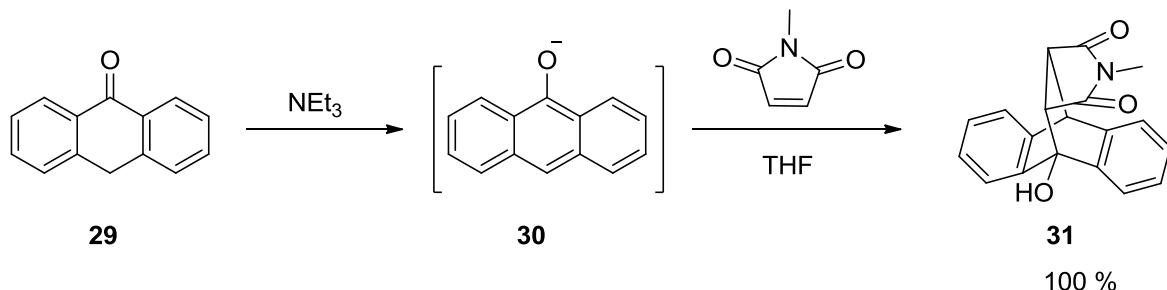
Scheme 14. Brønsted base catalysis in Diels-Alder reactions.

Asymmetric hydrocyanation reactions such as Strecker reaction[33] and cyano-hydrin synthesis[34] are also typical examples of Brønsted base catalysis. In these cases, hydrogen cyanide interacts with a Brønsted base to form a cyanide ion, which can further react with electrophiles.

1.1.5 Brønsted acid catalysis

Brønsted acid catalysis proceeds through a hydrogen bond between catalyst A-H and substrate S: or (partial) protonation of substrate S:, to generate intermediate A^--S^+H and A^--P^+H sequently, which liberates catalyst A-H and releases product P: (Scheme 15).
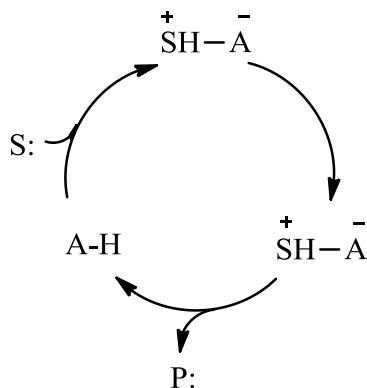
Scheme 15. Simplified general mechanism of Brønsted acid catalysis.

Generally chiral Brønsted acids are classified into two categories[35]: (1) Brønsted acids, such as thiourea and TADDOL derivatives, which are weakly acidic and may thus be considered to act as hydrogen-bonding catalysts, and (2) stronger

Brønsted acid, such as BINOL derivatives and phosphoric acid (Scheme 16). The pK_a of the selected Brønsted acid examples ranges from 25 to 1, which supplied a (partial) protonation mode to activate the substrates.

pKₐ range: ≈ 25 ≈ 12 ≈ 10 ≈ 1

Hydrogen-Bonding Catalysts   Stronger Brønsted acid catalysts
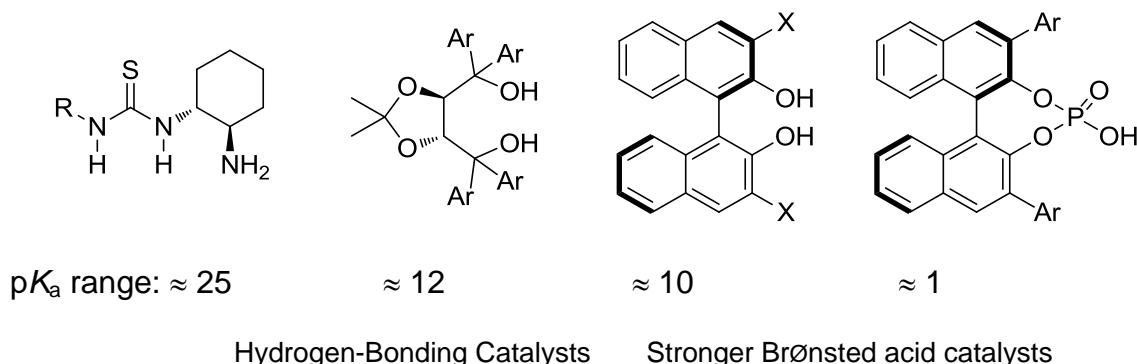
Scheme 16. Examples of four chiral Brønsted acid catalysts.[35]

Using their excellent urea and thiourea hydrogen-bonding type Brønsted acid catalysts, Jacobsen and co-workers developed a series of enantioselective Mannich-, Strecker-, hydrophosphonylation-, hydrocyanation-, cationic polycyclization-, cyanosilylation-, cycloaddition, Michael addition, Morita-Baylis-Hillman reactions and etc.[36] It was believed that the high reactivity and enantioselectivity were achieved by the activation of substrates through hydrogen bonding with Brønsted acid catalysts in a bridging mode.

Akiyama et al.[37] and Terada et al.[38] reported chiral phosphoric acid catalyzed Mannich reactions. As compared to hydrogen-bonding type Brønsted acid catalysis, protonation of the substrates is likely to occur in these cases. This series of chiral phosphoric acids has been applied widely[39] to promote Friedel-Crafts alkylation,[39a] hydrophosphonylation,[39b] Pictet-Spengler-,[39c] Strecker-,[39d] aza-Diels-Alder-,[39e] and transfer hydrogenation reactions[39f, 39g] etc. Quite recently, List et al. developed a new type of chiral disulfonimide **34**, which was shown to be a highly active catalyst for the Mukaiyama aldol reaction and gave full conversion and high enantioselectivity to the desired product **35** (Scheme 17).[40]
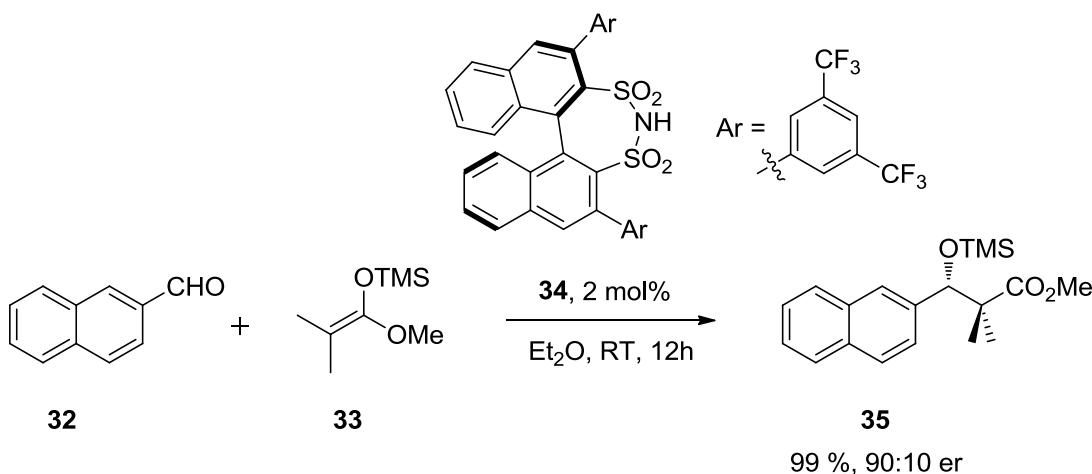
Scheme 17. Chiral disulfonimide catalyzed Mukaiyama aldol reaction.

Yamamoto and co-workers reported the nitroso Diels-Alder reaction of diene with nitrosobenzene catalyzed by binaphthol derivatives to furnish bicyclic ketones with excellent enantioselectivities.[41] Schaus and co-workers[42] developed an enantio-selective Morita-Baylis-Hillman reaction that involved the use of BINOL derivatives in the presence of Lewis base catalyst (see more detailed discussion in chapter 1.2.5).

1.1.6 Multifunctional Catalysis

Shibasaki et al.[43] have first developed the concept of multifunctional catalysis, wherein the catalysts exhibit both Lewis acidity and Brønsted basicity, using lanthanide complexes. Furthermore, a variety of asymmetric transformations have been realized by the above-mentioned concept.[44] An ideal set of multifunctional catalysts should conceptually contain two or more of Lewis- or Brønsted active sites, which act in several different activation modes or the substrate in a controlled chiral environment. The bi/multifunctional catalysts enable effective transformations, which generally are hard to achieve by the single functional catalyst.[45]

There are also a large number of multifunctional organocatalysts. Enamine catalysis, for example, may be described as bifunctional catalysis, because the amine-containing catalyst typically interacts with a ketone substrates to form an enamine intermediate, but simultaneously engages with an electrophilic reaction partner through either hydrogen bonding or electrostatic attraction.[4] Multifunctional catalysts have been successfully applied to Michael addition,[46a] Henry reaction,[46b]

Strecker reaction,[46c] kinetic resolution of alcohols,[46d] Morita-Baylis-Hillman reaction,[46e] and a wide range of enantioselective carbonyl α-functionlization processes.[19-22] A good example of bifunctional catalysis is reported by Jacobsen et al.[36h] The primary amine thiourea catalyst **37** is suitable for the direct conjugate addition of aldehydes to Michael acceptors to give very good results (up to >50:1 dr, up 99 % ee) (Scheme 18).
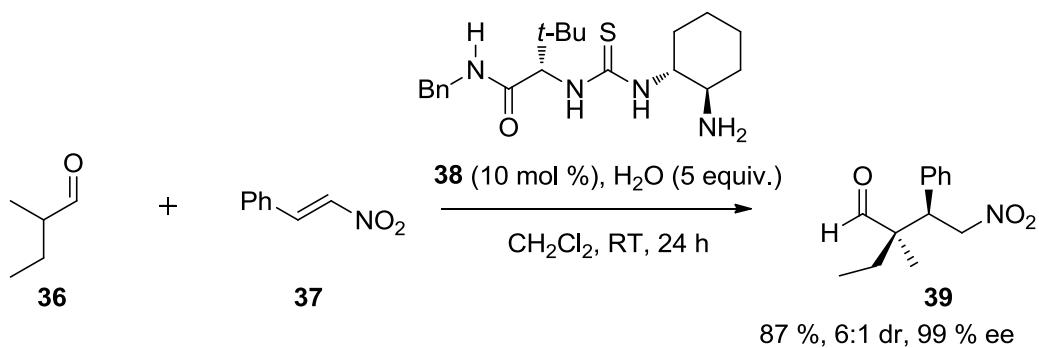
Scheme 18. Bifunctional catalysis of Michael addition.

The thiourea moiety of bifunctional catalyst **38** presumably interacts with the nitro group of Michael acceptor **37** via hydrogen bonding, whereas the primary amine group forms an enamine with aldehyde **36**. With this bifunctional activation mode, high yield and enantioselectivity of the Michael addition product **39** was achieved.[36h] Another reaction employing multifunctional/bifunctional chiral catalysis is the Morita-Baylis-Hillman reaction and its aza-counterpart,[46e] which will be discussed in detail in chapter 1.2.5.

1.2   Morita-Baylis-Hillman reaction

1.2.1 General aspects

The carbon-carbon bond formation remains an important challenge in organic synthesis. Numerous reactions for the formation of carbon-carbon bonds have been discovered and largely exploited. During the past decade, synthetic organic chemistry has seen enormous growth, not only in terms of the development of new methodologies for the construction of carbon-carbon bonds and functional group transformations, but also in terms of the development of new reagents, catalysts, strategies, transformations, and technologies often involving the concepts of atom economy and selectivity. Recent progress in organic chemistry has clearly

established that the efficent development of a reaction generally requires two main criteria: atom economy and (chemo-, regio-, stereo-) selectivity.[47] Because it combines two important requirements, atom economy and generation of functional groups, the Morita-Baylis-Hillman reaction was also considered as an important process for the formation of carbon-carbon bonds.[48]

1.2.2 Origin and development

The Morita-Baylis-Hillman (MBH) reaction was first discovered in 1968 by Morita,[49] and then in 1972 by Baylis and Hillman,[50] and it is essentially a three-component reaction involving the coupling of the α-position of activated alkenes with carbon electrophiles under the catalytic influence of a Lewis base providing a simple and convenient methodology for synthesis of densely functionalized molecules.[51a] After being ignored for a long time after its discovery, it was not until the 1980s that organic chemists started exploring various aspects of this promising and fascinating reaction. From a synthetic point of view the MBH reaction is particularly interesting because it can be used to convert cheap starting materials into highly functionalized compounds suitable for further transformations.[48] More recently asymmetric versions of the MBH reaction have also been developed.[51] The original process involved the use of an aldehyde. If the aldehyde is replaced by an imine the reaction is called aza-Morita-Baylis-Hillman (aMBH) reaction, which leads to very useful α-methylene-β-amino products and, in particular, to β-amino esters when an acrylate is used as Michael acceptor.[48f]

1.2.3 Mechanism

In the generally accepted mechanism the Morita-Baylis-Hillman reaction consists of a sequence of addition-elimination steps (Scheme 19). This mechanism was initially proposed by Hill and Isaacs,[52] and later refined by others.[53] For the prototypical MBH reaction of benzaldehyde with methyl vinyl ketone (MVK **41**) catalyzed by DABCO, the catalytic cycle starts with the Michael addition of DABCO **40** to the activated alkene, which generates the zwitterionic 3-ammonium enolate **42**. By an aldolic reaction enolate **42** adds to benzaldehyde (**43**) to yield another zwitterionic intermediate **44**, which undergoes intramolecular proton transfer to form intermediate **45**. In the last step, through E2 or E1$_{cb}$ elimination,

the product **46** is released with regenerated catalyst (Scheme 19). The aldol reaction step was commonly thought to be the rate determining step (RDS).
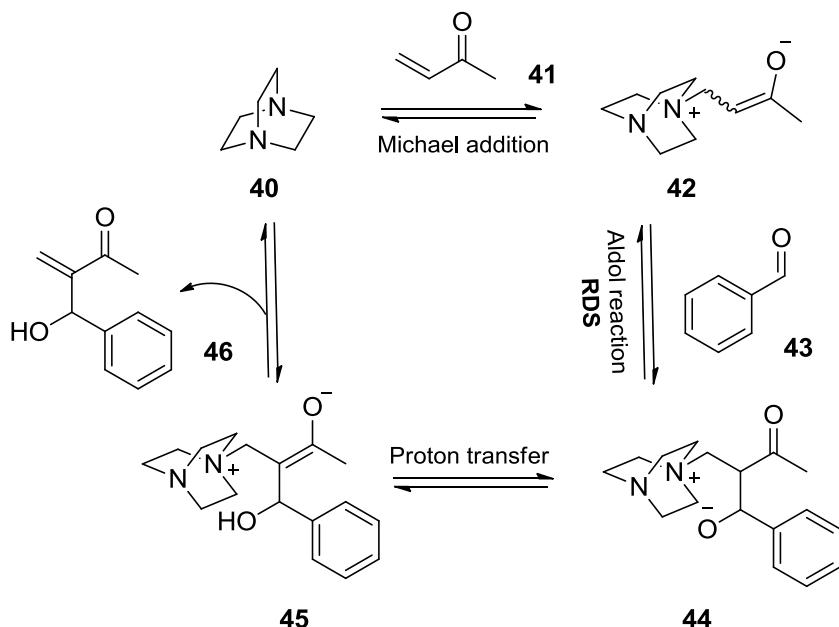
Scheme 19. Generally accepted MBH reaction mechanism.

Drewes et al.[54] reported the isolation of a type-**45** intermediate **48**, as a coumarin salt and characterized it by X-ray crystallography, by conducting the reaction of acryloyl chloride with 2-hydroxy-benzaldehyde in dichloromethane in the presence of DABCO (Scheme 20).
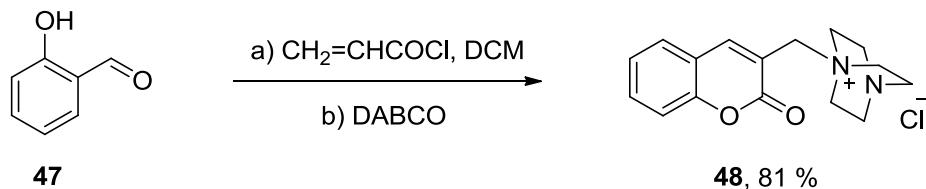
Scheme 20. The MBH reaction intermediate reported by Drewes et al.

Coelho, Eberlin and coworkers[55] have applied Electrospray Ionization Mass and Tandem Mass Spectrometry (EI-MS/MS) monitoring to probe the mechanism of the Morita-Baylis-Hillman reaction. In their study, type-**42** and **-44/-45** intermediates were all detected by ESI in their intact protonated forms, which were structurally characterized by tandem mass spectrometric (MS/MS) analysis.
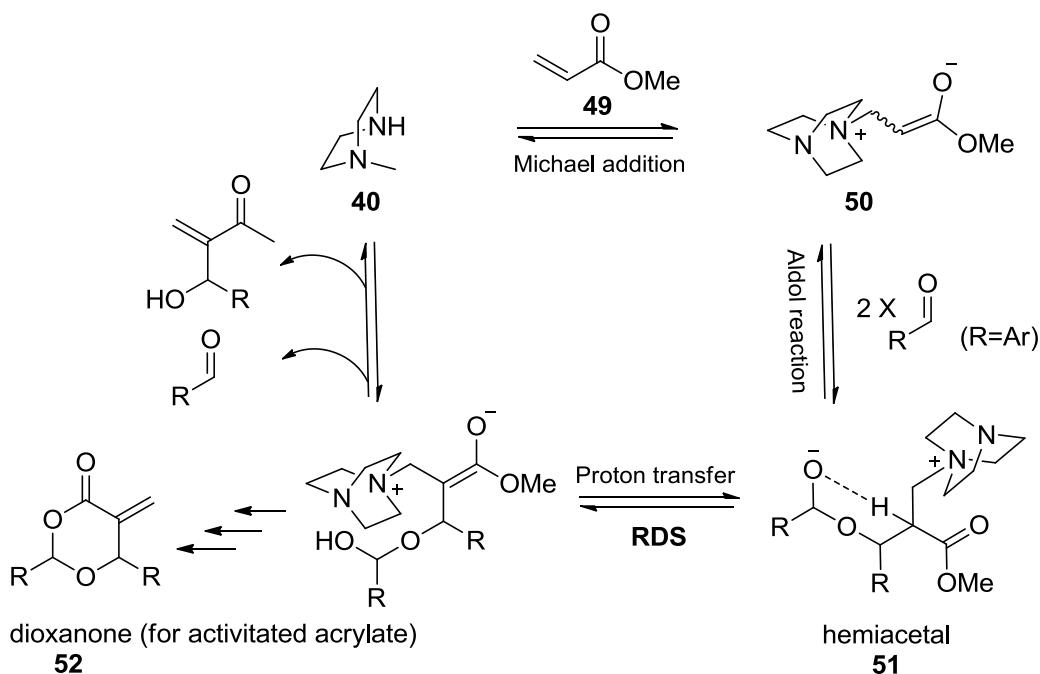
Scheme 21. The MBH reaction mechanism through a hemiacetal-intermediate as proposed by McQuade et al.[56]

Recent experimental results and theoretical studies regarding the proton transfer step of the standard MBH reaction suggested a dualistic nature for this mechanism. For the DABCO-catalyzed MBH reaction of aromatic aldehydes and methyl acrylate in non-polar, polar or even protic solvents, McQuade and coworkers[56] have presented two key observations: (1) The rate law is first order in DABCO and acrylate, and second order in aldehyde; and (2) a large kinetic isotope effect was observed when α-deuterioacrylate was employed. Based on these findings, McQuade et al. proposed a new mechanism for the MBH reaction, according to which the rate determining step is the proton transfer step through the hemiactal intermediate **51**. Another fact that supports this new hemiacetal-mode is the observation of dioxanone **52**, which could be detected when the concentration of aldehyde was high and the acrylate was an activitated ester (Scheme 21).

53
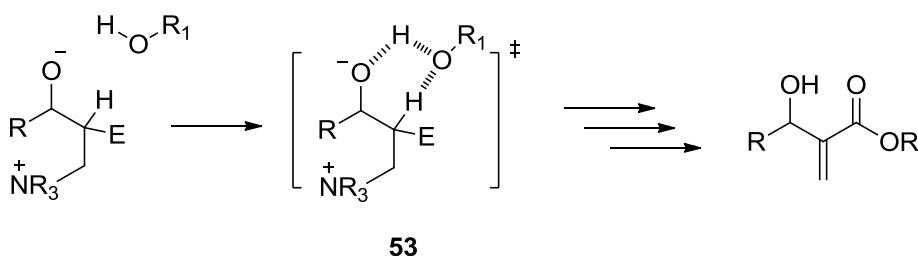
Scheme 22. The proton transfer step facilitated via transition state **53**.

Aggarwal and Lloyd-Jones et al.[57] investigated the reaction of ethyl acrylate with benzaldehyde catalyzed by quinuclidine without solvent. In the control reaction of α-deuterioacrylate and non-deuterioacrylate with aldehyde, it was observed that in the early stage of the reaction (≤20 % conversion), the non-deuterioacrylate was consumed more and as the reaction proceeded, both acrylates were consumed in the same ratio. This could be rationalized by a new catalysis mode: in the starting stage of the reaction, proton transfer is the rate determining step, which was verified by the higher consumption of non-deuterioacrylate due to a normal isotope effect; as the reaction proceeded, the aldol reaction became rate- determing, which was supported by the disappearance of the isotope effect. In this so-called autocatalysis mechanism, the product serves as hydrogen-donating co-catalyst to facilitate the proton transfer via transition state **53** (Scheme 22) to make this reaction autocatalytic. The autocatalysis mechanism was further supported by computational data which showed that the energy barrier for the ROH-promoted proton transfer was even somewhat lower than that envisioned in McQuade's mechanism.[58] It also explained the large rate enhancement caused by protic cosolvents.[59]

In contrast to the Morita-Baylis-Hillman reaction, only three mechanistic studies deal with the aza-version of this reaction.[60,61,62] In spite of the mechanistic analogies between the MBH and the aza-MBH reactions, there are still some relevant dissimilarities. Quite recently, Shibasaki, Berkessel and co-workers[62] investigated the aMBH reaction of phosphinoylimine with methyl acrylate and developed a new catalytic system, which contains the Lewis base DABCO, a phenol-type additive **57**, La(O-iPr)$_3$ as the Lewis acid and ligand **56**. They reported that no kinetic isotope effect was observed (k_H/k_D= 1), when α-deuterioacrylate was used, indicating that the proton transfer step is not the rate-determining step in this system. In the absence of phenol-additive **57** a kinetic isotope effect (k_H/k_D=

16

2.5) was observed, suggesting the importance of the proton source in the proton transfer step. Based on the kinetic data of a first-order dependence on acrylate, a 0th-order dependence on La(O-iPr)$_3$-Ligand complex, and a 1.4th-order dependence on DABCO, they proposed that the rate determining-step was Michael addition, and that the chiral La(O-iPr)$_3$-Ligand complex was involved in the enantio-discrimination step via the interaction with the zwitterionic enolate and the activation of the imine component (Scheme 23).
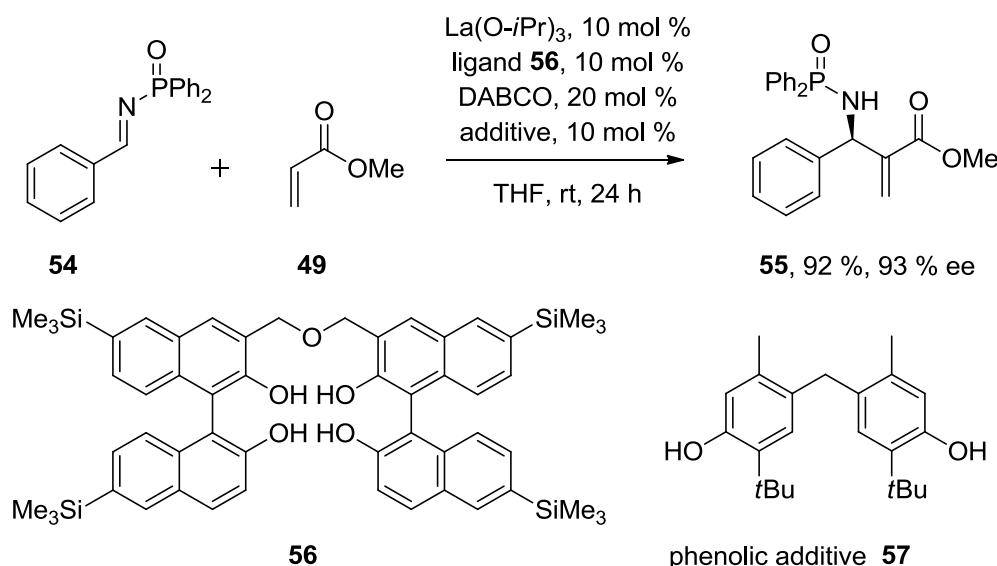
Scheme 23. La(O-iPr)$_3$ and DABCO cocatalyzed aMBH reaction.

Raheem and Jacobsen[60] reported that in the DABCO-promoted aza-MBH reaction of methyl acrylate and aromatic nosylimine in CHCl$_3$, a first-order kinetic dependence on both DABCO and methyl acrylate was observed (Scheme 24). In contrast to the MBH reaction,[56] it displayed rate saturation on nosylimine. When α-deuterioacrylate was used, a prominent primary kinetic isotope effect was also observed (k_H/k_D=3.8), strongly suggesting that the proton transfer step is rate-limiting.
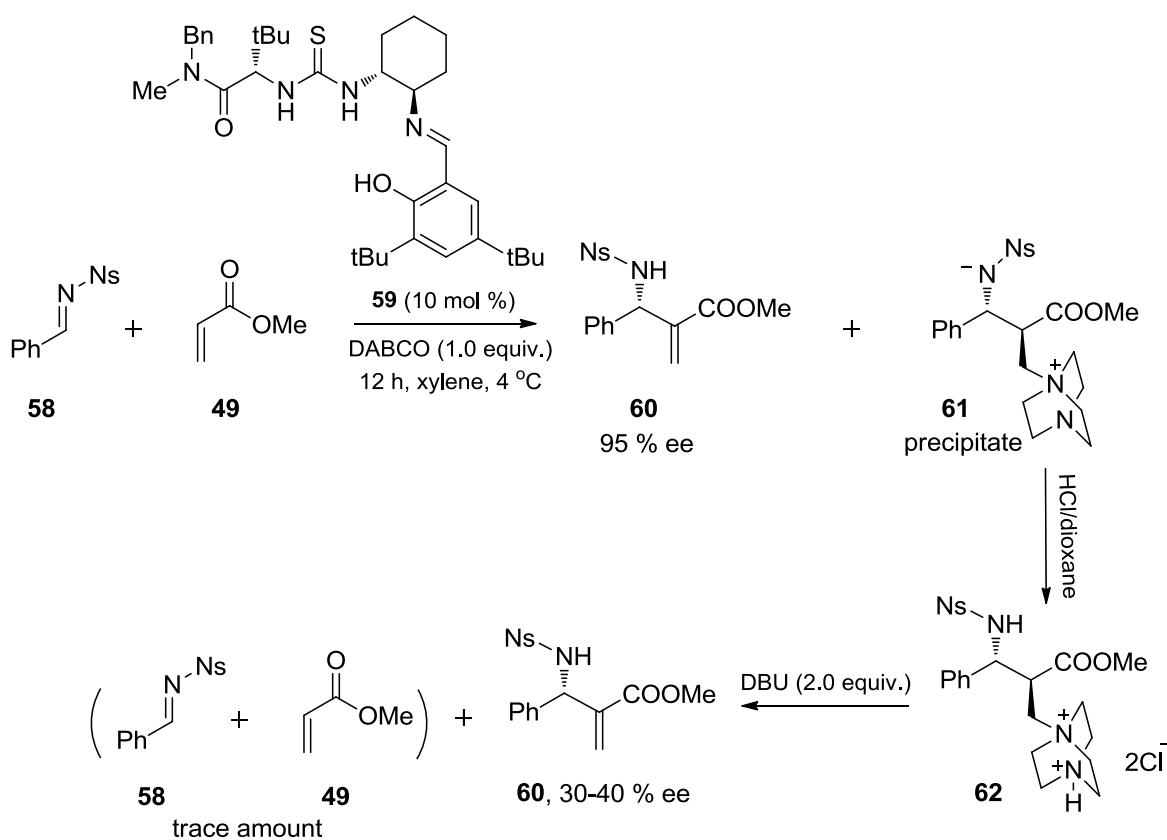
Scheme 24. The isolation and transformation of dihydrochloride salt **62**.

They also isolated and characterized dihydrochloride salt **62**, derived from type-**44** aldol reaction product **61**, which is insoluble in xylene and precipitates. The dihydrochloride salt **62** was highly diastereomerically pure and with the relative stereochemistry of the major isomer assigned as *anti*. When zwitterionic compound **61** was regenerated in d6-DMSO through deprotonation of **62** by DBU, methyl acrylate (**49**) and imine (**58**) were also detected, indicating that **61** undergoes reversion to its precursors (Scheme 24). This constitutes a racemization pathway for **61** in the presence of catalyst. The compound **61** generated in this manner underwent further proton transfer to provide product , consistent with the proposal that **61** is indeed an intermediate in the catalytic cycle.[60]

Since the zwitterionic species **61** exists as both *syn* and *anti* diastereomers, but only the *anti* isomer may undergo precipitation selectively in less polar solvent (xylene), they rationalized why solvents that effectively solubilize both diastereomers **61** lead to high yield but low enatioselective product **60**. The DBU-mediated deprotonation and further transformation of **62** in methanol shows first

order dependence on **62**. This is consistent with the rapid and irreversible deprotonation of **62** to **61**. Added imine had no effect on the rate of elimination, indicating that imine is not involved in the proton transfer step, which is different from the MBH hemiacetal[56] mechanism.
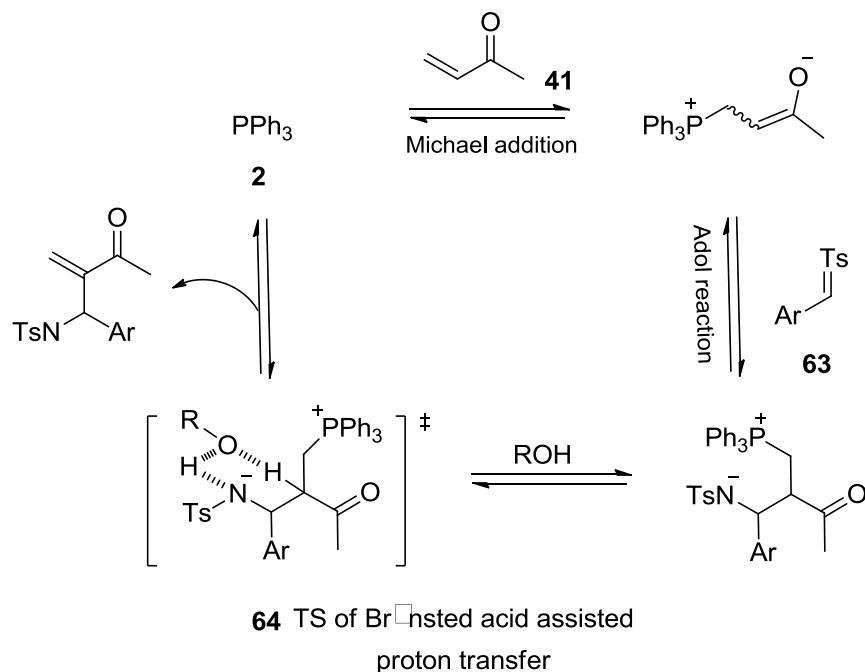
Scheme 25. Brønsted acid assisted proton transfer step reported by Leiter et al.[61]

Leitner et al.[61] studied the aza-MBH reaction of methyl vinyl ketone with tosylimine catalyzed by PPh$_3$ (**2**) in d$_8$-THF. They did not observe autocatalysis. A first-order kinetic dependence on methyl vinyl ketone (**41**) and triphenylphosphane (**2**), and a broken order of 0.5 on tosylimine **63** were observed, which indicates that the rate determining step is partially influenced by proton transfer. When a stoichiometric amount of phenol was used as co-catalyst, a new rate law was revealed, showing first-order dependence on imine. This clearly demonstrates that the elimination step is not involved in the rate determining step anymore, and the proton transfer must be accelerated by the phenol additives. This was rationalized by transition state **64** involving a Brønsted acid assisted proton transfer step, which is somewhat similar to autocatalysis (Scheme 25).

1.2.4 Substrate diversity

The Morita-Baylis-Hillman reaction is flexible with respect to the choice of starting materials. As electrophiles aldehydes are generally the primary source, but α–keto

esters, non-enolizable 1,2-diketones, and fluoro ketones, can also be used. Simple ketones require high pressure to undergo the MBH reaction.[48a] When aldimines such as tolsylimines, nosylimines, SES-imines, sulfinylimines, azodicarboxylates or phosphinoylimines are employed as electrophiles, the reaction is commonly referred as aza-Morita-Baylis-Hillman reaction. The aza-MBH reaction can also be performed as a three-component reaction in which aldehyde, activated alkene and tosylamide, SES-amide, or diphenylphosphane-amide are coupled in "one-pot".[48f] A variety of activated alkenes such as alkyl vinyl ketones, acrylates, acrylonitriles, vinyl sulfones, acrylamide, allenic esters, vinyl sulfonates, vinyl phosphonates, and acrolein, can be employed in the Morita-Baylis-Hillman reaction.[48a] However, activated alkenes with β-substituents such as crotononitrile, crotonic acid esters, and less reactive alkenes such as phenyl vinyl sulfoxides require more forcing reaction conditions.[48]

1.2.5 Catalysis

The Morita-Baylis-Hillman reaction is generally slow, reaction times often reaching several days. In order to improve both reaction rate and yield, various modifications to reaction conditions were studied. Polar or protic solvents that can solubilize the nonhomogeneous reaction mixture and stabilize the formed zwitterionic species, are the most appropriate for MBH reactions (e.g. DMSO, DMF, alcohols)[63].

Most MBH reactions were carried out at room temperature, but in some asymmetric cases, lower temperatures were also required to reach good enantioselectivities. Heating, such as microwave,[64] can accelerate the reaction, but can also accelerate side reactions such as olefin polymerization. According to the mechanism shown in Scheme 19, various nucleophilic Lewis bases can be employed to initiate the Morita-Baylis-Hillman reaction. This includes amine-[50], phosphane-[49] and chalcogenide-centered[65] Lewis bases. It is worth to mention here that $TiCl_4$ could also mediate MBH reactions to provide the corresponding MBH adducts exclusively.[66] In this thesis, only amine- and phosphane-centered Lewis bases will be discussed as catalysts in detail. Some reported nitrogen-centered Lewis bases for the MBH reaction are shown in Scheme 26, such as DABCO (**40**),[67] quinuclidine (**65**),[68] triethylamine (**66**),[69] tetramethylguanidine (**67**),[70] DBU (**68**),[71] imidazole (**69**),[72] and DMAP (**1**).[73]
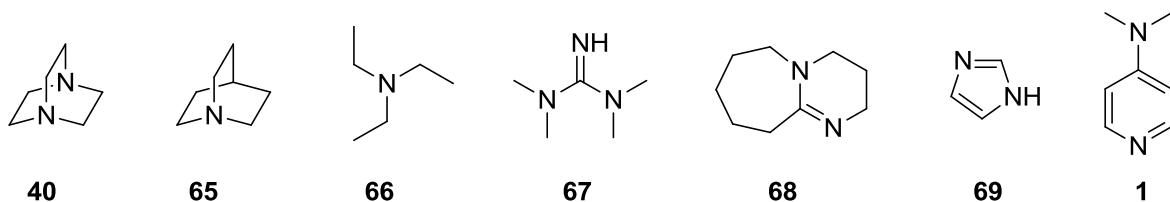
Scheme 26. Some N-centered Lewis bases used in the MBH reaction.

To determine how Brønsted basicity affects the efficiency of these catalysts in MBH reactions, Aggarwal et al.[68] examined the reactivity of a series of quinuclidine-based catalysts in the MBH reaction. They established a straightforward correlation between the basicity of the catalysts and reactivity, according to which more basic catalysts in this series are more reactive. Mayr et al.[74] studied the nucleophilicities of DABCO (**40**), quinuclidine (**65**) and DMAP (**1**). They reported that DABCO (**40**) and quinuclidine (**65**) were significantly better nucleophiles (about 10^3 times) and leaving groups (about 10^5 times) than DMAP (**1**). This interesting finding could be employed to rationalize the fact that DMAP (**1**) shows better performance than DABCO (**40**) in MBH reaction of cycloalkenones with formaldehyde[73a]: because of the higher carbon basicity of DMAP (**1**), a higher concentration of the zwitterionic intermediate was generated, which is probably more relevant in this reaction, comparing with the case catalyzed by DABCO (**40**) with higher rate of Michael addition and elimination.

Phosphane-centered Lewis bases useful for MBH reactions are compounds like tricyclohexylphosphane (**70**),[49] tributylphosphane (**71**),[75] triethylphosphane (**72**),[42] dimethylphenylphosphane (**73**),[76] and triphenylphosphane (**2**)[59a] (Scheme 27). As compared to their nitrogen analogues, P-centered Lewis bases have higher nucleophilicity and weaker proton-basicity, which are most likely attributed to their greater polarizability and lower electron density of the phosphorus atom. However, due to their high air-sensitivity, the potential efficiency of trialkylphosphanes in Morita-Baylis-Hillman reactions is somewhat reduced. Fu and coworkers[77] suggested that the air-stable conjugate acids of trialkylphosphane can be treated with base to regenerate the phosphane *in situ*. He et al.[78] reported the air-stable 1,3,5-triaza-7-phosphaadamantane (PTA, **74**) to be an effective catalyst for the MBH reaction.

70 **71** **72** **73** **2** **74**
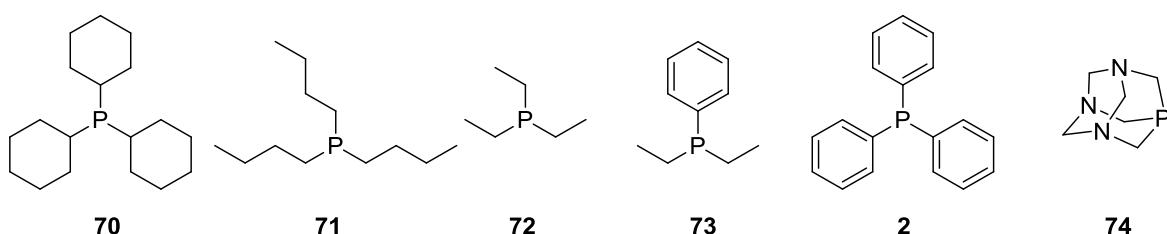
Scheme 27. Some P-centered Lewis bases used in the MBH reaction.

Various additives were used to accelerate the MBH reaction, such as La(OTf)$_3$,[79] lithium perchlorate,[80] 3,5-bistrifluoromethylphenol,[61] nitrophenol,[59a] octanol[59b] and urea.[81] The most commonly used co-catalysts are Brønsted acids, which supposedly accelerate the reaction through speeding up the proton transfer step. One of the very successful examples using a chiral Brønsted acid was reported by Schaus et al.[42a] In the triethylphosphane-promoted MBH reaction of 3-phenylpropanal with cyclohexenone, and BINOL derivative **75** as co-catalyst in THF, the product was obtained with high yield and enantioselectivity (Scheme 28). It was suggested that in this case the Brønsted acid might remain hydrogen-bonded to the resulting enolate in the enantioselectivity-determining adol addition step. Nagasawa and co-workers[81] developed a new bis-thiourea-type Brønsted acid **76**, which could promote the MBH reaction of cyclohexanecarboxaldehyde with cyclohexenone in the presence of DMAP to give the desired product with good yield and high entioselectivity (Scheme 29). Both of the thiourea moieties are necessary to reach high entioselectivity and yield, and it has been proposed that the aldehyde and the enone got activated via coordination to the thiourea units of **76** through hydrogen bonding interactions.
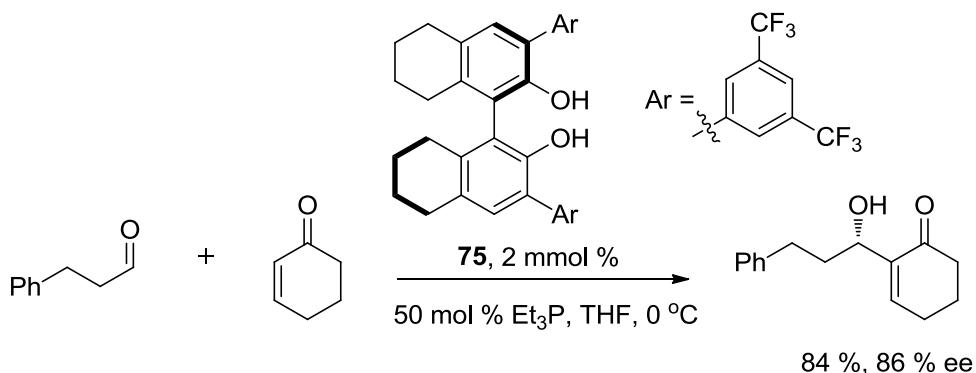
Scheme 28. BINOL derivative and PEt$_3$ co-catalyzed MBH reaction.
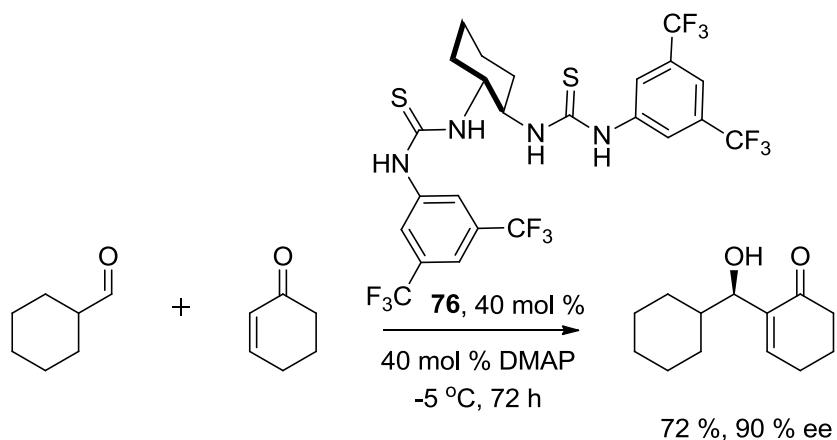
Scheme 29. DMAP and bis-thiourea co-catalyzed MBH reaction.

As mentioned in chapter 1.1.6, multifunctional/bifunctional catalysts, which combine two or more Lewis- or Brønsted type active sites in a well defined chiral environment, can effectively promote Morita-Baylis-Hillman reactions. One of the first successful chiral bifunctional catalysis in MBH reactions was developed by Hatakeyama et al.[46e] They reported that the cinchona alkaloid derivative **77** could catalyzed the asymmetric MBH reaction of aldehydes with activated acrylates. From the structure of compound **77**, there are two important potential features to achieve good enantioselectivity: (1) Increased nucleophilicity via reduced steric hindrance; (2) a free phenolic hydroxyl group (Scheme 30).
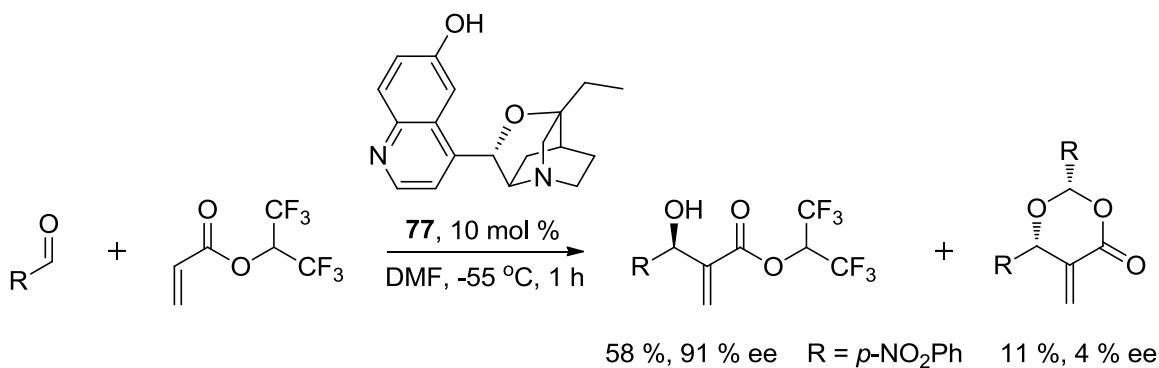
Scheme 30. Cinchona alkaloid derivative **77**-catalyzed asymmetric MBH reaction.

Later on, utilizing the same cinchona alkaloid derivative **77** as catalyst, Shi et al.[82] reported the formation of asymmetric aza-Morita-Baylis-Hillman reaction products of tosylimine and methyl vinyl ketone or methyl acrylate obtained with good yield

and enantioselectivity. They also rationalized that the key factor for high enantioselectivity is the hydrogen bond between the phenolic hydroxyl group and the nitrogen-centered anion, to give a relatively rigid transition state **78** (Scheme 31).
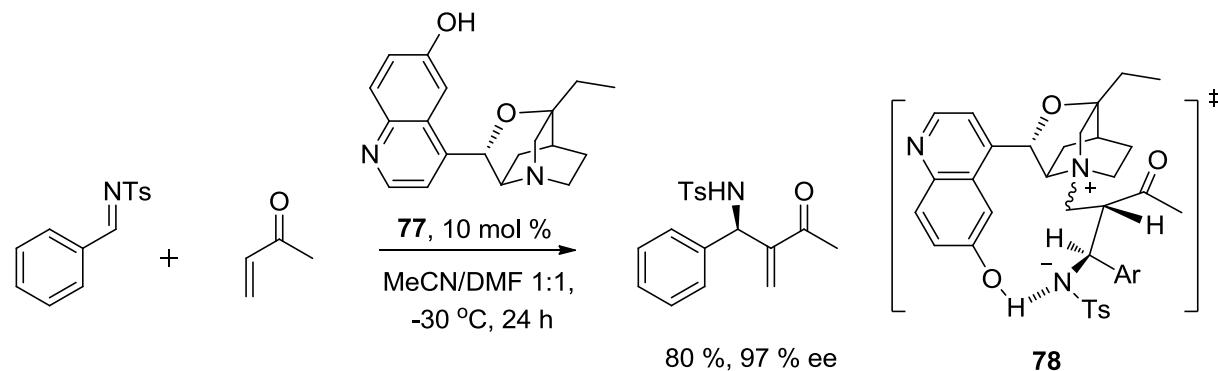
Scheme 31. Cinchona alkaloid derivative **77** catalyzed asymmetric aMBH reaction.

One of the most successful chiral bifunctional catalytic systems for aza-MBH reactions was also developed by Shi and coworkers.[83] The bifunctional catalyst **79** containing a phosphorus-centered Lewis base and a Brønsted acid moiety could promote the reaction of tosylimines with methyl vinyl ketone, acrylate, or acrolein to give the desired product with good yield and high enantioselctivity. They also carried out mechanistic studies to clearify that the phenolic hydroxyl Brønsted acid group is crucial for the efficiency of catalyst **79**. When the hydroxyl group was replaced by a methoxy group (as in catalyst **80**) significantly reduced catalytic reactivity and enantioselectivity was observed (Scheme 32).

72 %, 94 % ee   13 %, 20 % ee
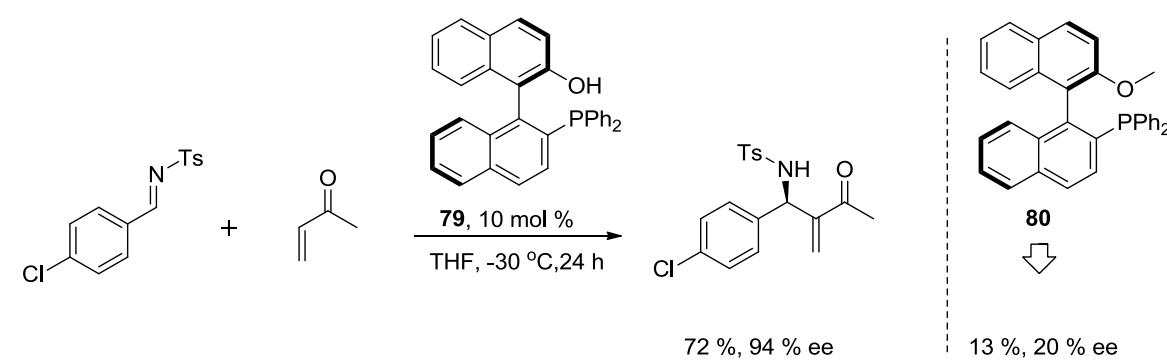
Scheme 32. Bifunctional phosphane catalyst **79** catalyzed asymmetric aMBH reaction.

Based on the same 1,1'-binaphthalene framework, a series of multi/bifunctional catalysts were also developed (Scheme 33). Shi et al. reported that more nucleophilic phosphane-BINOL-type bifunctional chiral catalysts **81**,[84] **82**,[84] and **83**[85] bearing multiple phenol groups, catalyst **84** containing an thiourea Brønsted acid moiety,[86] and dendrimer-supported catalyst **85**[87] were all efficient and enantioselective catalysts in aMBH reactions. Sasai and coworkers anchored phosphanes and aminopyridine units to the 3-position of BINOL to give catalysts **86**[88] and **87**,[89] which could mediate the aza-MBH reaction of imines with MVK, EVK, and acrolein with good yield and enantioselectivity. Liu and coworkers developed trifunctional catalyst **88**,[90] and fast and enantioselective aza-MBH reactions were achieved with benzoic acid as additive. Ito et al. also reported trifunctional catalyst **89**[91] for the aza-MBH reaction of imine and MVK, and with 1 mol % catalyst loading, high selectivity up to 96 % ee was achieved.
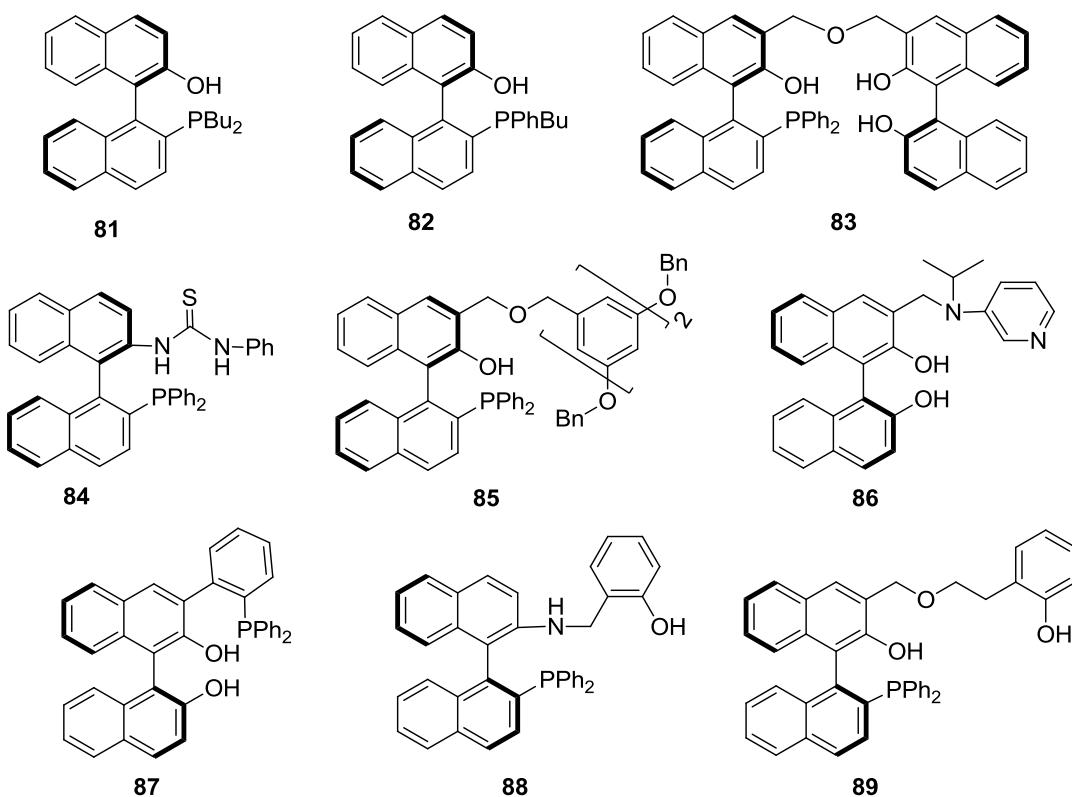
Scheme 33. Some phosphane-BINOL-type multi/bifunctional catalysts.

Another example for chiral phosphane-catalyzed MBH reactions were reported by Wu et al.[92] They employed a series of chiral phosphino-ureas derived from *trans*-2-amino-1-(diphenylphosphino)cyclohexane to promote the MBH reaction of

aromatic aldehydes with MVK. The MBH products were obtained in relatively short reaction times and with excellent enantioselectivity (Scheme 34).
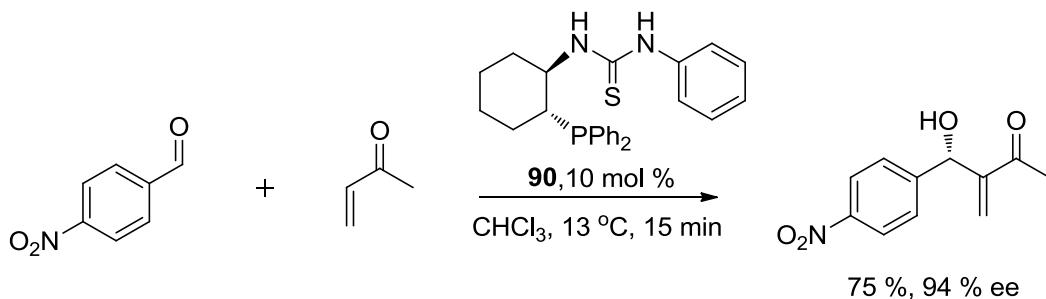
Scheme 34. MBH reaction of aldehyde and MVK catalyzed by **90**.

Until here, most cases of asymmetric MBH reactions mentioned in this introduction are carried out with a source of chirality in starting materials and catalysts. In 2006, Leitner et al.[93] reported the first example of highly enantioselective asymmetric MBH reaction in which only the reaction medium contains chiral information. The MBH reaction of MVK and imine catalyzed by PPh_3 was carried out in a chiral ionic liquid **91**, providing yields of up to 39 % and enantioselectivities up to 84 % (Scheme 35). They mentioned that the key to high enantioselectivity lay in strong interactions such as electrostatic attraction and hydrogen bonding between the ionic liquid solvent and the intermediates or transition states of the enantioselective reaction step.
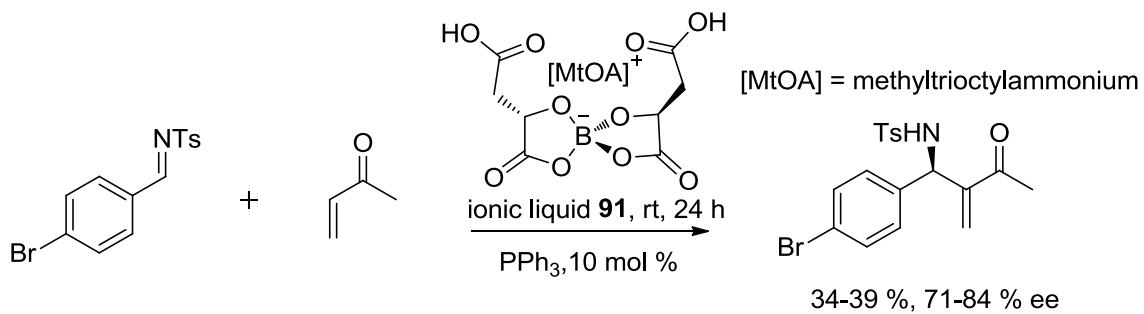
Scheme 35. Ionic liquid-assisted aMBH reaction.

1.3   Objective

To the best of our knowledge of organocatalysis and Mortia-Baylis-Hillman reaction till now, there are still some limitation for organocatalyzed MBH reaction, such as the turnover of organocatalyst and scopes of the subtrates. The objectives of this thesis are as follows:

(1) From the point of view of Brønsted acid-assisted MBH reaction, the generally accepted mechanism is that Brønsted acids accelerate the proton transfer step to speed up the catalytic cycle,[57] but there is still no kinetic data reported for the role of the proton source. We suppose that to clarify this point would help the understanding and design of new catalysts.

(2) Generally, the phosphane catalysts employed in MBH reactions are sensitive to oxygen and moisture in the atmosphere.[87] We plan to design and apply some new types of N-centered oxygen-tolerant Lewis bases in MBH reactions.

(3) Based on recent theoretical studies of organocatalysts,[94] we plan to predict the catalytic efficiency of a series of organocatalysts in the MBH reaction with theoretical methods and correlate them with experimental results.

(4) Design and development of some new multi/bifunctional organocatalysts for MBH reactions.

2   RESULTS AND DISCUSSION

2.1   Amine-catalyzed aza-Morita-Baylis-Hillman reaction

As mentioned in chapter 1.2.5, nitrogen-centered Lewis bases can effectively promote MBH reactions. The application of electron-rich pyridine-derived Lewis bases in Morita-Baylis-Hillman reactions will therefore be discussed in detail.

2.1.1   Pyridine-derived Lewis base catalysts

Donor-substituted pyridine derivatives, such as 4-(dimethylamino)pyridine (DMAP, (**1**)), play an important role as nucleophilic catalysts for a variety of organic reactions.[26a,95] The catalytic potential of DMAP was first discovered by the groups of Litvinenko and Steglich in the late 1960s.[5a,96] It is well known as a catalyst for the esterfication of alcohols by acid anhydrides and also for various other synthetically useful transformations, such as the synthesis of sulfonamides,[97] silylation,[98] CO_2 fixation,[99] kinetic resolution reaction,[100] and, of course, MBH reactions[73]. Recently, attention has been focused on the development of enantiomerically pure chiral pyridine derivatives for the kinetic resolution of alcohols and related enantioselective transformations.[101] 4-Substituted pyridine-derived Lewis bases (PDLB) act primarily as nucleophilic rather than general base catalysts for alcohol esterification. This follows from the dramatic loss of activity that accompanies 2-alkyl substitution despite the relatively marginal effect that this substitution has on the pK_a value of these derivatives.[26a] Such steric inhibition of catalysis was reported by Gold and Jefferson in the early 1950s[102] and quantified by Litvinenko and co-workers in 1981.[103] To enhance the reactivity of 4-substituted pyridines, our group developed a series of PDLBs based on the 3,4-diaminopyridine motif, which showed much better catalytic performance on acyl-transfer reactions than DMAP.[104] In acylation reactions catalyzed by DMAP, PPY, PDLB1, or PDLB2, the best results have been obtained with PDLB2, which has the highest nucleophilicity in this family.[104a,b] It is expected that PDLBs would also promote MBH reactions more effectively. Herein, we applied these catalysts in the aMBH reaction. Scheme 36 shows the PDLBs which were tested in aMBH reactions.
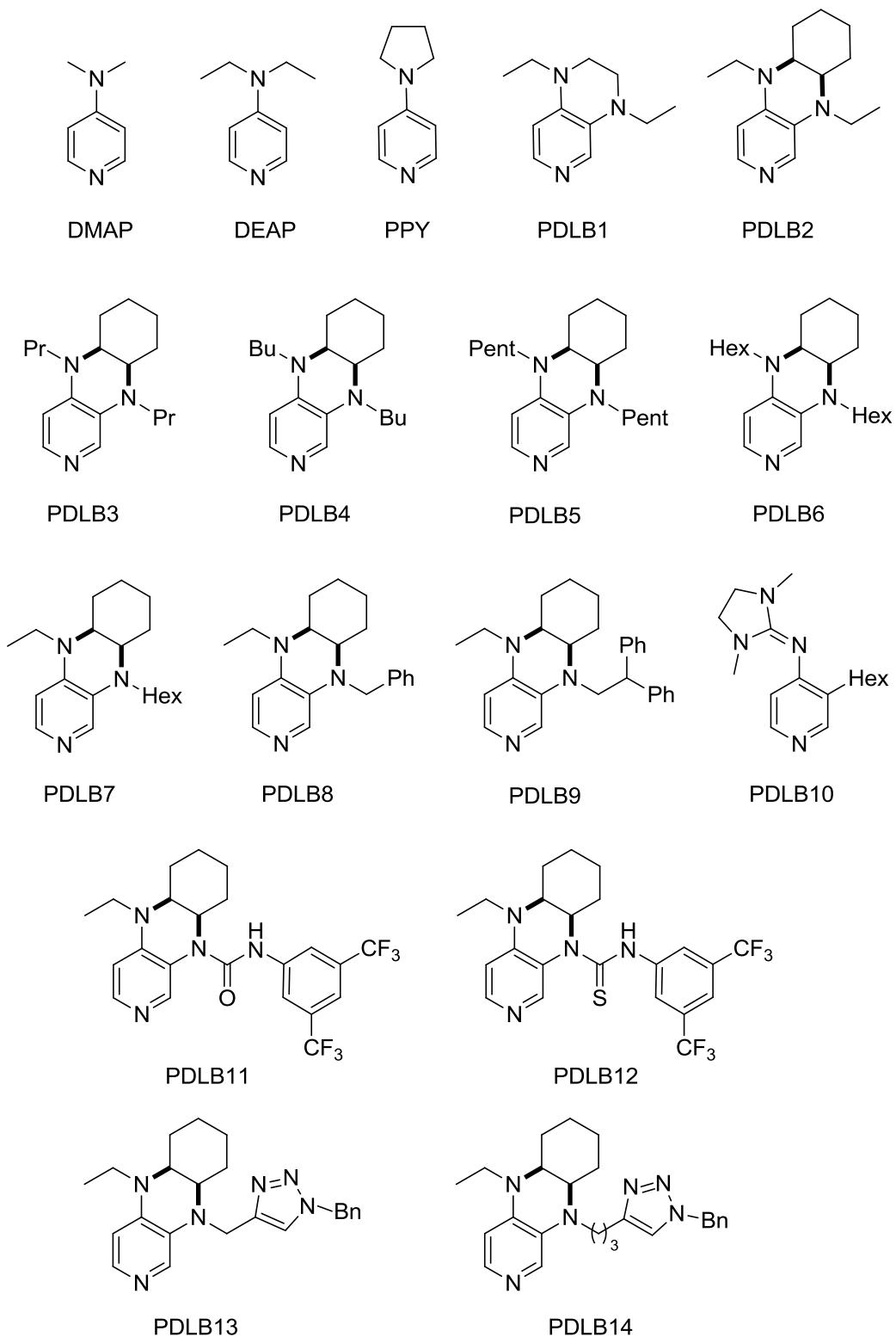
Scheme 36. Pyridine-derived Lewis bases (PDLB) tested in MBH reactions.

Most of the pyridines shown in Scheme 36 can efficiently be synthesized from 3,4-diaminopyridine in a three- or four-step sequence.[104a,105] The general procedure for the synthesis of PDLBs is shown in Scheme 37.
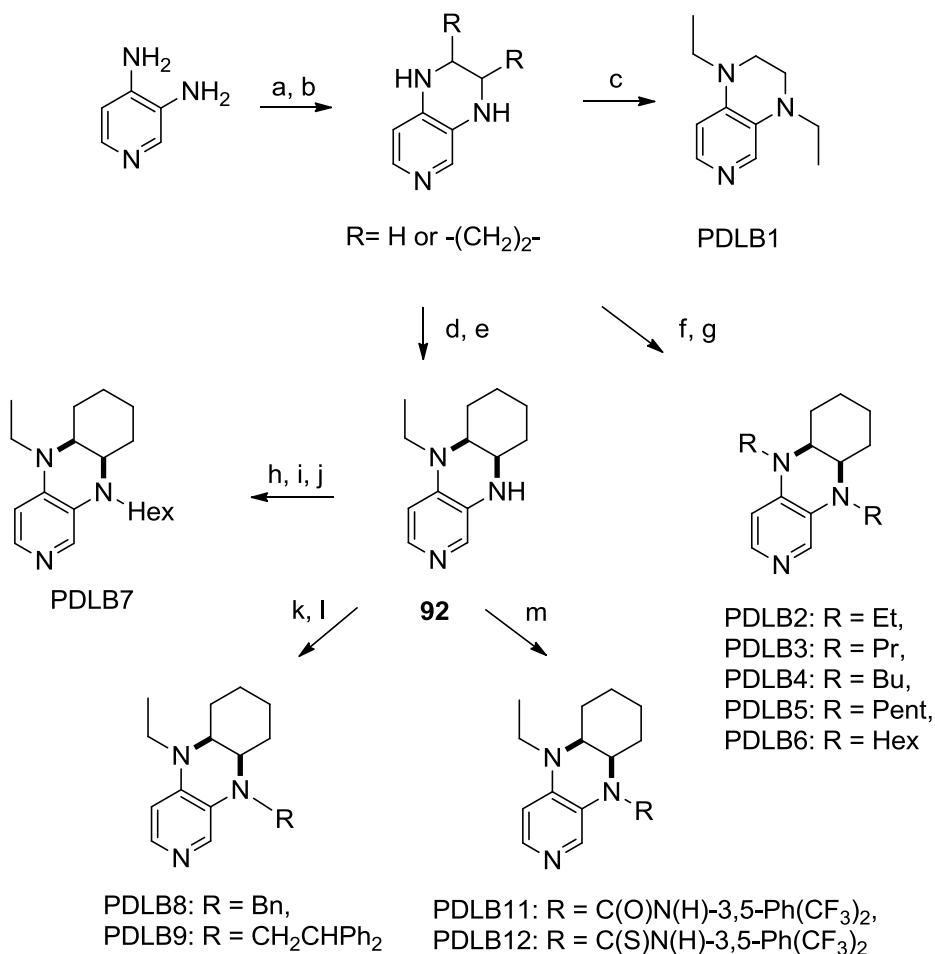
Scheme 37. Synthesis of 3,4-diaminopyridine catalysts. *Reagents and conditions:* a) glyoxal, or 1,2-cyclohexandione, EtOH, 70 °C. b) NaBH$_4$, EtOH, 40 °C. c) Ac$_2$O, pyridine, 100 °C; LiAlH$_4$, AlCl$_3$, MTBE, reflux. d) Ac$_2$O, PPY, Et$_3$N, CH$_2$Cl$_2$. e) LiAlH$_4$, AlCl$_3$,THF, reflux. f) Ac$_2$O, (C$_2$H$_5$CO)$_2$O, (C$_3$H$_7$CO)$_2$O, (C$_4$H$_9$CO)$_2$O, or (C$_5$H$_{11}$CO)$_2$O, PPY, pyridine, MW, 170 °C. g) LiAlH$_4$, AlCl$_3$, THF, reflux. h) BH$_3$SMe$_2$, THF. i) BuLi, then hexylbromide, THF, -78 °C. j) HCl/MeOH. k) benzoyl chloride or 2,2-diphenylacetyl chloride, pyridine, MW, 170 °C. l) LiAlH$_4$, AlCl$_3$, THF, reflux. m) RNCO, CH$_2$Cl$_2$, rt.

The utility of the pyridine catalysts shown in Scheme 36 was explored in the aMBH reaction by reacting N-tosylimines with methyl vinyl ketone (Table 1, 2, 3), ethyl acrylate (Table 4), or 2-cyclohexenone (Table 5, 6).

The kinetic measurements of the aMBH reactions described in Table1-7 were carried out in NMR tube experiments and monitored by ^{1}H NMR with the disappearance of the minor reaction component (N-tosylimine). Figure 1 shows a typical conversion-time plot of PDLB2-catalyzed aMBH reaction of N-tosylimine **93c** with methyl vinyl ketone. The turnover curve can be fitted to a simple first-order rate law model to give an effective rate constant k_{eff} or, equivalently, an

effective reaction half-life time $t_{1/2}$, which allows us to compare the performance of the catalysts in more quantitative terms.
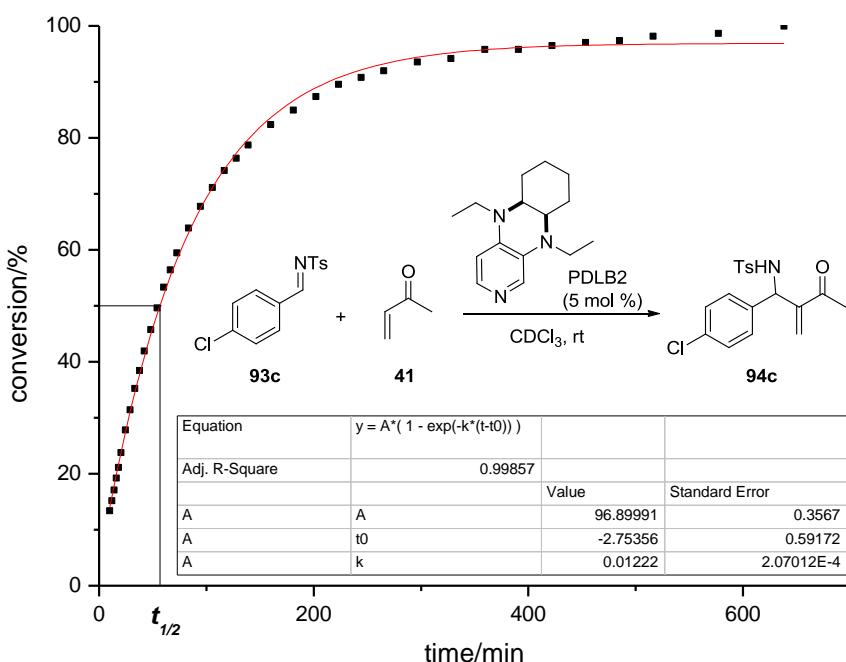
Figure 1. A typical conversion-time plot of PDLB2-catalyzed aMBH reaction of N-tosylimine **93c** with methyl vinyl ketone.

In the aMBH reaction of N-tosylimine **93c** with methyl vinyl ketone, DABCO did not promote the reaction very effectively, yielding only 8 % after 10 hours (entry 1, Table 1). For the pyridine catalysts DMAP, DEAP and PPY, up to 86 % conversion was achieved in the same time (entry 2-4, Table 1). Excellent results (entry 5-7, Table 2, 5 hour, up to 99 % conv.) were obtained when PDLB1, PDLB2 and PPh$_3$ were employed. It is worth mentioning that DEAP, which has two ethyl groups on the nitrogen atom, is 2.4 times more effective that DMAP with two methyl groups. PDLB2 is 1.5 times more effective than PDLB1, which is 11 times more reactive than DMAP and 4.3 times more reactive than PPY (Table 1).

Table **1**. Aza-MBH reaction of N-tosylimine **93c** with MVK in the presence of selected Lewis base catalysts.

Entry	Lewis base	Time/h	Conversion/%[a]	Half life/min
1	DABCO	10	8	-
2	DMAP	10	56	475
3	DEAP	10	83	195
4	PPY	10	86	176
5	PDLB1	5	98	44
6	**PDLB2**	**4**	**99(98)[b]**	**26**
7	PPh$_3$	4	99	38

a) Determined by ^{1}H NMR. b) Isolated yield. c) 0.125 M imine, 1.2 equiv. MVK.

Furthermore, we employed a series of pyridine catalysts at 5 % catalyst loading in the aMBH reaction of N-tosylimine **93c** with methyl vinyl ketone, and the results are shown in Table 2. Most of the PDLBs could promote this reaction effectively with 92-99 % conversion in 10 hours (entry 1-10, Table 2). PDLB2-6 showed almost the same $t_{1/2}$ and efficiency, which indicated the variation of ethyl, propyl, butyl, pentyl, and hexyl substituent groups on the nitrogen atoms of the 3,4-diaminopyridine motif (entry 2-6, Table 2) did not play a significant role as in the case of DMAP and DEAP. But in the case of PDLB8 and 9, the introduction of a benzyl or a 2,2-diphenylethyl group on the 3-nitrogen atom of 3,4-diaminopyridine motif resulted in a drop of catalytic activity by 2-fold comparing with PDLB2-6 (entry 2-3, Table 2). A 2-fold drop was observed when 4-guanidinylpyridine PDLB10 was employed. It is important to point out that bifunctional catalysts PDLB11 and PDLB12 with urea or thiourea framework on the 3-nitrogen atom (entry 10-11, Table 2) as hydrogen-donating groups, are much less reactive (12 % conv. in 12 h, and 67 % conv. in 24 h), probably due to the reduced nucleophilicity of the pyridine nitrogen by the inductive effect of the urea moiety, and similar effects were also observed in PDLB-catalyzed acylation reactions.[104a, 104b, 105b]

Table **2**. Aza-MBH reaction of N-tosylimine **93c** with MVK in the presence of pyridine catalysts.
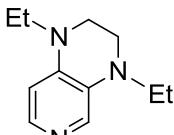
Entry	Lewis base		Time/h	Conversion/%[a]	Half life/min
1		PDLB1	10	97	78±1
2	R_1 = Et,	PDLB2	10	99/(92)[b]	57±1
3	R_1 = Pr,	PDLB3	10	99	52±1
4	R_1 = Bu,	PDLB4	10	99	55±1
5	R_1 = Pent,	PDLB5	10	99	54±1
6	R_1 = Hex,	PDLB6	10	99	55±1
7	R_2 = Hex,	PDLB7	10	97	66±1
8	R_2 = Bn,	PDLB8	10	92	102±2
9	R_2 = CH$_2$CHPh$_2$,	PDLB9	12	92	154±2
10	R_2 = C(O)N(H)-3,5-Ph(CF$_3$)$_2$,	PDLB11	12	12	-
11	R_2 = C(S)N(H)-3,5-Ph(CF$_3$)$_2$,	PDLB12	24	67	-
12	Hex	PDLB10	10	93	109±1
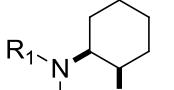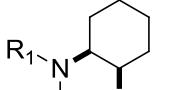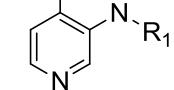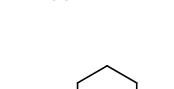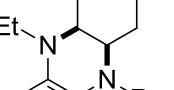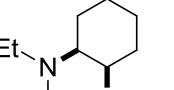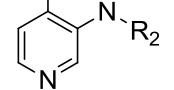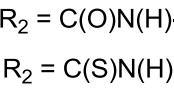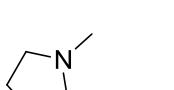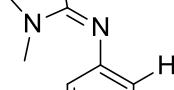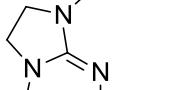
a) Determined by ^{1}H NMR. b) Isolated yield. c) 0.125 M imine, 1.2 equiv. MVK.

Using PDLB2 as catalyst, we next examined a variety of tosyl imines, and the results are shown in Table 3. For aryl imines with an electron-withdrawing group on the aromatic ring (*p*-cyano, *p*-nitro, *p*-chloro, *o*-chloro, *p*-bromo) and the imine derived from benzaldehyde, the corresponding aMBH reaction products were obtained in good to high yields (entry 1-6, Table 3). But for the electron-rich imine (*p*-methyl, *p*-methoxy), longer reaction times were needed and only moderate

yields and conversions were achieved (entry 7-8, Table 3). The aMBH product was also obtained in good yield for the aliphatic tosyl imine (entry 9, Table 3).

Table **3**. Aza-MBH reaction of N-tosylimines **93** with MVK in the presence of catalyst **PDLB2**.

Entry	Ar	Tosylimine	Time/h	Yield/%[a]	Conversion/%[b]
1	p-CNC$_6$H$_5$,	**93a**	1.5	**94a**, 94	99
2	p-NO$_2$C$_6$H$_4$,	**93b**	1.5	**94b**, 90	99
3	p-ClC$_6$H$_4$,	**93c**	15	**94c**, 92	99
4	o-ClC$_6$H$_4$,	**93d**	18	**94d**, 81	93
5	p-BrC$_6$H$_4$,	**93e**	14	**94d**, 86	93
6	C$_6$H$_4$,	**93f**	15	**94f**, 73	99
7	p-MeC$_6$H$_4$,	**93g**	20	**94g**, 80	89
8	p-MeOC$_6$H$_4$,	**93h**	48	**94h**, 74	85
9	$trans$-Ph-CH=CH-,	**93i**	20	**94i**, 78	90

a) Isolated yield. b) Determined by ^{1}H NMR. c) 0.125 M imine, 1.2 equiv. MVK.

Given the promising results for the reactive substrate MVK, we turned our attention to the less reactive Micheal acceptors: ethyl acrylate and cyclohexenone. In the comparatively slow reaction of N-tosylimine **93c** with ethyl acrylate, PPh$_3$ and DABCO showed better catalytic performance than most pyridine catalysts. The best result was obtained when PPh$_3$ was employed (93 % conv., 5 days) (entry 1, 2, Table 4). With increasing nucleophilicity of PDLBs, higher conversion was achieved. PDLB2 led to 75 % conversion in 5 days, which was not so satisfying, but the best in this pyridine derivative family (entry 3-6, Table 4). The different activities of pyridine catalysts and DABCO in aMBH reactions can be rationalized by the study of nucleophilicities of DABCO and DMAP from Mayr et

al.[74] When the much less reactive ethyl acrylate was employed in the aMBH reactions, the Michael addition step might be slowed down to be somewhat rate-limiting, in which DABCO with higher nucleophilicity would lead to faster reaction rates as compared to DMAP with lower nucleophilicity.[74]

Table **4**. Aza-MBH reaction of N-tosylimine **93c** with ethyl acrylate in the presence of selected Lewis base catalysts.
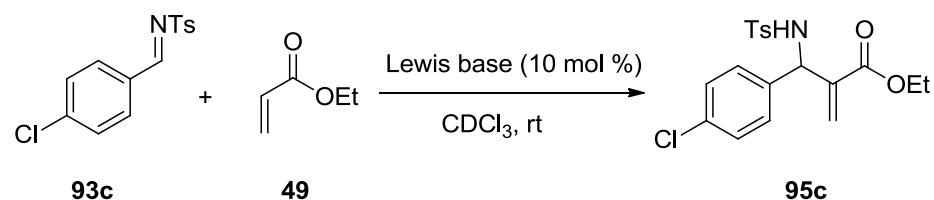

Entry	Lewis base	Time/d	Conversion/%[a]
1	**PPh$_3$**	**5**	**93**
2	DABCO	5	86
3	DMAP	5	40
4	PPY	5	60
5	PDLB1	5	63
6	PDLB2	5	75

a) Determined by ^{1}H NMR. b) 0.17 M imine, 2 equiv. ethyl acrylate.

To further explore the scope and utility of these PDLB catalysts in aMBH reactions, 2-cyclohexenone was employed to react with tosyl imines under the catalysis of PDLBs. As compared with methyl vinyl ketone, the β-substituents on the activated alkene of 2-cyclohexenone interfere with the MBH reaction to proceed smoothly.[48a] Some other potential nucleophilic catalysts, including PPh$_3$, CyclohexylPPh$_2$, DABCO, quinuclidine, DMAP and PPY, were also screened. It was found that PPh$_3$ and CyPPh$_2$ showed almost no reactivity, and DABCO showed a very low reaction rate, whereas quinuclidine, DMAP and PPY could promote this reaction with low conversion (up to 43 % conv., 40 h). Notable result (99 % conv., 98 % yield, 40 h) was achieved when PDLB2 was employed (Table 5).

Table **5**. Aza-MBH reaction of N-tosylimine **93c** with cyclohexenone in the presence of selected Lewis base catalysts.

Entry	Lewis base	Time/h	Conversion/%[a]
1	PPh$_3$	30	< 3
2	CyPPh$_2$	100	< 3
3	DABCO	40	4
4	Quinuclidine	40	25
5	DMAP	40	36
6	PPY	30	43
7	**PDLB2**	**40**	**99(98)[b]**

a) Determined by ^{1}H NMR. b) Isolated yield. c) 0.25 M imine, 4 equiv. cyclohexenone.

We investigated the scope of the PDLB2 catalyzed aMBH reaction of cyclohexenone by examining a variety of electrophiles (Table 6). For electron-deficient imines, the catalyst system is very efficient: aMBH products of most of the electron-deficient imines and 2-cyclohexenone were obtained in excellent yield (85 - 99 %, entry 1-5, Table 6). Additionally, this system also afforded reasonable yields for electron-rich imines. 69 % yield and 90 % conversion were achieved for the electron-rich *p*-methoxy tosylimines (entry 7, Table 6). For the aliphatic imine (entry 8) the aMBH product was also obtained with 87 % yield. It is worth mentioning that the long reaction time (such as 15 h, entry 3, Table 3; 120 h, entry 7, Table 6) for the PDLB-catalyzed aMBH reaction are partially due to the low concentrations of substrates used here. Reactivity measurements for different catalysts were perfomed in NMR tube experiments and monitored by ^{1}H NMR. The concentrations of reactants and catalysts were therefore selected to be compatible with this analytical approach and deuterated solvents were used throughout.

Table **6**. Aza-MBH reaction of N-tosylimines with cyclohexenone in the presence of pyridine catalyst **PDLB2**.

Entry	Ar	Time/h	Yield/%[a]	Conversion/%[b]
1	p-CNC$_6$H$_5$	24	**97a**, 88	99
2	p-NO$_2$C$_6$H$_4$	24	**97b**, 85	99
3	p-ClC$_6$H$_4$	40	**97c**, 98	99
4	o-ClC$_6$H$_4$	48	**97d**, 84	95
5	p-BrC$_6$H$_4$	60	**97e**, 90	99
6	C$_6$H$_4$	60	**97f**, 83	95
7	p-MeOC$_6$H$_4$	120	**97h**, 69	90
8	*trans*-Ph-CH=CH-	54	**97i**, 87	96

a) Isolated yield. b) Determined by ^{1}H NMR. c) 0.25 M imine, 4 equiv. cyclohexenone.

To determine relative reactivites of different Michael acceptors in aMBH reactions, the PDLB2-catalyzed aMBH reactions of tosylimine **93c** (0.25 M) with different Michael acceptors (MVK, cyclohexenone, ethyl acrylate)(1M) were carried out under otherwise identical conditions, and the turnover curves are shown in Figure 2. The reaction of tosylimine **93c** with MVK proceeded too rapidly to follow (98 % conv., 5 min.), and the half life time $t_{1/2}$ was roughly estimated as 1 min. As shown in Figure 3, the PDLB2-catalyzed aMBH reaction of tosylimine **93c** (0.25 M) with cyclohexenone is 430 times slower as compared to MVK, and is 2 times faster than the case of ethyl acrylate. This implies that the reactivity of Michael acceptors in the pyridine catalyst-catalyzed aMBH reactions distinctly depends on both the electrophilicity and steric hindrance of β-subtituents on the activated alkene.
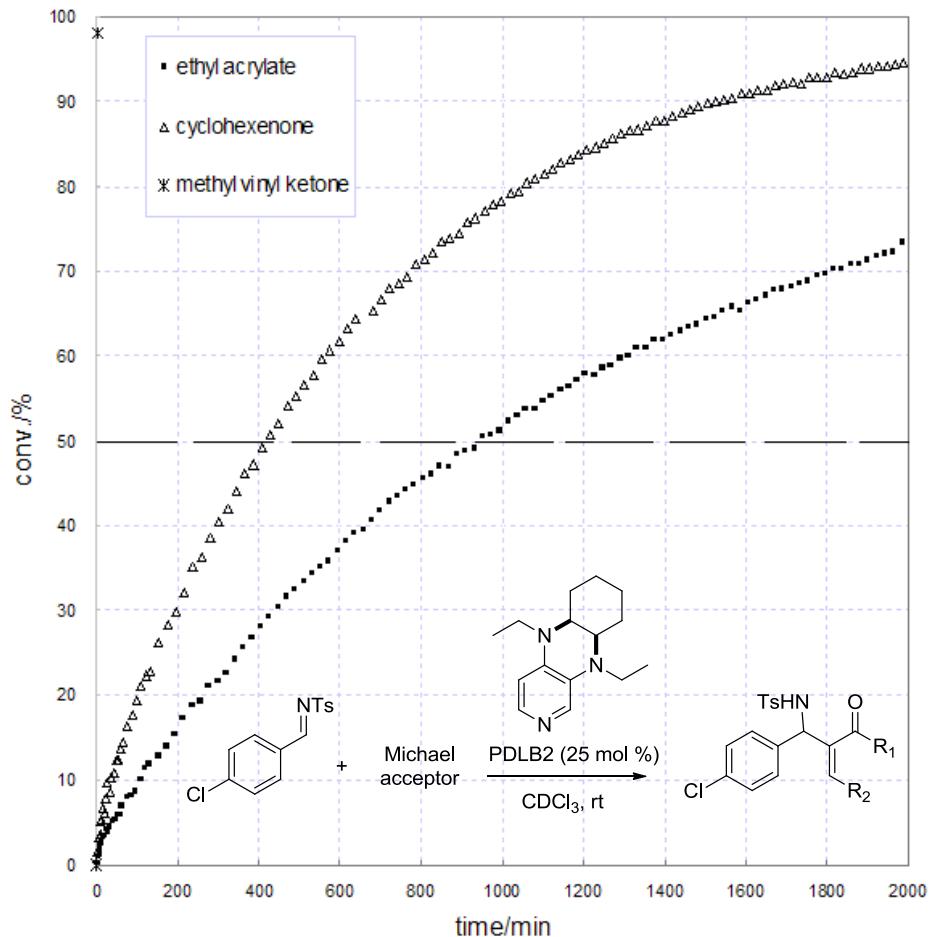
Figure 2. The conversion-time plots of PDLB2-catalyzed aMBH reactions of tosylimine **93c** (0.25 M) with Michael acceptors (MVK, cyclohexenone, ethyl acrylate)(1M).
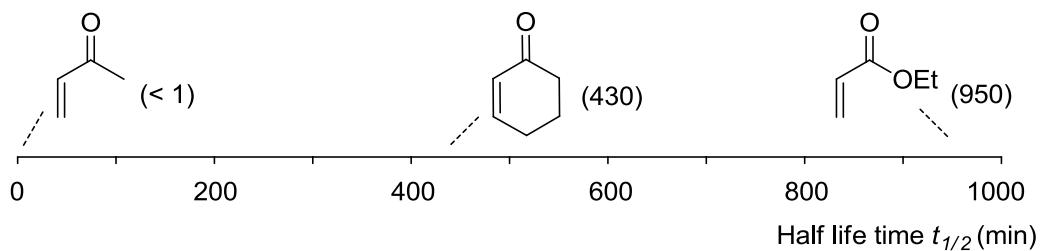

Figure 3. Reaction half life times $t_{1/2}$ of PDLB2-catalyzed aMBH reactions of tosylimine **93c** with different Michael acceptors.

As mentioned before, appropriately chosen proton sources are able to accelerate aMBH reactions. We also tried to introduce proton donor groups into the PDLB

motif to furnish bifunctional catalysts. Unfortunately, these bifunctional catalysts did not give promising results (entry 10-11, Table 2). In an attempt to accelerate the PDLB-mediated aMBH reaction, p-nitrophenol (PNP), an additional proton source, was used as co-catalyst in the reaction of tosylimine with methyl vinyl ketone. The results are shown in Table 7. In the DABCO-promoted aMBH reaction, the addition of PNP was able to speed up this reaction, but still did not give a satisfactory conversion (entry 1-2, Table 7). In the case of DMAP, when PNP was used as additive, a 1.5-fold rate acceleration was observed (entry 3-4, Table 7). For PPY, there was almost no rate change (entry 5-6, Table 7). But in the case of PDLB2, the reaction was slowed down by a factor of 1.4 (entry 7-8, Table 7). This could be rationalized by the protonation of the highly nucleophilic catalyst with PNP. Comparing with DMAP, less PDLB2, which is more nucleophilic and basic, could survive from protonation with PNP to promote the reaction. When diphenylurea was employed as co-catalyst for the PDLB2-catalyzed aMBH reaction, a small acceleration effect was observed (entry 9, Table 7), probably due to the lower acidity of diphenylurea as compared with PNP (pK_a in DMSO: 19.5 for diphenylurea, 10.8 for PNP).[106]

In summary, we have applied a series of PDLBs in the aMBH reaction of tosyl imines with three different activated alkenes: ethyl acrylate, methyl vinyl ketone, cyclohexenone. PDLBs did not show promising results in the case of ethyl acrylate. The catalytic potential of PDLBs in the reaction of tosylimine with MVK had been studied in detail, and PDLB2-6, which are the most nucleophilic in this family, show also the best catalytic performance. The best results were observed in the case of 2-cyclohexenone, in which PDLB2 showed the best catalytic potential compared with the other Lewis bases. The scope of these reactions for different N-tosylimines has also been investigated.

Table **7**. Aza-MBH reaction of N-tosylimine **93c** with MVK assisted by Lewis bases and co-catalysts.

| Entry	Lewis base	Co-catalyst	Time/h	Conversion/%[a]	Half life/min
1	DABCO	none	10	8	-
2	DABCO	PNP (10 mol %)	10	26	-
3	DMAP	none	10	56	475
4	DMAP	PNP (10 mol %)	10	64	385
5	PPY	none	10	85	176
6	PPY	PNP (10 mol %)	10	85	174
7[c]	PDLB2	none	10	99	57
8[c]	PDLB2	PNP (5 mol %)	10	96	78
9[c]	PDLB2	Urea (5 mol %)	10	99	48

a) Determined by ^{1}H NMR. b) 0.125 M imine, 1.2 equiv. MVK. c) 5 mol % Lewis base.

2.1.2 Immobilized catalysts

With the advent of the "green chemistry" concept[107] and the rising call for better sustainability, factors like catalysts recoverability[108] and recyclability are becoming increasingly important. Efforts have therefore been undertaken to support DMAP on cross-linked polystyrene beads.[109] Although these catalysts showed a good degree of recoverability and can apparently be reused without any sensible loss of activity, the catalytic performance of these heterogeneous catalysts is often significantly lower than that of their homogeneous equivalents. In the last few years, new elegant immobilization strategies have been explored including the immobilization of DMAP on mesoporous silica nanospheres,[110] on silica coated magnetic particles [111] or the microencapsulation of linear DMAP polymer.[112] In spite of these remarkable advances, a heterogeneous system able to approach or even surpass the performance of the homogenous catalysts has not been reported yet. Tricyclic DMAP derivative PDLB2 has recently been shown to exhibit excellent activity in acylation reactions in homogeneous solution.[104] Therefore we planned to

immobilize PDLB2 on a polystyrene support, hoping for catalysts of unprecedented catalytic activity, while preserving the benefits of facile recoverability and recyclability.

The catalytically active PDLB2 units were attached to the polystyrene support using the copper-catalyzed Huisgen reaction between azides and alkynes. A number of alkyne-substituted derivatives of PDLB2 were therefore synthesized and attached to an azide-modified Merrifield resin as shown in Scheme 38. In order to characterize the influence of the linker structure on the catalytic activity in acylation reactions, soluble catalysts with variable side chains have also been synthesized following the synthetic protocol shown in Scheme 38. This includes soluble catalyst PDLB7 with a simple *n*-hexyl side chain as well as catalysts PDLB13 and 14 with triazolyl-substituted side chains of variable length.[*]
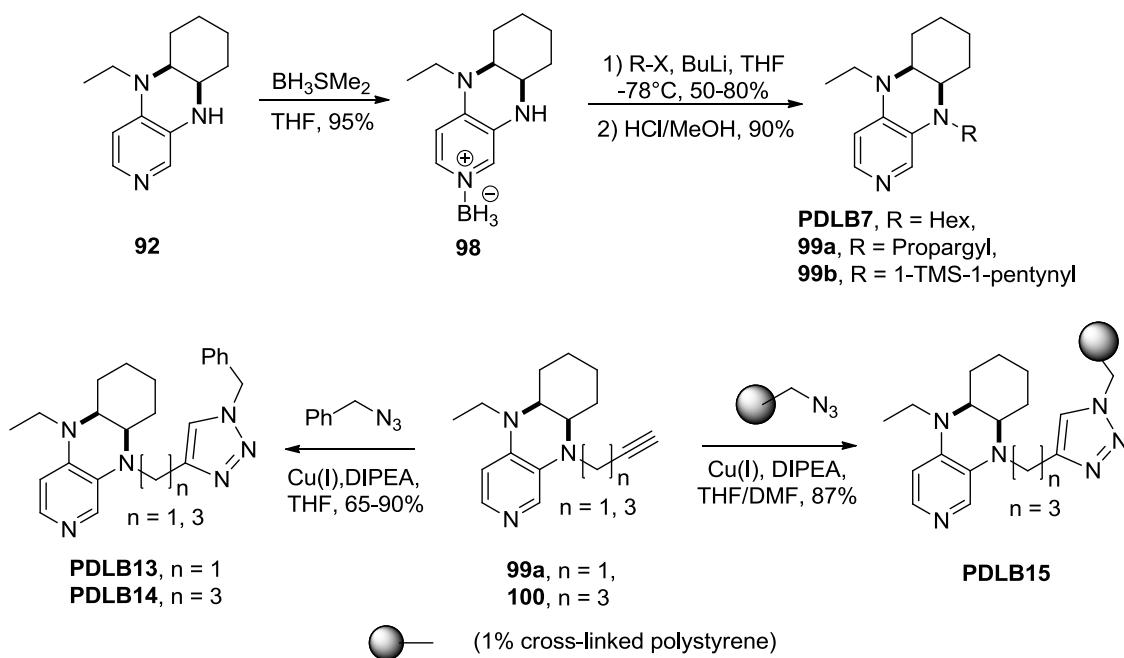
Scheme 38. Synthesis of immobilized catalyst PDLB15 and its soluble counterparts PDLB13 and 14.

The catalytic potential of catalyst PDLB13, 14, 15 in the aMBH reaction has been explored using the benchmark reaction of tosyl imines with methyl vinyl ketone. Using PPY as a reference (homogeneous) catalyst at 5 % loading we find that the

---

[*] PDLB7, 13-15 were prepared by Dr. Valerio D'Elia.

reaction proceeds moderately fast with a reaction half-life time of 385 min, providing 84 % conversion after 20 h reaction time. The diaminopyridine catalysts PDLB7, 13, 14 are significantly more active under otherwise identical conditions, providing essentially complete conversion after 10 h. The shortest reaction half-life of 53 min is determined for catalyst PDLB14 (entry 1-5, Table 8). Perusal of the kinetic data for the soluble 3,4-diaminopyridine catalysts shows that variation of the side chain attached to the nitrogen substituent at C3 position of the pyridine ring has no major influence on the catalytic activity. Experiments with supported catalysts (at 10 % catalyst loading) show a large influence of the catalyst structure: while only slow turnover is observed for the commercial PS-DMAP polymer (base loading ≈ 3.0 mmol/g DMAP, polystyrene crosslinked with 2 % of DVB), fast reactions and synthetically useful yields are obtained with resin PDLB15. Measured $t_{1/2}$ values indicate an intrinsic activity difference of ten for this selected substrate pair (entry 6-7, Table 8).

Whether the immobilized catalysts synthesized here can be used repeatedly after separation from the reaction mixture by filtration has been explored for repeated batches of the reaction shown in Table 8 with catalyst PDLB15. These experiments were conducted such that the catalyst was filtered off from the reaction mixture, washed abundantly with chloroform, dried in vacuum for 12 h and then reused without any further modification. This procedure is accompanied by only minimal losses of catalyst (approx. 1 to 2 %) per cycle. PDLB15 could be successfully reused for five more runs, although a slight loss of activity is noticed in the last of these cycles (entry 8-12, Table 8), or for the synthesis of other aMBH products (entry 13-15). The $t_{1/2}$ values assembled in Table 8 also allow us to quantify the effect of the resin and linker structure on the catalyst activity. Assuming a linear dependence of the catalyst loading on the reaction rate, the reaction half-life time of 110 min measured for PDLB15 and that of 57 min for PDLB2 imply that immobilization reduces the catalyst activity by a factor of 4.

Table **8**. Catalytic activity of immobilized and soluble pyridine catalysts in the aza-MBH reaction.
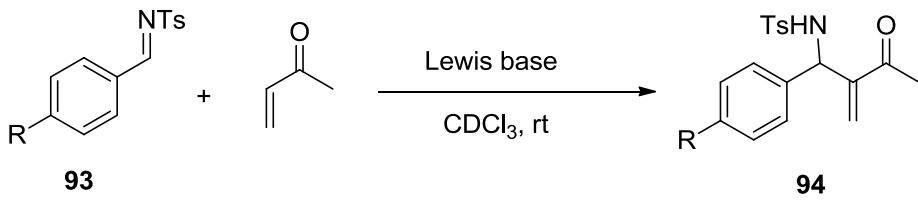
93
a, R = CN, b, R = NO$_2$,
c, R = Cl , f, R = H,

Entry	Lewis base	Product	$t_{1/2}$/min	Time/h	Conversion/%[a]
		Soluble catalysts (5 mmol %)			
1	PPY	**94c**	385±2	20	84
2	PDLB2	**94c**	57±1	10	99
3	PDLB7	**94c**	66±1	10	97
4	PDLB13	**94c**	57±1	10	98
5	PDLB14	**94c**	53±1	10	98
		Immobilized catalysts (10 mmol%)			
6	PS-DMAP	**94c**	1125±100	21	54
7	PDLB15	**94c**	110±7	12	93(87)[d]
8[c]	PDLB15	**94c**	-	12	92
9[c]	PDLB15	**94c**	-	12	90
10[c]	PDLB15	**94c**	-	12	92
11[c]	PDLB15	**94c**	-	20	95
12[c]	PDLB15	**94c**	-	25	90
13[e]	PDLB15	**94a**	-	16	94(81)[d]
14[e]	PDLB15	**94b**	-	16	90(78)[d]
15[e]	PDLB15	**94f**	-	16	89(63)[d,f]

R = Hexyl, PDLB7

n = 3, PDLB14
n = 1, PDLB13

n = 3, PDLB15

a) Determined by ^{1}H NMR. b) Imine 0.125 M, 1.2 equiv. MVK. c) The catalyst is recycled from the former entry. d) Isolated yield after column chromatography. e) The catalyst had been already employed for the reactions in entries 7-12. f) 20 % of benzaldehyde (hydrolysis of **93f**) was also recovered.

The deactivation of immobilized DMAP after its repeated use could be caused by covalent attachment of methyl vinyl ketone to the pyridine nitrogen of the polymer.[113] In order to split off the attached MVK and thus regain the initial activity of the immobilized catalyst PDLB15, the partially deactivated catalyst PDLB15 was submitted to treatment with base. This is in analogy to the catalyst recovery from reaction intermediates described in Scheme 24. Unfortunately not much activity recovery occurs upon contacting the polymer with a 2 M NaOH solution at 60 °C for 1 h.

Figure 4: When the agitation is stopped, the resin floats on top of the reaction solution allowing the facile sampling.

After tosylimine, methyl vinyl ketone and immobilized catalyst were added to the reaction flask, the reaction mixture was mechanically shaken at a rotation speed of 480 turns/minute. Periodically, the agitation was interrupted for about one minute until all the resin floated on top of the solution, thus allowing the sampling from the bottom of the reaction mixture using a syringe as shown in Figure 4. The sample was subsequently submitted to ^{1}H NMR spectroscopy to determine the kinetic information. At the end of the reaction, the immobilized catalyst was easily recovered by filtration, washing with chloroform and drying under vaccum.

In conclusion, the immobilization of 3,4-diaminopyridines on polystyrene support by aid of the copper-catalyzed Huisgen reaction leads to new catalysts of high activity and facile recoverability. The measured half-lifes of aMBH reactions depend significantly on the nature of the pyridine catalyst. This active combination of resin and PDLB has been found to exceed the catalytic activity of commercially available polystyrene-DMAP by 10-fold for the aza-aMBH reaction.

2.2 Phosphane-catalyzed (aza) Morita-Baylis-Hillman reaction

2.2.1 Phosphane catalysts and their MCAs

Phosphanes are well known not only as ligands for transition metal complexes, but also as versatile catalysts for acylation reactions,[114] MBH reactions,[59] Rauhut–Currier reactions,[115] or Michael addition reactions.[116] In these areas of application as catalysts, phosphanes react with carbon-centered electrophiles and thus activate these substrates for subsequent steps in the catalytic cycle. The affinity of phosphanes towards a reference carbon electrophile will thus help to correlate observed catalytic reactivity with the phosphane substitution pattern. In our group a quantum mechanical protocol was therefore established for the reliable calculation of the reaction of N- and P-centered nucleophiles with the methyl cation, the smallest C-centered electrophile.[94] In contrast to gas or solution phase proton affinities, methyl cation affinities (MCAs) provide a much more realistic assessment of the nucleophilic potential of phosphanes in organocatalytic processes. The MCA values for a wide variety of phosphanes have been reported and predicted.[117] In an effort to correlate the catalytic potential of phosphorus-based nucleophiles used in organocatalytic processes with their MCA values, we select the aMBH reation as a benchmark reaction. The phosphanes tested in the aMBH reaction are shown in Scheme 39.
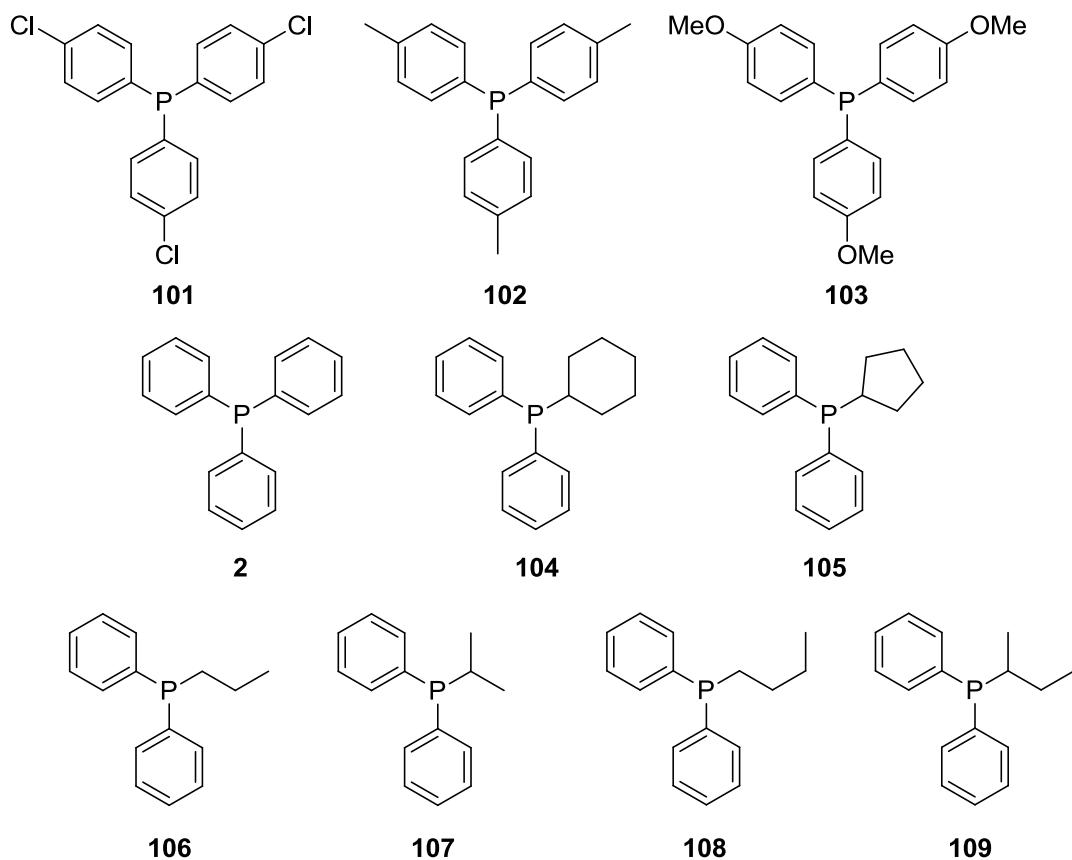
Scheme 39. Phosphanes tested in aMBH reactions.

MCAs of phosphane bases have been calculated as the gas phase reaction enthalpy at 298.15 K and 1 atm pressure for the methyl cation detachment reaction shown in equation 1. This is in analogy to the mass spectrometric definition of proton affinities.

$$PR_3\text{-}CH_3^+ \longrightarrow PR_3 + CH_3^+ \qquad (1)$$

The MCAs of phosphanes tested in the aMBH reaction are shown in Table 9.[*] The MCAs ranged from 586.5 kJ/mol (for **101**) to 651.0 kJ/mol (for **103**). The catalytic performance of these phosphanes for the aMBH reaction was investigated in the benchmark reaction of tosylimine **93c** with methyl vinyl ketone. PPh₃ was used as reference catalyst with 10 % loading, and the reaction proceeded moderately fast with a reaction half-life time of 38 min. Phosphane **101** is significantly less active under otherwise identical conditions, providing 69 % conversion after 18 h (entry 1, Table 9). The shortest reaction half-life time of 17 min is observed for phosphane

---

∗ The MCA values were calculated by Christoph Lindner.

106 (entry 7, Table 9). Most of these phosphanes promote the aMBH reaction effectively with 99 % conversion in 5 h.

Table 9. Aza-MBH reaction of N-tosylimine **93c** with MVK in the presence of phosphane catalysts.

Entry	Phosphane	MCA values (kJ/mol)	Time/h	Conversion/%[a]	Half life/min
1	R_1 = Cl, **101**	586.5	18	69	574±7
2	R_1 = H, PPh$_3$ (**2**)	618.4	4	99	38±0.2
3	R_1 = Me, **102**	637.2	4	99	37±2
4	R_1 = MeO, **103**	651.0	4	99	40±2
5	R_2 = Cyclohexyl, **104**	630.2	3	99	24±1
6	R_2 = Cyclopentyl, **105**	630.5	5	99	39±1
7	R_2 = Propyl, **106**	623.6	3	99	17±0.3
8	R_2 = iPropyl, **107**	623.0	3	98	31±0.1
9	R_2 = Butyl, **108**	624.6	3	99	19±0.5
10	R_2 = iButyl, **109**	625.8	3	99	28±0.5
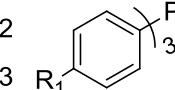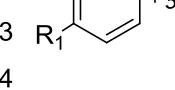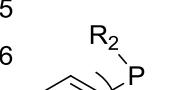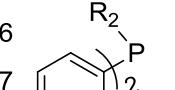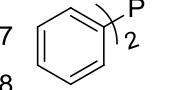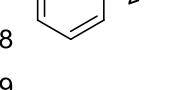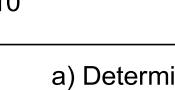
a) Determined by ^{1}H NMR. b) 0.125 M imine, 1.2 equiv. MVK.

Given the experimentally measured reaction half-life $t_{1/2}$ and calculated MCAs for the phosphane catalysts, we next turned our attention to the correlation of MCAs with reaction rates. Since the rate constant k is inversely proportional to $t_{1/2}$, including the data from Table 9, a linear correlation of the MCA values and reaction rates was obtained (Figure 5), which can be briefly expressed by the equation MCA = 11.79 $\times$ Ln(1/$t_{1/2}$) + 668.32. The quality of the correlation (R^2 = 0.5089) is moderate and does not allow for very precise predictions. It is notable to mention that triarylphosphanes Ph$_3$P (**2**), (p-MeOPh)$_3$P (**103**) and (p-MePh)$_3$P (**102**) gave similar results ($t_{1/2}$ = 37-40 min.), but (p-ClPh)$_3$P (**101**) showed significantly lower reactivity ($t_{1/2}$ = 574 min). This probably implies that the rate determining step in the case of (p-ClPh)$_3$P (**101**) is different as compared to the other

triarylphosphanes. We rationalized the deviation of MCAs and reactivity of phosphanes in aMBH reactions by the following reasons:

(1) The MCA value describes the detachment reaction enthalpy of phosphanes with methyl cation, which represents the stability of the phosphane-methyl cation complex. On the other side, the reaction rate is reflected by the Gibbs free energy of the transition state, which is not fully dependent on the enthalpy. And this deviation could be caused by ignoring kinetic aspects.

(2) The rate determining step in the aMBH reaction is considered to be the proton transfer step, but not the Michael addition step, which could be more accurately depicted by MCAs. We expect better correlation of MCA and reaction rate if another MBH benchmark reaction is selected, using different substrates, in which the Michael addition step is the rate limiting step.
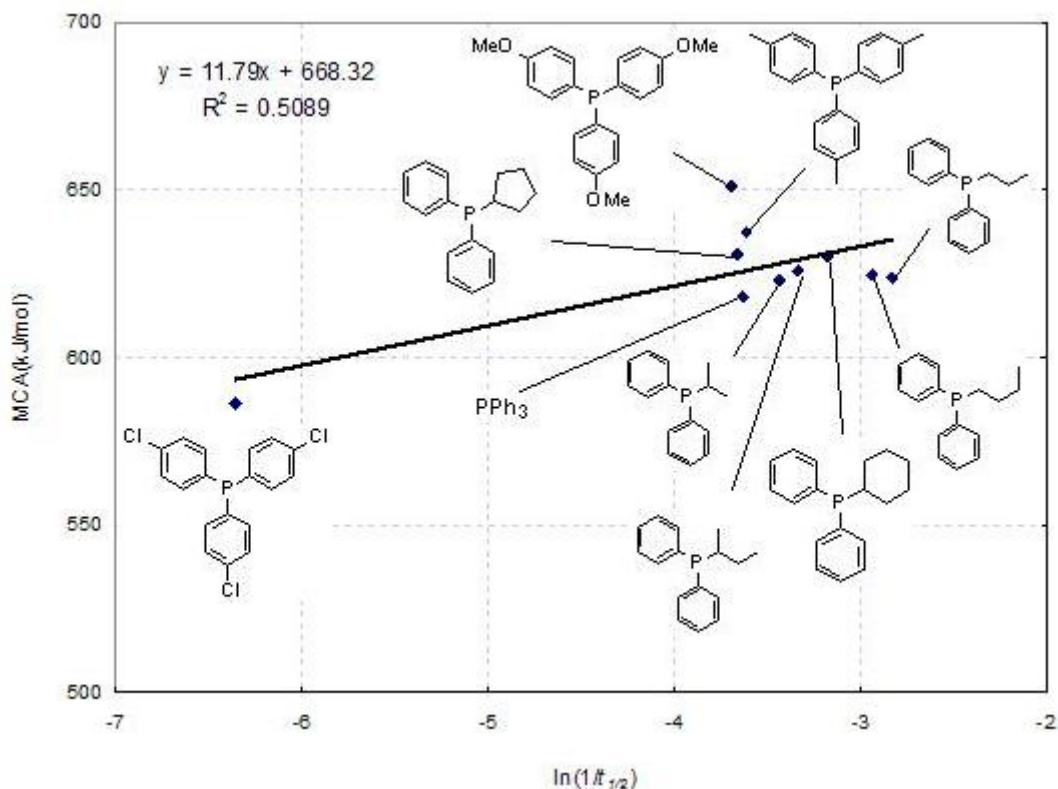
Figure 5. Correlation between the MCA values and relative reaction rates.

2.2.2 PPh$_3$-catalyzed aza-Morita-Baylis-Hillman reaction

The aza-Morita-Baylis-Hillman reaction (aMBH) can be mediated by nucleophilic Lewis bases such as phosphanes and tertiary amines in various solvents. The synergistic action of Lewis bases with Lewis or Brønsted acids is often employed

to accelerate the aMBH reaction. Polar and/or protic solvents are generally preferred to accelerate the MBH reaction due to the stabilization of the formed zwitterionic intermediates.[63] The very broad range of Lewis bases used in these reactions in combination with an equally broad range of solvents and acidic/protic co-catalysts suggests on first sight that no simple guidelines exists for efficient combinations of catalysts, co-catalysts and solvents. For the example of triphenylphosphane (PPh$_3$ (**2**)) as the Lewis base and *p*-nitrophenol (PNP) as the phenolic co-catalyst we show here that this is mainly due to large solvent effects, which substantially modify the effectiveness of Lewis basic catalysts and protic co-catalysts.

Currently available rate studies of the aMBH reaction indicate that reactions are first order in the Lewis base catalysts and the Michael acceptor. The reaction is between zero and first order on imine, depending on the used catalyst system and the concentration of the imine itself.[60,61,62] For the catalyst/co-catalyst combination of Ph$_3$P/PNP selected here we find that turnover curves can be fitted to a simple first-order rate law model in all cases. This implies that the reaction rate can be characterized by an effective rate constant k_{eff} or, equivalently, by an effective reaction half-life time $t_{1/2}$. The latter option is particularly helpful as approximate values of the reaction half-life time can also be obtained from visual inspection of turnover curves.

Table 10. Reaction half-life time $t_{1/2}$ (min) for the reaction shown in Figure 6.

Solvent	AN[b]	$t_{1/2}$ /min
d-Chloroform	23.1	38.1±0.1
d$_2$-DCM	20.4	83.1±1.3
d$_6$-DMSO	19.3	129.1±0.6
d$_7$-DMF	16.0	192.0±2.8
d$_8$-THF	8.0	628.2±6.0[a]

a) Determined using linear fit of turnover to reaction time
b) AN = Gutmann acceptor numer
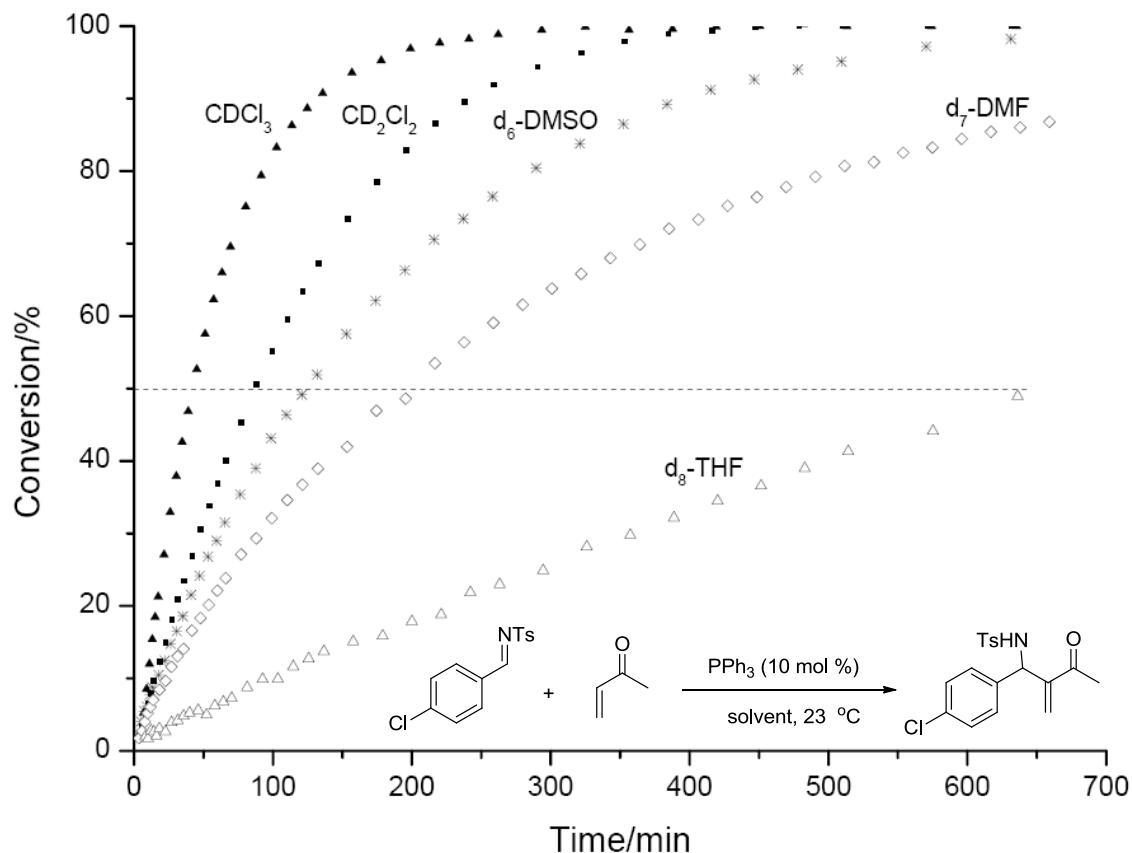
Figure 6. Turnover curves for the aMBH reaction of N-tosylimine **93c** with methyl vinyl ketone using PPh₃ (**2**) (10 mol %) as the catalyst in selected solvents.

First experiments were performed for the reaction of *p*-chlorotosylimine with methylvinyl ketone (MVK) using Ph₃P as catalyst in various aprotic solvents (Figure 6). The reaction proceeds swiftly in chloroform as a solvent with a reaction half-life time $t_{1/2}(CDCl_3) = 38.1$ min, while the reaction is much more sluggish in THF with $t_{1/2}(THF) = 628.2$ min. These solvent effects can be correlated with the electron-pair acceptor ability of the solvent as quantified by the Gutman acceptor number AN,[118] which is also known as solvent polarity-polarizability for aprotic solvents (Table 10). The faster reactions observed in chloroform (a solvent with good electron-pair acceptor ability) as compared to THF are compatible with the formation of (zwitterionic) enolate intermediates and their stabilization through dipole-dipole interactions with the surrounding solvent. A promising linear correlation between the Gutman acceptor number and reaction rates could be briefly expressed by the equation $\ln(1/t_{1/2}) = 0.1749AN - 7.9614$ ($R^2 = 0.945$, Figure 7). The effect that increasing the electron-pair acceptor ability of the solvent

increases the rate, was previously also observed in the epoxidation of alkenes.[119] At this stage we exclude protic solvents such as CH_3OH, whose mode of action may also involve hydrogen-transfer catalysis.
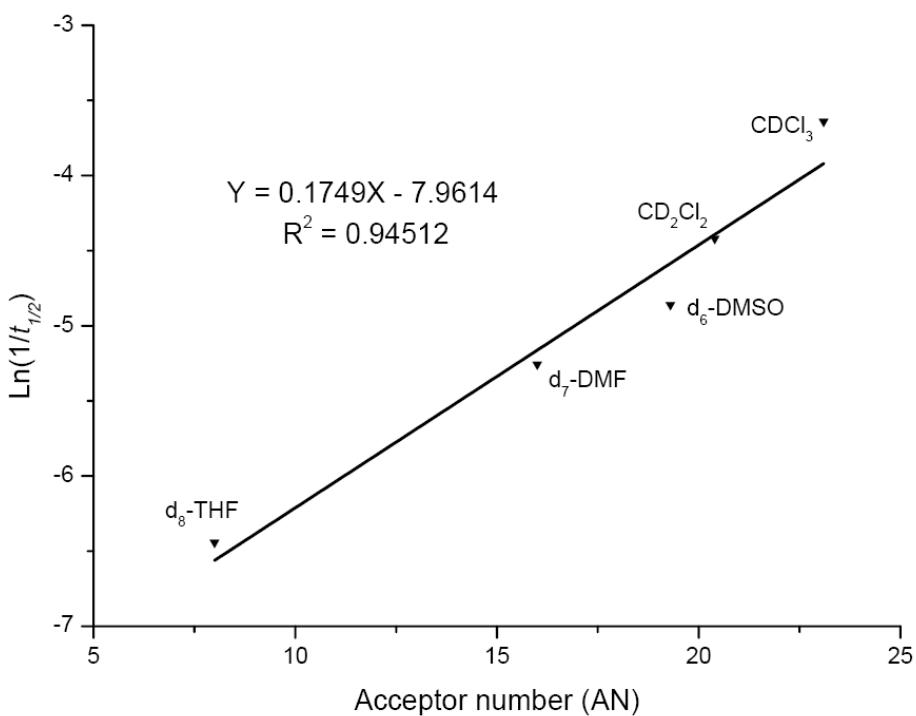
Figure 7. Correlation between the solvent acceptor number and relative reaction rates.

The aMBH reactions shown in Figure 6 can also be evaluated with initial rate methods (Figure 8, Table 11).[62] A similar linear correlation between the Gutman acceptor number and initial reaction rate r_{init} is obtained and can be expressed by the equation $\ln(r_{init}) = 0.1809AN - 4.0282$ ($R^2 = 0.9607$, Figure 9). This also testified that the solvent with good electron-pair acceptor ability could accelerate the aMBH reaction by stabilizing the zwitterionic enolate intermediatess through dipole-dipole interactions with the surrounding solvent.
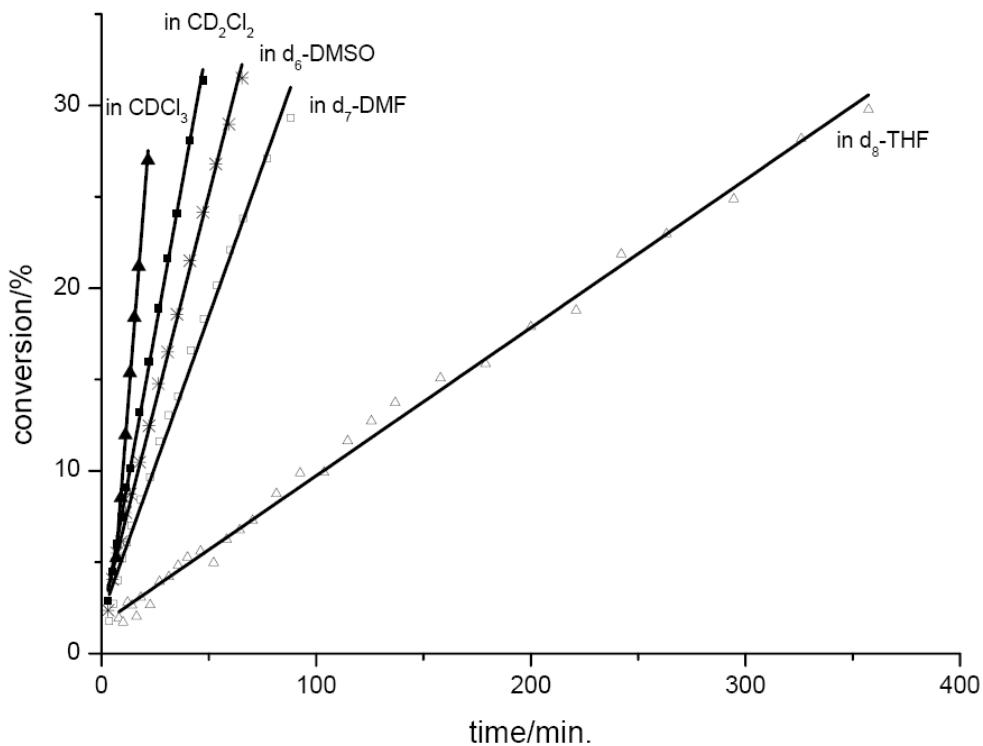
Figure 8. Initial rates r_{init} for the PPh$_3$-catalyzed aMBH reaction of N-tosylimine **93c** with MVK in selected solvents.

Table 11. Initial rates r_{init} for the reactions shown in Figure 8.

Solvent	AN	r_{init} (M/min)	Ln(r_{init} (M/min))
d-Chloroform	23.1	1.49064	0.399206
d$_2$-DCM	20.4	0.64525	-0.43812
d$_6$-DMSO	19.3	0.45995	-0.77664
d$_7$-DMF	16.0	0.32854	-1.1131
d$_8$-THF	8.0	0.081	-2.51331

As a second step in this study we analyzed the variation of the reaction rate as a function of the imine substitution pattern. In order to avoid the simultaneous influence of electronic and steric effects, we limit ourselves here to variations of the *para* substituents of the imine substrate in chloroform (CDCl$_3$) as the solvent (Figure 10).
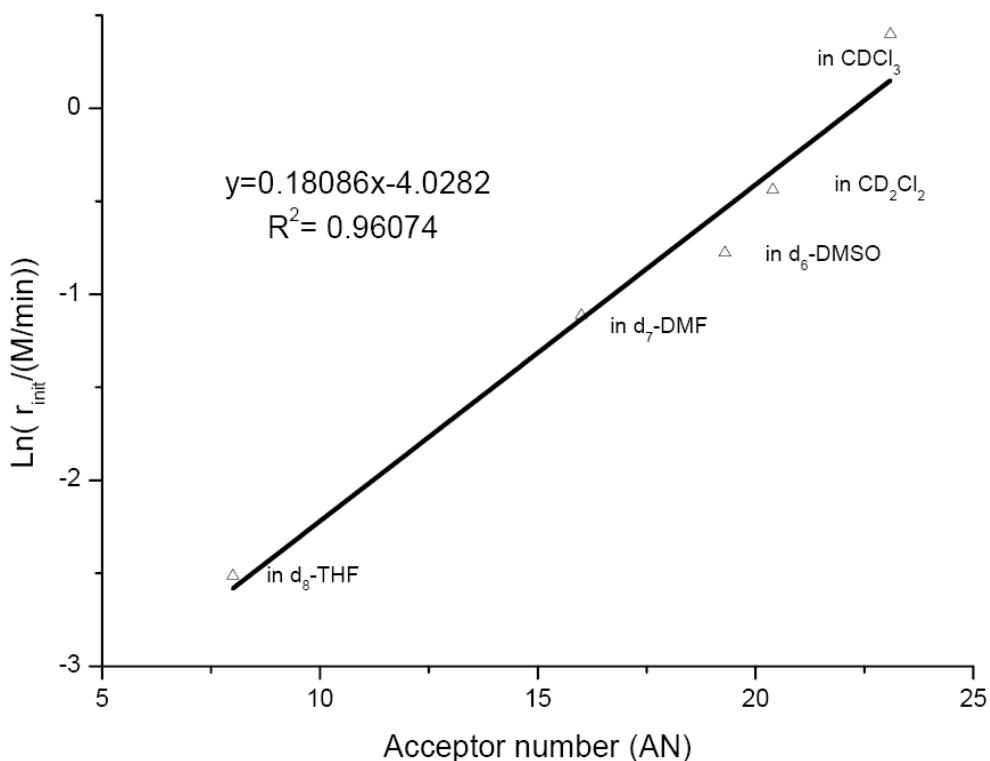
Figure 9. Correlation between the solvent acceptor number and initial reaction rates.

As expected for reactions involving nucleophilic attack on the imine substrate we observed here that the reaction rate for X = CN is significantly faster than for X = OMe. The turnover-curves could be fitted well to a simple first order rate law to give the effective rate constant k_{eff} as shown in Table 12. Therefore, the sensitivity of the reaction rate to the electronic substituent effect can most easily be characterized by the Hammett plot shown in Figure 11. Hammett plot reveals that positive ρ-value (0.68) is relatively small as compared to those observed in other reactions of imines.[120] And the rather poor quality (R^2 = 0.6718) of the Hammett correlation line is certainly not fully in line with expectation for the rate-limiting attack of the enolate nucleophile onto the imine substrate. Both of these indicate that proton transfer is indeed the most plausible rate-determining step.
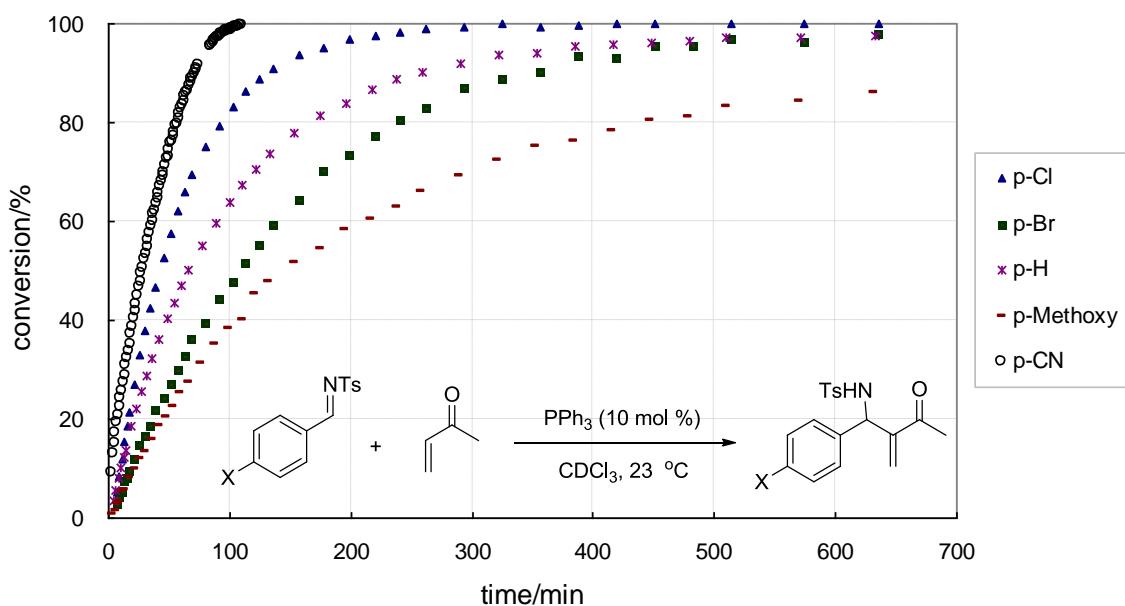
Figure 10. Turnover-curves for the aMBH reaction of tosylimines with MVK using PPh₃ (10 mol %) as catalyst in CDCl₃.
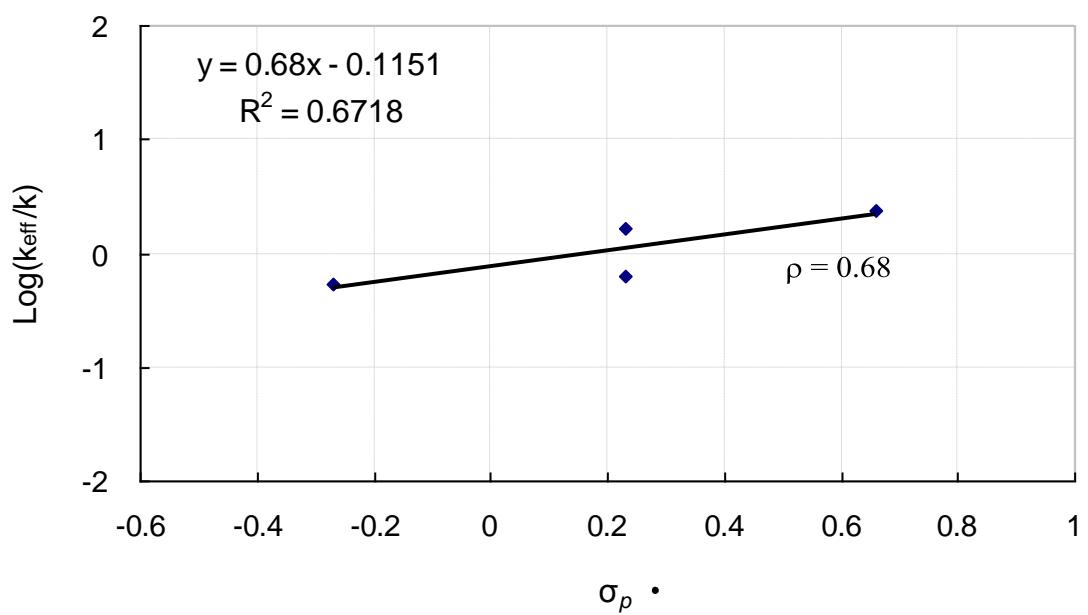
Figure 11. Hammett plot of PPh₃-catalyzed aMBH reactions of tosylimines with MVK in CDCl₃.

Table 12. The kinetic data for the Hammett plot of aMBH reactions shown in Figure 10.
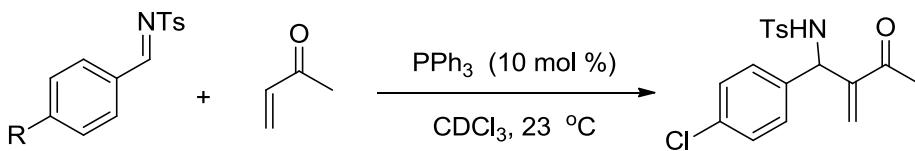
R	k_{eff} /(s^{-1})	Log(k_{eff}/k_H)	σ_p[121]
p-CN	0.02515	0.36752	+0.70
p-Cl	0.01818	0.22657	+0.24
p-Br	0.00670	-0.20695	+0.26
p-MeO	0.00580	-0.26959	-0.28
H	0.01079	0.00000	0.00

With the results for the Lewis base catalyzed reaction in hand we can now turn to the effect of protic co-catalysts. The effects of phenols as co-catalysts have repeatedly been studied in the past for synthetic purposes, in particular in cases involving chiral phenols based on the BINOL motif. The reaction of *p*-chlorotosylimine with MVK using Ph_3P as the catalysts was therefore studied in the presence of *p*-nitrophenol (PNP) in various concentrations (Figure 12).

The addition of small amounts of PNP (0-10 mol %) accelerates the reaction by a small margin, while higher concentrations are found to slow down the reaction considerably. This is best seen when plotting the reaction half-life $t_{1/2}$ against the imine/phenol ratio as shown in Figure 13. Repeating this type of measurement for solvents of lower Gutman acceptor number such as CD_2Cl_2 and THF-d_8 we can observe, that the rate acceleration is significantly larger now and peaks at much higher concentration as compared to $CDCl_3$. For THF as a frequently used solvent in asymmetric aMBH reactions the effects of added PNP are particularly pronounced with largest rate enhancements achieved at PNP/imine ratios of around 0.5. The successful use of chiral phenols in asymmetric aMBH reactions is thus accompanied by a large rate acceleration through these additives, an effect not necessarily found in chloroform or DCM. This also implies that catalyst/co-

catalyst systems optimized for one particular organic solvent will not necessarily be effective in other reaction media.
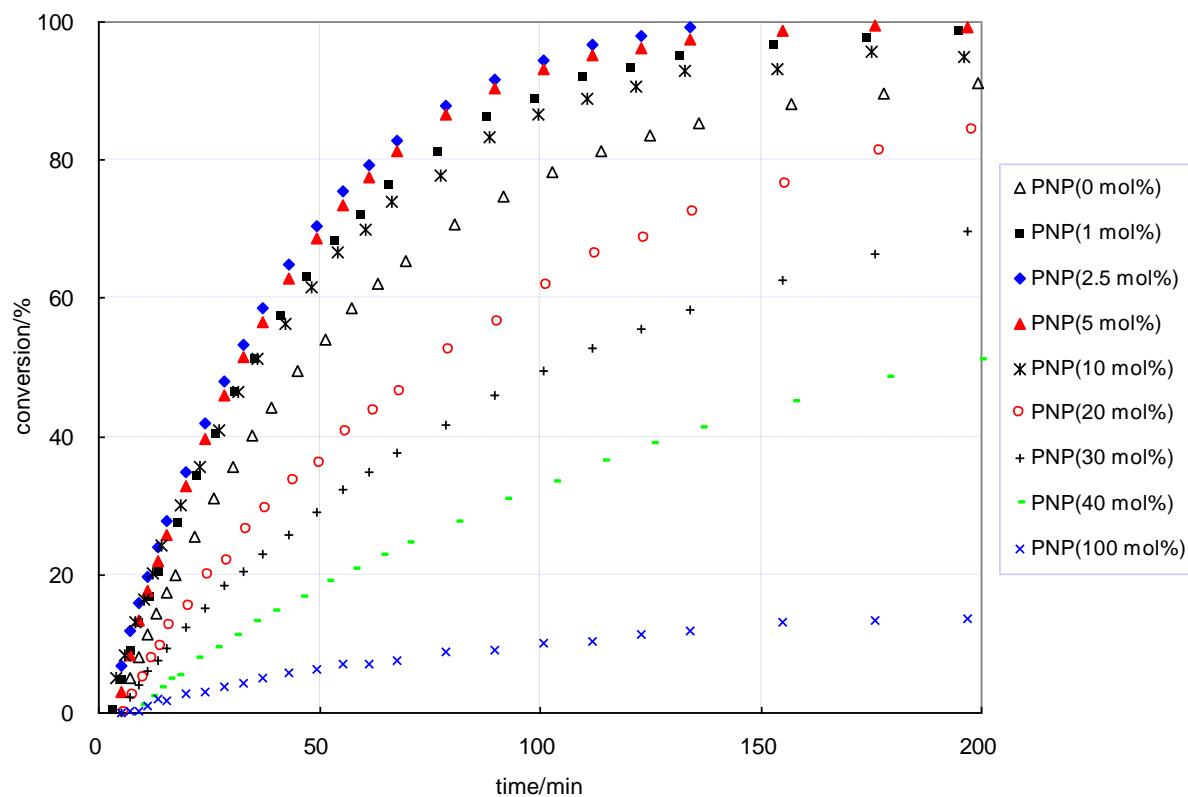

Figure 12. Turnover-curves for the PPh_3 (10 mol %) catalyzed aMBH reaction of tosylimine **93c** with MVK (120 mol %) in the presence of various concentrations of PNP in $CDCl_3$.

Table 13. Reaction half-life times $t_{1/2}$ (min) for the reaction shown in Figure 13.

PNP(x mol/%)	$t_{1/2}$[min] in $CDCl_3$	$t_{1/2}$[min] in CD_2Cl_2	$t_{1/2}$[min] in d_8-THF
0	38.1±0.1	83.1±1.3	628.2±6.0
1	30.0±0.2	-	-
2.5	27.0±0.4	60.1±1.0	-
5	27.1±0.2	59.2±0.9	-
10	32.0±0.3	58.4±0.1	300±3.5
20	63.8±0.9	111.1±1.8	153.7±2.3
30	101±0.6	288.8±10.9	-

40	200±0.9	-	-
50	-	2603.3±107.2	100.1±1.4
70	-	-	102.7±1.1
100	1184.2±63.8	4402.6±581.5	111.1±0.2
120	-	-	195.8±3.5
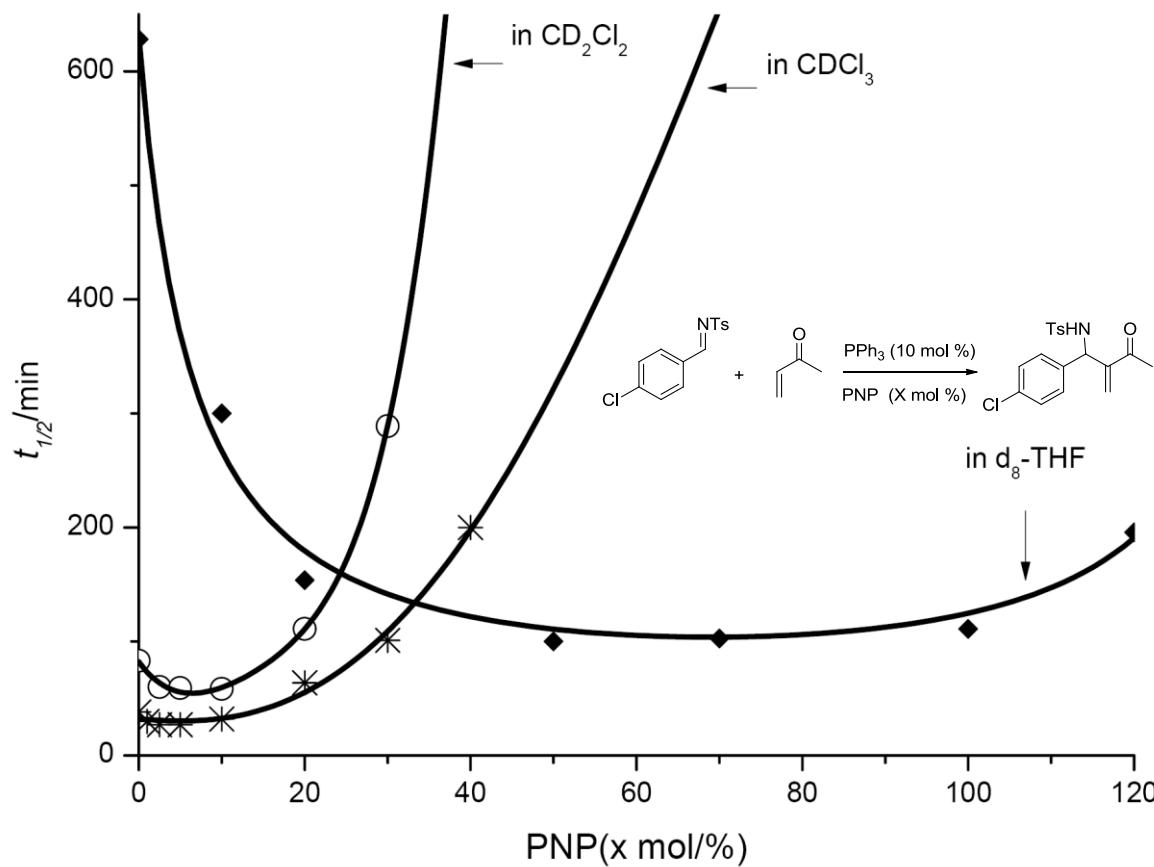
Figure 13. The effect of PNP on relative rates of PPh$_3$ (10 mol %)-catalyzed aMBH reaction of tosylimine **93c** with MVK (120 mol %) in CDCl$_3$, CD$_2$Cl$_2$, or d$_8$-THF.

With the interdependent effects of solvent and co-catalyst in hand, we carried out a series of control reactions of PPh$_3$, MVK and PNP in different solvents to discover the correlation of solvent and co-catalyst. As shown in Figure 14, the ^{31}P NMR spectrum of the reaction of PPh$_3$, MVK and PNP in CDCl$_3$ showed a new signal at +25.93 ppm in addition to the signal of PPh$_3$ at -4.38 ppm. This new peak was assigned to be phosphonium intermediate **140**. By comparing the integrals of

the two ^{31}P NMR signals, the yield of the phosphonium intermediate **140** could be easily calculated.
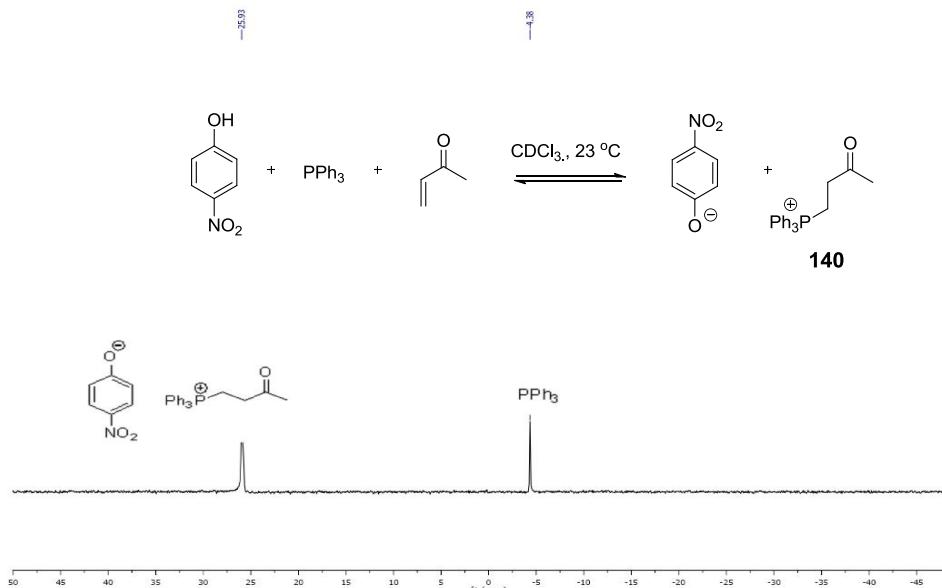
Figure 14. The ^{31}P NMR spectrum of the reaction of PPh$_3$, MVK and PNP in CDCl$_3$.
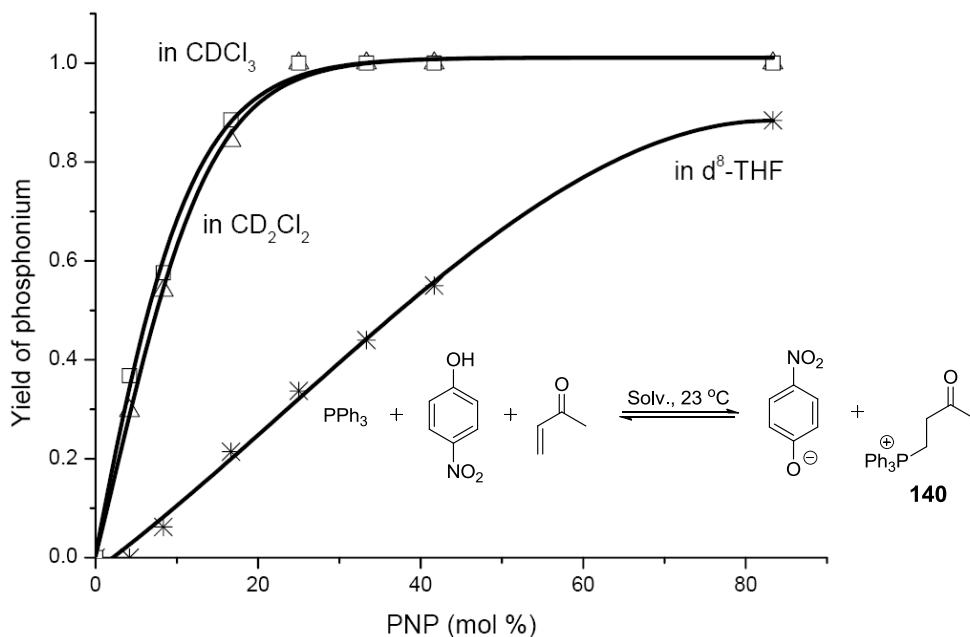
Figure 15. The yield of phosphonium ion **140** in the reaction of PPh$_3$ (8.33 mol%), PNP(X mol%), MVK (0.15 M) in CDCl$_3$ CD$_2$C$_2$ and d$_8$-THF based on ^{31}P NMR.

With the variations of the concentration of PNP, the reactions were carried out in different solvents. And the yields of the phosphonium intermediate for different concentrations of PNP in d$_8$-THF, CD$_2$Cl$_2$ and CDCl$_3$ were obtained and are shown

in Figure 15. It was observed that the enolate generated from the Michael addition of PPh$_3$ and MVK would be more easily protonated by PNP in CDCl$_3$ and CD$_2$Cl$_2$ as compared with in d_8-THF (Figure 15). The reaction of PPh$_3$, MVK and PNP will be discussed in more detail in chapter 2.3.1. In the ^{31}P NMR spectrum of the reaction of p-chlorobenzaldehyde, PPh$_3$, MVK and PNP, no other signals were detected in addition to the two peaks shown in Figure 14. This implies that the co-catalyst can also interfere the MBH reaction with a manner of keeping the catalyst in a "resting state".

One example for the combined effects of co-catalyst and solvent is shown in Scheme 41. Catalyst **79** can be thought of as assembled from PPh$_3$ and one equiv. phenol, which worked more effectively in THF than in CH$_2$Cl$_2$ (76 % vs 38 %). This result can be rationalized well by the results shown in Figure 15: the hydroxyl group in **79** played a vital role in the chirality transfer from catalyst to product, but it would also play another role to quench this reaction by intramolecular proton transfer, which is easier in CH$_2$Cl$_2$ than in THF.

THF: 76 %, 88 % ee
CH$_2$Cl$_2$: 38 %, 82 % ee
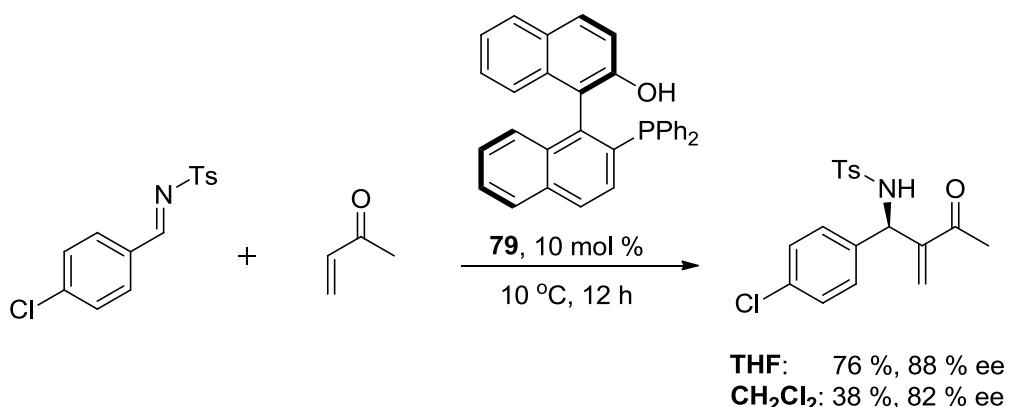
Scheme 41. Bifunctional catalyst **79** catalyzed aMBH reaction reported by Shi.[83]

In summary, the aza-Morita-Baylis-Hillman (aMBH) reaction has been studied in a variety of solvents and with a broad selection of catalysts and co-catalysts. From the results it is clearly apparent that the effects of solvent and co-catalysts are strongly interdependent. These results are most easily reconciled in a mechanistic model involving the reversible protonation of zwitterionic intermediates of the catalytic cycle as shown in Scheme 25.

2.2.3 Bifunctional phosphane catalysts

In chapter 2.2.2, the Brønsted acid co-catalyst effect in the aMBH reaction has been discussed. In this chapter, we prepared a new family of bifunctional catalysts by combining Lewis basic centers and Brønsted acid moieties, and tested their application in the aMBH reactions.

2.2.3.1   Synthesis of bifunctional phosphane catalysts

Based on the reported bifunctional phosphane catalyst systems, we designed a new family of bifunctional phosphane catalysts (BPC) by anchoring a tunable Brønsted acid group to the triphenylphosphane framework. Varying the amide group, a series of Brønsted acids with different acidities could be installed into these BPCs. These bifunctional phosphane catalysts (BPC) could be prepared by the coupling of compound **110** with acid chlorides or anhydrides (equation 2).
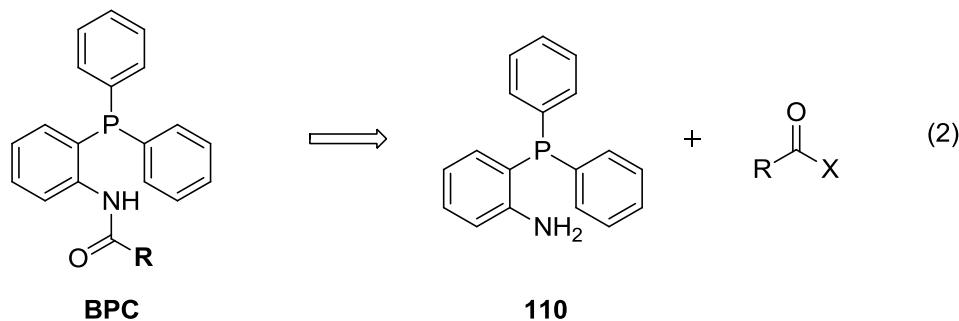
We first prepared BPC1 with cheap starting materials. The pivaloyl-protected aniline **111** was *ortho*-metalated with butyl lithium and subsequently treated with chlorodiphenylphosphane to give BPC1 in 59 % yield. The crystal structure is shown in Figure 16, in which the amide shows Z-configuration and the hydrogen in the amide group points to the phosphorus center. Depivaloylation of BPC1 to access aminophosphane **110** was, unfortunately, not successful, neither under basic nor acidic conditions (Scheme 42).
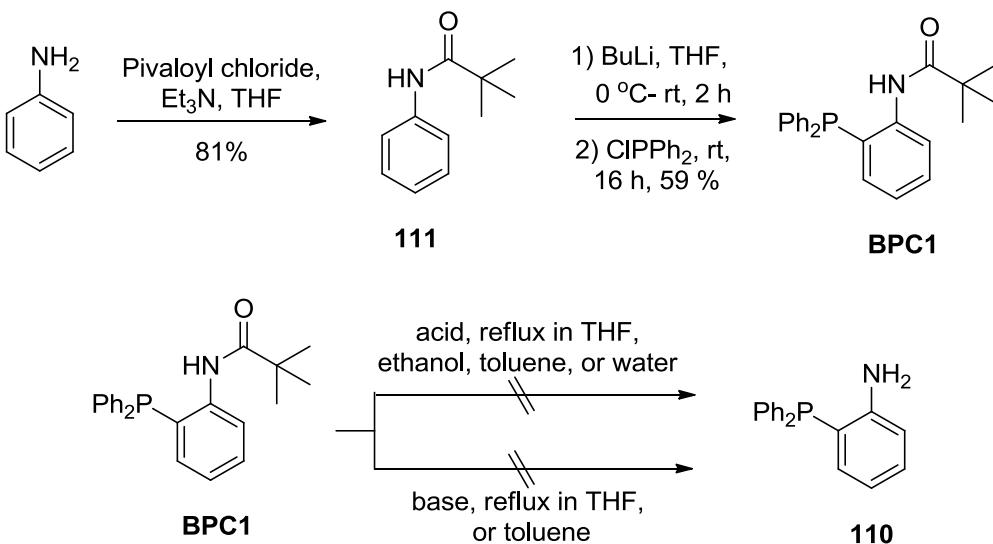
Scheme 42. Synthesis of BPC1 and compound **110**.
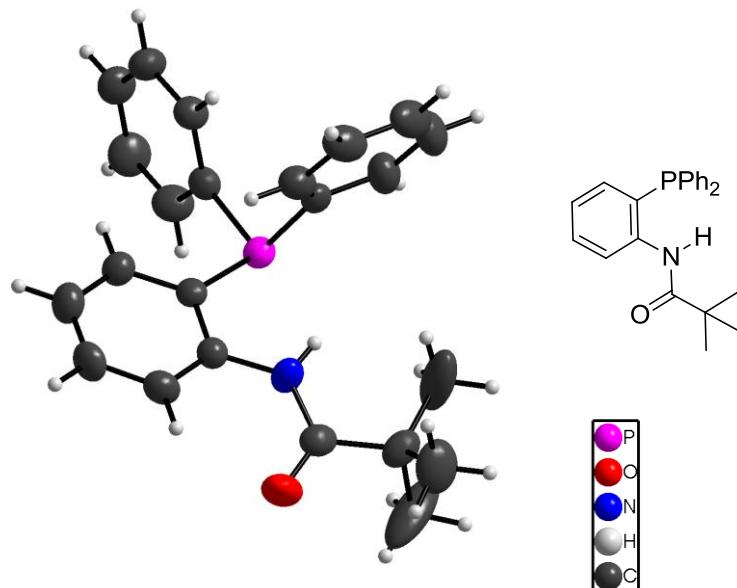
Figure 16. Crystal structure of BPC1.

The synthesis of compound **110** was subsequently accomplished by Stelzer's method,[122] with the coupling of 2-iodoaniline with diphenylphosphane. 2-Diphenyl-phosphinoaniline **110** was obtained with 83 % yield (Scheme 43).
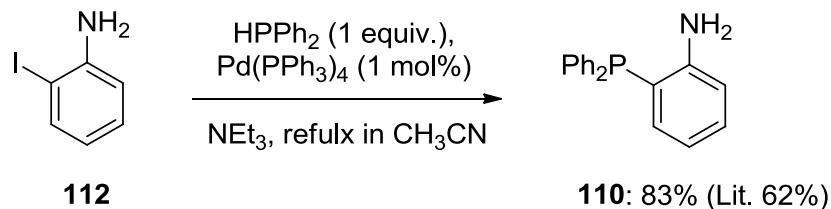

Scheme 43. Synthesis of 2-diphenylphosphinoaniline **110**.

With 2-Diphenylphosphinoaniline **110** in hand, we carried out a series of acylation reactions to prepare bifunctional phosphane catalyst (BPC1-9) as shown in the synthesis protocol in Scheme 44.

R= Me,   **BPC2**, 61 %
R= Ph,   **BPC3**, 72 %
R= CF$_3$,   **BPC4**, 35 %
R= *p*-MeOPh, **BPC5**, 40 %

R= *p*-CNPh, **BPC6**, 37 %
R= *i*Pr,   **BPC7**, 35 %
R= *m,m*-diMeOPh, **BPC8**, 51 %

BPC9, 33 %

79, Shi's catalyst
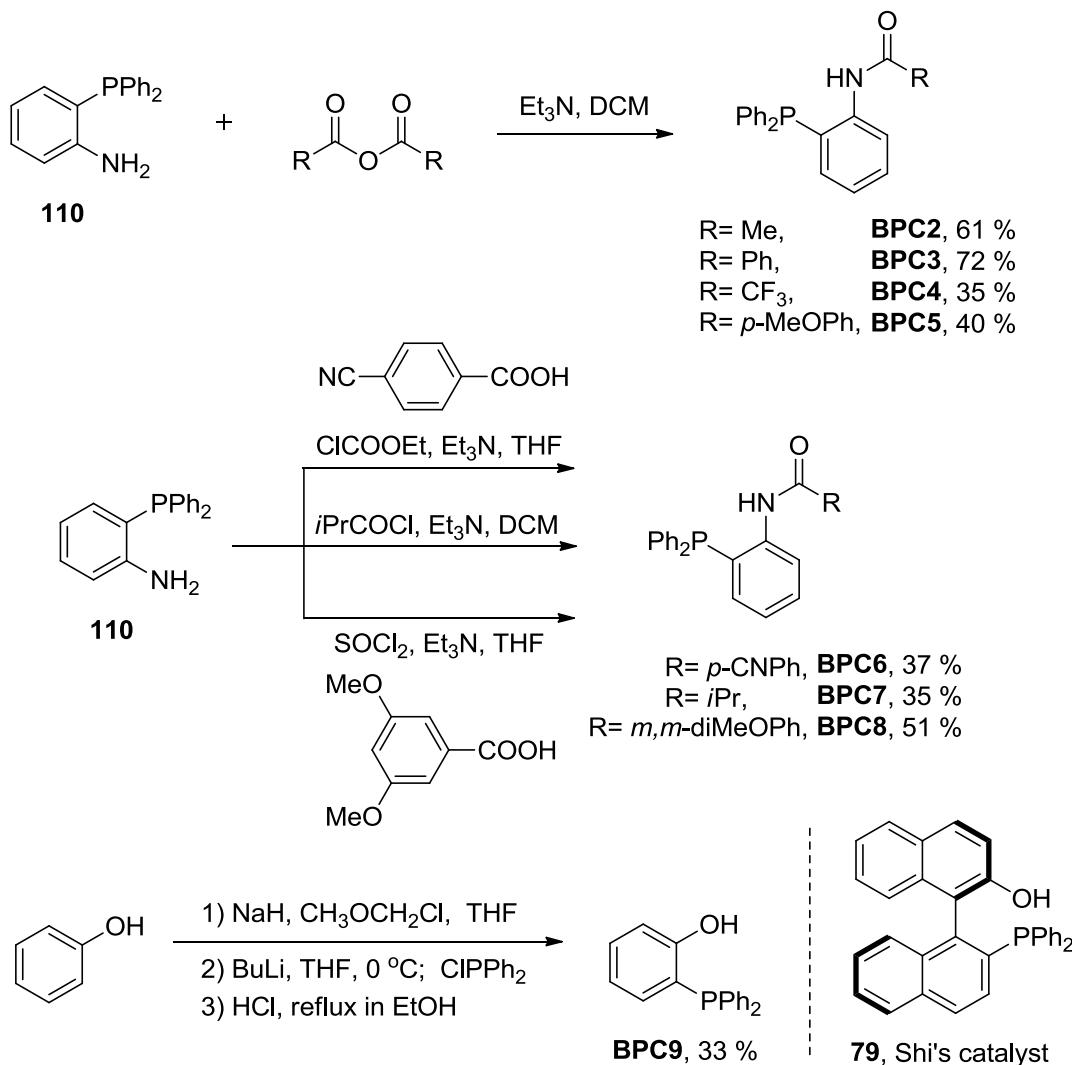
Scheme 44. Synthesis of bifunctional phosphane catalysts (BPC1-9).

Bifunctional phosphane catalysts BPC2-5 were prepared by the acylation of **110** with the corresponding acid anhydrides. For the less reactive m,m-dimethoxy homolog, the acid chloride was first made with thionyl chloride for the further amidation to BPC8. To introduce the acyl group with increased steric hindrance (iPrCOCl, BPC7), the respective acid chlorides were employed. When electron-deficient *p*-cyanobenzoic acid chloride was used in this reaction, there was no desired product formed, but instead only the phosphane oxide was isolated. *p*-Cyanobenzoic acid was therefore treated with ethyl chloroformate to form the mixed anhydride *in situ*, which furnish BPC6 in 37 % yield after the reaction with

110. Starting from phenol, after protection with MOMCl, *ortho*-metalation with butyl lithium, quenching with chlorodiphenyl-phosphane and deprotection with HCl in a one-pot reaction, we also get BPC9, with a hydroxyl group near the Lewis base center, which could be thought as a version of Shi's catalyst **79** (Scheme 44).
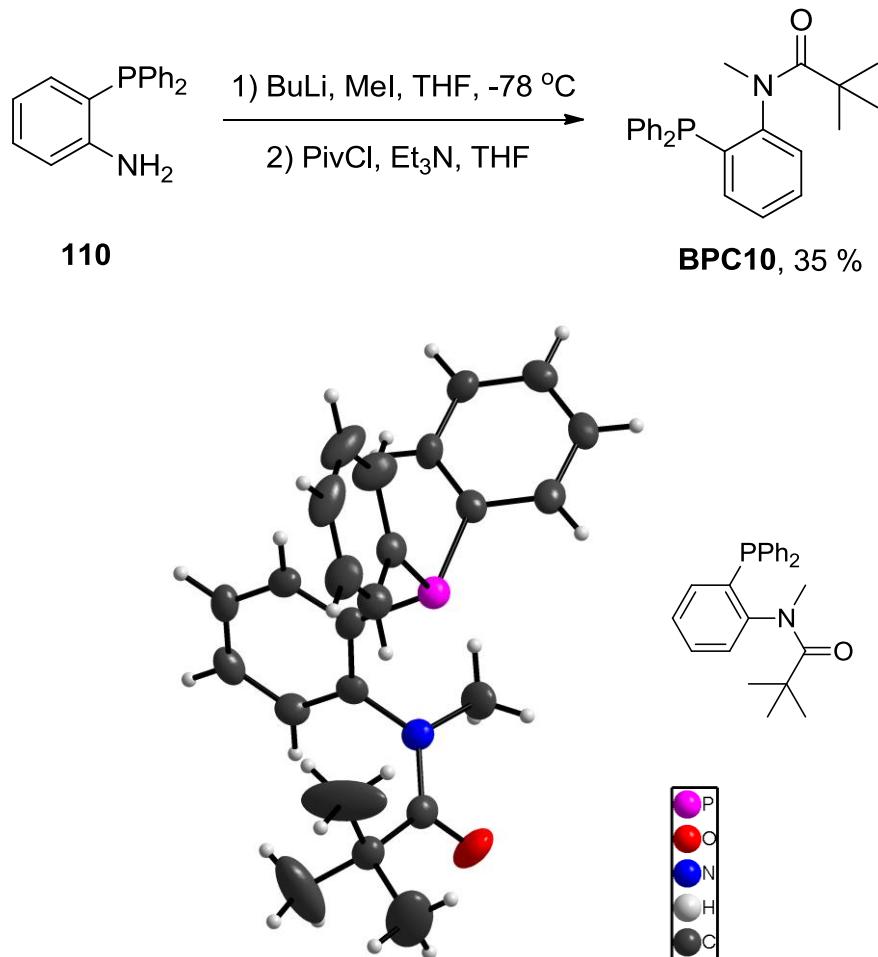
Scheme 45. Synthesis and crystal structure of BPC10.

To explore the role of hydrogen donor in BPCs catalyzed aMBH reactions, we also synthesized BPC10, in which the hydrogen in the N-H group was replaced with a methyl group. After deprotonation of the amino group on **110** with butyl lithium, methyl iodide and pivaloyl chloride were added subsequently to obtain the desired product BPC10 with 35 % yield. The crystal structure is also shown in Scheme 45, in which the amide shows E-configuration and the methyl group in the amide group points to the phosphorus center. This can increase the steric hindrance to the phosphane Lewis base center.

2.2.3.2 Application in aza-Morita-Baylis-Hillman Reactions

With these bifunctional phosphane catalysts in hand, we explored their catalytic performance in the benchmark aMBH reaction of *p*-chlorotosylimines with methyl vinyl ketone. The results are shown in Table 14 and Figure 17.

Table 14. Aza-MBH reaction of N-tosylimine **93c** with MVK in the presence of bifunctional phosphane catalysts
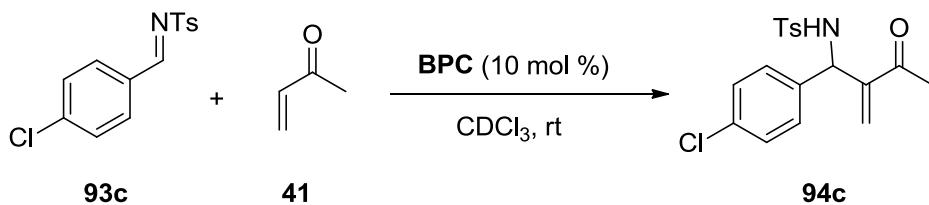
Entry	Lewis base	Time/h	Conversion/%[a]	Half life/min
1	PPh₃ (**2**)	4	99	38.1±0.1
2	R = pivaloyl, BPC1	5	98	71.7±0.6
3	R = Me, **BPC2**	**2**	**99(91)[b]**	**12.4±0.3**
4	R = Ph, BPC3	4	99	33.4±0.2
5	R = CF₃, BPC4	10	8	-
6	R = *p*-MeOPh, BPC5	4	99	38.1±0.1
7	R = *p*-CNPh, BPC6	4	99	25.8±0.1
8	R = *i*Pr, BPC7	2	99	16.6±0.1
9	R = *m,m*-diMeOPh, BPC8	6	98	37.4±0.5
10	BPC9	8	12	-
11	BPC10	10	2	-

a) Determined by ¹H NMR. b) Isolated yield. c) 0.125 M imine, 1.2 equiv. MVK.

With 10 mol % catalyst loading, the aMBH reaction proceeded very effectively with up to 99 % conversion (entry 1-4, 6-9). The best result was achieved with BPC2, which gives 99 % conversion in 2 hours. BPC4 showed very poor reactivity (10 h, 8 % conversion). BPC9, which was thought to be similar to Shi's catalyst **79**,

showed just a slightly higher catalytic activity (8h, 12 % conversion) as compared with BPC4.

The turnover plots (Figure 17) can be fitted well to a simple first order rate law equation, thus the half life time $t_{1/2}$ was determined to evaluate the catalytic performance of BPCs. BPC2 with acetamide as a hydrogen donating group gave the best result (12.4 min.) BPC7 with isobutyramide (16.6 min), BPC6 with benzamide (25.8 min) and BPC3 (33.4 min) showed better performance than PPh_3. Similar reactivity to PPh_3 was determined with BPC5 and BPC8, which have less acidic amide groups. BPC1 with a pivaloyl amide group was less reactive than PPh_3 by a factor of 2, probably due to steric effects from the bulky pivaloyl group.

Surprisingly, for BPC10, in which the amide proton was replaced with methyl group, there was almost no reactivity observed, reflecting the importance of the acidic proton of the amide group for catalytic activity in aMBH reaction. Blocking this proton with methyl group in BPC10 diminished the catalytic activity completely, and this amplified the crucial role of a proton donating group in accelerating the aMBH reaction.
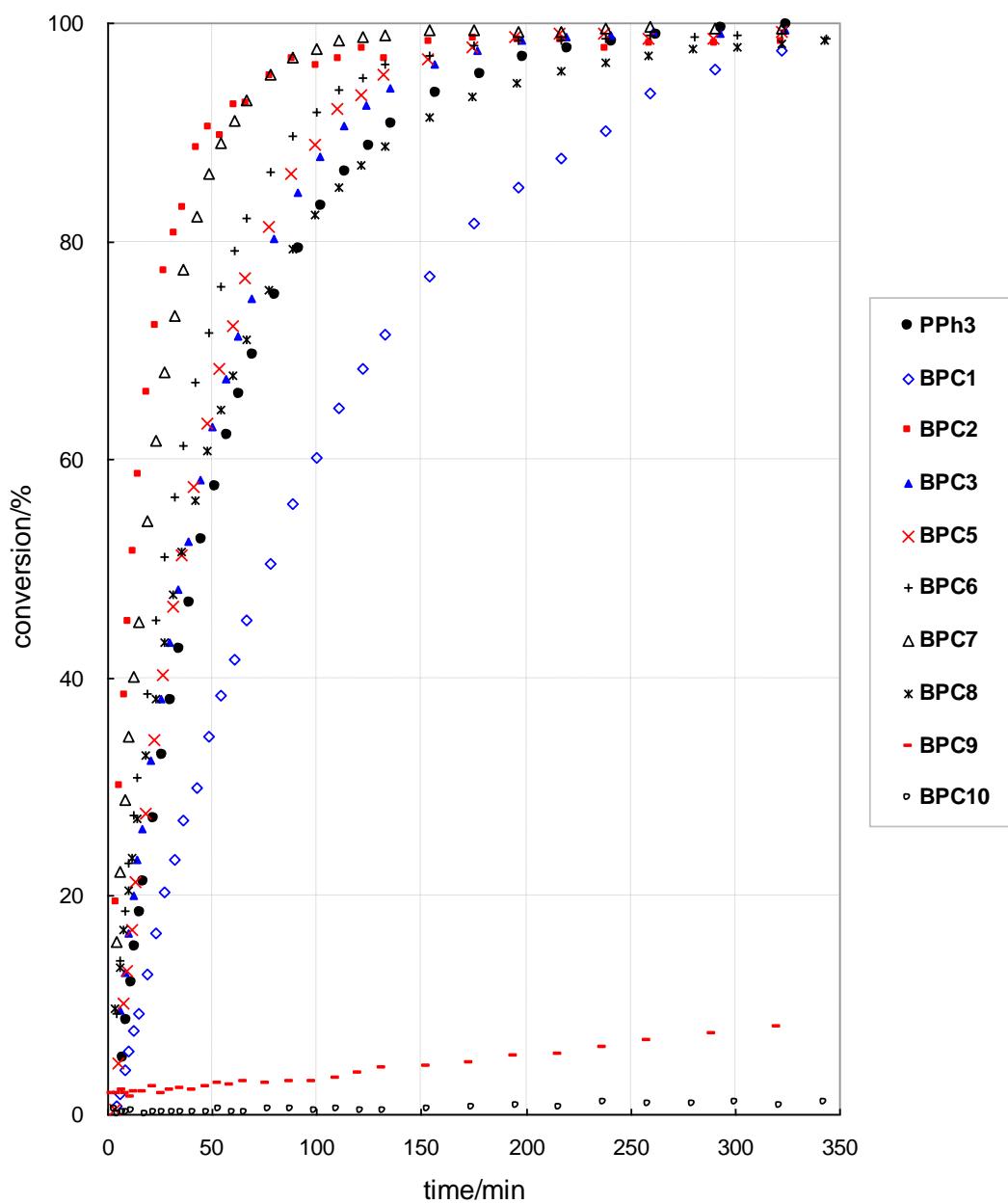
Figure 17. Turnover plots of bifunctional phosphane-catalyzed aMBH reaction in CDCl$_3$.

To clarify the different reactivities of BPCs, we carried out a series of ^{31}P NMR measurements. ^{31}P NMR spectroscopy was measured during the aMBH reaction to follow the catalytic cycle and identify possible intermediates.
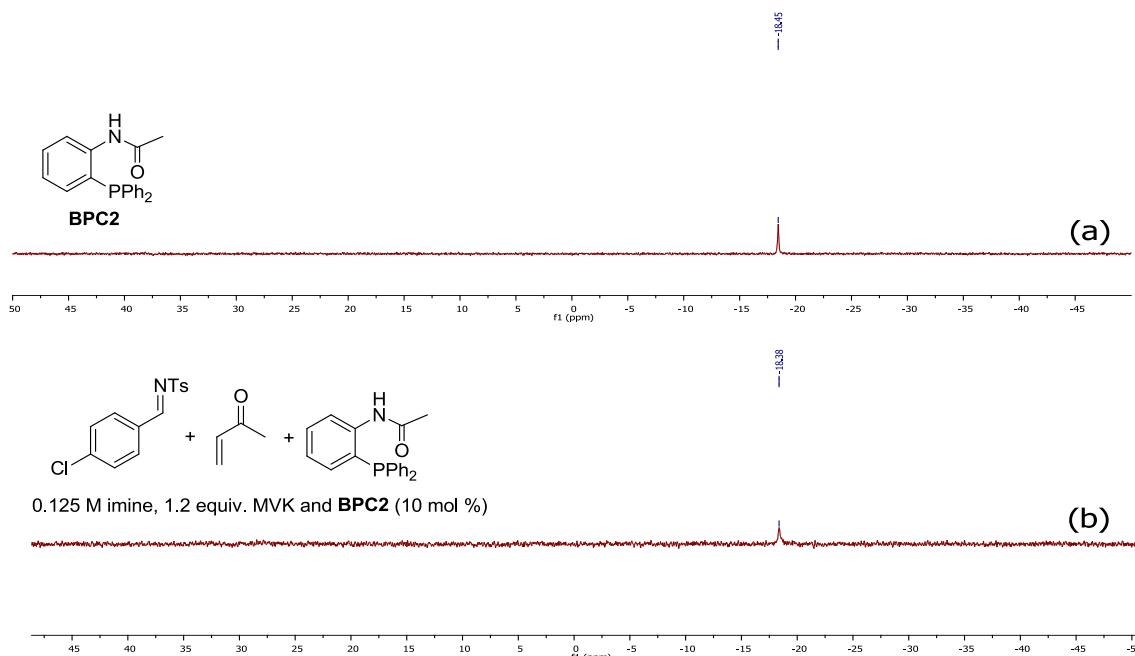
Figure 18. The ^{31}P NMR of the BPC2-promoted aMBH reaction in CDCl$_3$.

The ^{31}P NMR spectroscopy of BPC2 in CDCl$_3$ was first measured to obtain a peak at -18.46 ppm (Figure 18a). In the BPC2 promoted aMBH reaction of tosylimine with methyl vinyl ketone, only one peak at -18.38 ppm was observed throughout from ^{31}P NMR spectroscopy (Figure 18b). This signal is identical to that of the catalyst BPC2 alone, which reflects that there are no other obvious phosphine intermediates emerged in the reaction.

In the BPC6-promoted aMBH reaction of tosylimine with methyl vinyl ketone, in addition to the peak of BPC6 at -19.58 ppm, a new peak at +23.32 ppm was observed in the ^{31}P NMR, which is assigned to intermediate **113** (Figure 19b, Scheme 46). This finding reflected that part of the catalysts stayed in the "resting state", which can explain that BPC6 is less reactive in MBH reaction as compared to BPC2.

In the BPC4-promoted aMBH reaction, the peak of BPC4 at -20.94 ppm disappears, and a new peak at + 24.04 ppm is observed in the ^{31}P NMR spectrum, which is assigned to intermediate **114** (Figure 20b, Scheme 46). This reflected that all the catalyst stayed in the "resting state", which is responsible for the low catalytic efficency of BPC4 in aMBH reactions.
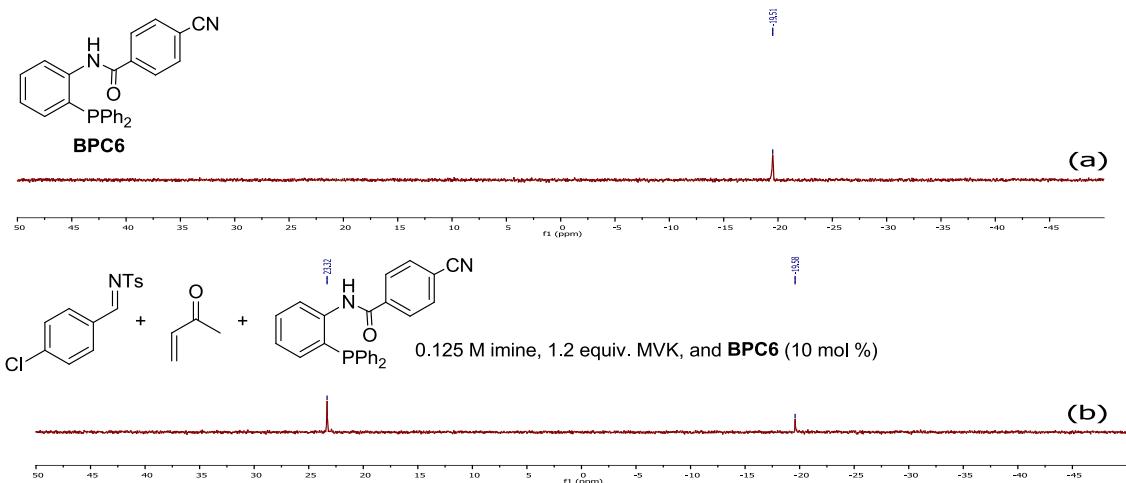
Figure 19. The ^{31}P NMR of the BPC6-promoted aMBH reaction in CDCl$_3$.
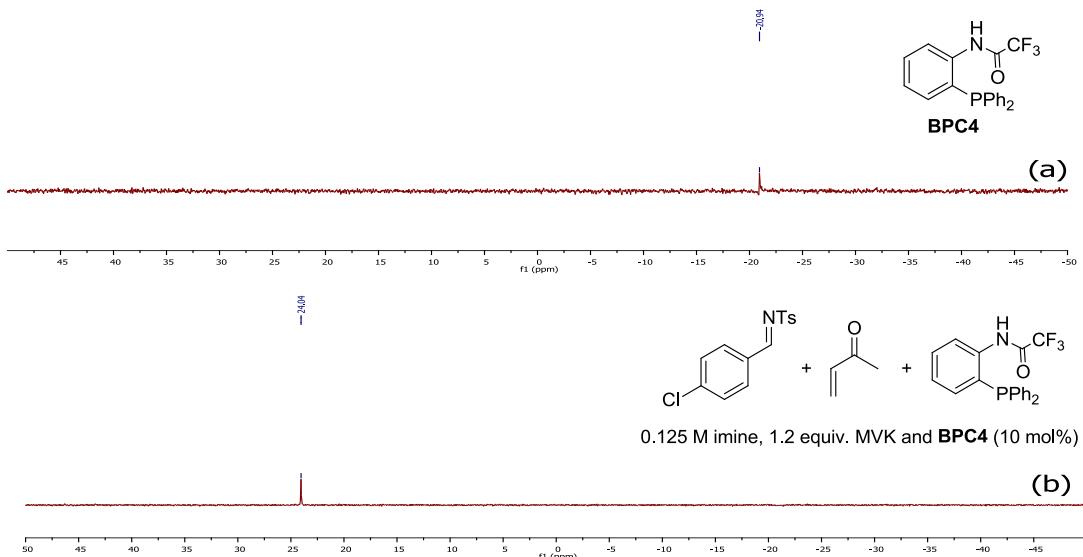

Figure 20. The ^{31}P NMR of the BPC4-promoted aMBH reaction in CDCl$_3$.

In the BPC9-promoted aMBH reaction, a similar result as for BPC4 was observed: the peak at -27.93 ppm disappears, and a new peak at +22.33 ppm is detected in the ^{31}P NMR spectrum, which was believed to be intermediate **115** (Figure 21, Scheme 46). A similar catalytic reactivity was also observed for BPC9 as for BPC4.
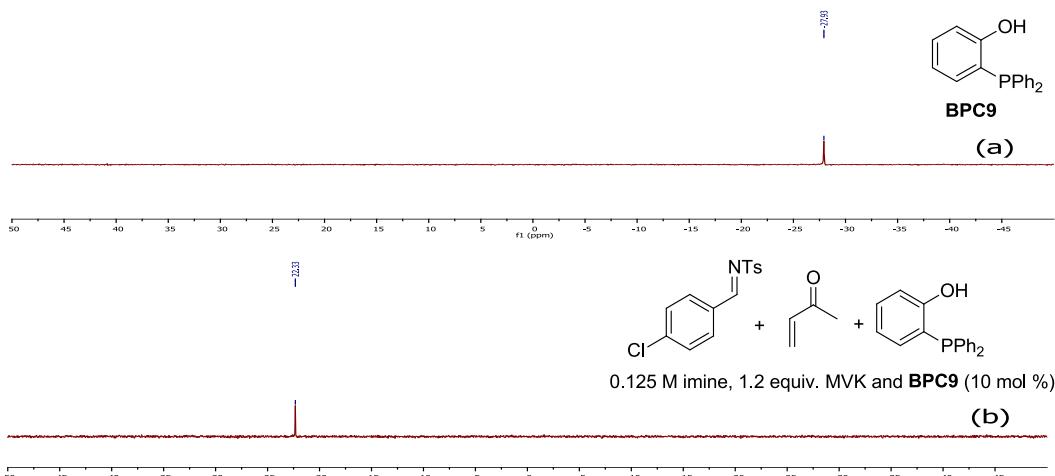
Figure 21. The ^{31}P NMR of the BPC9-promoted aMBH reaction in CDCl$_3$.
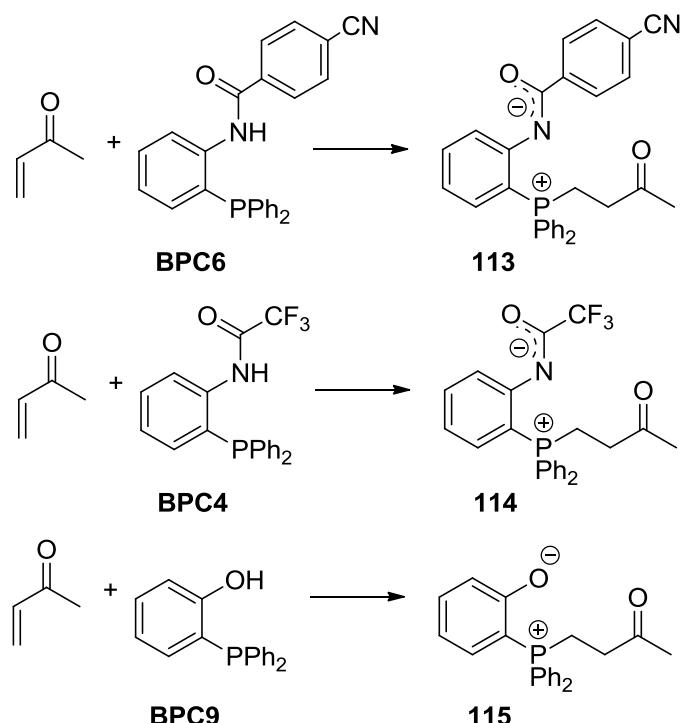
Scheme 46. Reaction intermediates formed in the BPC6, 4, 9-assisted aMBH reaction.

The type-115 intermediate was also observed in the reaction of PPh$_3$, MVK and PNP in CDCl$_3$ as shown in Figure 14. The characterization of type-115 protonated intermediates will be described in detail in chapter 2.3. With all these ^{31}P NMR data and the catalytic performance of BPCs in hand, we can draw the conclusion that: (1) a properly placed intramolecular proton donor is essential for the

69

acceleration of aMBH reactions. (2) proton donors with high acidity will slow down this reaction, by the generation of protonated intermediates, such as **113**-**115**.

In chapter 2.2.2, it was demonstrated that the effects of co-catalyst are strongly interdependent with solvents. It could thus be possible that the BPCs, which did not work properly in CHCl$_3$, would be more effective in some other solvents. The co-catalyst effect was also tested in the BPC-promoted aMBH reaction, the results are shown in Table 15. For BPC2 (5 mol % loading and 5 mol % PNP), there was almost no additive effect. A negative additive effect was detected for BPC8. These findings illustrate that an intermolecular hydrogen donor was not necessary any more to accelerate the reaction in the presence of an intramolecular hydrogen bond.

Table 15. Aza-MBH reaction of tosylimine **93c** with MVK assisted by bifunctional phosphane catalysts and co-catalyst.
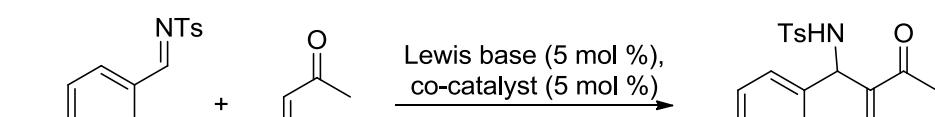
Entry	Lewis base	Co-catalyst	Time/h	Conversion/%[a]	Half life/min
1		BPC2	none	4	99	22.4±0.4
2		BPC2	PNP	4	99	23.7±0.4
3		BPC5	none	5	98	57.1±0.6
4		BPC8	none	5	97	56.7±1.2
5		BPC8	PNP	5	92	70.7±0.5

a) Determined by ^{1}H NMR. b) 0.125 M imine, 1.2 equiv. MVK.

The scope of the BPC2-catalyzed aMBH reaction was investigated by examining a variety of electrophiles (Table 16). For electron-deficient imines, the system is very efficient: most of the electron-deficient imines react rapidly with excellent

conversion (up to 98 %, entry 1-5). Still reasonable conversions for electron-rich and aliphatic imines (91 % and 94 % conversion in 4 hours) were also achieved.

Table 16. Aza-MBH reaction of N-tosylimines with MVK in the presence of bifunctional phosphane catalyst BPC2.
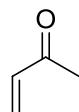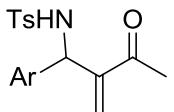

Entry	Ar	Time/min	Conversion/%[a]
1	p-CNC$_6$H$_5$	15	98
2	p-NO$_2$C$_6$H$_4$	15	97
3	p-ClC$_6$H$_4$	120	95
4	o-ClC$_6$H$_4$	120	98
5	p-BrC$_6$H$_4$	120	95
6	C$_6$H$_4$	120	94
7	p-MeOC$_6$H$_4$	240	91
8	trans-Ph-CH=CH-	240	94

a) Determined by ^{1}H NMR. b) 0.125 M imine, 1.2 equiv. MVK.

2.2.3.3 Application in Morita-Baylis-Hillman Reactions

Given the excellent performance of BPCs in aMBH reactions we next turned our attention to the Morita-Baylis-Hillman (MBH) reaction, which could also be accelerated by protic additives, such as PNP or octanol as reported.[59] The reaction of p-chlorobenzaldehyde with methyl vinyl ketone (MVK) was selected as the benchmark reaction. To a solution of p-chlorobenzaldehyde (0.4 M), PPh$_3$ (0.08 M), trimethoxybenzene (0.125 M) and PNP (0.12 M) in THF, was added MVK (1.2 M) at rt. At appropriate time intervals 10 µL of the reaction mixture was diluted into 1.5 mL of DCM for GC analysis. The disappearance of the minor starting material (aldehyde) was monitored by GC to follow the reaction.

Table 17. MBH reaction of *p*-chlorobenzaldehyde with MVK assisted by BPC catalysts and PNP as co-catalyst.
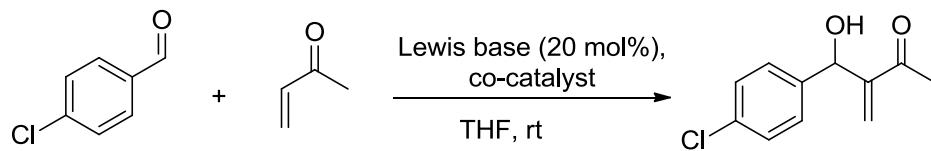
Entry	Lewis base	Cocatalyst	Time/h	Conversion/%[a]
1	PPh$_3$	none	15	19
2	PPh$_3$	PNP(15 mol%)	20	56
3	**PPh$_3$**	**PNP(30 mol%)**	**20**	**60**
4	PPh$_3$	PNP(50 mol%)	22	51
5	PPh$_3$	PNP(100 mol%)	20	6

Entry	Lewis base	Cocatalyst	Time/h	Conversion/%[a]
6	BPC1	none	22	64
7	**BPC1**	**PNP(30 mol%)**	**20**	**87**
8	BPC2	none	20	62
9	BPC2	PNP(30 mol%)	20	72
10	BPC3	none	20	47
11	BPC3	PNP(30 mol%)	20	65
12	BPC4	none	12	2
13	BPC4	PNP(30 mol%)	12	8
14	BPC5	none	20	53
15	BPC5	PNP(30 mol%)	21	70
16	BPC6	none	19	12
17	BPC6	PNP(30 mol%)	19	22
18	BPC8	none	21	57
19	BPC8	PNP(30 mol%)	21	71

R (entries 6–7) = *tert*-butyl; R = Me (8–9); R = Ph (10–11); R = CF$_3$ (12–13); R = *p*-OMe-phenyl (14–15); R = *p*-CN-phenyl (16–17); R = 3,5-diOMe-phenyl (18–19)

a) Determined by GC with internal standard. b) 0.4 M aldehyde, 1.2 equiv. MVK.

We first test the co-catalyst effect combined with PPh$_3$ as the Lewis base in THF. As shown in Table 17, the best result was obtained in the case of 30 mmol %

PNP. Similar to the aMBH reaction, more or less additive showed no positive effect on the conversion. In the next step, a series of BPCs were employed in this benchmark reaction. In most cases, the combination of BPCs with 30 mmol % PNP gave better results than that performing the reaction without additive. The best conversion was determined for BPC1, yielding 87 % conversion in 20 h. A slightly better but not so promising result than PPh_3 was achieved in the case of BPC2, 3, 5 and 8. For BPC4 and BPC6, probably due to the protonation described in Scheme 46, only 8 % and 22 % conversion was achieved.

Since BPC1 showed the best catalytic performance in this family of catalysts, another three new BPCs were prepared to test how the position of the hydrogen donor affects the catalytic reactivity. All these BPCs could be prepared in 2 steps, including the palladium-catalyzed coupling reaction and the following pivaloylation (Scheme 47).[123]
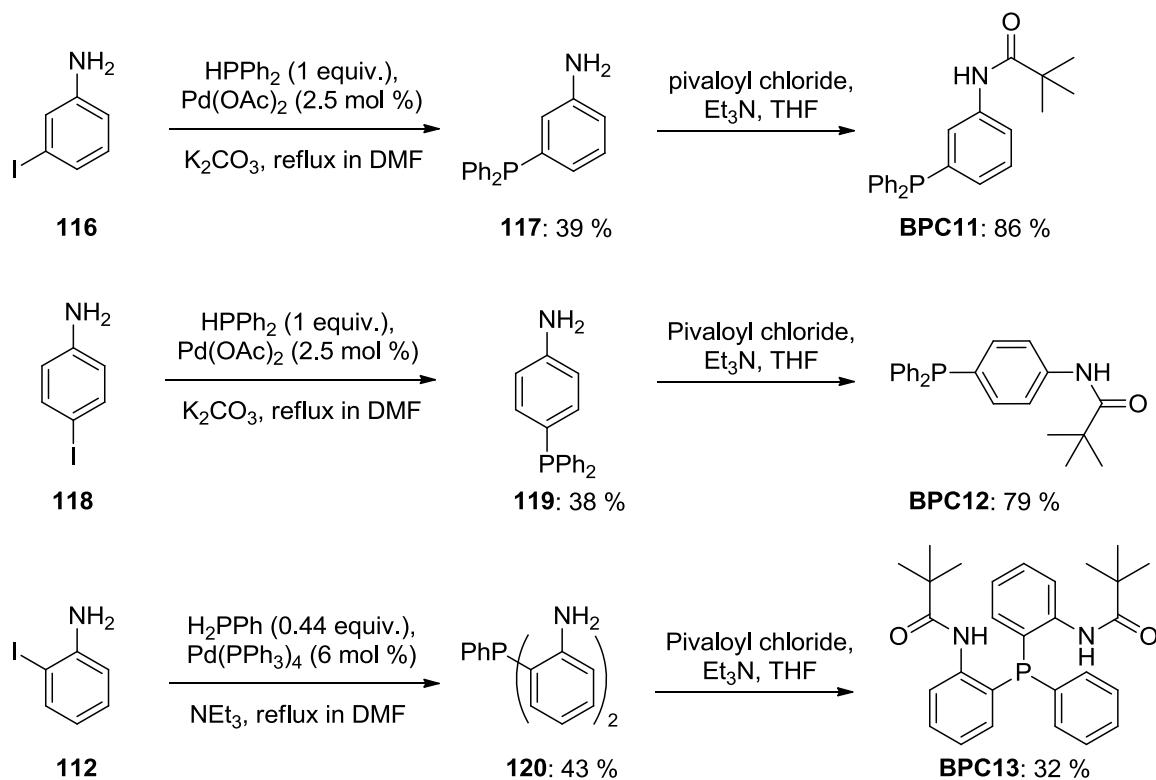
Scheme 47. The synthesis of BPC11, 12, 13.

Table 18. MBH reaction of *p*-chlorobenzaldehyde with MVK promoted by BPC and co-catalyst.

Entry	Lewis base	Co-catalyst	Conversion/%[a]
1		BPC1	none	64
2		**BPC1**	**PNP (30 mol %)**	**87**
3		BPC11	none	35
4		BPC11	PNP (30 mol %)	46
5		BPC12	none	63
6		BPC12	PNP (30 mol %)	62
7		BPC13	none	15
8		BPC13	PNP (30 mol %)	50

a) Determined by GC with internal standard. b) 0.4 M aldehyde, 1.2 equiv. MVK.

As shown in Table 18, when the geometry of the hydrogen donor changed, the catalytic performance of BPC11 dropped siginificantly; BPC12 showed good reactivity probably due to the better nucleophilicity of phosphane with amide group on the *para* position. When PNP was employed as co-catalyst, BPC1 showed better catalytic reactivity than BPC11. In the case of BPC13, not as we expected, two pivaloylamide groups near the phosphorus atom brought more steric hindrance, which slowed down this reaction by blocking the catalytically active phosphorus atom.

2.2.4 Asymmetric phosphane catalysts

2.2.4.1 Design and synthesis of asymmetric phosphane catalysts

Based on the reported multi/bifunctional catalysts (chapter 1.2.5) and the results from our own group (chapter 2.2), we designed a series of new chiral multifunctional phosphane catalysts. From our hypothesis, there are three activation modes for the control of transfer of chirality: Mode (A): Near the hydrogen-donating amide group a chiral steric hindrance group is anchored to supply the chiral environment; Mode (B): Introduction of another chiral proton donating group; Mode (C): Introduction of additional functional groups (e. g. *sec*-amine) able to stabilize transient intermediates. Herein, type-**121** and -**122** catalysts were prepared based on different activation modes.
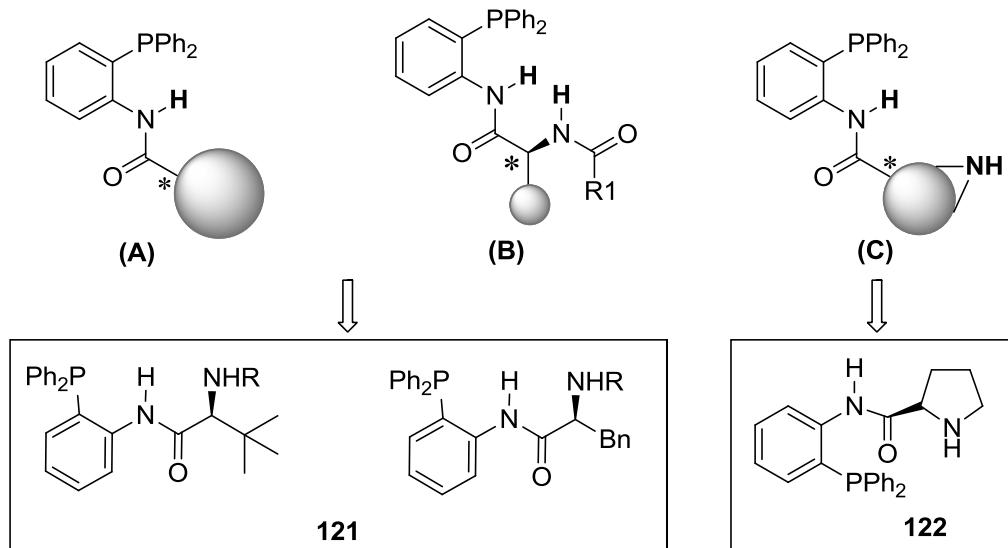
Scheme 48. The design of asymmetric phosphane catalysts.

The synthesis of asymmetric phosphane catalysts is shown in Scheme 49. Starting from the Boc-protected phenylalanine, proline, valine and *tert*-leucine, after coupling with amine **110** mediated by ethyl chloroformate or DCC, catalysts **124**, **127**, **130**[124] and **132**[124] were obtained. Deprotection of **124** and **127** with TFA produced catalysts **125** and **128**.
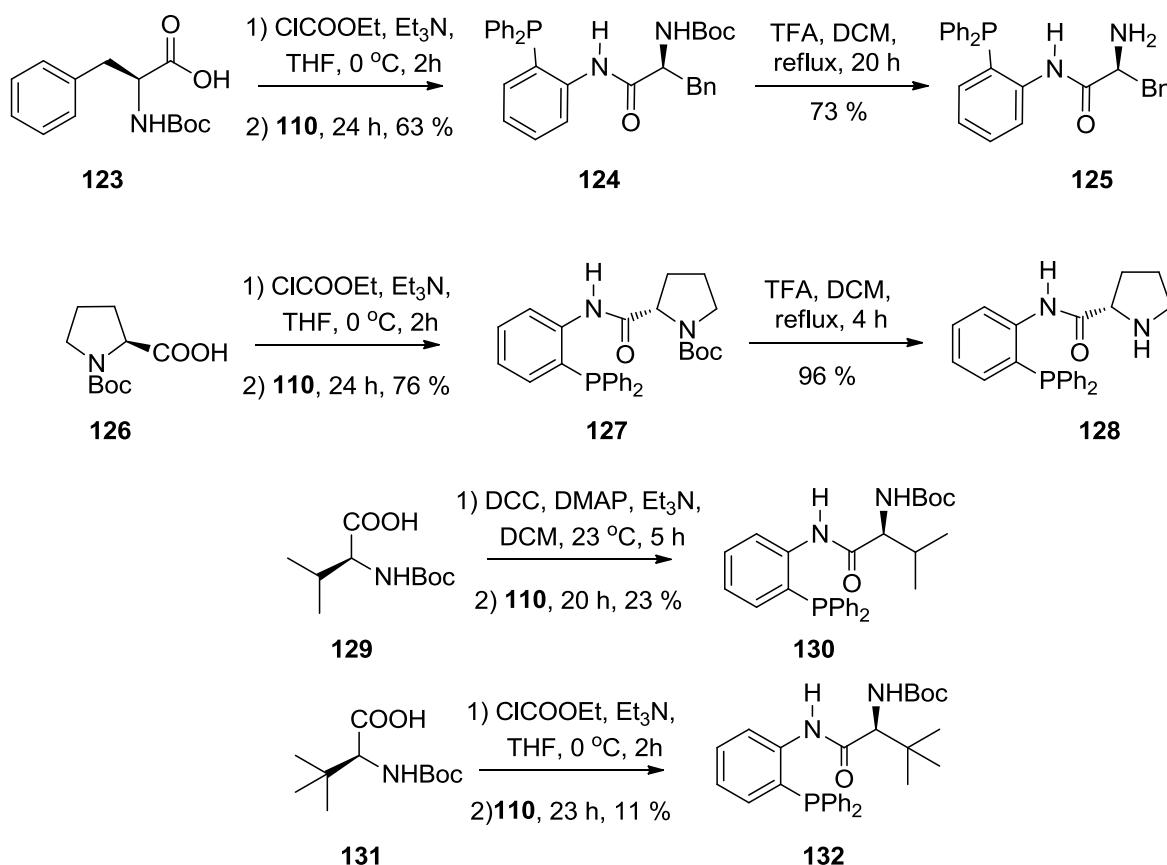
Scheme 49. The synthesis of asymmetric phosphane catalysts.

2.2.4.2 Asymmetric phosphane catalyzed (a)MBH reaction

Only a few asymmetric (a)MBH reaction examples regarding the application of asymmetric phosphane catalysts mentioned in Scheme 49 were carried out and the results are shown in Table 19. In the BPC1-catalyzed MBH reation of *p*-chlorobenzaldehyde with methyl vinyl ketone, when *s*-BINOL was employed as co-catalyst, the product was obtained with moderate yield and poor enantioselectivity (11 % and 15 % ee). This is in accordance with the results described in Table 18 (entry 1, 2), which indicates that the external chiral proton source might still be necessary to accelerate the MBH reaction and obtain enantioselective products. Unfortunately catalysts **124**, **127** and **128** could not promote this reaction. In the catalyst **128**-assisted aMBH reation of tosylimines with MVK, the aMBH products were obtained in good yield, but no enantioselectivity.

Table **19**. (a)MBH reaction of aldehyde or N-tosylimine with MVK promoted by phosphanes and co-catalyst.
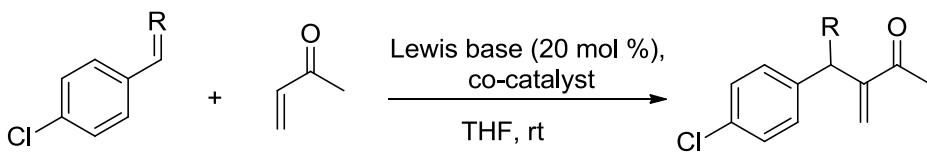
Entry	R	Lewis base	Co-catalyst	Time/h	Yield/%^{a}	ee^b/%
1	O	BPC1	s-BINOL(30 mol%)	40	87	11
2	O	BPC1	s-BINOL(20 mol%)	52	65	15
3	O	**124**	none	118	52	8
4	O	**127**	none	96	-^{d}	-
5	O	**128**	none	96	-^{d}	-
6	O	**128**	PNP (30 mol%)	96	-^{d}	-
7	NTs	**128**	none	18	87	1^f
8	NTs	**128**	PNP (30 mol%)	18	88	1^f

a) isolated yield. b) determined with chiral GC. c) 0.4 M aldehyde, 1.2 equiv. MVK. d) no reaction. f) determined with chiral HPLC.

2.3 Mechanistic studies of the Morita-Baylis-Hillman reaction

In this chapter mechanistic studies of the MBH reaction are discussed together with recent results from theoretical studies.

2.3.1 Protonation/deprotonation equilibria in the catalytic cycle

The mechanism of the Morita-Baylis-Hillman reaction has recently been found to be quite variable, depending on the particular nature of the reactants, the catalysts and the solvent used. Recent spectroscopic, kinetic, and theoretical studies suggest that, under these conditions, the reaction follows the mechanism outlined in Scheme 50 (shown here using the PPh$_3$ (**2**)-catalyzed reaction of methyl vinyl ketone (MVK, **41**) as an example).
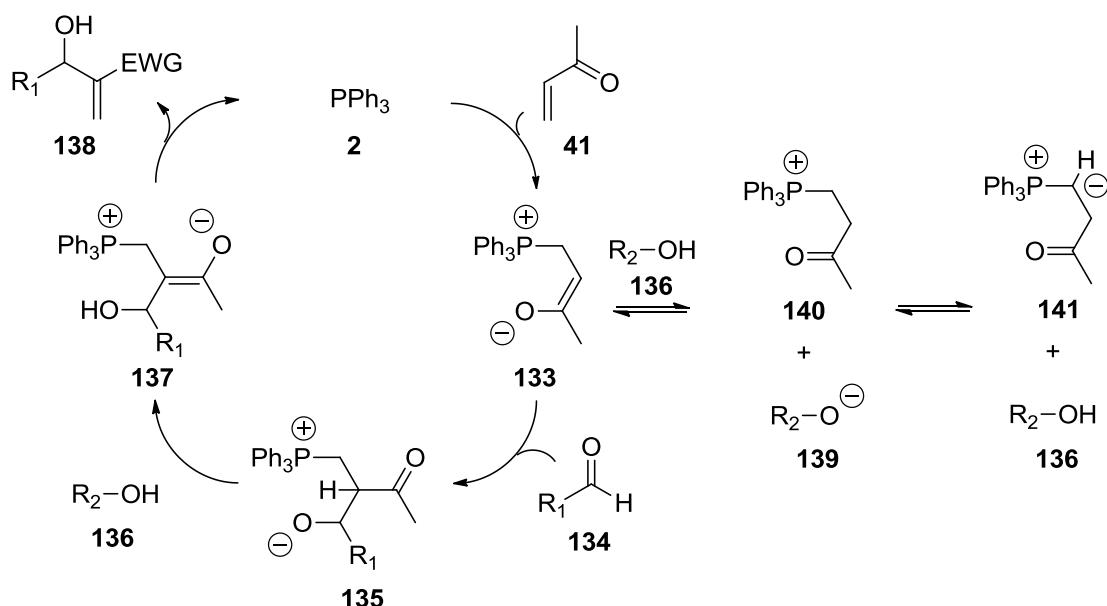
Scheme 50. A general mechanism for the MBH reaction.

In this mechanism the phosphane catalyst **2** is expected to add to the Michael acceptor **41** in a rapid and reversible manner, forming the zwitterionic adduct **133** as the first transient intermediate. This is followed by nucleophilic addition to aldehyde **134**, yielding a second zwitterionic intermediate **135** as the product. Subsequent intramolecular hydrogen transfer within intermediate **135** to yield enolate zwitterion **137** is considered to be rate-limiting for many systems and is catalyzed by protic co-catalysts or solvents R_2-OH **136**. The catalytic cycle is completed by elimination of the phosphane catalyst **2** and generation of the MBH product **138**. In addition to accelerating the hydrogen-transfer step in intermediate **135**, the protic co-catalysts **136** may also react with enolate zwitterions **133** and **135** in protonation/deprotonation equilibria. This is shown in Scheme 50 for zwitterion **133**, whose reaction with alcohol **136** leads to formation of alkoxide **139** and phosphonium cation **140**. Depending on the solvent system used these may either exist as solvent-separated ions (e.g. in DMSO) or as tight ion pairs (e.g. in THF). Protonation/deprotonation may, of course, also involve the position directly adjacent to the phosphorous atom, yielding ylide **141** as a potential additional intermediate. Ylids such as **141** can subsequently react with a second equivalent of MVK **41**, forming unwanted side products together with oxidized (and thus deactivated) phosphane catalyst **2**. Even though quantitative data for the basicity of intermediates **133**, **137**, and **141** appear not to be available in the contemporary literature, indirect evidence suggests that the equilibrium between **133** and **140** is

shifted far to the right under most experimental conditions. This is supported by the abundant detection of type-**140** intermediates as well as protonated forms of intermediate **137** in reaction solutions of MBH reactions by ESI-MS.[55] β-Ketophosphonium cations such as **140** have also been characterized by NMR spectroscopic techniques in the mechanistically related phosphane-mediated addition of alcohols to Michael acceptors.[116a] In this latter case cations such as **140** are considered to represent the resting state of the phosphane catalysts. The large success of phenolic co-catalysts in a variety of MBH reactions thus raises the question of the actual basicity of zwitterionic enolates **133** and **137** in different solvent systems, especially compared to the acidity of phenolic co-catalysts. We are using here a combination of theoretical and experimental studies to clarify this point.

Both Leitner and Shi have reported that triphenylphosphane (PPh$_3$) can catalyze (a)MBH reactions well in the presence of a catalytic amount of Brønsted acid with proper acidity.[61,59a] To clarify the interaction of Brønsted acid and enolate-**133** in the catalytic cycle, we carried out NMR spectroscopic measurements of PPh$_3$ and PNP co-catalyzed MBH reaction to monitor the intermediates. As a first step PPh$_3$ (0.32 M) and methyl vinyl ketone (3.3 M) were dissolved in CDCl$_3$. Aside from the signal for PPh$_3$ at -4.7 ppm, new signals appeared at +29.5 ppm and around -60 ppm as shown in Figure 22. The signal at +29.5 ppm is identical to that of O=PPh$_3$. The group of signals at around -60 ppm were assigned to some cyclic P(V) intermediates according to the ^{31}P NMR calculation results.[*]

---

[*] The computational study about ^{31}P NMR was proceeded by Boris Maryasin, Ph.D thesis **2011**.
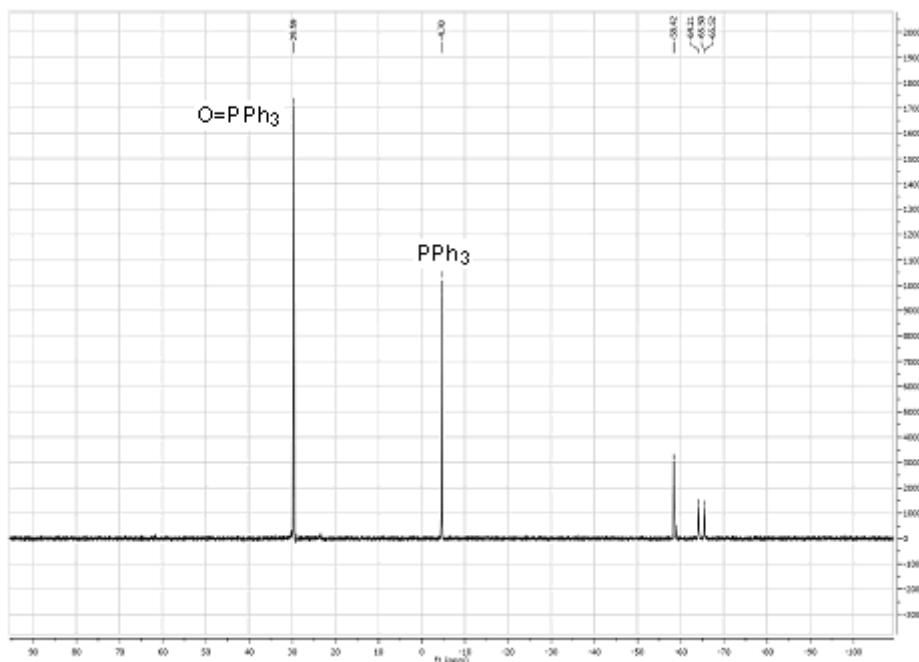
Figure 22. The ^{31}P NMR of PPh$_3$ (0.32 M) and MVK (3.2 M) in CDCl$_3$ after 50 mins.
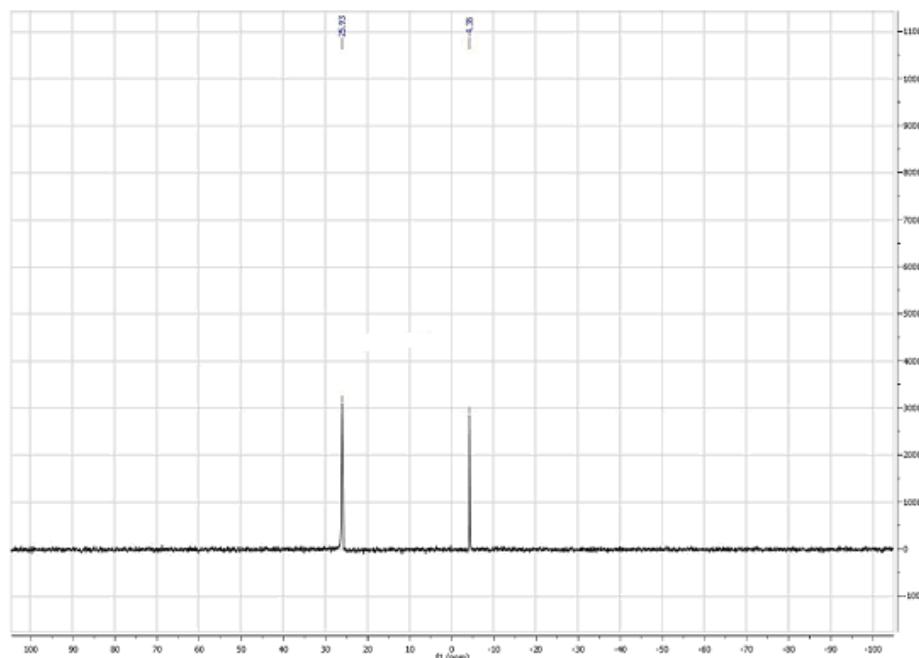
Figure 23. The ^{31}P NMR of PPh$_3$ (0.32 M), PNP (0.48 M) and MVK (3.2 M) in CDCl$_3$ after 5 mins.

In the next step PPh$_3$ (0.32 M), PNP (0.48 M) and MVK (3.2 M) were dissolved in CDCl$_3$. A new signal appeared at +25.72 ppm, in addition to the signal for PPh$_3$ at -4.7 ppm (Figure 23). The new signal can be shown to be intermediate **140**, which can be characterized by ^{1}H NMR and 2D NMR (see experimental part). This really

brings the argument of how could protonated enolate intermediate continue to react as a normal enolate. Taking this in mind, the ^{31}P NMR measurement of the reaction of PPh$_3$ (0.32 M), PNP and MVK (3.2 M) (molar ratio 1: x: 10) in CDCl$_3$ with the variation of PNP molar concentration were performed (Figure 24). By comparing the integrals of ^{31}P NMR signals at +25.72 ppm and -4.7 ppm, the ratio of PPh$_3$ and intermediate **140** can be obtained to give the yield of intermediate **140** (Figure 25). These ^{31}P NMR measurements with different concentrations of PNP showed clear protonation/deprotonation equilibria between PPh$_3$, MVK, PNP and intermediate **140** and phenolate **139**. These equilibria indicated that intermediate **140** could work as an enolate bath and also clarified the interaction between the Brønsted acid and the enolate intermediate in the MBH reaction.
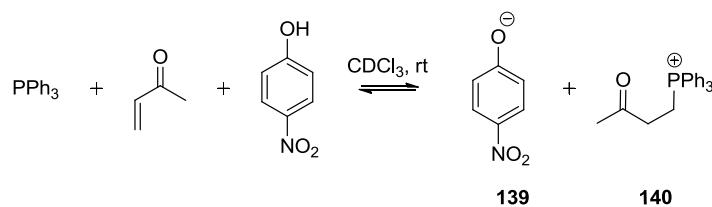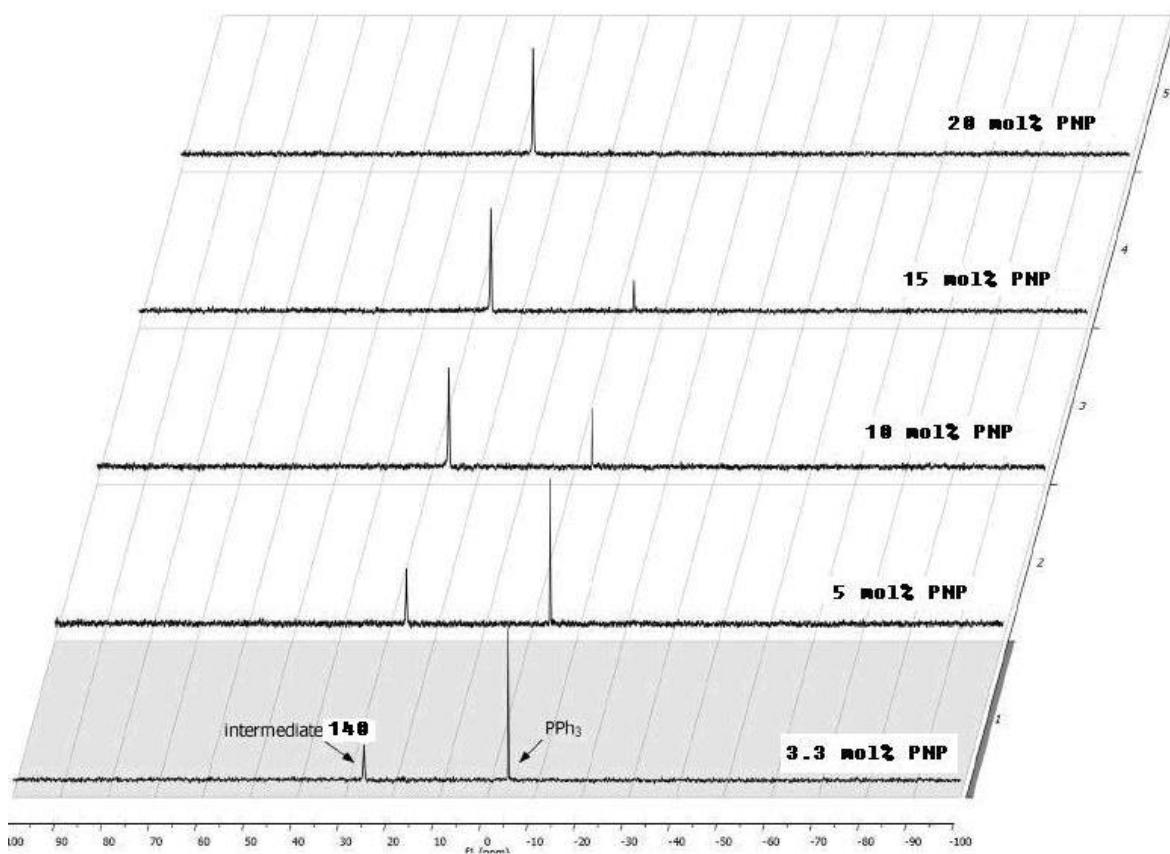
Figure 24. The ^{31}P NMR spectroscopy of the equilibria of MVK (3.2 M), PPh$_3$ (10 mol %) and PNP (x mol %) in CDCl$_3$.
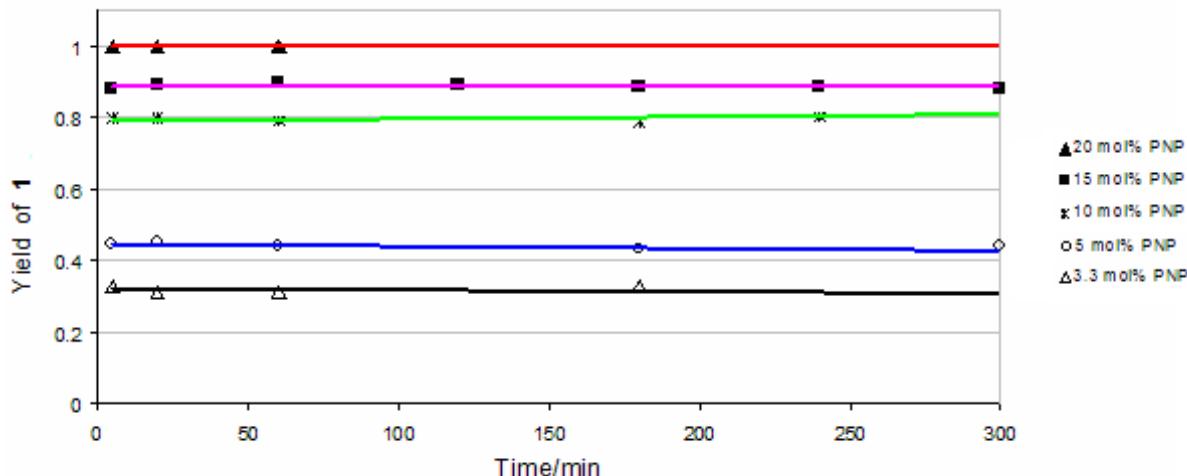
Figure 25. The yield of intermediate **140** determined with ^{31}P NMR in the reaction of MVK (3.2 M), PPh$_3$ (10 mol %) and PNP (x mol %) in CDCl$_3$.

The analogue of **140** could also be prepared by the reaction of PPh$_3$, MVK and HBr in CDCl$_3$, (equation 3) which showed a similar ^{31}P NMR resonance at +26.84 ppm.

(3)
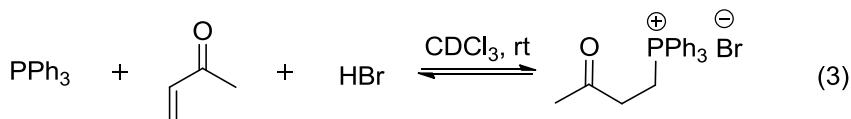
The equilibrium between PPh$_3$, MVK and PNP (molar ratio 1:10:1.5) in THF could also be monitored by ESI-MS. An aliquot of the reaction mixture (10 μL) was taken, diluted in 1 mL THF and injected into the ESI source. Two cationic species ([PPh$_3$+H]$^+$ of m/z 263, **140** of m/z 333) and one anionic species (**139** of m/z 138), which were related to the proposed protonation/deprotonation equilibrium of the enolate intermediate, were detected (Figure 26a). Identically, ESI-MS of the mixture of PPh$_3$, ethyl vinyl ketone, and PNP (molar ratio 1:10:1.5) in THF showed two cationic species ([PPh$_3$+H]$^+$ of m/z 263, **142** of m/z 347) and one anionic species (**139** of m/z 138) (Figure 26b).

(a)   (b)
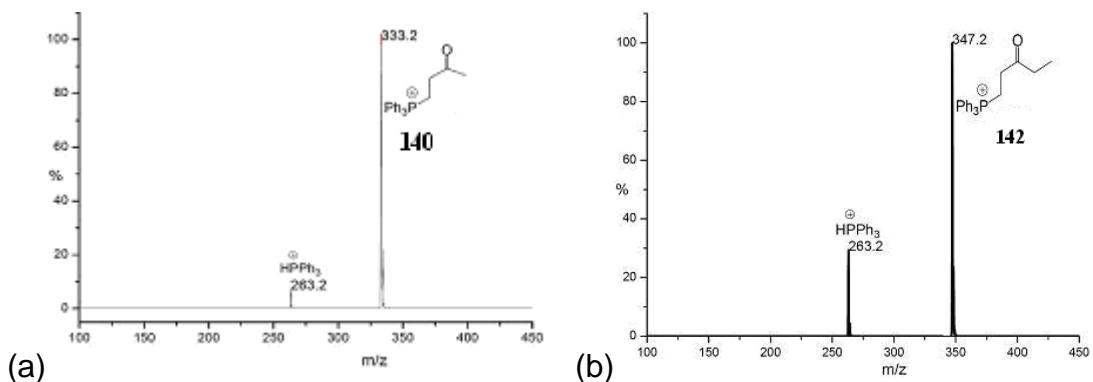
Figure 26. ESI (+)-MS of PNP (15 mol %), PPh₃ (10 mol %) and (a) MVK or (b) EVK in THF.

As mentioned before, the mixture of PPh$_3$ and MVK in CDCl$_3$ (molar ratio 1:10) shows a ^{31}P NMR resonance of O=PPh$_3$ at +29.54 ppm. After 10 h, almost all of the PPh$_3$ was converted to O=PPh$_3$, which could probably be generated from the reaction of MVK with the phosphonium zwitterionic ylide **141** (equation 4).
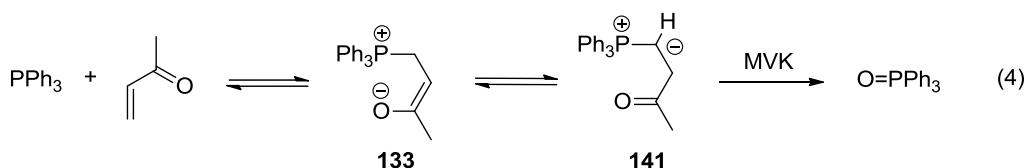
In the presence of PNP, there was no ^{31}P NMR resonance of O=PPh$_3$, but intermediate **140** is observed instead. This implied that the role of PNP here is to convert the PPh$_3$ catalyst to the resting state **140**. It should be noted that, aside from the deprotonation/protonation equilibrium between **133** and **140**, there could be another equilibrium between **140** and ylide **141** (Scheme 51). This raised the question about the acidity of the α- and β-position of the phosphonium cation **140**.
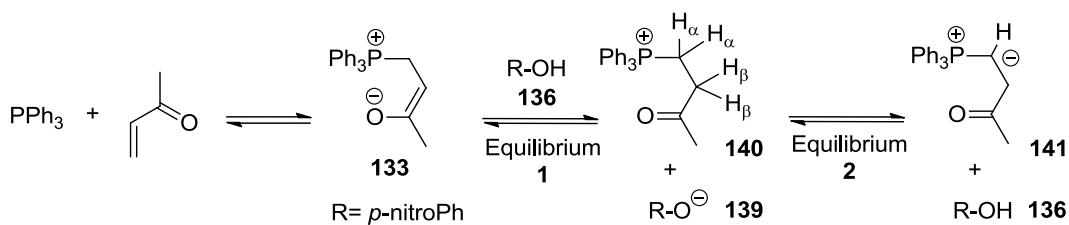
Scheme 51. The protonation/deprotonation equilibria.

Herein Boris Maryasin carried out theoretical calculation to estimate the pK_a of **140** with reference to experimentally known systems such as phosponium cations **142**

and **143**[106] as outlined in Scheme 52.* The acidity of the β-hydrogens (pK_a(DMSO) = 19.5±0.4) of the phosphonium cation **140** is about 3 pK_a units higher than that of the α-position (pK_a(DMSO) = 22.4±0.4). Therefore deprotonation on the β-position of **140** to form **133** is much more favorable, which could clarify that in the resting state the catalyst was protected from the Wittig reaction (via **141** to O=PPh₃) due to the more favorable equilibrium between **133** and **140**. As compared with protic co-catalysts such as PNP, which are much more acidic with a pK_a(DMSO) value +10.8, we can assume that the equilibrium between enolate **133** and its protonated analogue **140** is shifted far to the side of the latter, leaving a small amount of zwitterionic enolate **133** behind to progagate the catalytic cylcle.
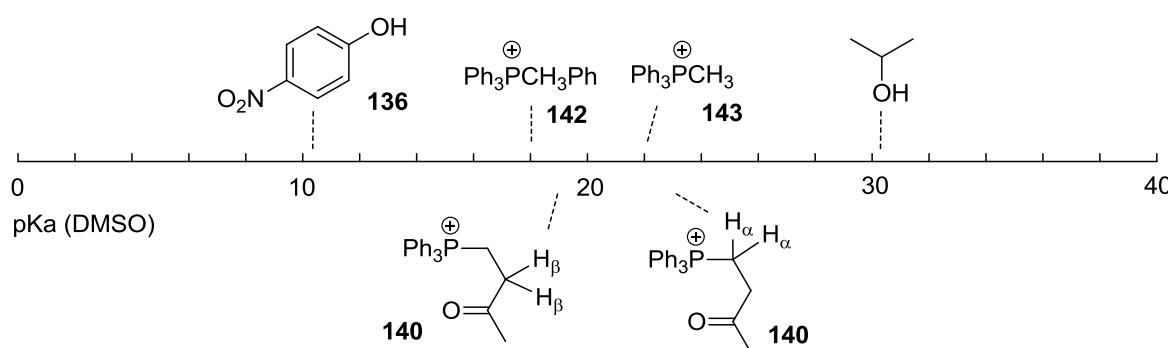
Scheme 52. The pK_a scale of **140**.
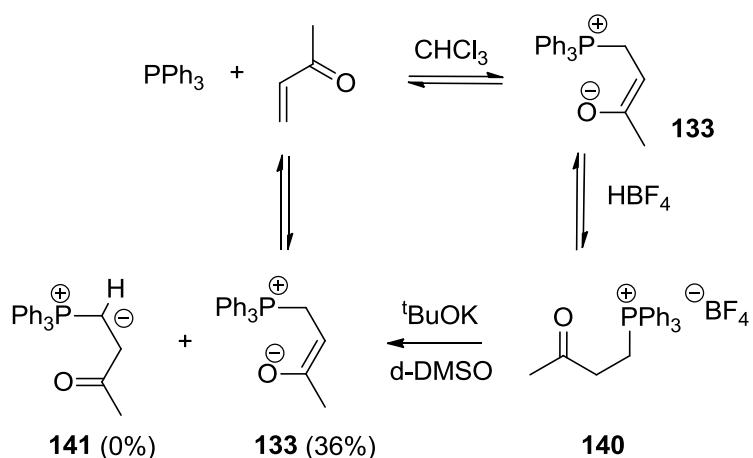
Scheme 53. Deprotonation of **140** with tBuOK.

---

* The comp, utional study about pK_a value of compound **140** was performed by Boris Maryasin.

84
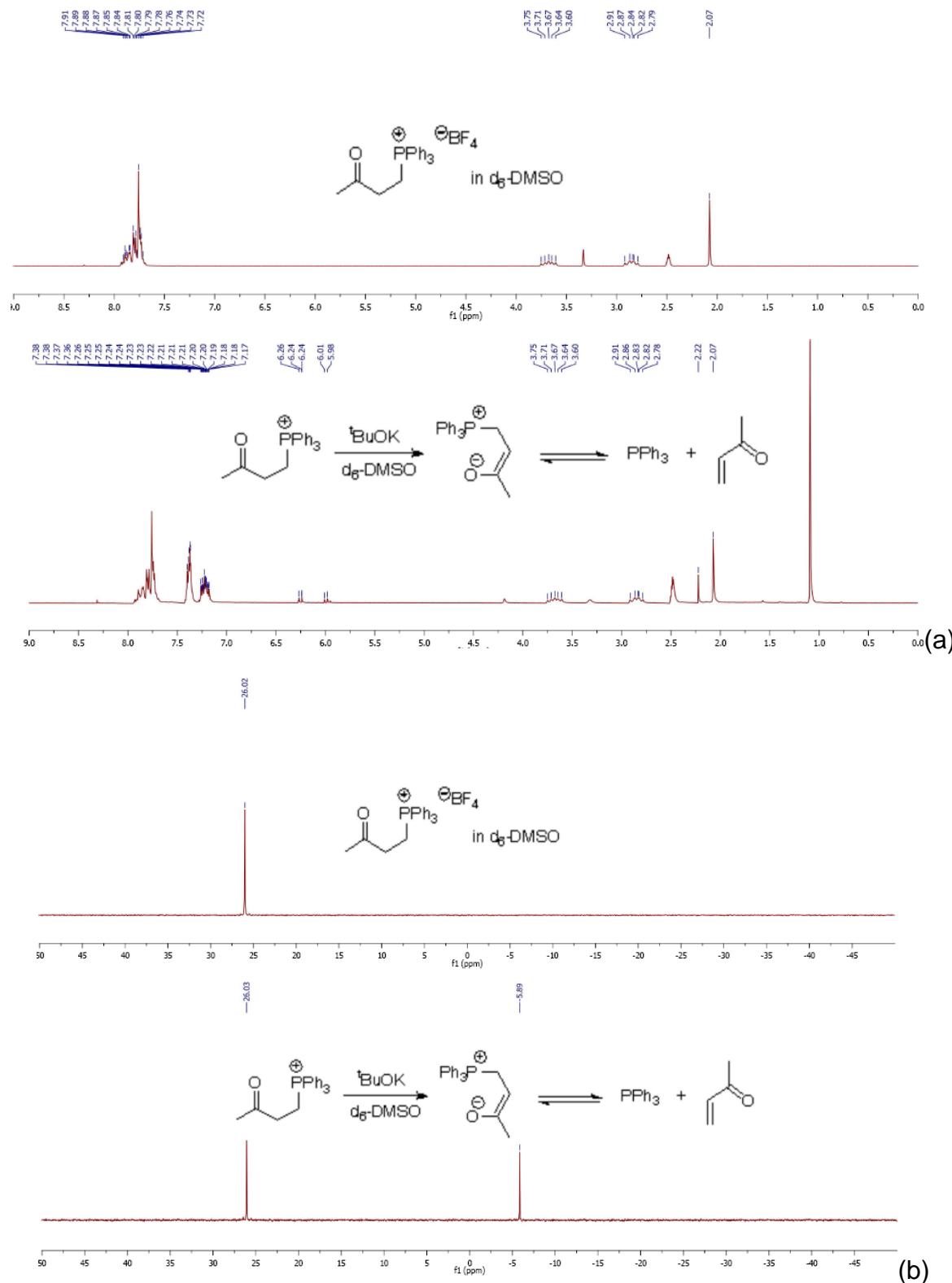
Figure 27. The ^{1}H NMR (a) and ^{31}P NMR (b) spectroscopy of the control reaction of **140** with *t*BuOK.

That **140** is more acidic at H$_\beta$ than at H$_\alpha$ could be easily testified by the control reaction depicted in Scheme 53. When **140** with ionic pair of $^-$BF$_4$ in d$_6$-DMSO

solution was treated with 0.8 equiv. *t*-BuOK, instantly regenerated PPh$_3$ and MVK were detected by ^{1}H NMR and ^{31}P NMR spectroscopy, but no **141** was observed. This could not exclusively exclude the formation of **141**, but it can somewhat prove that the β-position of **140** is more preferably deprotonated (Figure 27).

Actually in the real MBH reaction, when aldehyde is present, it should compete with Brønsted acid in reacting with the enolate. The ^{31}P NMR measurement of PPh$_3$, PNP, MVK, and *p*-chlorobenzaldehyde (molar ratio 1: 1.5: 10: 5) in CDCl$_3$ still showed the intermediate **140** signal at +25.72 ppm and the peak for PPh$_3$ at -4.63 ppm. This implied that after the Michael addition step the phenolic co-catalysts would render the enolate less active and slow down the MBH reaction. It is, however, found that phenolic co-catalysts promote a variety of MBH reactions rather well. We can rationalize this with the role phenolic co-catalyst played in the hydrogen transfer step, where its acceleration effect is bigger than its slowdown effect after the Michael addition step. The theoretical study to describe this PPh$_3$ and PNP co-catalytic cycle in detail is still under way.

2.3.2 Kinetic studies of the protonation/deprotonation process

In the most recent mechanism studies, the rate determining step in (a)MBH reaction is the proton transfer step or the aldol addition step. Quite recently, Shibasaki, Berkessel and co-workers reported that the Michael addition step was determined to be rate-limiting in the aMBH reaction of phosphinoylimine with methyl acrylate, which recall us the crucial role of the Michael acceptors. As also shown in chapter 2.1.1, the rate of aMBH reaction does strongly depend on Michael acceptors and catalysts. For instance, PPh$_3$ showed energetic catalytic performance for the aMBH reaction of tosylimine with MVK, but no reactivity in the reaction of 2-cyclohexenone with imine. Pyridine derivatives can promote the aMBH reaction of tosylimine with 2-cyclohexenone much more effectively than PPh$_3$, and they are as effective as PPh$_3$ with MVK as substrate. Pyridine derivatives showed less reactivity compared with PPh$_3$ when ethyl acrylate was employed. This really raises our interest to disclose the interaction of catalysts with activated alkenes in the Michael addition step.

At first the reaction of PPh$_3$, MVK and PNP in THF was taken as benchmark reaction to study the Michael addition step. As discussed in chapter 2.3.1, the

zwitterionic compound **133** generated for the Michael addition of PPh_3 with MVK would react instantly with PNP to form **140** and phenolate **139** (equation 5).
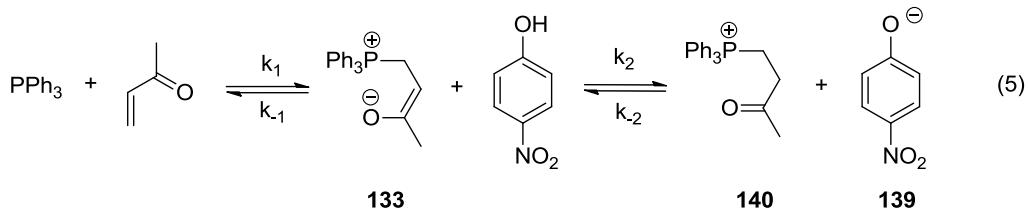
With the assumption that $\frac{d[\textbf{133}]}{dt} = 0$, $k_2 >> k_{-2}$, one obtains equation (6):

$$k_1[PPh_3][MVK] = k_{-1}[\textbf{133}] + k_2[\textbf{133}][PNP] \quad \text{(6a)}$$

$$[\textbf{133}] = \frac{k_1[PPh_3][MVK]}{k_{-1} + k_2[PNP]} \quad \text{(6b)}$$

The rate law of the reaction of PPh_3, MVK and PNP in THF could be described as equation 7c,

$$\frac{d[\textbf{139}]}{dt} = \frac{d[\textbf{140}]}{dt} \quad \text{(7a)}$$

$$\frac{d[\textbf{139}]}{dt} = k_2[\textbf{133}][PNP] \quad \text{(7b)}$$

$$\frac{d[\textbf{139}]}{dt} = \frac{k_1 k_2[PPh_3][MVK][PNP]}{k_{-1} + k_2[PNP]} \quad \text{(7c)}$$

$$\frac{d[\textbf{139}]}{dt} = \frac{k_1 k_2[PPh_3][MVK][PNP]}{k_{-1}} \quad \text{(7d)}$$

$$\frac{d[\textbf{139}]}{dt} = k_{obv}[PNP], \quad k_{obv} = \frac{k_1 k_2[PPh_3][MVK]}{k_{-1}} \quad \text{(7e)}$$

From equation 7c, if $k_{-1} >> k_2[PNP]$, one can get equation 7d, which means the reaction is first order in PNP. The rate law can be expressed by equation 7e. If $k_{-1} \approx k_2[PNP]$, the rate law can be expressed by equation 7c, in which the PNP is partially involved in the rate-determining step. If $k_{-1} << k_2[PNP]$, the rate law can be expressed by equation 7f, which implies that the reaction is zero order inPNP and the Michael addition step is rate determining.

$$\frac{d[139]}{dt} = k_1[PPh_3][MVK] \quad \text{(7f)}$$

At first we carried out this reaction with an excess amount of MVK and PPh_3, the proton transfer step will be the rate determining step according to the rate law shown in equation 7e. The rates of the reaction at different concentrations of MVK, PNP and PPh_3 were determined photometrically in THF at 20 ^{o}C (Scheme 54). In a similar manner, the reactions of MVK, PNP and PPh_3 were carried out with variation of concentrations of MVK and PNP (Scheme 55, 56).
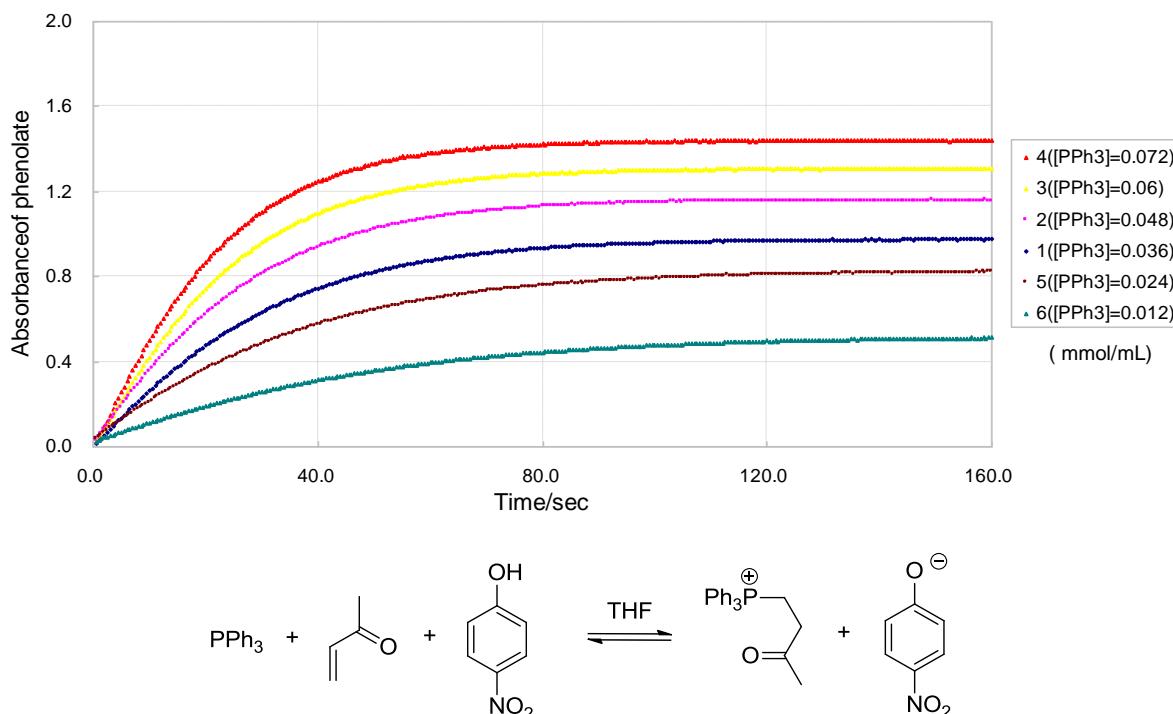
Scheme 54. Exponential increase of the absorbance of phenolate in the reaction of MVK (0.072 M), PPh_3 (0.012-0.072 M) and PNP (0.003 M) in THF.
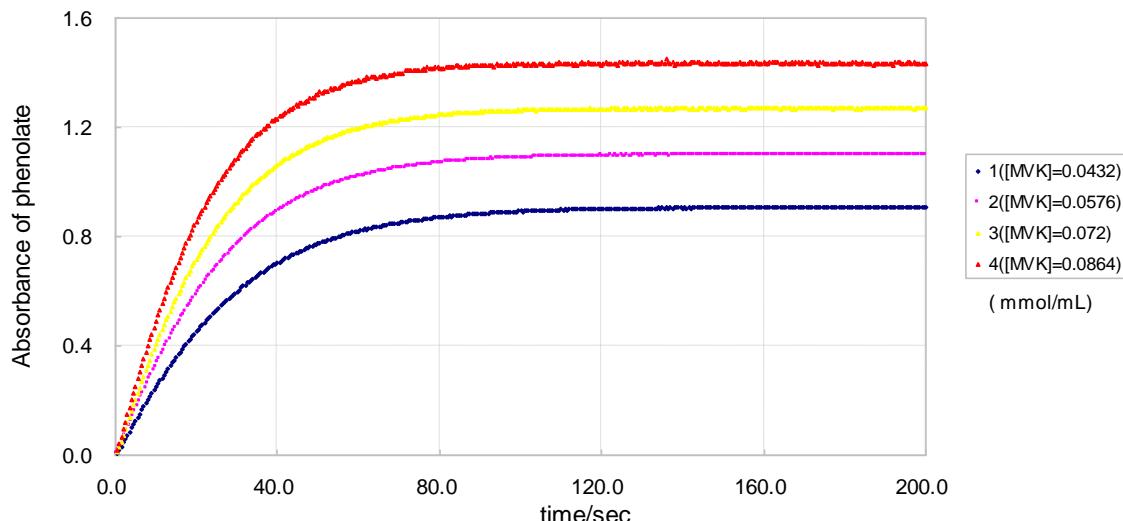
Scheme 55. Exponential increase of the absorbance of phenolate in the reaction of MVK (0.0432-0.0864 M), PPh$_3$ (0.06 M) and PNP (0.003 M) in THF.
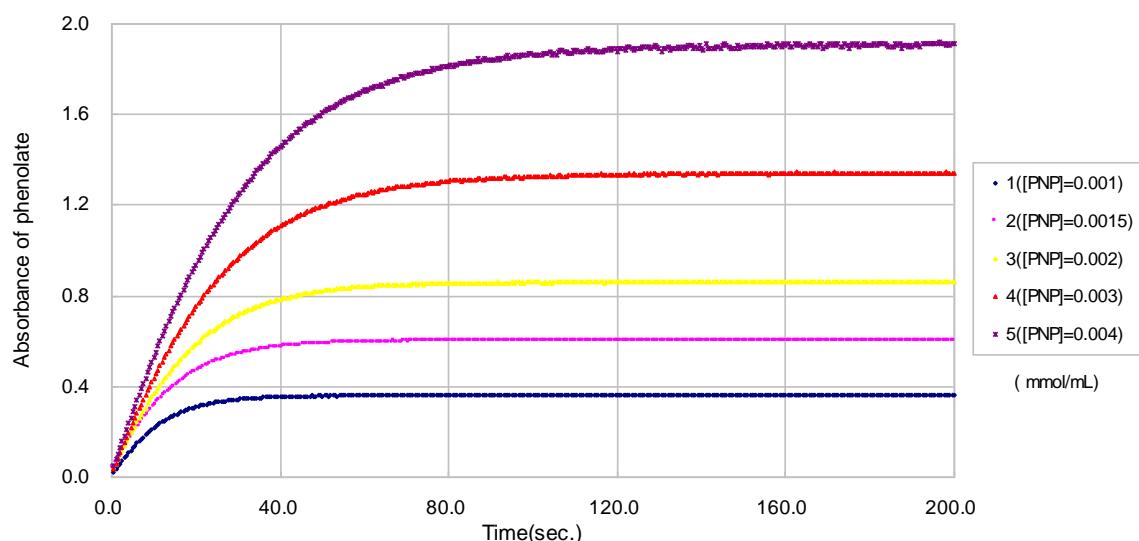
Scheme 56. Exponential increase of the absorbance of phenolate in the reaction of MVK (0.072 M), PPh$_3$ (0.06 M) and PNP (0.001-0.004 M) in THF.

To testify the rate law and determine the partial reaction order of MVK, PPh$_3$, and PNP , we applied the intital rate method to evaluate these kinetic measurements. It is found that the reaction rate had a first-order dependence on MVK, a first-order dependence on PPh$_3$, and a broken order of 0.5 on PNP (Figure 28, 29, 30), which implies that the rate-determining step is partly influenced by the proton transfer step. This indicates that the rate law shown in equation 7c is more relevant to this series of reactions with these concentrations of substrates. With the intial rate data,

a plot of $\dfrac{1}{rate}$ versus $\dfrac{1}{[PNP]}$ is linear to give the intercept as $\dfrac{1}{k_1[PPh_3][MVK]}$,

which allows us to obtain the Michael addition rate constant k_1 (0.00186 $M^{-1}s^{-1}$) as shown in Figure 31.

$$rate = \frac{d[\mathbf{139}]}{dt} = \frac{k_1 k_2 [PPh_3][MVK][PNP]}{k_{-1} + k_2[PNP]} \tag{7c}$$

$$\frac{1}{rate} = \frac{dt}{d[\mathbf{139}]} = \frac{k_{-1}}{k_1 k_2 [PPh_3][MVK][PNP]} + \frac{1}{k_1[PPh_3][MVK]} \tag{7g}$$

$$\frac{1}{rate} = \frac{dt}{d[\mathbf{139}]} = k_{obv}\frac{1}{[PNP]} + \frac{1}{k_1[PPh_3][MVK]}, \quad k_{obv} = \frac{k_{-1}}{k_1 k_2 [PPh_3][MVK]} \tag{7h}$$
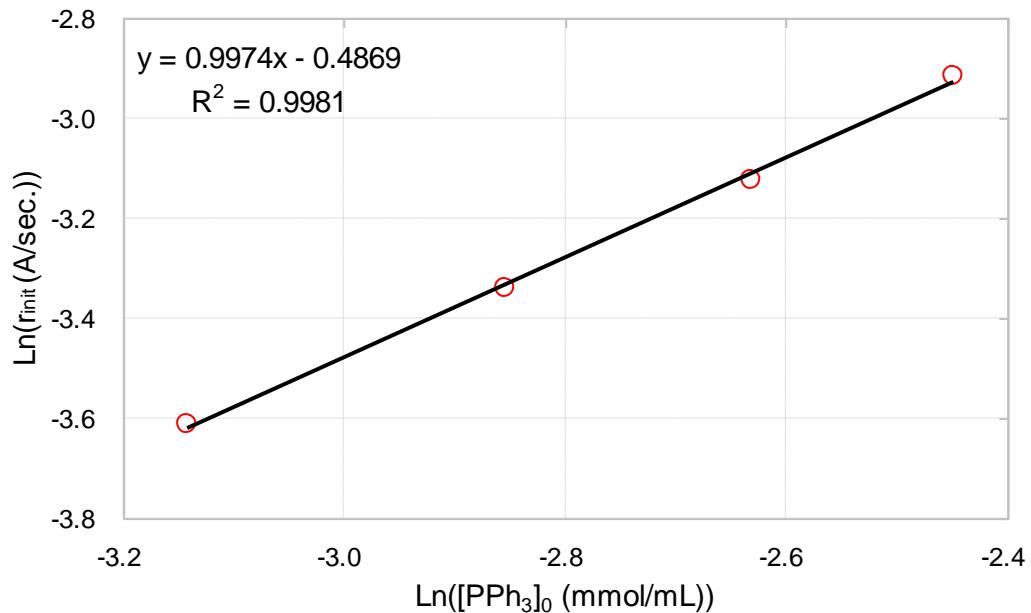
Figure 28. The partial order of PPh_3 in the reaction of MVK, PPh_3, and PNP.

90
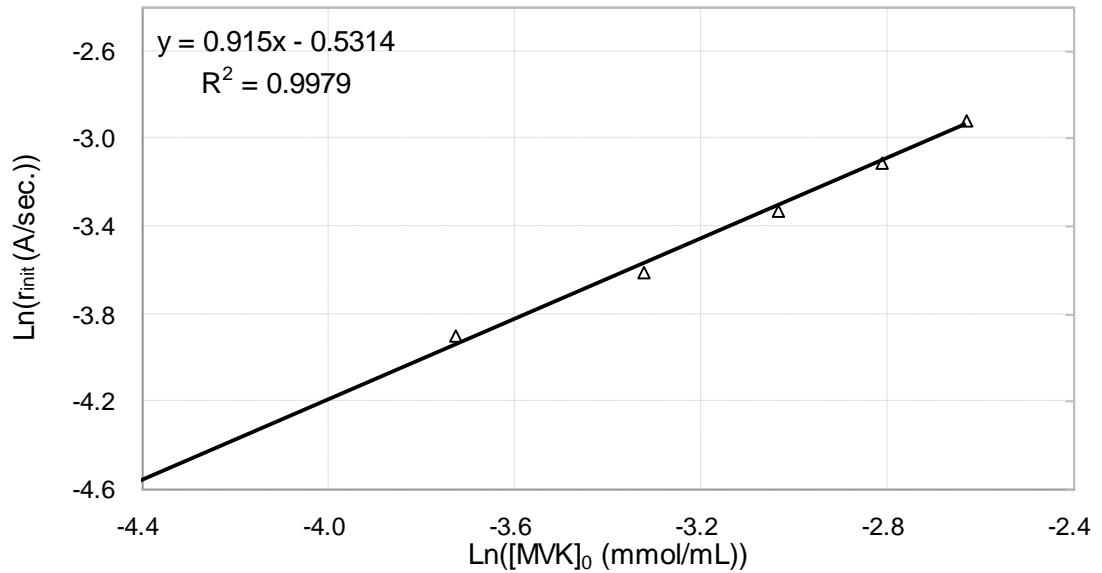
Figure 29. The partial order of MVK in the reaction of MVK, PPh$_3$, and PNP.
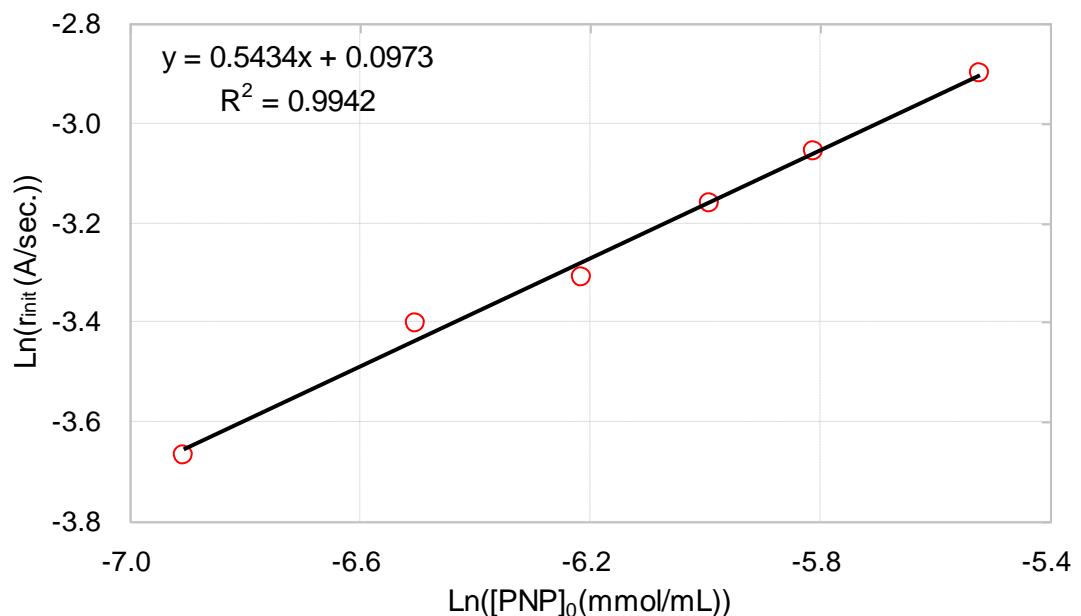
Figure 30. The partial order of PNP in the reaction of MVK, PPh$_3$, and PNP.
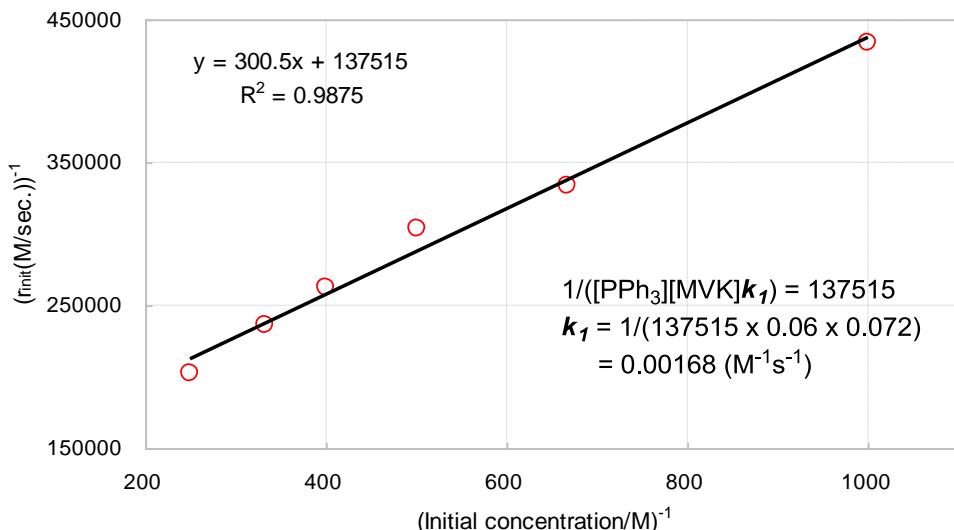
Figure 31. Determination of the rate constant k_1.

In an analogous fashion, we also carried out the reaction of ethyl acrylate, PPh$_3$, and PNP. As compared with the reaction with MVK as substrate, this reaction proceeded much more slowly and reached the maximum conversion in 5 hours, which clarified the different reactivity of MVK with ethyl acrylate in this reaction (Scheme 57). There could be other activated alkenes, such as acrylamide and acrolein, used in this reaction and measured with this method. Given this second-order rate constant, it is possible to evaluate the electrophilicity of activated alkenes for Michael addition with E parameter which was developed with Mayr group.[125] There is still much more effort needed to complete this.
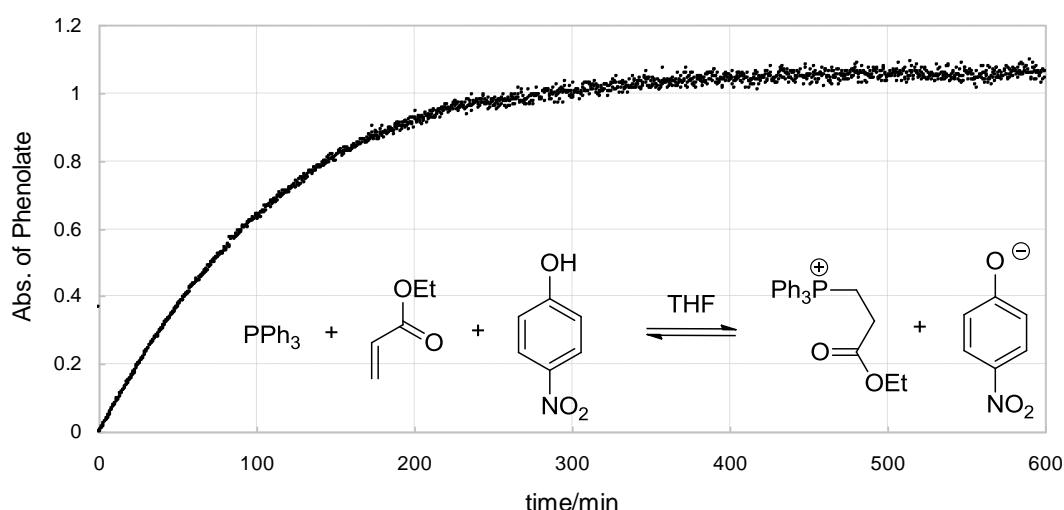
Scheme 57. The turnover plot of the reaction of ethyl acrylate (0.5 mmol/mL), PPh$_3$ (0.14 mmol/mL) and PNP (0.0018 mmol/mL) in THF.

3 CONCLUSION AND OUTLOOK

CONCLUSION: In this thesis, the organo-catalyzed (aza)-Morita-Baylis-Hillman ((a)MBH) reaction was investigated with different Lewis base catalytic systems:
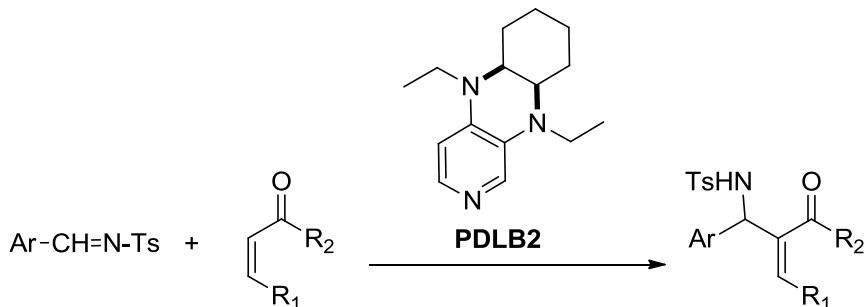

A series of pyridine-derived Lewis bases (PDLBs) were applied in the aMBH reaction of tosyl imine with a variety of activated alkenes: ethyl acrylate, methyl vinyl ketone, 2-cyclohexenone. PDLBs showed excellent catalytic performance in the case of MVK. The best activity was determined when 2-cyclohexenone and PDLB2 was employed, as compared with the other Lewis bases. The scope of these reactions for different tosyl imines has also been investigated.
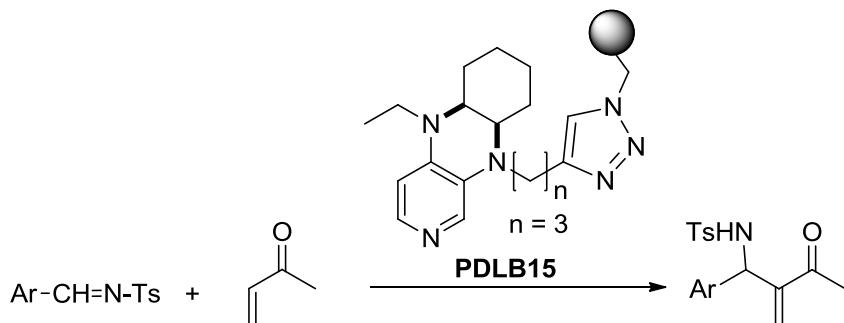
The immobilization of PDLB2 on a polystyrene support leads to a catalyst of unprecedented catalytic activity in aMBH reactions, while preserving the benefits of easy recoverability and recyclability. This heterogeneous catalytic system in aMBH reactions is able to approach or even surpass the performance of the homogenous catalysts.
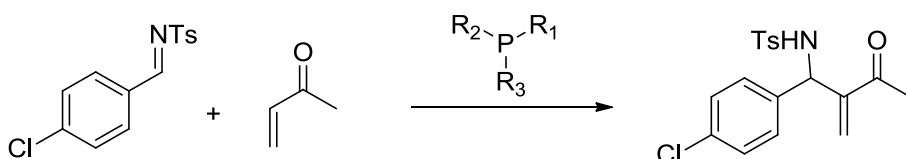

The catalytic acitivity of a series of phosphanes in aMBH reactions was investigated, and correlated with the MCA values of these phosphanes, which did not give a promising correlation.
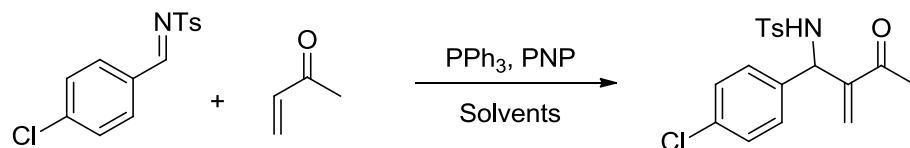
The PPh$_3$ and PNP co-catalyzed aMBH reaction was studied in detail about the co-catalyst effect in a variety of solvents, documenting the strong interdependence of the solvent and co-catalyst effect. This implied the importance of the selection of solvents for some special combined asymmetric co-catalytic system.
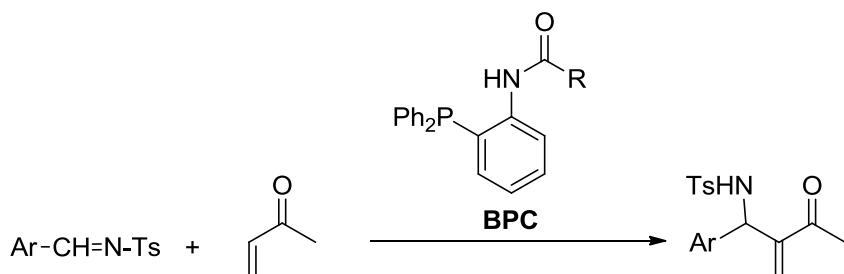
A series of bifunctional phosphorus catalysts were synthesized and tested in the (a)MBH reaction. The catalytic performance was found to be strongly dependent on the acidity and steric effect of the Brønsted acid. Several asymmetric bifunctional phosphorus catalysts were also prepared and applied in the (a)MBH reaction, which did not afford satisfying results.
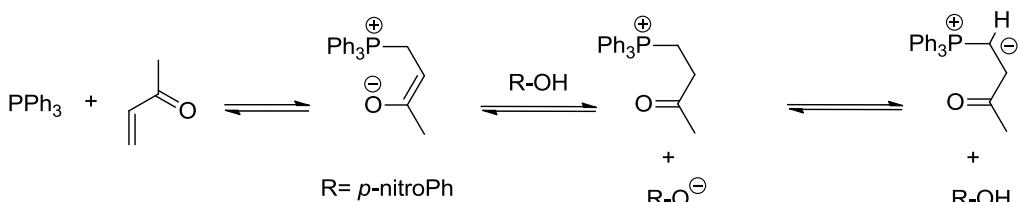
The equilibria in the Lewis base and Brønsted acid co-catalyzed MBH reaction were investigated by kinetic and theoretical calculation methods. The intermediate was characterized by ^{31}P NMR spectroscopy and ESI-MS. We had attempted to discover the interaction of Lewis base and activitated alkene in Michael addtion with kinetic method.

OUTLOOK: In this stage of this thesis, there are still a few parts of the research not completed yet, which are worthy for futher study.

There could also be some other attempts to fertilize the PDLBs catalyzed aMBH reaction, such as to combine equimolar amounts of proper chiral Lewis acid or Brønsted acid, which could supply a chiral environment to promote enantio-selective aMBH reaction.

The application of catalysts **124-132** in (a)MBH reactions could be further explored in different substrates and solvents. There could be also further modification to supply new catalysts based on catalysts **124-132**. For catalyst **128**, acrolein could be tested as Michael acceptor to form a rigid type-**144** intermediate.
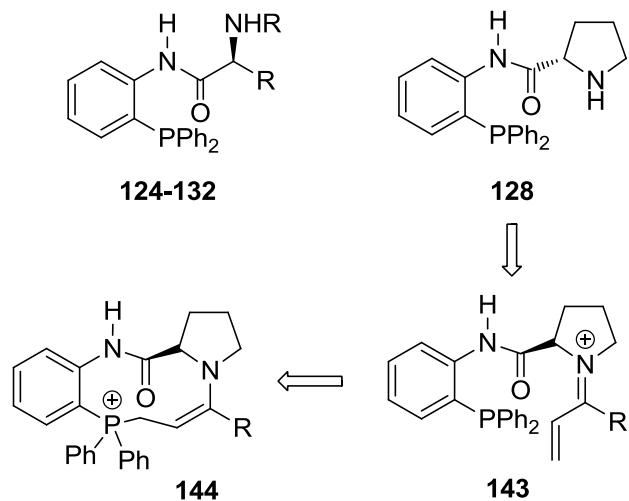
This equilibrium between Lewis base, Michael acceptor and PNP could be extended to a big range of Lewis base and Michael acceptor, in which the nucleophilicity of Lewis base and the electrophilicity of Michael acceptor for Michael addition could be determined.
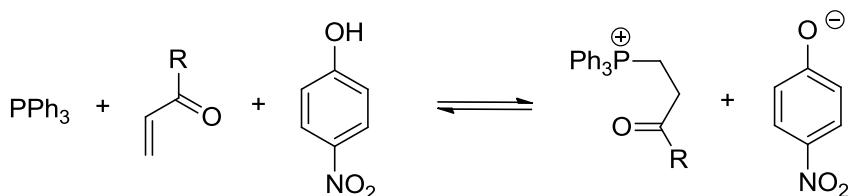
In summary, the thesis described a N- or P-centered Lewis base-catalyzed aMBH reaction with mechanistic study. We hope our finding here would be helpful for the organocatalysts design and better understanding of the MBH reaction in the future.

4   EXPERIMENTAL PART

General information

All air and water sensitive manipulations were carried out under a nitrogen atmosphere using standard Schlenk techniques. Schlenk flasks were dried in the oven at 120 °C for at least 12 hours prior to use and then assembled quickly while still hot, cooled under a nitrogen stream and sealed with a rubber septum. All commercial chemicals were of reagent grade and were used as received unless otherwise noted. Dichloromethane and chloroform were refluxed for at least one hour over CaH_2 and subsequently distilled. Methyl vinyl ketone, cyclohexenone, ethyl acrylate were distilled freshly before use. Commercial PS-DMAP polymer (base loading ≈ 3.0 mmol/g DMAP, polystyrene crosslinked with 2 % of DVB) and Merrifield´s resin (Mesh: 100-200, loading: 2.0 to 3.0 mmol/g Cl^-, polystyrene crosslinked with 1 % DVB) were purchased from Sigma-Aldrich and dried overnight under vacuum at 60 °C before use. ^1H and ^{13}C NMR spectra were recorded on Varian 300 or Varian INOVA 400 machines at ambient temperature. All ^1H chemical shifts are reported in ppm (δ) relative to $CHCl_3$ (7.26); ^{13}C chemical shifts are reported in ppm (δ) relative to $CDCl_3$ (77.16). ^1H NMR kinetic data were measured on a Varian Mercury 200 at 23 °C. HRMS spectra (ESI-MS) were carried out using a Thermo Finnigan LTQ FT instrument. IR spectra were measured on a Perkin-Elmer FT-IR BX spectrometer mounting ATR technology. All the reactions promoted by polymer supported catalysts were mechanically shaken on a IKA KS 130 shaker; for each reaction the rotation speed was set at 480 turns/minute. Analytical TLC were carried out using aluminium sheets coated with silica gel Si 60 F_{254}.

The experimental procedures, compound data, kinetic data and graphics described in the **Experimental Part** are ordered according to the chapters in the **Results and Discussion** section.

4.1 Amine-catalyzed Morita-Baylis-Hillman reaction

4.1.1 Synthesis of tosylimines[126]

$$\text{Ar-CHO} \quad + \quad \text{TsNH}_2 \quad \xrightarrow[160\,^\circ\text{C}]{\text{Si(OEt)}_4} \quad \text{Ar}-\text{CH}=\text{NTs}$$

93a-i
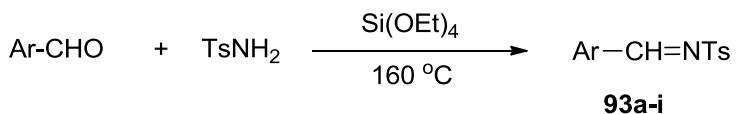
93a: Ar = p-CNC$_6$H$_5$,   **93b**: Ar = p-NO$_2$C$_6$H$_4$,   **93c**: Ar = p-ClC$_6$H$_4$,
93d: Ar = o-ClC$_6$H$_4$,   **93e**: Ar = p-BrC$_6$H$_4$,   **93f**: Ar = C$_6$H$_4$,
93g: Ar = p-MeC$_6$H$_4$,   **93h**: Ar = p-MeOC$_6$H$_4$,   **93i**: Ar = $trans$-C$_6$H$_4$-CH=CH

Under nitrogen atmosphere aldehyde (20 mmol), p-toluenesulfonamide (20 mmol, 3.4 g) and tetraethyl orthosilicate (24 mmol, 5.4 mL) were added to a 100 mL flask with condenser and distillation setup. The reaction mixture was heated to 150 $^\circ$C by microwave irradiation for 10 hours, and the ethanol generated from the reaction was removed by distillation. The residue was dissolved in 20 mL of dichloromethane, and poured into 400 mL of cold isohexane, and this cold mixture was stirred for another 30 min to precipitate the imine. After filtration and drying under high vaccum for 5 hours, the tosyl imine was isolated as a white solid (60-90 % yield).

93a: ^{1}H NMR (200 MHz, CDCl$_3$): δ 2.45 (3H, s, Me), 7.35 (2H, d, J = 7.4Hz, Ar), 7.77 (2H, d, J = 7.6 Hz, Ar), 7.89 (2H, d, J = 8.0 Hz, Ar), 8.01 (2H, d, J = 8.0 Hz, Ar), 9.05(1 H, s).

93b: ^{1}H NMR (200 MHz, CDCl$_3$): δ 2.46 (3H, s, Me), 7.39 (2H, d, J = 7.9Hz, Ar), 7.91 (2H, d, J = 8.0 Hz, Ar), 8.12 (2H, d, J = 8.6 Hz, Ar), 8.34 (2H, d, J = 8.6 Hz, Ar), 9.11(1 H, s).

93c: ^{1}H NMR (200 MHz, CDCl$_3$): δ 2.44 (3H, s, Me), 7.36 (2H, d, J = 7.9 Hz, Ar), 7.47 (2H, d, J = 8.6 Hz, Ar), 7.86 (2H, d, J = 8.6 Hz, Ar), 7.88 (2H, d, J = 7.9 Hz, Ar), 9.00 (1 H, s).

93d: ^{1}H NMR (200 MHz, CDCl$_3$): δ 2.45 (3H, s, Me), 7.38-7.38(3H, m, Ar), 7.45-7.56 (2H, m, Ar), 7.88-7.93 (2H, m, Ar), 8.16 (1H, dd, J_1 = 7.8 Hz, J_2 = 1.2 Hz, Ar), 9.50 (1 H, s).

93e: ^{1}H NMR (200 MHz, CDCl$_3$): δ 2.43 (3H, s, Me), 7.35 (2H, d, J = 7.9 Hz, Ar), 7.62 (2H, d, J = 8.5 Hz, Ar), 7.86 (2H, d, J = 8.6 Hz, Ar), 7.88 (2H, d, J = 7.9 Hz, Ar), 8.97 (1 H, s).

93f: ^{1}H NMR (200 MHz, CDCl$_3$): δ 2.44 (3H, s, Me), 7.35 (2H, d, J = 8.6 Hz, Ar), 7.47 (2H, dd, J = 7.4 Hz, J = 7.9 Hz, Ar), 7.59-7.65 (1H, m, Ar), 7.88-7.94 (4H, m, Ar), 9.03 (1 H, s).

93g: ^{1}H NMR (200 MHz, CDCl$_3$): δ 2.42 (3H, s, Me), 2.43 (3H, s, Me), 7.28 (2H, d, J = 8.5 Hz, Ar), 7.34 (2H, d, J = 7.9 Hz, Ar), 7.81 (2H, d, J = 8.5 Hz, Ar), 7.88 (2H, d, J = 7.9 Hz, Ar), 8.99(1 H, s).

93h: ^{1}H NMR (200 MHz, CDCl$_3$): δ 2.42 (3H, s, Me), δ 3.87 (3H, s, Me), 6.96 (2H, d, J = 6.9Hz, Ar), 7.31 (2H, d, J = 7 Hz, Ar), 7.86 (4H, m, Ar), 8.93 (1 H, s).

93i: ^{1}H NMR (200 MHz, CDCl$_3$): δ 2.41 (3H, s, Me), 6.99 (1H, dd, J_1 = 15.6 Hz, J_2 = 9.3 Hz, Ar), 7.34 (2H, d, J = 8.1 Hz, Ar), 7.42-7.56 (6H, d, J = 8.1 Hz, Ar), 7.86 (2H, d, J = 8.1 Hz, Ar), 8.78 (1H, d, J = 9.3 Ar).

4.1.2 aMBH reaction of tosylimines and activated alkenes

4.1.2.1 Procedure for the aMBH reaction of tosylimine and methyl vinyl ketone catalyzed by PDLBs.
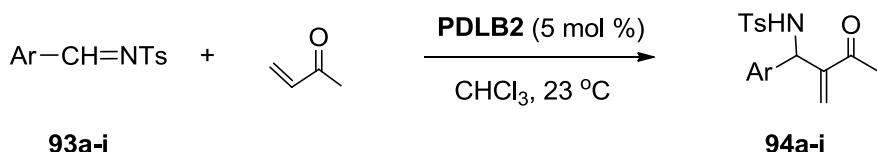
a: Ar = p-CNC$_6$H$_5$,   b: Ar = p-NO$_2$C$_6$H$_4$,   c: Ar = p-ClC$_6$H$_4$,
d: Ar = o-ClC$_6$H$_4$,   e: Ar = p-BrC$_6$H$_4$,   f: Ar = C$_6$H$_4$,
g: Ar = p-MeC$_6$H$_4$,   h: Ar = p-MeOC$_6$H$_4$,   i: Ar = $trans$-C$_6$H$_4$-CH=CH

Two stock solutions were first prepared, *A*: methyl vinyl ketone (0.9 mmol, 73 mg), tosylimine (0.75 mmol) and trimethoxybenzene (0.2 mmol, 33 mg) in 5 mL chloroform. *B*: catalyst **PDLB2** (0.1875 mmol, 46 mg) in 5 mL chloroform. 0.5 mL stock solution *A* and 0.1 mL stock solution *B* were mixed under nitrogen atmosphere. The reaction was monitored by ^{1}H NMR until the disappearance of all starting material (tosylimine) was observed. The reaction mixture was directly subjected to silica gel column chromatography and eluted with EtOAc / isohexane = 1/4 to give the corresponding aMBH product.

94a: ¹H NMR (200 MHz, CDCl₃): δ 2.12 (3H, s, Me), 2.39 (3H, s, Me), 5.30 (1H, d, *J* = 9.2 Hz), 6.04 (1H, s), 6.09 (1H, s), 6.14 (1H, d, *J* = 9.4 Hz), 7.24 (4H, m, Ar), 7.45 (2H, d, *J* = 6,7 Hz, Ar), 7.64 (2H, d, *J* = 7.2 Hz, Ar).


94b: ¹H NMR (200 MHz, CDCl₃): 2.15 (3H, s, Me), 2.42 (3H, s, Me), 5.32 (1H, d, *J* = 9.4 Hz), 5.91 (1H, d, *J* = 9.4 Hz), 6.08 (1H, s), 6.13 (1H, s), 7.30 (4H, m, Ar), 7.64 (2H, d, *J* = 8.3 Hz, Ar), 8.06 (2H, d, *J* = 8.7 Hz).
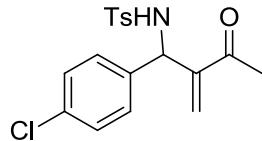

94c: ¹H NMR (200 MHz, CDCl₃): δ 2.15 (3H, s, Me), 2.41 (3H, s, Me), 5.22 (1H, d, *J* = 8Hz, NH), 5.72 (1H, d, *J* = 8.4 Hz, CH), 6.05 (1H, s), 6.09 (1H, s,), 7.01 (2H, d, *J* = 8.7Hz, Ar), 7.15 (4H, m, Ar), 7.62 (2H, d, *J* = 8.0Hz, Ar).
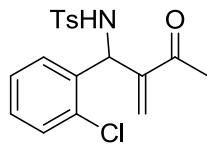
94d: ¹H NMR (200 MHz, CDCl₃): 2.21 (3H, s, Me), 2.37 (3H, s, Me), 5.68 (1H, d, *J* = 8.6 Hz), 5.78 (1H, d, *J* = 8.6 Hz), 6.16 (1H, s), 6.17 (1H, s,), 7.06-7.15 (2H, m, Ar), 7.20 (2H, d, *J* = 8.4Hz, Ar), 7.21-7.24 (1H, m, Ar), 7.30-7.33 (1H, m, Ar), 7.63 (2H, d, *J* = 8.4Hz, Ar).
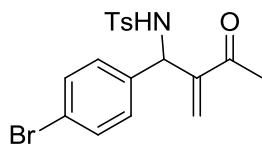

94e: ¹H NMR (200 MHz, CDCl₃): δ 2.17 (3H, s, Me), 2.52 (3H, s, Me), 5.26 (1H, d, *J* = 9.1 Hz), 5.67 (1H, d, *J* = 9.1 Hz), 6.16 (1H, s), 6.19 (1H, s), 7.12 (2H, d, *J* = 7.8 Hz), 7.29 (4H, m, Ar), 7.54 (2H, *J* = 7.8 Hz).


99
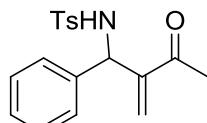
94f: ^{1}H NMR (200 MHz, CDCl$_3$): δ 2.15 (3H, s, Me), 2.43 (3H, s, Me), 5.26 (1H, d, J = 8.6 Hz), 5.61 (1H, d, J = 8.6 Hz), 6.10 (1H, s), 6.11 (1H, s), 7.11 (2H, m, Ar), 7.21-7.27 (5H, m, Ar), 7.68 (2H, d, J = 8.1 Hz, Ar).
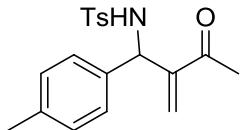
94g: ^{1}H NMR (200 MHz, CDCl$_3$): δ 2.15 (3H, s, Me), 2.26 (3H, s, Me), 2.41 (3H, s, Me), 5.23 (1H, d, J = 8.4 Hz), 5.66 (1H, d, J = 8.4 Hz), 6.09 (2H, s), 6.86-7.03 (4H, m, Ar), 7.24 (2H, m, Ar), 7.63 (2H, d, J = 8.0 Hz, Ar).


94h: ^{1}H NMR (200 MHz, CDCl$_3$): δ 2.16 (3H, s, Me), 2.41 (3H, s, Me), 3.74 (3H, s, Me), 5.22 (1H, d, J = 8.4 Hz, NH), 5.49 (1H, d, J = 8.4 Hz, CH), 6.09 (2H, s), 6.72 (2H, d, J = 8.2 Hz, Ar), 6.99 (2H, d, J = 8.8 Hz, Ar), 7.23 (2H, d, J = 8.0 Hz, Ar), 7.65 (2H, d, J = 8.2 Hz, Ar).
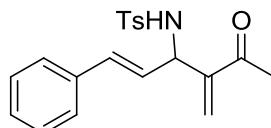
94i: ^{1}H NMR (200 MHz, CDCl$_3$): δ 2.19 (3H, s, Me), 2.33 (3H, s, Me), 4.77 (1H, dd, J_1 = 4.2 Hz, J_2 = 7.2 Hz, CH), 5.65 (1H, d, J = 8.6Hz, NH), 5.98 (1H, s), 5.99 (1H, dd, J_1 = 4.2 Hz, J_2 = 16.0 Hz), 6.00 (1H, s), 6.28 (1H, d, J = 16.0 Hz), 7.10-7.28 (7H, m, Ar), 7.69 (2H, d, J = 8.0 Hz, Ar).

4.1.2.2 Procedure for the aMBH reaction of tosylimine and 2-cyclohexenone catalyzed by PDLBs.
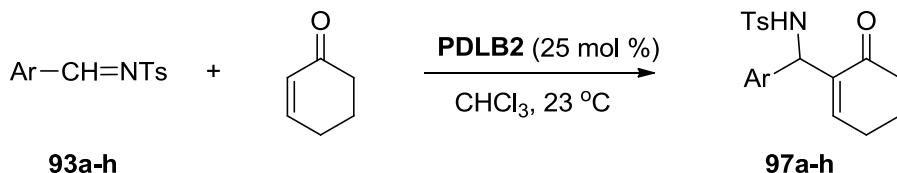

a: Ar = p-CNC$_6$H$_5$, **b**: Ar = p-NO$_2$C$_6$H$_4$, **c**: Ar = p-ClC$_6$H$_4$,
d: Ar = o-ClC$_6$H$_4$, **e**: Ar = p-BrC$_6$H$_4$, **f**: Ar = C$_6$H$_4$,
g: Ar = p-MeOC$_6$H$_4$, **h**: Ar = trans-C$_6$H$_4$-CH=CH

Two stock solutions were first prepared, *A*: cyclohexenone (6 mmol, 575 mg) and trimethoxylbenzene (0.4 mmol, 67.2 mg) in 5 mL chloroform. *B*: catalyst **PDLB2**

(0.4 mmol, 48.8 mg) in 1 mL chloroform. To a mixture of 0.5 mL stock solution *A* and 0.1 mL stock solution B was added tosylimine (0.15 mmol). The reaction was monitored by ^{1}H NMR until the disappearance of all starting material (tosylimine) was dectected. The reaction mixture was directly subjected to silica gel column chromatography and eluted with EtOAc / isohexane = 1/4 to give the corresponding aMBH product.
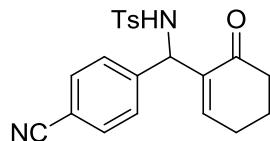

N-((4-cyanophenyl)(6-oxocyclohex-1-en-1-yl)methyl)-4-methylbenzenesulfon-amide **97a**: white solid. IR: 3265 (NH), 3300, 2954, 2924, 2225, 1662 (C=O), 1606, 1598, 1501, 1495, 1423, 1396, 1330, 1305, 1287, 1248, 1160, 1094, 1079, 1043, 1018, 980, 927, 906, 876, 865, 826, 811, 733, 706 cm^{-1}. ^{1}H NMR (CDCl$_3$, 300 MHz): 1.64-1.74 (1H, m, CH$_2$), 1.76-1.79 (1H, m, CH$_2$), 2.05-2.17 (2H, m, CH$_2$), 2.22-2.30 (2H, m, CH$_2$), 2.41 (3H, s, CH$_3$), 5.09 (1H, s), 6.02 (1H, s), 6.81 (1H, t, *J* = 3.0 Hz), 7.25 (1H, d, *J* = 9.0 Hz, Ar), 7.34 (2H, d, *J* = 9.0 Hz, Ar), 7.51 (2H, d, *J* = 6.0 Hz, Ar), 7.63 (2H, d, *J* = 6.0 Hz, Ar). ^{13}C NMR (CDCl$_3$, 75 MHz): 21.49, 21.87, 25.84, 38.24, 59.50, 111.27, 118.53, 126.98, 127.23, 129.52, 132.14, 136.07, 137.69, 143.52, 144.64, 150.09, 151.07. MS (EI): *m/e* 331, 281, 253, 207, 155 (MePhSO$_2$$^+$), 91 (MePh$^+$). HRMS (ESI) [M-H]$^+$ Calcd. for C$_{21}$H$_{19}$N$_2$O$_3$S: requires 379.1116, Found: 379.1123.


97b: ^{1}H NMR (CDCl$_3$, 200 MHz): 1.57-1.95 (2H, m, CH$_2$), 2.02-2.37 (4H, m, CH$_2$), 2.41 (3H, s, CH$_3$), 5.14 (1H, d, *J* = 9.4 Hz), 6.07 (1H, d, *J* = 9.4 Hz), 6.84 (1H, t, *J* = 4.2 Hz), 7.25 (2H, d, *J* = 6.8 Hz, Ar), 7.39 (2H, d, *J* = 8.8 Hz, Ar), 7.63 (2H, d, *J* = 8.4 Hz, Ar), 8.08 (2H, d, *J* = 7.0 Hz, Ar).


97c: ^{1}H NMR (CDCl$_3$, 200 MHz): 1.55-1.96 (2H, m, CH$_2$), 2.00-2.34 (4H, m, CH$_2$), 2.41 (3H, s, CH$_3$), 5.05 (1H, d, *J* = 9.4 Hz), 5.96 (1H, d, *J* = 9.6 Hz), 6.80 (1H, t, *J* = 4.4 Hz), 7.09-7.27 (6H, m, Ar), 7.61 (2H, d, *J* = 7.6 Hz, Ar).

N-((2-chlorophenyl)(6-oxocyclohex-1-en-1-yl)methyl)-4-methylbenzenesulfon-amide **97d**: A white solid. IR: 3260 (NH), 2953, 2922, 2854, 1675, 1594, 1575, 1494, 1472, 1438, 1379, 1328, 1306, 1286, 1258, 1154, 1136, 1088, 1078, 1037, 980, 952, 913, 854, 815, 756, 744, 715, 705, 699, 608 cm^{-1}. ^{1}H NMR (CDCl$_3$, 300 MHz): 1.75-1.83 (2H, m, CH$_2$), 2.16-2.30 (4H, m, CH$_2$), 2.36 (1H, s, CH$_3$), 5.53 (1H, d, J = 6.0 Hz), 6.13 (1H, d, J = 6.0 Hz), 6.99 (1H, t, J = 6.0 Hz), 7.08-7.10 (2H, m, Ar), 7.17 (2H, d, J = 6.0 Hz, Ar), 7.21-7.22 (1H, m, Ar), 7.42-7.44 (1H, m, Ar), 7.62 (2H, d, J = 6.0 Hz, Ar).^{13}C NMR (CDCl$_3$, 75 MHz): 21.44, 21.51, 25.83, 38.47, 56.24, 126.44, 126.71, 127.23, 128.52, 129.21, 129.31, 129.48, 129.68, 132.42, 135.77, 136.38, 143.13, 150.14, 199.0 HRMS (ESI) [M+Na]$^+$ Calcd. for C$_{20}$H$_{20}$ClNNaO$_3$S: requires 412.0750, Found: 412.0743.


N-((4-bromophenyl)(6-oxocyclohex-1-en-1-yl)methyl)-4-methylbenzenesulfon-amide **97e**: white solid. IR: 3356 (NH), 3259, 3187, 2925, 2865, 1668 (C=O), 1597, 1527, 1486, 1454, 1423, 1387, 1335, 1303, 1286, 1158, 1092, 1078, 1051, 1007, 980, 957, 933, 917, 905, 814, 797, 736, 708, 688, 660, 633 cm^{-1}. ^{1}H NMR (CDCl$_3$, 300 MHz): 1.61-1.74 (1H, m, CH$_2$), 1.78-1.88 (1H, m, CH$_2$), 2.07-2.10 (2H, m, CH$_2$), 2.20-2.28 (2H, m, CH$_2$), 2.41 (3H, s, CH$_3$), 5.03 (1H, d, J = 6.9 Hz), 5.99 (1H, d, J = 6.9 Hz), 6.80 (1H, t, J = 3.3 Hz), 7.06 (1H, d, J = 6.3 Hz, Ar), 7.23 (2H, d, J = 6.3 Hz, Ar), 7.33 (2H, d, J = 6.3 Hz, Ar), 7.61 (2H, d, J = 6.3 Hz, Ar). ^{13}C NMR (CDCl$_3$, 75 MHz): 21.48, 21.93, 25.80, 38.33, 59,15, 121.372, 127.26, 128.02,129.44, 131.40, 136.49, 137.72, 138.38, 143.31, 149, 33, 198.87. MS (EI): m/e 334, 281, 264 (M$^+$+1-170), 207, 183(MePhSO$_2$NHCH$_2$$^+$), 171(MePhSO$_2NH_2$$^+$), 155 (MePhSO$_2$$^+$), 91 (MePh$^+$), HRMS (ESI) [M]$^+$ Calcd. for C$_{20}$H$_{24}$O$_3$N$_2$BrS: requires 451.0691, Found: 451.0687.
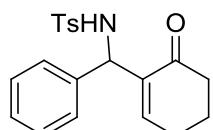
97f: ^{1}H NMR (CDCl$_3$, 200 MHz): 1.60-1.70 (2H, m, CH$_2$), 1.73-1.84 (4H, m, CH$_2$), 2.39 (3H, s, CH$_3$), 5.11 (1H, d, J = 9.2 Hz), 6.05 (1H, d, J = 9.4 Hz), 6.84 (1H, t, J = 4.2 Hz), 7.12-7.28 (6H, m, Ar), 7.62 (2H, d, J = 8.6 Hz, Ar).
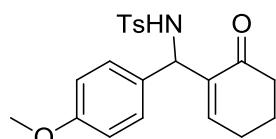

97h: ^{1}H NMR (CDCl$_3$, 200 MHz): 1.58-1.92 (2H, m, CH$_2$), 2.03-2.30 (4H, m, CH$_2$), 2.40 (3H, s, CH$_3$), 3.74 (3H, s, CH$_3$), 5.06 (1H, d, J = 9.2 Hz), 5.92 (1H, d, J = 9.4 Hz), 6.71-6.81 (3H, m), 7.08 (1H, d, J = 6.8 Hz), 7.22 (2H, d, J = 8.6 Hz, Ar), 7.62 (2H, d, J = 8.2 Hz, Ar).
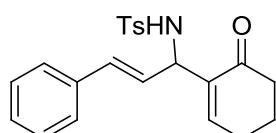
(E)-4-methyl-N-(1-(6-oxocyclohex-1-en-1-yl)-3-phenylallyl)benzenesulfonamide **97i**: IR: 3288 (NH), 3026, 2955, 2924, 2867, 1732, 1660, 1596, 1493, 1447, 1426, 1385, 1326, 1304, 1250, 1213, 1160, 1151, 1090, 1028, 974, 914, 883, 841, 815, 757, 747, 698, 632 cm^{-1}. ^{1}H NMR (CDCl$_3$, 300 MHz): 1.68-1.75 (1H, m, CH$_2$), 1.78-1.88 (1H, m, CH$_2$), 2.11-2.28 (4H, m, CH$_2$), 2.35 (3H, s, CH$_3$), 4.64 (1H, t, J = 6.0 Hz), 5.85 (1H, d, J = 9.0 Hz), 6.08 (1H, dd, J = 9.0 Hz, J = 6.0 Hz), 6.33 (1H, d, J = 18 Hz), 6.79 (1H, t, J = 6.0 Hz), 7.19-7.28 (7H, m, Ar), 7.69 (2H, d, J = 9.0 Hz, Ar). ^{13}C NMR (CDCl$_3$, 75 MHz): 21.40, 22.03, 25.77, 38.37, 59.19, 126.45, 126.48, 127.38, 127.80, 128.40, 129.41, 131.53, 136.15, 143.13, 148.53, 199.11. HRMS (ESI) (M+Na) Calcd. for C$_{22}$H$_{23}$NNaO$_3$S: requires 404.1296, Found: 404.1291.

4.1.2.3 The procedure of aMBH reaction of tosylimine and ethyl acrylate catalyzed by PDLBs.
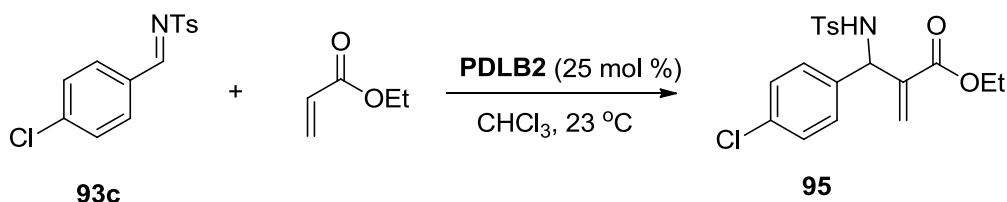
To a solution of tosyl imine (0.15 mmol, 44 mg), ethyl acrylate (0.6 mmol, 60 mg) and trimethoxybenzene (0.02 mmol, 3.5 mg) in 0.6 ml chloroform, was added **PDLB2** (0.04 mmol, 10 mg). The reaction was monitored by ^{1}H NMR spectroscopy following the disappearance of starting material (tosylimine).

4.1.2.4 Kinetic measurements of PDLB catalyzed aMBH reaction (**Analysis**)

If not noted, all the rate meausurements in this thesis are proceeded by this procedure.


TMB   **16a-d**
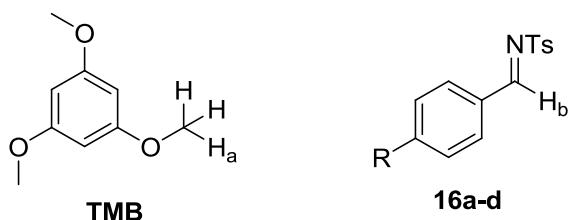
Trimethoxybenzene. ^{1}H NMR (200 MHz, CDCl$_3$): 3.74(9H, s), 6.06(3H, s).

I_{H_a} is the overall intensity of the methyl groups of the internal standard 1,3,5-trimethoxybenzene (**TMB**), I_{H_b} is the intensity of the imine proton of the substrate, $I_{H_{a0}}$ is the overall intensity of the methyl groups of **TMB** at the reaction start, $I_{H_{b0}}$ is the intensity of the imine proton of the substrate at the reaction start.

$$\text{conversion (\%)} = (1 - \frac{I_{H_b} \times I_{H_{a0}}}{I_{H_a} \times I_{H_{b0}}}) \times 100$$

Rate measurements have been performed through following the disappearance of the minor reaction component (tosylimine) by the integral of the proton signal at 8.99 ppm comparing with the proton signal of trimethoxylbenzene at 3.74 ppm.
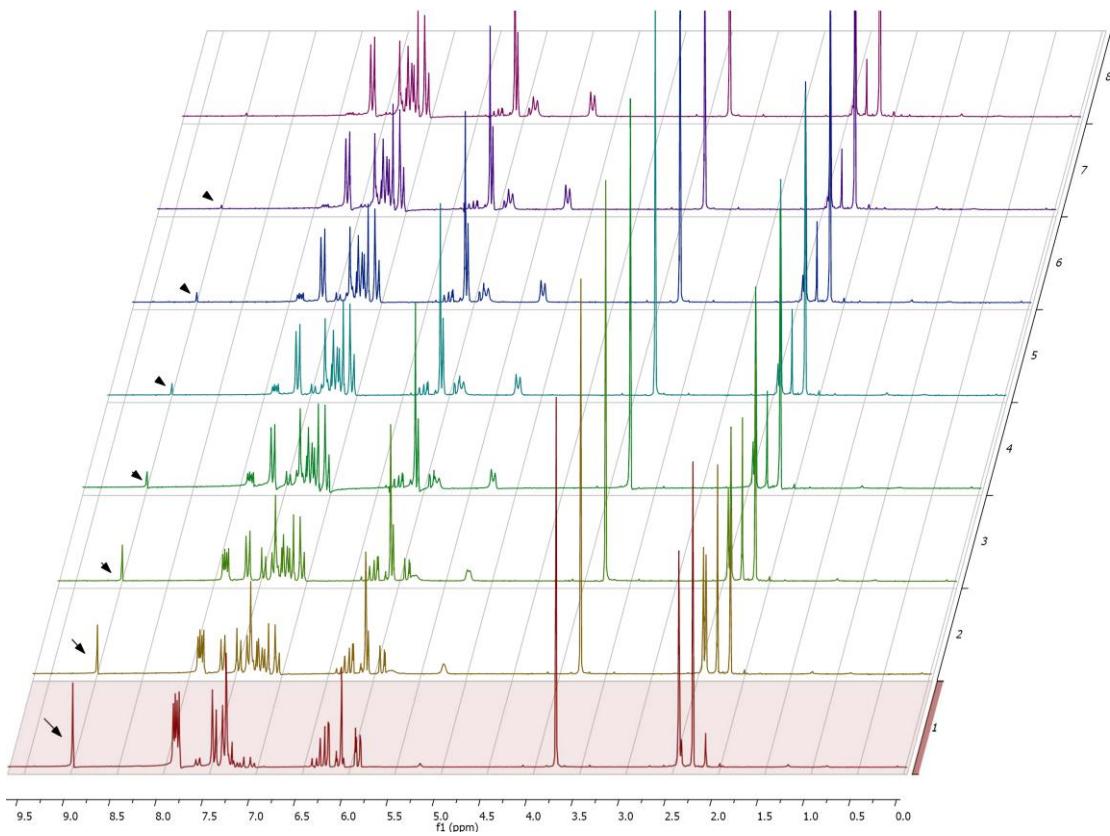
Fitting:

The kinetic data collected for the aMBH reaction were found to fit perfectly in the following rate law:

$$\text{conversion (\%)} = c_0\left(1 - \exp(-k(t - t_0))\right) \times 100$$

parameters: c_0 (final conversion), k(rate constant), t_0 (starting time)

Half-life time:

$$t_{1/2} = \frac{\ln 2}{k}$$

4.1.2.5 Kinetic measurements of PDLBs-catalyzed aMBH reactions (**graphics**).

The kinetic data of PDLBs catalyzed aMBH reaction of tosylimine with methyl vinyl ketone, cyclohexenone and ethyl acrylate are shown in Figure IV-1-5.
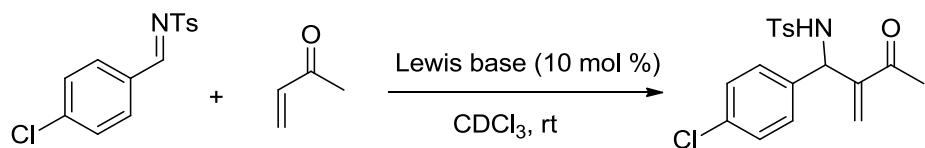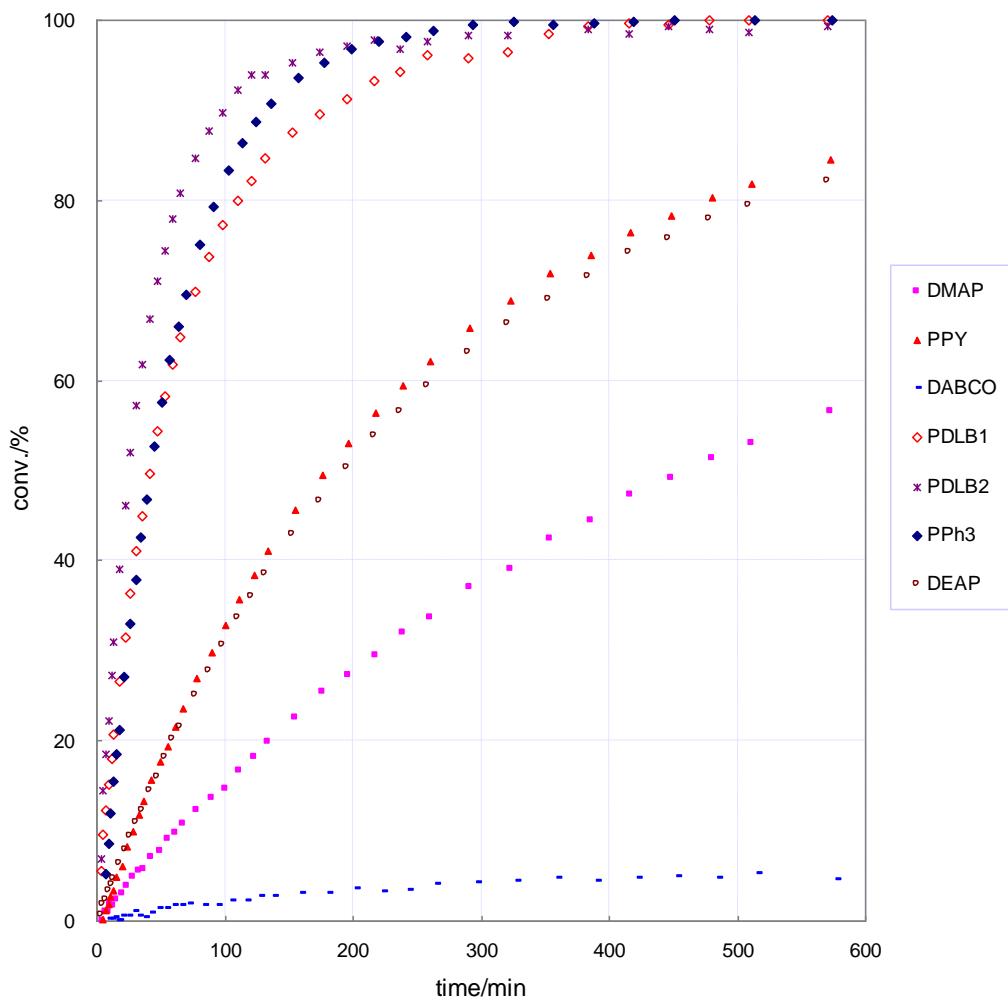
Figure IV-1. aMBH reactions of *N*-tosylimine with MVK in the presence of Lewis base.
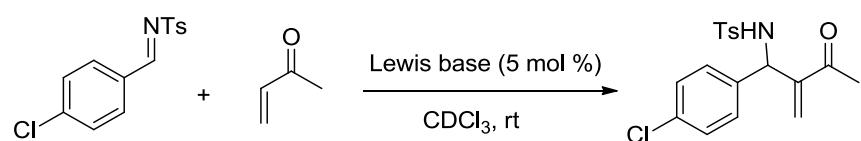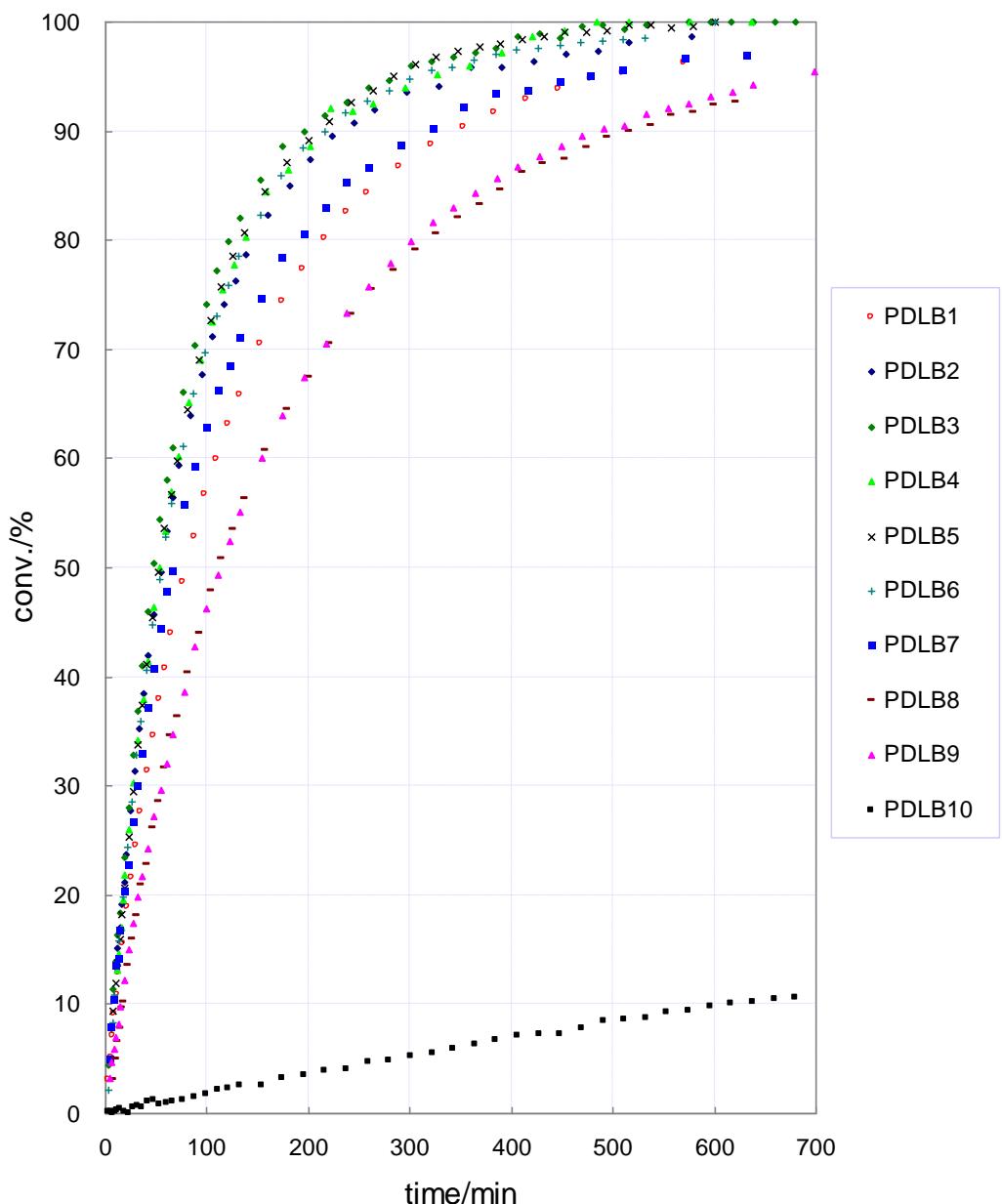
Figure IV-2. aMBH reactions of *N*-tosylimine with MVK in the presence of PDLBs.
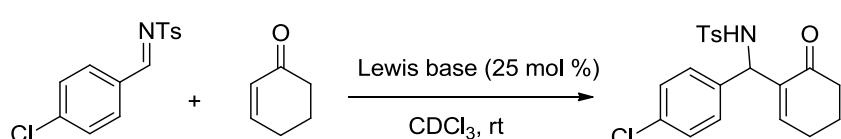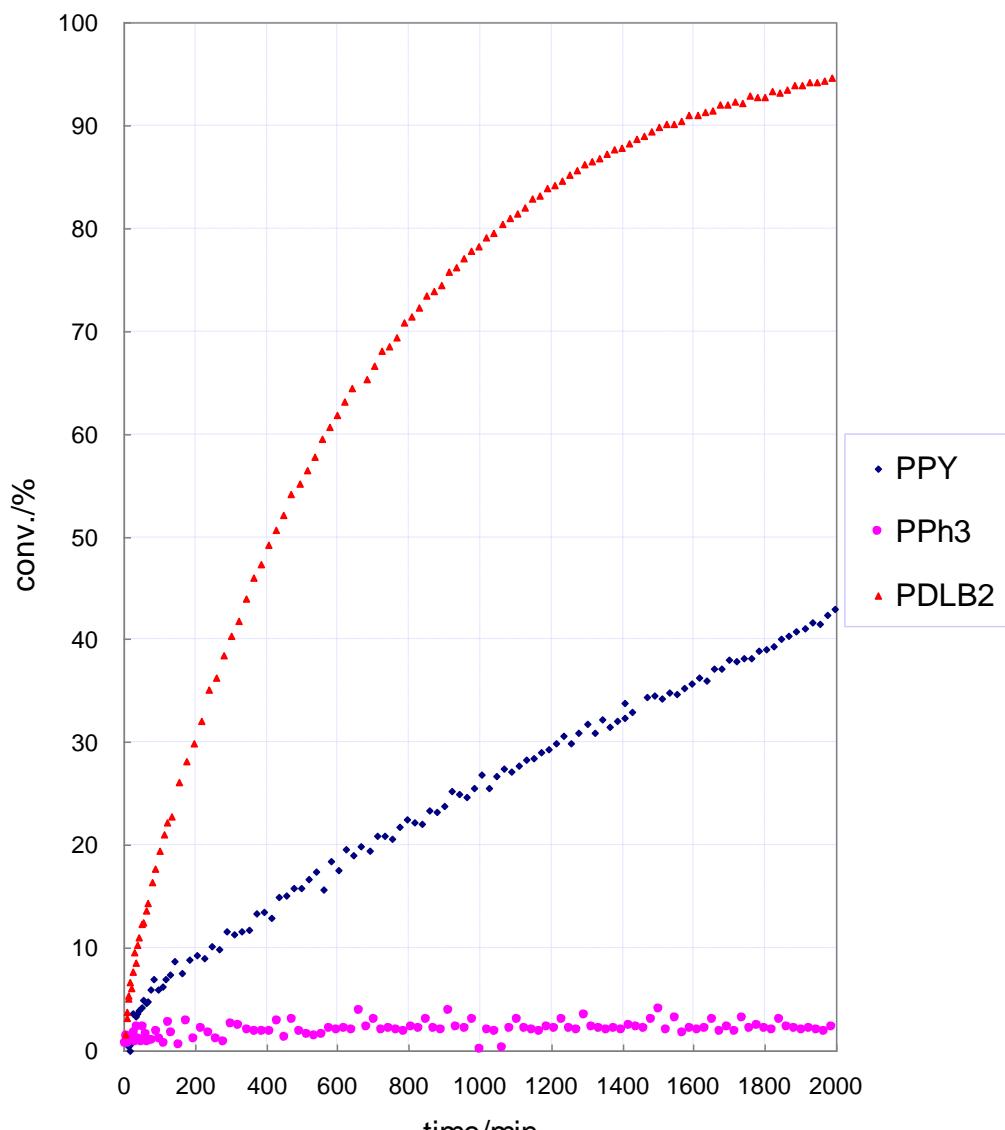
Figure IV-3. aMBH reactions of *N*-tosylimine with cyclohexenone in the presence of Lewis bases.
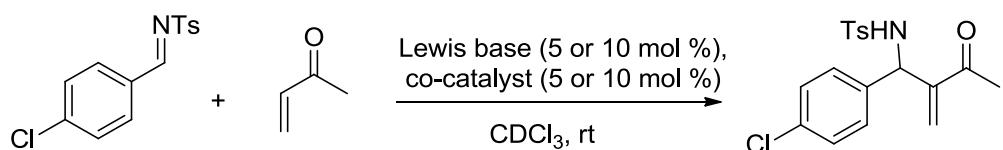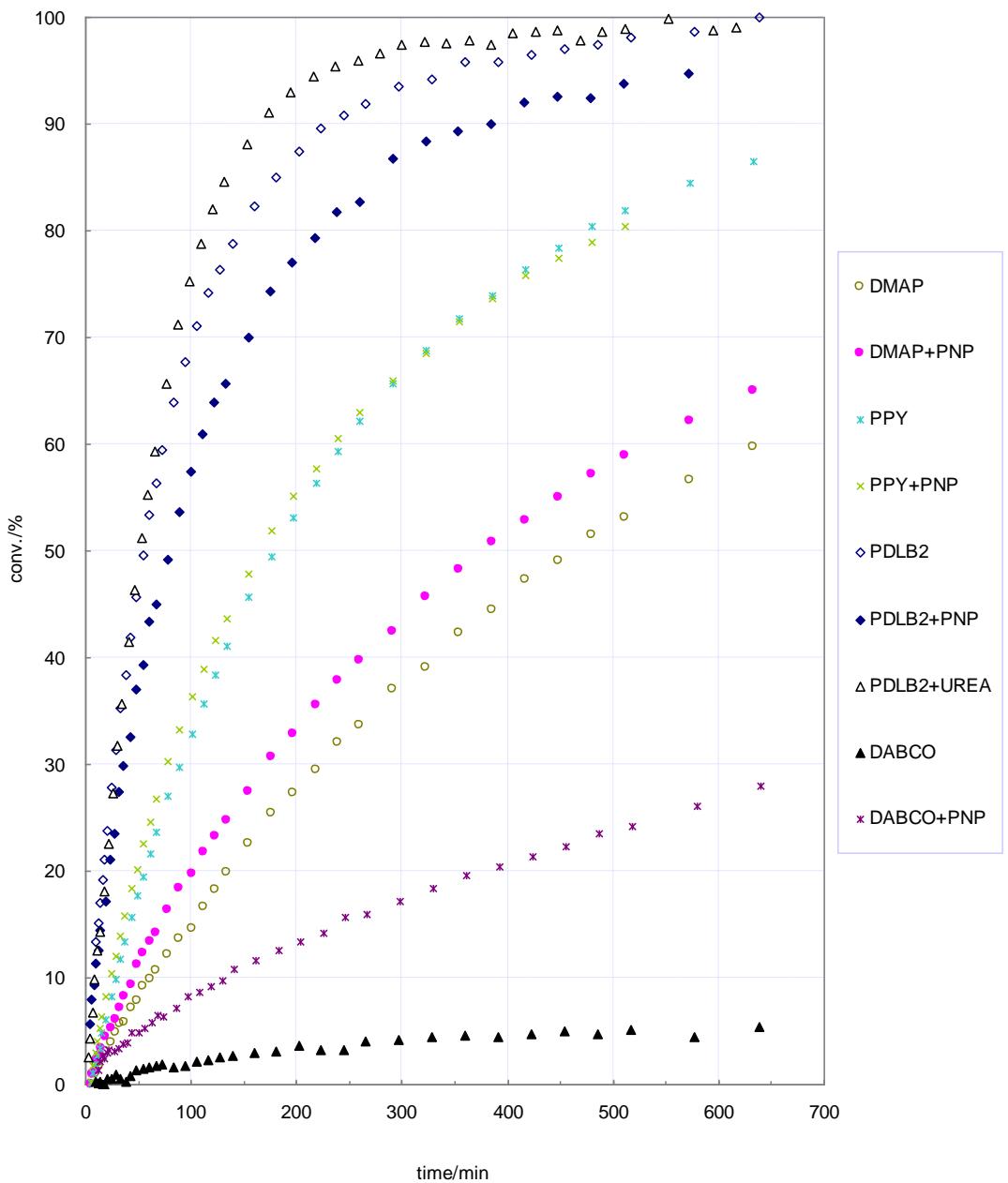
Figure IV-4. aMBH reactions of *N*-tosylimine with MVK catalyzed by Lewis bases and Brönsted acid (UREA =1,3-diphenylurea).

4.1.2.6 Homogeneous and heterogeneous PDLBs-catalyzed aMBH reactions.

Homogeneous catalysis:

Two stock solutions were prepared in dry calibrated 5 mL flasks; stock solution A: 0.15 M in tosylimine, 0.18 M in methyl vinyl ketone and 0.1 M in 1,3,5-trimethoxy benzene (internal standard) in $CDCl_3$, stock solution B: 0.0375 M in catalyst in $CDCl_3$. Under a nitrogen atmosphere, 0.5 mL of stock solution A and 0.1 mL of stock solution B were injected into a NMR tube, which was sealed by melting its opening with a flame. The sample was periodically submitted to NMR analysis in order to collect the kinetic information.

Heterogenous catalysis and catalyst recovery:

0.375 mmol of supported catalyst were added to a solution of tosylimine (3.75 mmol), methyl vinyl ketone (4.5 mmol, 315 mg) and 1,3,5-trimethoxybenzene (1.0 mmol, 168 mg, internal standard) in 30 mL of $CDCl_3$. The reaction vessel was shaken at room temperature (480 turns/min). Periodically, the agitation was interrupted for about one minute until all the resin would float on top of the solution, thus allowing the removal of 100 µL of a solid-free sample from the bottom of the reaction mixture using a syringe. The sample was diluted with 0.6 mL of $CDCl_3$ solution and subsequently submitted to ^{1}H NMR spectroscopy in order to determine the kinetic information.

At the end of the reaction the heterogeneous mixture was filtered under reduced pressure on a Büchner funnel covered by a disc of filter paper. The catalyst was washed with $CHCl_3$ (3 x 50 mL), collected in a dry 50 mL flask and dried overnight under high vacuum at 60 °C.

Isolation of the aMBH products:

The filtrate was evaporated under reduced pressure. The crude material was purified through column chromatography on silica gel (4:1 hexanes/EtOAc) affording the desired aMBH product along with 2 to 20 % of aromatic aldehyde derived from the partial hydrolysis of the tosylimine substrates.

The kinetic plots of homogeneous and heterogeneous PDLB catalyzed aMBH reactions are shown in Figure IV-5.
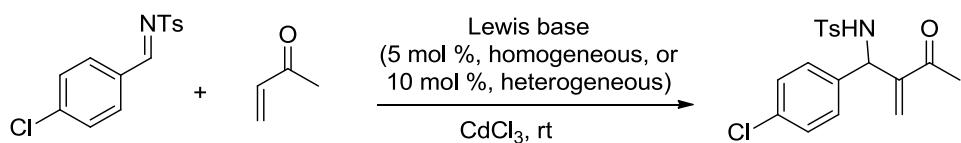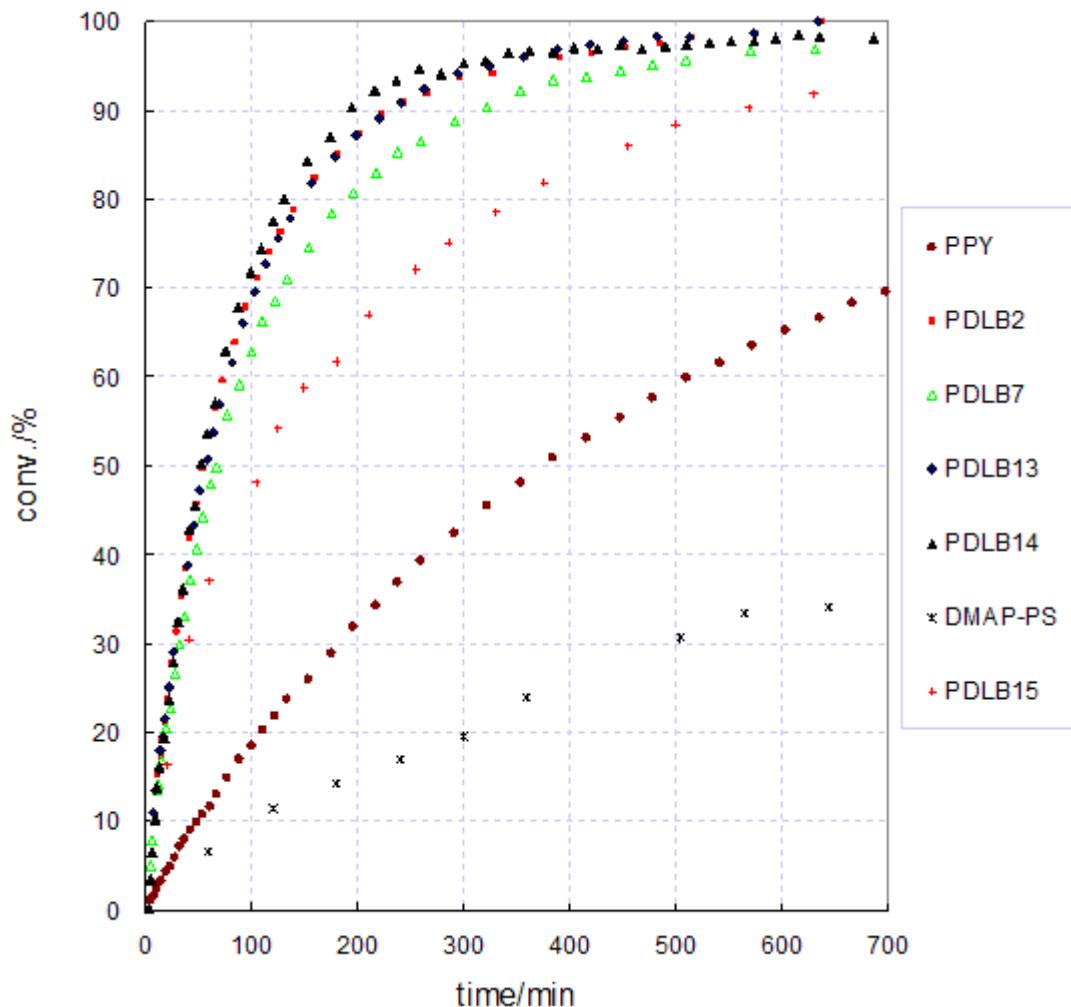
Figure IV-5. aMBH reactions of *N*-tosylimine with MVK in the presence of different Lewis bases and immobilized catalysts.

4.2 Phosphane-catalyzed aza-Morita-Baylis-Hillman reactions

4.2.1 Phosphane catalysts

4.2.1.1 Procedure for the aMBH reactions of tosylimine and methyl vinyl ketone catalyzed by tertiary phosphanes.

Two stock solutions were prepared in dry calibrated 5 mL flasks; stock solution *A*: 0.15 M in tosylimine, 0.18 M in methyl vinyl ketone and 0.1 M in 1,3,5-trimethoxy benzene (internal standard) in $CDCl_3$, stock solution *B*: 0.075 M in phosphane in $CDCl_3$. Under a nitrogen atmosphere, 0.5 mL of stock solution *A* and 0.1 mL of stock solution *B* were injected into a NMR tube. The sample was periodically submitted to NMR analysis in order to collect the kinetic information.

4.2.1.2 The kinetic graphic of Phosphane catalyzed aMBH reaction was shown in Figure IV-6.
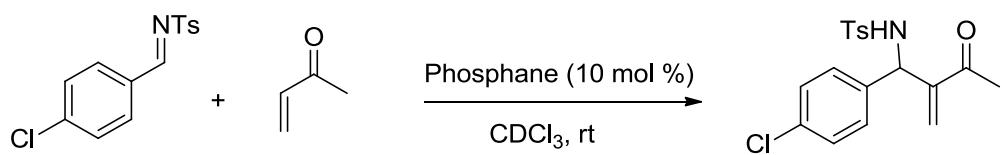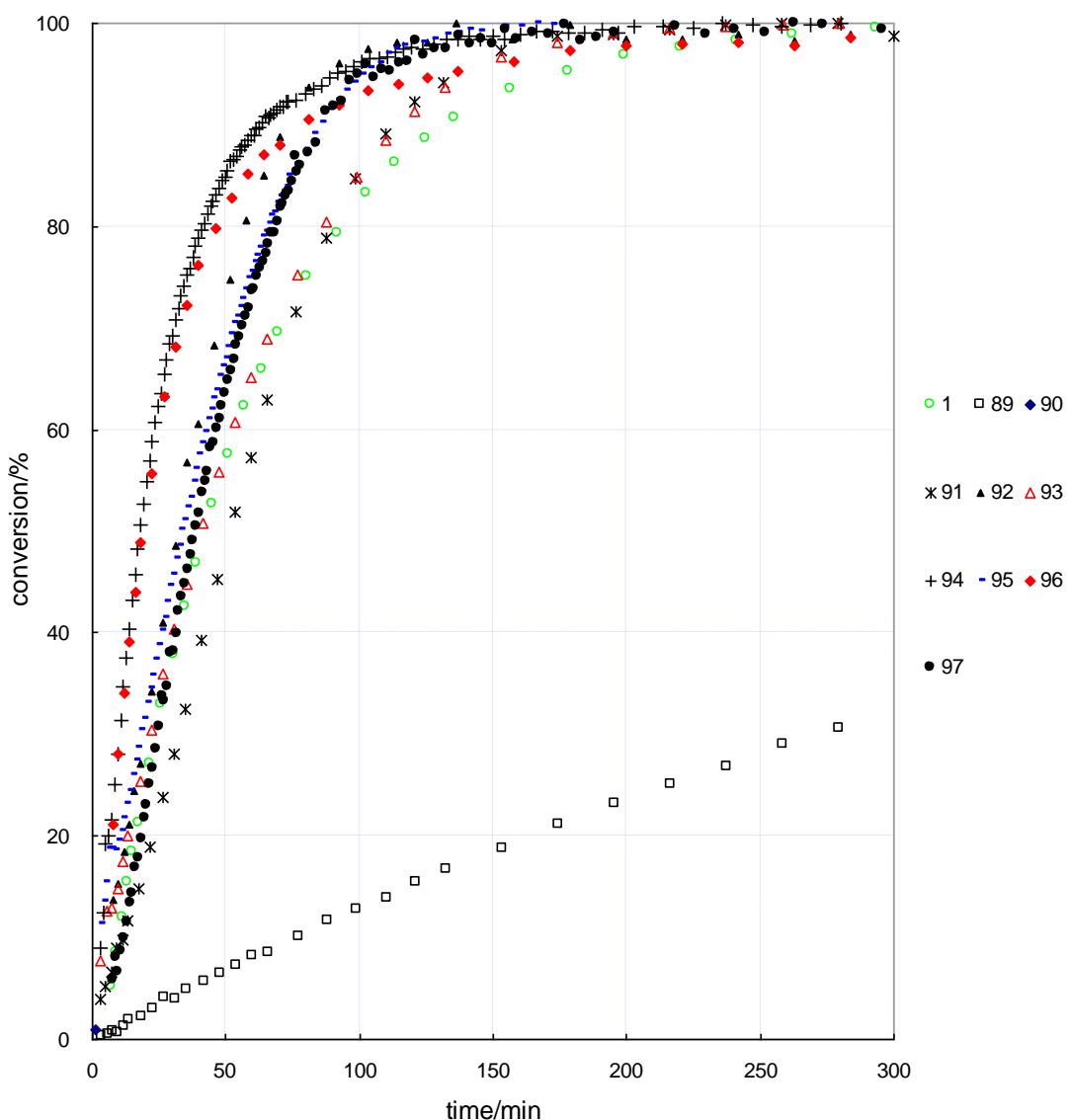
Figure IV-6. aMBH reactions of *N*-tosylimine with MVK in the presence of phosphanes.

4.2.2 PPh$_3$-catalyzed aza-Mortia-Baylis-Hillman reaction

The kinetic measurements were proceeded following the procedures described in **4.1.2.4**.
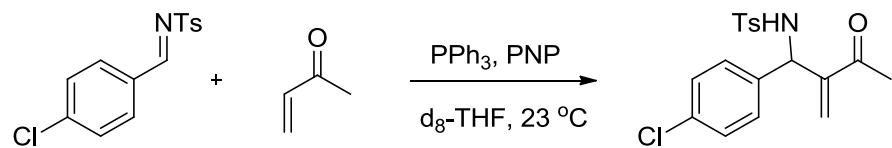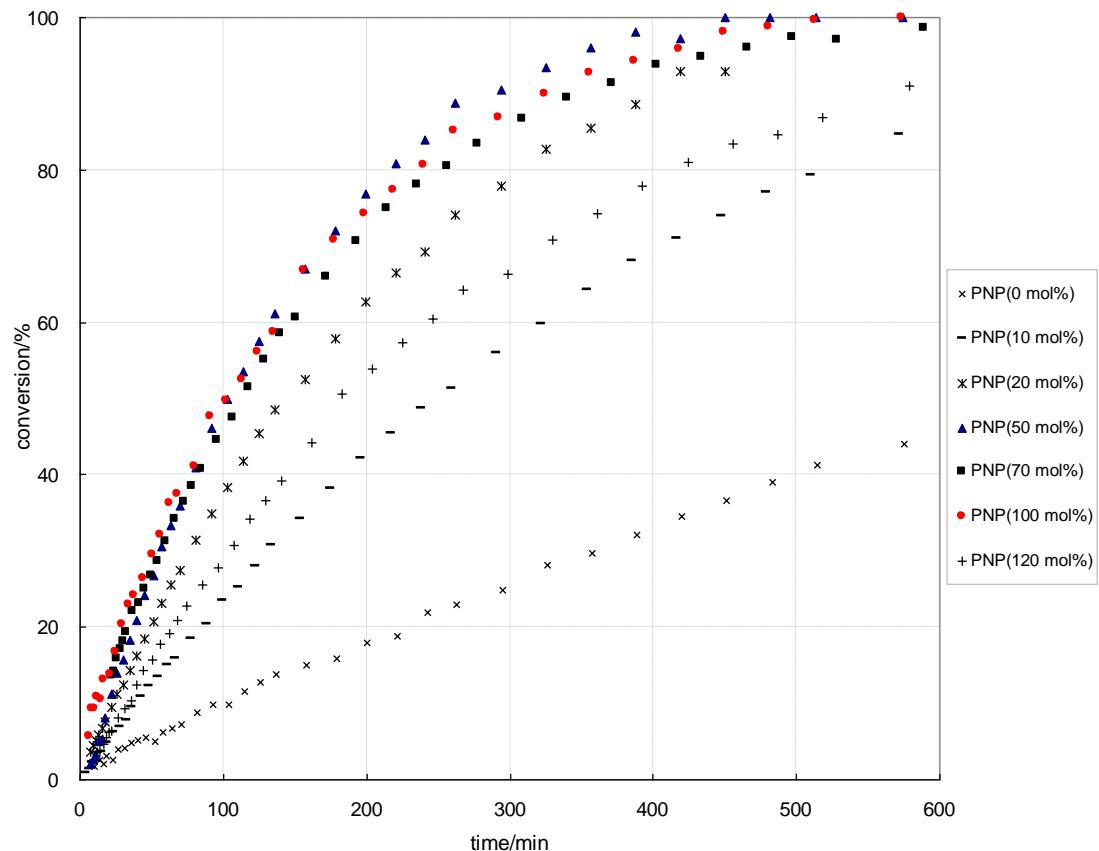
Figure IV-7. Co-catalyst effect in the PPh$_3$ (10 mol %) catalyzed aMBH reaction of *p*-chlorotosylimine (0.125 mmol/mL), MVK (120 mol %) and PNP (x mol %) in *d$_8$*-THF.

.
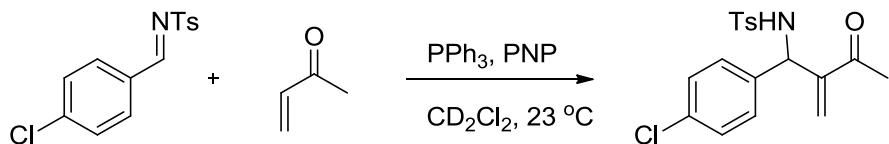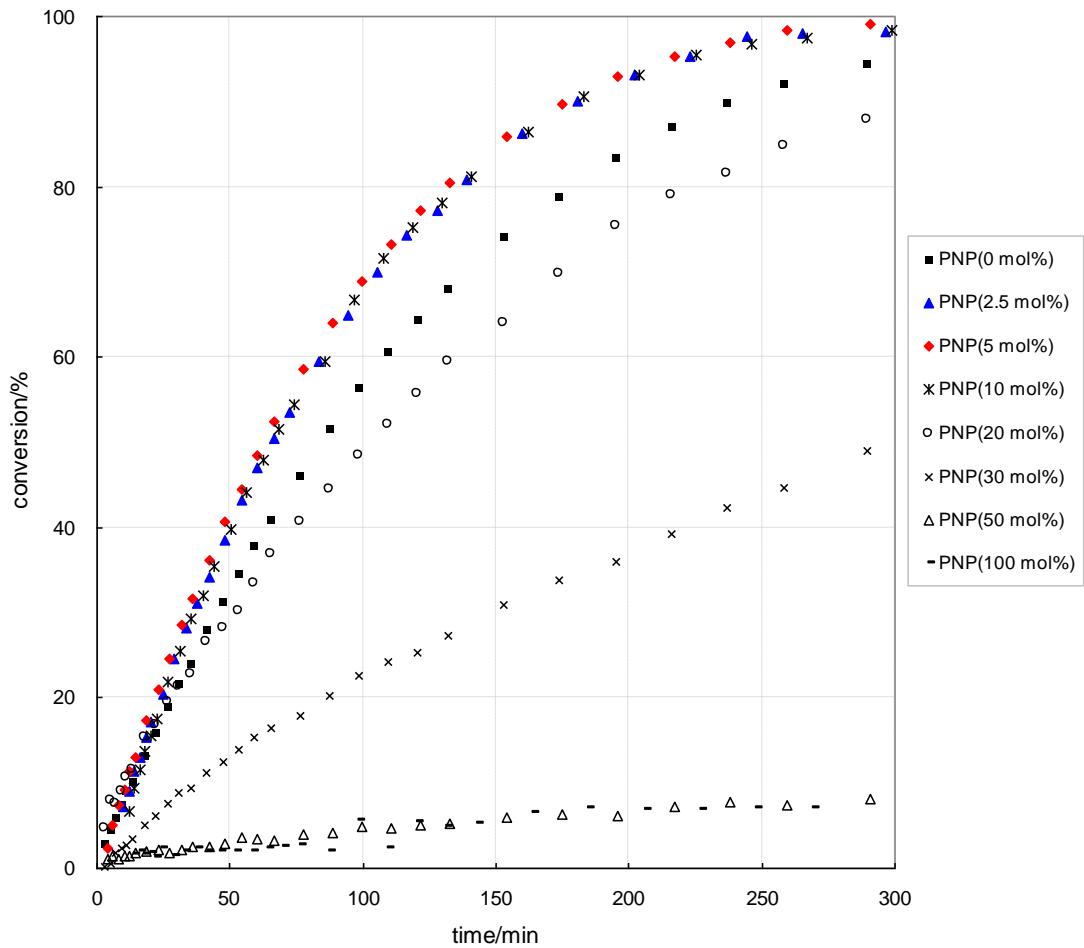
Figure IV-8. Co-catalyst effect in the PPh$_3$ (10 mol %) catalyzed aMBH reaction of
p-chlorotosylimines (0.125 mmol/mL), MVK (120 mol %) and PNP (x mol %) in
CD$_2$Cl$_2$.

4.2.3 Bifunctional phosphane catalysts

4.2.3.1 Synthesis of bifunctional phosphane catalysts
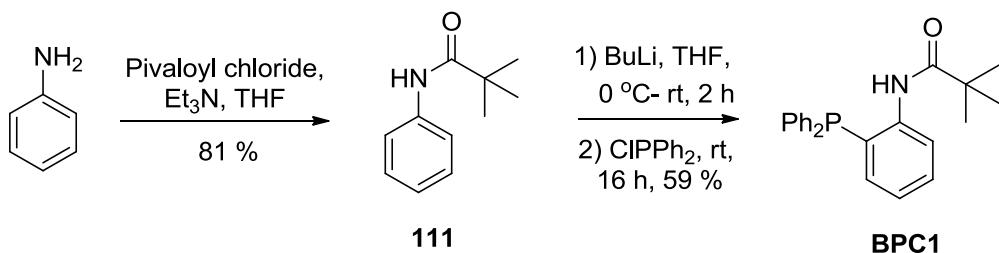
Synthesis of **111**: A solution of pivaloyl chloride (5.28 g, 44 mmol) in 20 mL THF was added dropwise r.t. to a solution of aniline (4 g, 43 mmol) and triethylamine (4.36 g, 43 mmol) in 40 mL THF. The resulting thick white suspension was stirred for 18 hours. After filtration, the filtrate was concentrated in vaccum, and the residue was recrystalized from diethyl ether to form a white solid (6.2g, 81 %). ^{1}H NMR (CDCl$_3$, 200 MHz): δ 1.31 (9H, s, Me), 7.04-7.55 (5H, m, Ar).

N-(2-(diphenylphosphino)phenyl)pivalamide **BPC1**. To a solution of **111** (438 mg, 2.5 mmol) in 40 ml dry THF was added dropwise butyl lithium (6 mmol, 2.4 mL of 2.5 M solution in Hexane) at 0 ^{o}C. The solution was stirred r.t.for 2 hours before chlorodiphenylphosphane (0.55 ml, 3 mmol) was added. After 16 hours, 1 mL water was injected to quench the reaction. After extraction, the organic phase was dried over MgSO$_4$ and evaporated in vaccum, and the residue was purified through column chromatography on silica gel (1:4 EtOAc/ihexane) affording **BPC1** (0.532 g, 1.47 mmol, 59 %) as a white solid. IR: 3265 (NH), 3349, 3052, 2957, 2866 1685 (C=O), 1573, 1506, 1440, 1395, 1364, 1294, 1274, 1154, 1123, 1090, 1026, 997, 918, 867, 741, 694 cm^{-1}. ^{1}H NMR (CDCl$_3$, 400 MHz): δ 1.10 (9H, s, CH$_3$), 6.82 (1H, m, Ar), 7.03 (1H, t, J = 7.2 Hz, Ar), 7.26-7.39 (11H, m, Ar), 8.18-8.21 (2H, m, Ar). ^{13}C NMR (CDCl$_3$, 100 MHz): 27.27, 39.84, 121.93, 124.42, 126.43, 128.80, 129.31, 130.01, 133.24, 133.80, 134.14, 140.82, 176.34. ^{31}P NMR (CDCl$_3$, 108 MHz): -18.73. MS (EI): m/e 361, 346, 304, 277, 226, 198, 183, 107, 77, 57. HRMS (ESI) (M+H) Calcd. for C$_{23}$H$_{25}$NOP: requires 362.1674, Found: 362.1669.

110: 83 % (Lit. 62 %)
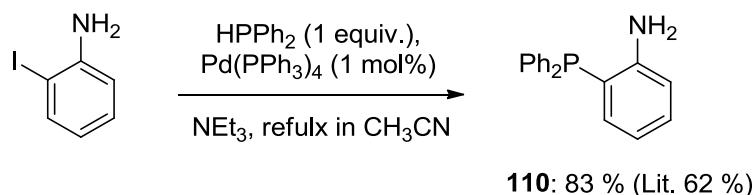
2-(diphenylphosphino)aniline **110**: 2-iodoaniline (1.095 g, 5 mmol), triethyl amine (508 mg, 5 mmol) and diphenylphosphane (931 mg, 5 mmol) were dissolved in 40 mL CH$_3$CN. To this solution was added Pd(PPh$_3$)$_4$ (58 mg, 0.05 mol). After refluxing for 18 hours, TLC control (1:4, EtOAc/*i*Hexane, R$_f$ = 0.90) showed the complete conversion of the starting material (2-iodoaniline). The solvent was removed under reduced pressure and the raw material was extracted with water (5 mL) and DCM (10 mL x 3). The organic phase was dried over Na$_2$SO$_4$ and the solvent was subsequently evaporated under reduced pressure. The residue was was purified through column chromatography on silica gel (1:4, EtOAc/*i*hexane) affording **110** (1.145 g, 83 %) as white solid. ^{1}H NMR (CDCl$_3$, 200 MHz): δ 4.15 (2H, s, NH$_2$), 6.65-6.79 (3H, m, Ar), 7.14-7.22 (1H, m, Ar), 7.27-7.37 (10H, m Ar). ^{31}P NMR (CDCl$_3$, 54 MHz): -19.33.

| R= Me, | **BPC2**, 61% | R= CF$_3$, | **BPC4**, 35 % |
| R= Ph, | **BPC3**, 72% | R= *p*-MeOPh, | **BPC5**, 40 % |
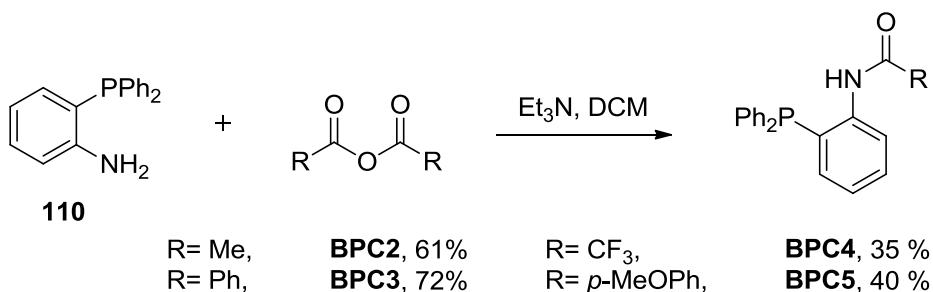
General Procedure for the synthesis of **BPC2-5**:

To a solution of **110** and triethylamine (2 equiv.) in DCM was dropwise added the corresponding acid anhydride at 0 °C. The reaction was further stirred at r.t. for another 5 hours and quenched with water. After extraction, the aqueous phase was washed with DCM (10 mL x 3). The organic phase was combined and dried over Na$_2$SO$_4$. The solvent was removed under reduced pressure and the crude material was purified through column chromatography on silica gel (1:4, EtOAc/*i*hexane) affording **BPC2-5** as white solids.

N-(2-(diphenylphosphino)phenyl)acetamide **BPC2**:

^{1}H NMR (CDCl$_3$, 200 MHz): δ 1.96 (3H, s, CH$_3$), 6.90-6.98 (1H, m, Ar), 7.03- 7.10 (1H, m, Ar), 7.25-7.40 (10H, m, Ar), 7.95 (1H, s, Ar), 8.12-8.16 (1H, m, Ar),. ^{31}P

NMR (CDCl$_3$, 54 MHz): -19.12. HRMS (ESI) (M+H) Calcd. for C$_{20}$H$_{19}$NOP: requires 320.1204, Found: 320.1203.

N-(2-(diphenylphosphino)phenyl)benzamide **BPC3**:

^{1}H NMR (CDCl$_3$, 200 MHz): δ 6.94-7.07 (1H, m, Ar), 7.10- 7.14 (1H, m, Ar), 7.30-7.52 (13H, m, Ar), 7.59-7.69 (2H, m, Ar), 8.41-8.47 (1H, m, Ar), 8.83 (1H, s, NH). ^{1}P NMR (CDCl$_3$, 54 MHz): -19.89.

N-(2-(diphenylphosphino)phenyl)-2,2,2-trifluoroacetamide **BPC4:**

IR: 3364 (NH), 3073, 1725, 1570, 1523, 1478, 1458, 1437, 1331, 1310, 1277, 1231, 1198, 1172, 1149, 1124, 1089, 1069, 1026, 997, 948, 956, 763, 751, 736, 675, 609 cm^{-1}. ^{1}H NMR (CDCl$_3$, 300 MHz): 7.01-7.06 (1H, m, Ar), 7.03 (1H, t, J = 4.5 Hz, Ar), 7.29-7.48 (11H, m, Ar), 8.13 (1H, t, J = 4.2 Hz, Ar), 8.90 (1H, s, NH). ^{13}C NMR (CDCl$_3$, 75 MHz): 122.23 (d, J = 1.5 Hz), 126.58 (d, J = 1.5 Hz), 128.21 (d, J = 12 Hz), 128.95, 129.04, 129.63 (d, J = 0.75 Hz), 130.49, 133.44 (d, J = 5.3 Hz), 133.57, 133.83, 134.14 (d, J = 1.5 Hz), 138.18 (d, J = 18 Hz) ^{19}F NMR (CDCl$_3$, 282 MHz): -76.01. ^{31}P NMR (CDCl$_3$, 81 MHz): -20.76. MS (EI): m/e 373, 304, 277, 283, 152, 107, 77. HRMS (ESI) (M+H) Calcd. for C$_{20}$H$_{16}$NOF$_3$P: requires 374.0922, Found: 374.0920.

N-(2-(diphenylphosphino)phenyl)-4-methoxybenzamide **BPC5**

IR: 3311 (NH), 3349, 3050, 2964, 2837, 1648 (C=O), 1605, 1567, 1529, 1497, 1439, 1311, 1293, 1249, 1189, 1086, 1027, 911, 842, 761, 749, 695, 641 cm^{-1}. ^{1}H NMR (CDCl$_3$, 600 MHz): 3.85 (3H, s, OMe), 6.89 (2H, d, J = 8.6 Hz, Ar), 6.98 (1H, t, J = 6.1 Hz, Ar), 7.07 (1H, t, J = 7.5 Hz, Ar), 7.35-7.38 (11H, m, Ar), 7.60 (2H, d, J = 8.6 Hz, Ar), 8.41 (1H, d, J = 8.0 Hz, Ar), 8.80 (1H, s, NH). ^{13}C NMR (CDCl$_3$, 75 MHz): 55.40, 113.83, 121.66, 124.50, 126.99, 128.84, 128.90, 133.65, 133.77, 133.94, 133.96, 141.43 (d, J = 16.8 Hz), 162.40, 164.65. ^{31}P NMR (CDCl$_3$, 162 MHz): -19. HRMS (EI) (M+) Calcd. for C$_{26}$H$_{22}$NO$_2$P: requires 411.1388, Found: 411.1380.
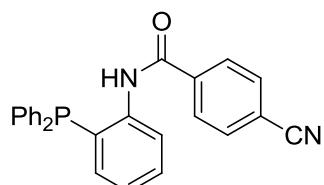
4-Cyano-N-(2-(diphenylphosphino)phenyl)benzamide **BPC6**:

p-Cyanobenzoic acid (294 mg, 2 mmol) and triethylamine (242 µL, 2 mmol) were dissolved in 30 mL THF. Ethylchloroformate (190 µL, 2 mmol) was added to this

solution at 0 ^{o}C. The reaction mixture was stirred at r.t. for 2 hours till **110** was added. After 18 hours, the reaction was quenched with 5 mL water. The mixture was extracted and the aqueous phase was washed with DCM (20 mL x 3). The organic phase was combined and dried over Na_2SO_4. After evaporation of the solvent, the residue was purified through column chromatography on silica gel (1:4, EtOAc/*i*hexane) obtaining **BPC6** as white solid (300 mg, 37 %). IR: 3311 (NH), 2507, 2233, 2161, 2023, 1973, 1676, 1572, 1525, 1498, 1477, 1432, 1317, 1301, 1246, 1208, 1181, 1117, 1094, 995, 974, 946, 893, 829, 749, 697, 644 cm^{-1}. ^{1}H NMR (CDCl$_3$, 400 MHz): 6.99 (1H, t, J = 8.0 Hz, Ar), 7.13 (1H, t, J = 8.0 Hz, Ar), 7.31-7.40 (10H, m, Ar), 7.46 (1H, t, J = 8.0 Hz, Ar), 7.69 (4H, s, Ar), 8.35 (1H, dd, J = 4.0 Hz, J = 4.0 Hz, Ar), 8.76 (1H, d, J = 8.0 Hz, NH). ^{13}C NMR (CDCl$_3$, 100 MHz): 115.26, 117.94, 121.90, 125.42 (d, J = 2.0 Hz), 127.59, 128.96, 129.04, 129.56, 130.50, 132.50, 133.66, 133.79, 133.85, 134.08 (d, J = 4.0 Hz), 138.57, 140.35 (d, J = 17.0 Hz), 163.27. ^{31}P NMR (CDCl$_3$, 108 MHz): -19.466. HRMS (ESI) (M+H) Calcd. for C$_{26}$H$_{22}$N$_2$OP: requires 407.1313, Found: 407.1311.
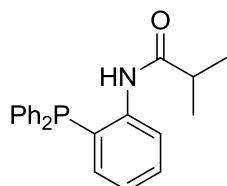
N-(2-(diphenylphosphino)phenyl)isobutyramide **BPC7**:

To a solution of **110** (450 mg, 1.625 mg) and triethylamine (242 µL, 2 mmol) in 10 mL DCM was dropwise added isobutyryl chloride (173 mg, 1.625 mmol) during 1 hour at 0 ^{o}C. The reaction mixture was stirred at r.t. for 2 hours and quenched with 3 mL water. The mixture was extracted and the aqueous phase was washed with DCM (3 x 10 mL). All the organic phase was combined and dried over Na_2SO_4. After evaporation of the solvent, the residue was purified through column chromatography on silica gel (1:4, EtOAc/*i*hexane) obtaining **BPC7** as white solid (200 mg, 35 %). IR: 3293 (NH), 3052, 2966, 2930, 2871, 1686, 1604, 1573, 1505, 1478, 1432, 1382, 1286, 1234, 1190, 1155, 1119, 1095, 1069, 1026, 997, 938, 868, 828, 742, 617 cm^{-1}. ^{1}H NMR (CDCl$_3$, 300 MHz): 1.06 (3H, d, J = 3.0 Hz, CH$_3$), 1.07 (1H, d, J = 3.0 Hz, CH$_3$), 2.35 (1H, m, J = 6.0 Hz, CH), 6.91 (1H, t, J = 6.0 Hz, Ar), 7.06 (1H, t, J = 6.0 Hz, Ar), 7.30-7.43 (11H, m, Ar), 7.96 (1H, t, J = 3.0 Hz, Ar), 8.21 (1H, s NH). ^{13}C NMR (CDCl$_3$, 75 MHz): 19.26, 36.71, 122.09, 124.53, 128.80, 128.90, 129.30, 130.20, 133.57, 133.67 (d, J = 3.0 Hz), 133.83, 134.34 (d, J = 6.0

Hz), 140.91 (d, J = 16.5 Hz), 174.88. ^{31}P NMR (CDCl$_3$, 81 MHz): -18.90. MS (EI): m/e 347, 332, 304, 277, 198, 183, 152, 107, 77, 43. HRMS (ESI) (M+H) Calcd. for C$_{22}$H$_{23}$NOP: requires 348.1517, Found: 348.1511.
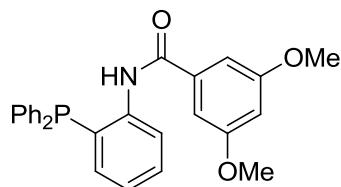
N-(2-(diphenylphosphino)phenyl)-3,5-dimethoxybenzamide **BPC8** :

m,m-Dimethoxylbenzoic acid (546.5 mg, 3 mmol) and thionyl chloride (1.19 g, 10 mmol) was dissolved in 30 mL THF. The mixture was refluxed for 2 hours Then the solvent and excess thionyl chloride were removed under vaccum. The residue was dissolved in 20 mL DCM and triethylamine (484 µL, 4 mmol) and to this solution was added **110** (1.91 mmol). After stirring at r.t. for 16 hours, 5 mL water was added to quench this reaction. The mixture was extracted and the aqueous phase was washed with DCM (3 x 10 mL). The organic phase was combined and dried over Na$_2$SO$_4$. After evaporation of the solvent, the residue was purified through column chromatography on silica gel (1:4, EtOAc/iHexane) obtaining **BPC8** as white solid (430 mg, 51 %). IR: 3360 (NH), 3053, 3008, 2957, 2837, 1672, 1584, 1571, 1507, 1477, 1443, 1431, 1348, 1327, 1300, 1275, 1231, 1201, 1155, 1132, 1094, 1062, 1051, 1025, 998, 943, 923, 893, 869, 848, 825, 778, 697, 676, 624 cm^{-1}. ^{1}H NMR (CDCl$_3$, 300 MHz): 3.81 (6H, s, OMe), 6.60 (1H, t, J = 3.0 Hz, Ar), 6.88 (2H, d, J = 3.0 Hz, Ar), 6.99 (1H, t, J = 3.0 Hz, Ar), 7.12 (1H, t, J = 6.0 Hz, Ar), 7.33-7.41 (10H, m, Ar), 7.48 (1H, t, J = 6.0 Hz, Ar), 8.45 (1H, dd, J = 6.0 Hz, J = 9.0 Hz,, Ar), 8.85 (1H, J = 9.0 Hz, NH). ^{13}C NMR (CDCl$_3$, 75 MHz): 55.58, 104.35, 104.69, 121.70, 124.86, 126.35 (d, J = 9.8 Hz), 128.88, 128.97, 129.39, 130.46, 133.58, 133.84, 133.96 (d, J = 2.3 Hz), 134.26 (d, J = 6 Hz), 137.04, 141.15 (d, J = 17.3 Hz), 160.93, 166.07. ^{31}P NMR (CDCl$_3$, 81 MHz): -21.00. HRMS (EI) (M+) Calcd. for C$_{27}$H$_{24}$NO$_3$P: requires 441.1494, Found: 441.1490.

1) NaH, CH$_3$OCH$_2$Cl, THF
2) BuLi, THF, 0 °C; ClPPh$_2$
3) HCl, reflux in EtOH

BPC9, 33 %
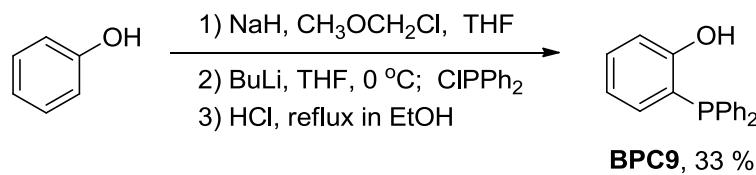
2-(diphenylphosphino)phenol **BPC9**:

To a solution of phenol (1.49 g, 15.9 mmol) in 50 mL THF was added NaH (800 mg, 20 mmol). After stirring for 1 hour, methoxylmethyl chloride (1.47 mL,16 mmol)

was added. After 10 hour, the reaction was quenched by 10 mL water. The mixture was extracted and the aqueous phase was washed with DCM (30 mL x 3). The organic phase was combined and dried over Na_2SO_4. After evaporation of the solvent and drying under high vaccum overnight, the product was dissolved in 30 mL dry THF. To this solution was added dropwise butyl lithium (11.72 mmol, 4.69 mL of 2.5 M solution in Hexane) at 0 $^{\circ}$C. The mixture was stirred at room temperature for 2 hours before chlorodiphenylphosphane (2.2g, 12 mmol) was added. After 16 hours, 2 mL conc. HCl was added to quench the reaction, which was allowed to reflux for 2 hours. The resulting solution was extracted and the aqueous phase was washed with DCM (20 mL x 3). All the organic phase was combined and dried over Na_2SO_4. After evaporation of the solvent, the residue was purified through column chromatography on silica gel (1:2, EtOAc/*i*hexane) obtaining **BPC9** as white solid (1.45 g, 33 %). ^{1}H NMR (CDCl$_3$, 200 MHz): 6.18 (1H, s, OH), 6.85-7.03 (4H, m, Ar), 7.24-7.38 (10H, m, Ar). ^{31}P NMR (CDCl$_3$, 54 MHz): -27.80.

110   **BPC10**, 35 %
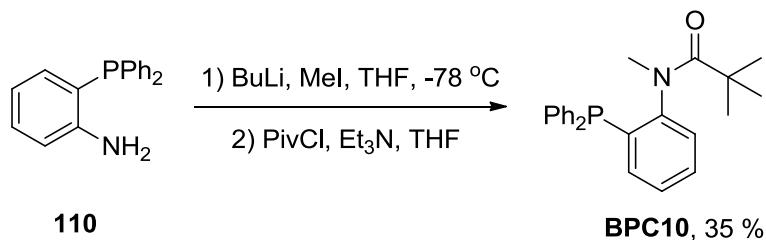
N-(2-(diphenylphosphino)phenyl)-N-methylpivalamide **BPC10**:

To a solution of **110** (1108 mg, 4 mmol) in 20 mL THF was added dropwise butyl lithium (4.4 mmol, 2.75 mL of 1.6 M solution in Hexane) at -78 $^{\circ}$C. After further stirring for 2 hours, methyl iodide (625 mg, 4.4 mmol) was added dropwise at -78 $^{\circ}$C. After 1 hour, the mixture was warmed to r.t. for another 18 hours stirring. Pivaloyl chloride (1.46 g, 5 mmol) and triethylamine (1 mL, 8.5 mmol) was injected to the reaction mixture. In 10 hours the reaction was quenched by adding 10 mL water and the solvent was subsequently removed under reduced pressure. The aqueous layer was washed with 10 mL of DCM and the combined organic layers were dried over Na_2SO_4, filtered and evaporated under reduced pressure to yield an oil that was purified through column chromatography on silica gel (1:8 EtOAc/iHexane) affording **BPC10**. IR: 3049, 2958, 1627, 1580, 1562, 1477, 1465, 1433, 1414, 1392, 1336, 1289, 1255, 1205, 1129, 1117, 1085, 1010, 898, 888, 740, 719, 670 cm^{-1}. ^{1}H NMR (CDCl$_3$, 300 MHz): 1.17 (9H, s, (CH$_3$)$_3$), 2.89 (3H, s,

Me), 7.14 (1H, m, Ar), 7.20-7.27(3H, m, Ar), 7.29-7.43 (10H, m, Ar). ^{13}C NMR (CDCl$_3$, 75 MHz): 29.35, 40.87, 41.34, 128.11, 128.47, 128.55, 129.11, 130.09, 133.51, 134.37, 135.47, 136.54, 149.73 (d, J = 25.5 Hz), 177.77. ^{31}P NMR (CDCl$_3$, 81 MHz): -16.97. HRMS (EI) (M+H) Calcd. for C$_{24}$H$_{27}$NOP: requires 376.1830, Found: 376.1812.

4.2.3.2 Application in the aza-Morita-Baylis-Hillman reaction

Kinetic measurements followed the procedure described in **4.1.2.4**.

The BPC catalyzed aMBH reactions of *N*-tosylimines with MVK followed the same procedure described in **4.1.2.1**.
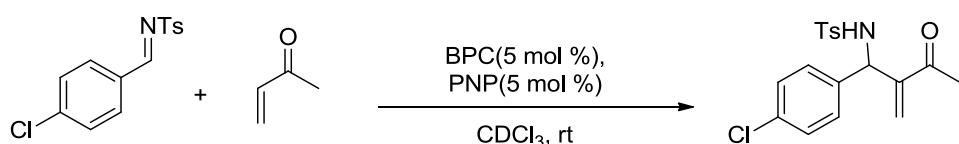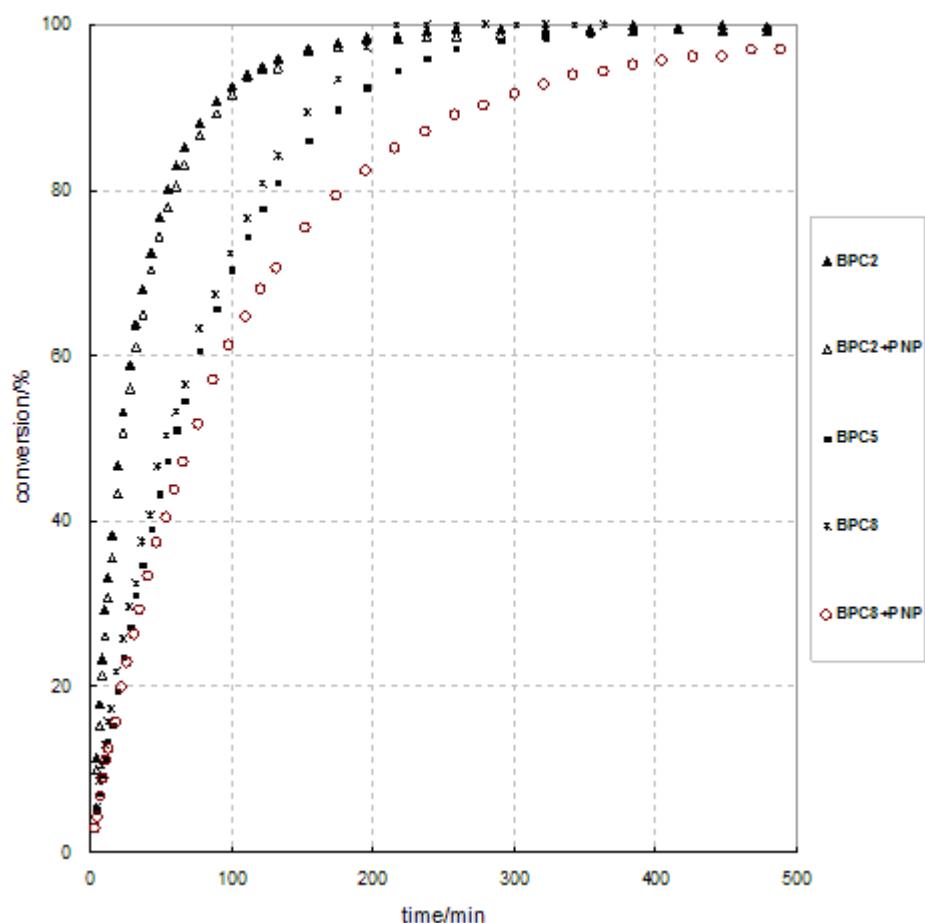

Figure IV-9. aMBH reactions of *N*-tosylimines with MVK in the presence of BPCs.

4.2.3.3 Application in the Morita-Baylis-Hillman reaction

(a) The synthesis of compound **117**, **119**, **120** followed a literature method.[122]

3-Iodoaniline (10 mmol), potassium acetate (12 mmol), and diphenylphosphane (10 mmol, 1.85 g) were dissolved in 60 mL DMF. To this solution was added Pd(OAc)$_2$ (52 mg, 0.25 mol). After refluxing overnight, TLC control (EtOAc/*i*hexane 1:4, R$_f$ = 0.90) showed the complete conversion of the starting material 3-iodoaniline. The solvent was removed under reduced pressure and the raw material was extracted with water (250 mL) and DCM (1 L). The organic phase was dried over Na$_2$SO$_4$ and the solvent was subsequently evaporated under reduced pressure. The residue was purified through column chromatography on silica gel (1:4, EtOAc/*i*Hexane) affording **117** (1.07 g, 39 %) as white solid. The synthesis of **119**, **120** followed the similar procedure.
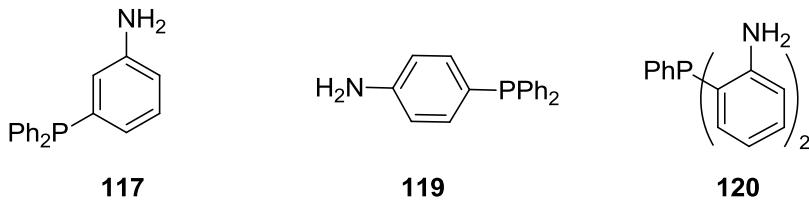
117: ^{1}H NMR (CDCl$_3$, 200 MHz): δ 3.62 (s, 2H, NH$_2$), 6.83-6.51 (3H, m, Ar), 7.14 (1H, m, Ar), 7.33 (10H, m, Ar). ^{31}P NMR (CDCl$_3$, 54 MHz): -3.79.

119: ^{1}H NMR (CDCl$_3$, 200 MHz): δ 3.77 (2H, s, br, NH$_2$), 6.66 (2H, dd, J = 8.6, 1.0 Hz, Ar), 7.15 (2H, dd, J = 8.5, 7.8 Hz, Ar), 7.35-7.27 (10H, m, Ar). ^{31}P NMR (CDCl$_3$, 54 MHz): -5.81.

120: ^{1}H NMR (CDCl$_3$, 200 MHz): δ 4.10 (2H, s, NH$_2$), 6.76-6.63 (4H, m, Ar), 6.89-6.76 (2H, m, Ar), 7.25-7.10 (2H, m Ar). 7.36 (5H, dd, J = 4.8, 1.6 Hz, Ar). ^{31}P NMR (CDCl$_3$, 54 MHz): -32.23.

(b) The synthesis of BPC**11**, **12**, **13**

To a solution of **117** (550 mg, 1.98 mg) and triethylamine (200 mg, 2 mmol) in 8 mL THF was dropwise added pivaloyl chloride (240 mg, 1.625 mmol) during 1 hour at 0 °C. The reaction mixture was stirred at room temperatue for another 48 hours and quenched with 20 mL water. The mixture was extracted and the aqueous phase was washed with DCM (3 x 20 mL). The organic phase was combined and dried over Na$_2$SO$_4$. After evaporation of the solvent, the residue was purified through column chromatography on silica gel (1:4, EtOAc/*i*Hexane)

obtaining **BPC11** as white solid (620 mg, 86 %). The synthesis of **BPC12**, **BPC13** followed this similar procedure.

| **BPC11** | **BPC12** | **BPC13** |
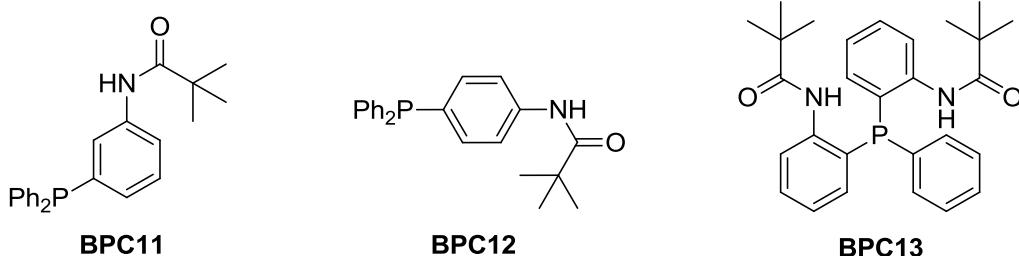
N-(3-(diphenylphosphino)phenyl)pivalamide **BPC11**: IR: 3296, 2960, 2926, 2868, 1727, 1654, 1593, 1532, 1468, 1432, 1295, 1260, 1230, 1168, 1091, 1025, 927, 901, 795, 743, 694 cm^{-1}. ^{1}H NMR (400 MHz, CDCl$_3$): δ 1.29 (9H, d, J = 3.0 Hz, C(CH$_3$)$_3$), 6.98 (1H, ddt, J = 7.7 Hz, 6.8 Hz, 1.2 Hz), 7.41 – 7.17 (12H , m), 7.84 (ddd, J = 8.2 Hz, 2.2 Hz, 0.9 Hz , 1H). ^{13}C NMR (101 MHz, CDCl$_3$): δ = 176.5, 138.2, 138.1, 136.9, 136.8, 133.8, 133.6, 129.3, 129.3, 129.2, 129.2, 128.8, 128.5, 128.5, 125.0, 124.7, 120.8, 39.6, 27.6. ^{31}P NMR (CDCl$_3$, 108 MHz): -4.98. MS (EI) m/z (%): 361 (M$^+$, 100), 277 (Ph$_2$PPh-NH$_2$$^+$, 17), 198 (PhPPhN, 10), 183 (PPh$_2$$^+$-2H, 12), 169 (3), 108 (2), 83 (5), 57 (t-Bu$^+$, 16). HRMS (ESI) (M+H) Calcd. for C$_{23}$H$_{24}$NOP: requires 361.1596, Found: 362.1671.

N-(4-(diphenylphosphino)phenyl)pivalamide **BPC12**: IR: 3285, 2975, 1650, 1582, 1515, 1477, 1432, 1392, 1312, 1286, 1243, 1170, 1090, 1026, 924, 823, 744, 694.cm^{-1}. ^{1}H NMR (CDCl$_3$, 400 MHz): 1.31 (s, 9H, C(CH$_3$)$_3$), 7.39 – 7.26 (m, 12H), 7.57 – 7.49 (dd, J = 8.0 Hz, 1.2 Hz, 2H, H). ^{13}C NMR (CDCl$_3$, 101 MHz): 176.6, 138.8, 137.0, 136.9, 134.8, 134.6, 133.6, 133.4, 128.7, 128.5, 128.4, 119.8, 119.8, 39.7, 27.6. ^{31}P NMR (CDCl$_3$, 108 MHz): -6.44. MS (EI) m/z (%): 361 (M$^+$, 100), 277 (Ph$_2$PPh-NH$_2$$^+$, 8), 198 (PhPPhN, 10), 169 (8), 152 (2), 107 (2), 83 (2), 57 (t-Bu$^+$, 16). HRMS (ESI) (M+H) Calcd. for C$_{23}$H$_{24}$NOP: requires 361.1596, Found: 362.1671.

N,N'-((phenylphosphanediyl)bis(2,1-phenylene))bis(2,2-dimethylpropanamide)**BPC13**: IR: 3337, 2961, 1684., 1672, 1574, 1514, 1494, 1432, 1395, 1362, 1298, 1276, 1233, 1156, 1026, 920, 853, 761, 752, 696 cm^{-1}. ^{1}H NMR (CDCl$_3$, 300 MHz): 1.10 – 1.04 (m, 18H), 6.89 – 6.74 (m, 2H), 7.05 (t, J = 7.5 Hz, 2H), 7.47 – 7.28 (m, 7H), 7.96 (d, J = 6.8 Hz, 2H), δ 8.17 (dd, J = 7.5 Hz, 4.9 Hz, 2H). ^{13}C NMR (75 MHz, CDCl$_3$): δ 176.4, 141.0, 134.4, 134.1, 133.2, 131.2, 130.7 , 130.2, 129.4, 129.3, 125.0, 123.7, 123.7, 122.6, 39.9, 27.3. ^{31}P NMR (CDCl$_3$, 81 MHz): -31.49. MS (EI) m/z (%): 403 (M$^+$-t-Bu, 100), 404 (M$^+$-

C_4H_8, 25), 57 (t-Bu$^+$, 9), 460 (M$^+$, 5). HRMS (ESI) (M+) Calcd. for $C_{28}H_{33}N_2O_2P$: requires 460.2280, Found: 460.2277.

(c) Procedure for the BPCs-catalyzed MBH reactions.

To a solution of *p*-chlorobenzaldehyde (224 mg, 1.6 mmol), catalyst (0.32 mmol), trimethoxylbenzene (84 mg, 0.5 mmol) and *p*-nitrophenol (66 mg, 0.48 mmol) in 4 mL THF, was added MVK (436 µL, 4.8 mmol) at rt. The reaction was monitored by diluting 10 µL of the reaction mixture into 1.5 mL of DCM at appropriate time intervals for GC analysis.

4.2.4 Asymmetric phosphane catalysts

(a) Synthesis of chiral phosphane catalysts

124
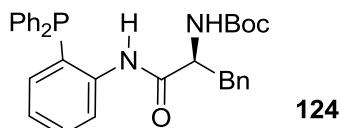
(S)-tert-butyl-1-(2-(diphenylphosphino)phenylamino)-1-oxo-3-phenylpropan-2-ylcarbamate **124**.

To a solution of N-*t*-Boc-*L*-Phenylalanine(1.06 g, 4 mmol) and triethylamine (1 mL, 8mmol) in THF (50 mL) was added ethyl chloroformate (0.390 mL, 4 mmol) at r.t. After stirring for 2 hours, 2-(diphenylphosphino)aniline **110** (831mg, 3 mmol) was added. The mixture was stirred for 20 hours, then 1 mL water was added to quench the reaction. THF was removed under reduced pressure and the residue was washed with water (20 mL) and extracted with DCM (2 X 20 mL). The organic phase was combined and dried over Na_2SO_4. After the solvent was removed by rotary evaporation, the residure was purified by silica gel column chromatography (Eluent: 1:4 EtOAc/ isohexane) to give product (715 mg) as a white powder. IR (ATR): 3301(br), 3055, 3028, 2976, 2930, 1676(br), 1574, 1511, 1434, 1365, 1295, 1246, 1163, 1081, 1048, 1025.8, 999.6, 917.0, 851 cm^{-1}. ^{1}H NMR (300 MHz, CDCl$_3$): 1.43 (9H, s), 2.80 (1H, b), 3.09(1H, dd, *J* = 5.6 Hz, *J* = 14 Hz), 4.45 (1H, b), 4.70 (1H, b), 6.89-6.92 (1H, m), 7.11-7.21 (3H, m), 7.34 (14H, m), 8.18-8.21 (1H, m), 8.59 (1H, d, *J* = 7.1 Hz). ^{13}C NMR (CDCl$_3$, 75.45 MHz): δ 28.27, 38.13, 56.23, 80.20, 122.03. 125.06, 126.91, 127.05, 128.64, 128.80, 128.90, 129.23, 129.32, 130.22, 133.56, 133.70, 133.82, 133.96, 134.52, 134.62, 136.37, 140.16,

140.40, 155.14, 169.31. ^{31}P NMR (CDCl$_3$, 81 MHz): -16.81. HRMS (ESI) for C$_{32}$H$_{33}$ N$_2$O$_3$P+1: requires 525.2262; Found: 525.2297.

128
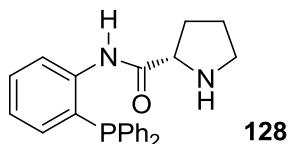
(S)-N-(2-(diphenylphosphino)phenyl)pyrrolidine-2-carboxamide **128** was prepared in a similar procedure as **124**. IR (ATR): 3154, 3009, 1838, 1833, 1814, 1793, 1676, 1586, 1521, 1467, 1457, 1423, 1371, 1315, 1285, 1281, 1167, 1160, 1091, 1054, 1015, 964, 938, 881, 846, 738, 712, 686, 637, 607 cm^{-1}. ^{1}H NMR (300 MHz, CDCl$_3$): δ 1.26-1.62 (2H, m), 1.83-2.08 (2H, m), 2.61-2.72 (1H, m), 2.82-2.94 (1H, m), 3.72 (1H, q, *J* = 4.8 Hz), 6.76 (1H, t, *J* = 6.0 Hz), 7.00 (1H, t, *J* = 7.2 Hz), 7.23-7.41 (11H, m, Ar), 8.25-8.32 (1H , m), 10.41 (1H, s, NH). ^{13}C NMR (CDCl$_3$, TMS, 75.45 MHz): δ 25.86, 30.78, 47.46, 61.15, 121.08, 124.27, 126.60 (d, *J* = 11.3 Hz), 129.12 (d, *J* = 7.5Hz), 129.86, 133.14 (d, *J* = 0.8 Hz), 133.71 (d, *J* = 19.6 Hz), 134.15 (d, *J* = 19.6 Hz), 140.69, 140.7 (d, *J* = 18.1 Hz), 173.58. ^{31}P NMR (CDCl$_3$, 81 MHz): -16.61. HRMS (ESI) (M+H) for C$_{23}$H$_{24}$N$_2$OP: requires 375.1626; Found: 375.1621.

130
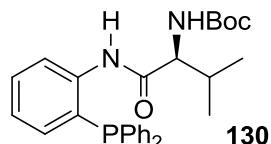
*(S)-t-*butyl(1-((2-(diphenylphosphino)phenyl)amino)-3-methyl-1-oxobutan-2-yl)carbamate **130** was synthesized in a in a similar procedure as **124**. IR (ATR): 3301(br), 3317, 3056, 2986, 2932, 2874, 2249, 1816, 1682, 1574, 1499, 1453, 1434, 1391, 1366, 1325, 1297, 1275, 1233, 1157, 1091, 1042, 1026, 1016, 908, 874, 802, 728, 695, 646, 618 cm^{-1}. ^{1}H NMR (300 MHz, CDCl$_3$): δ 0.65 (3H, d, *J* = 9Hz), 0.84 (3H, d, *J* = 9 Hz), 1.45 (s, 9H), 2.03-2.14 (1H, m), 4.06-4.13 (1H, m), 4.90 (1H, d, *J* =12 Hz), 6.88 (1H, t, *J* = 9 Hz), 7.04 (1H, t, *J* = 12 Hz), 7.27-7.33 (11H, m, Ar), 8.18-8.24 (1H, m), 8.53 (1H, d, *J* = 9 Hz, NH). ^{13}C NMR (CDCl$_3$, TMS, 75.45 MHz): δ 26.0, 27.7, 34.3, 63.1, 79.5, 122.3, 124.5, 128.2, 129.4, 131.2, 133.2 (d, *J* = 19 Hz), 134.0, 134.3, 134.9, 141.0 (d, *J* = 19 Hz), 154.9, 170.1. ^{31}P NMR (CDCl$_3$, 81 MHz): -19.88. HRMS (ESI) (M+H) for C$_{28}$H$_{34}$N$_2$O$_3$P: requires 477.2307; Found: 477.2303.
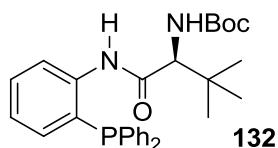
(S)-*t*-butyl(1-((2-(diphenylphosphino)phenyl)amino)-3,3-dimethyl-1-oxobutan-2-yl) carbamate **132** was synthesized in a similar procedure as **124**. IR (ATR): 3297, 3051, 2959, 1831, 1714, 1693, 1667, 1568, 1511, 1477, 1454, 1433, 1366, 1325, 1283, 1249, 1168, 1156, 1090, 1058, 1038, 1026, 1012, 965, 936, 880, 815, 760, 743, 722, 676, 634, 606 cm^{-1}. ^{1}H NMR (300 MHz, CDCl$_3$): δ 0.90 (9H, s), 1.45 (9H, s), 3.91 (1H, d, J = 9.3 Hz), 5.23 (1H, d, J = 9.3 Hz), 6.87 (1H, t, J = 7.6 Hz), 7.08 (1H, t, J = 9 Hz), 7.26-7.38 (11H, m, Ar), 8.23-8.36 (1H , m), 8.38 (1H, d, J = 9.0 Hz, NH). ^{13}C NMR (CDCl$_3$, TMS, 75.45 MHz): δ 26.5, 28.3, 34.8, 63.5, 79.8, 121.5, 124.8, 128.8, 128.9, 130.0, 133.7 (d, J = 19.6 Hz), 134.2, 134.6, 134.7, 140.8 (d, J = 18.8 Hz), 155.6, 169.3. ^{31}P NMR (CDCl$_3$, 81 MHz): -21.58. HRMS (ESI) (M+H) for C$_{29}$H$_{36}$N$_2$O$_3$P: requires 491.2464; Found: 491.2442.

(b) Asymmetric phosphane catalyzed MBH reaction

To a solution of *p*-chlorobenzaldehyde (224 mg, 1.6 mmol), catalyst (0.32 mmol), in 4 mL THF, was added MVK (436 μL, 4.8 mmol) at rt. The mixture was stirred at room temperature for another 50 h. After evaporation of the solvent, the residue was purified through column chromatography on silica gel (1:4, EtOAc/*i*hexane) obtaining MBH product as white solid.
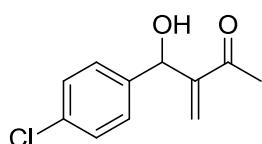

^{1}H NMR (200 MHz, CDCl$_3$): δ 2.35 (3H, s), 5.58 (1H, s), 5.98 (1H, s), 6.21 (1H, s), 7.29-7.30 (4H, m, Ar).

4.3 Mechanistic studies of the Morita-Baylis-Hillman Reaction

4.3.1 Protonation/deprotonation equilibria in the catalytic cycle

4.3.1.1 The ^{31}P NMR measurement

(**a**) PPh$_3$ and MVK in CDCl$_3$
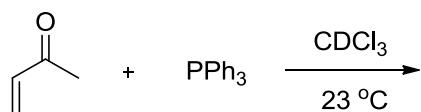
PPh$_3$ (44 mg, 0.16 mmol), MVK (145 µL, 1.6 mmol) and 0.5 mL freshly distilled *d*-chloroform were added to an NMR tube under N$_2$ atmosphere. After 10 min the ^{31}P NMR measured at 23 °C showed a peak at -4.627 ppm (PPh$_3$) and a new peak at 29.54 ppm which was proved to be triphenylphosphane oxide and a group of little new peaks at around -58.45 ppm, which are thought to be cyclic phosphorus(V) intermediates (Figure IV-10). With increasing time all new peaks increased and only the peak at -4.627 ppm decreased (Figure IV-11). After 10 hours the peak at -4.627 ppm disappeared (Figure IV-12).
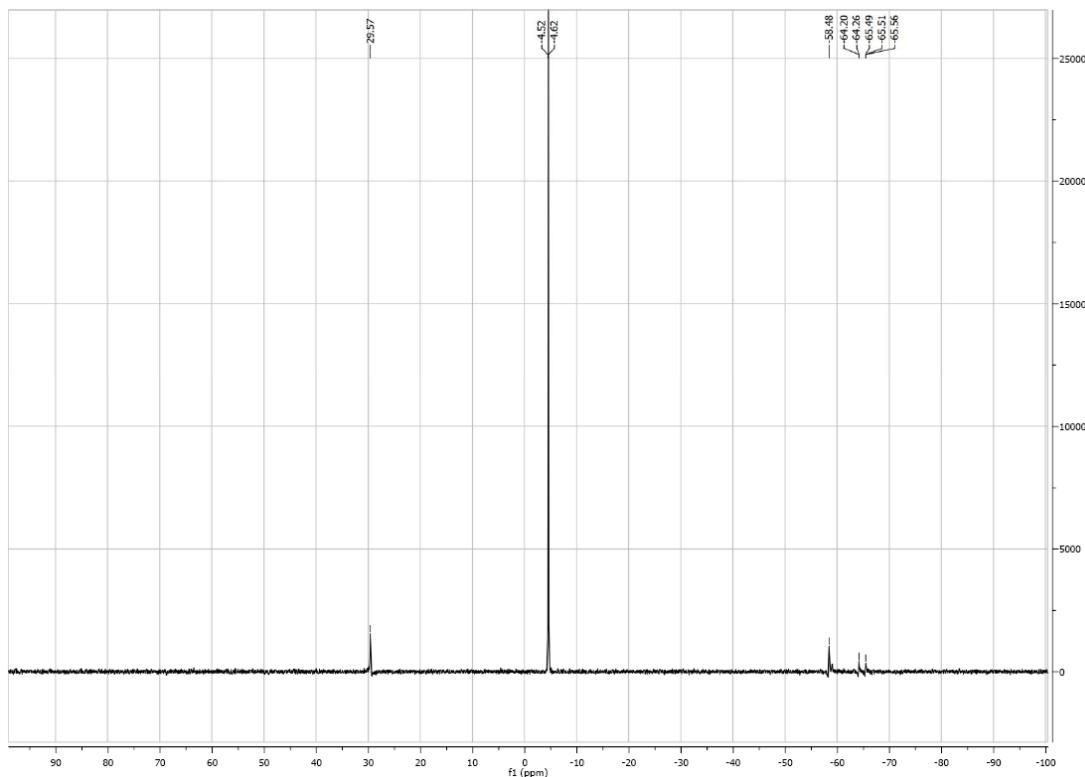

Figure IV-10. ^{31}P NMR spectrum (108 MHz) obtained from the reaction of PPh$_3$ and MVK in CDCl$_3$ after 10 min.
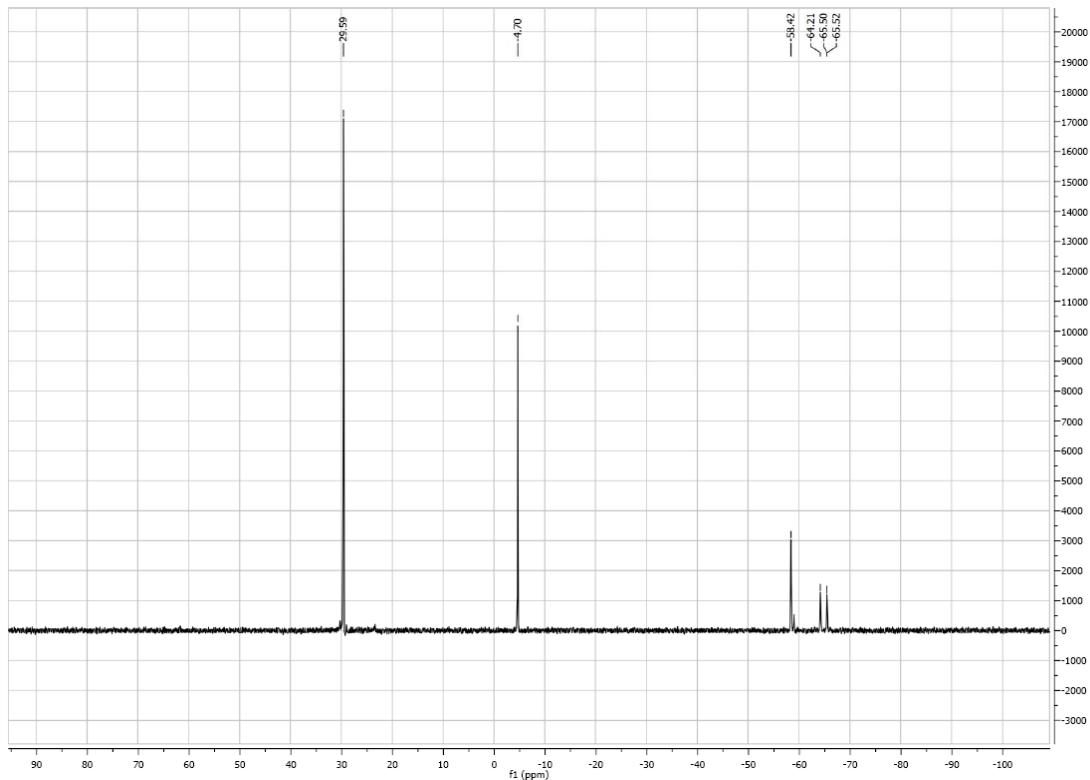
Figure IV-11. ^{31}P NMR spectrum (108 MHz) obtained from the reaction of PPh$_3$ and MVK in CDCl$_3$ after 50 min.
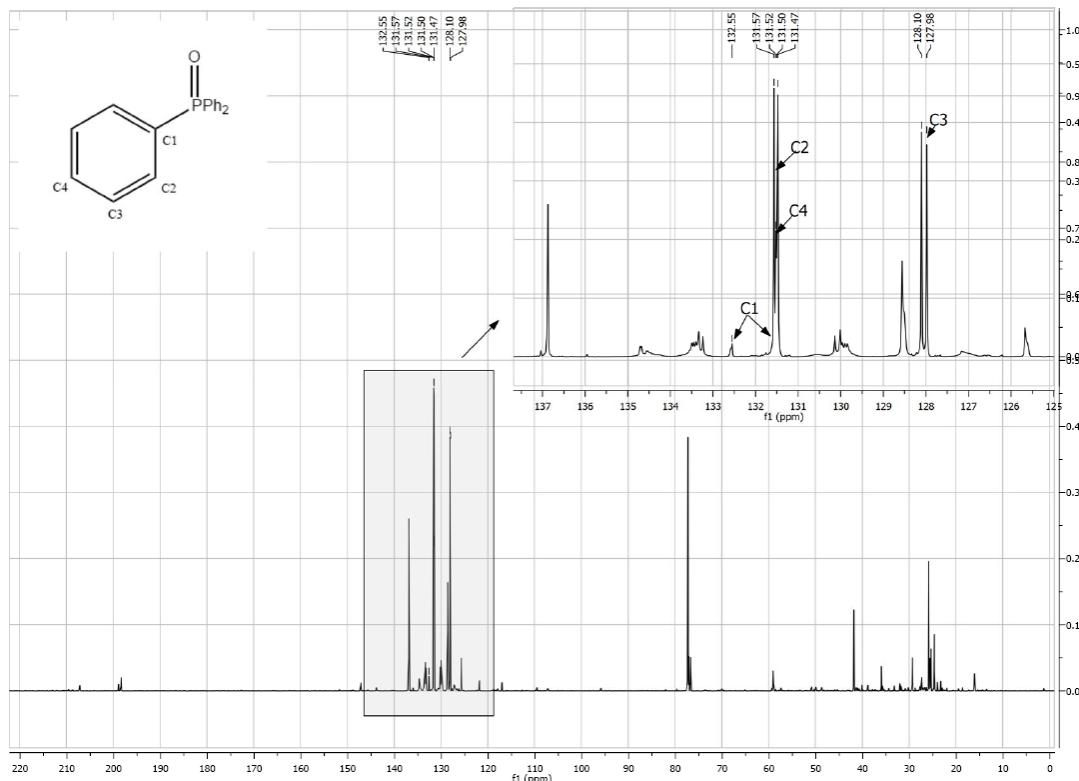
Figure IV-12. ^{13}C NMR spectrum (100 MHz) obtained from the reaction of PPh$_3$ and MVK in CDCl$_3$ after 10 hours.

(b) PPh$_3$, MVK and PNP in CDCl$_3$
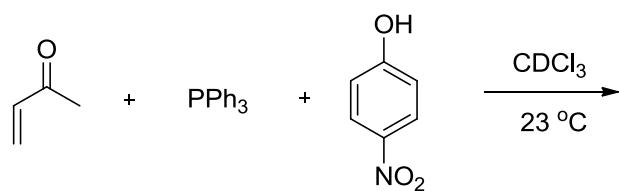
PPh$_3$ (44 mg, 0.16 mmol), PNP (33 mg, 0.24 mmol) and 0.5 mL freshly distilled *d*-chloroform were added to a NMR tube under N$_2$ atmosphere. The PNP did not dissolve well instantly, but after MVK (145 µL, 1.6 mmol) was added, PNP all dissolved and gave a yellow transparent solution. In ^{31}P NMR spectrum two single peaks at -4.373, 25.936 ppm were observed, and the ratio of two peaks integrals didn't change as time went on (Figure IV-13). With the variation of molar amount of PNP (0.053, 0.08, 0.16, 0.24, 0.32 mmol), it shows different ratios of two peaks integrals (Figure 24). ^{13}C NMR and 2D NMR were also measured (Figure IV-15-19). After 24 hours, ^{1}H and ^{13}C NMR shows that there is a large amount of MVK dimer formed (Figure IV-20, 21).
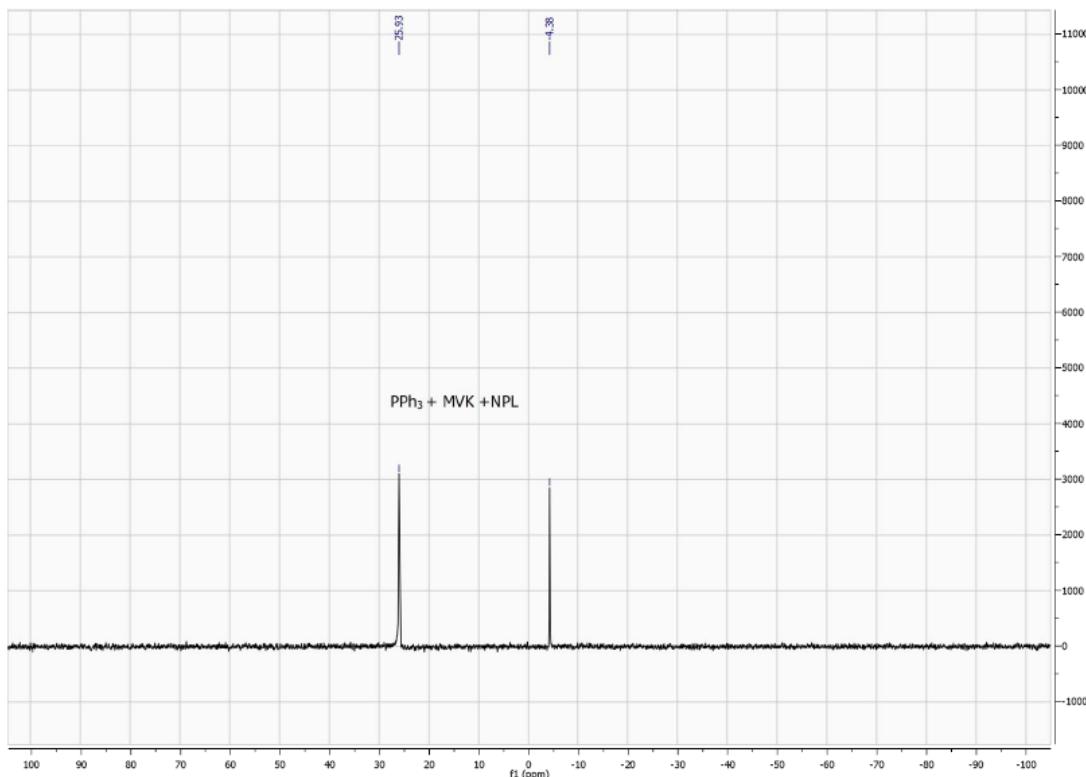
Figure IV-13. ^{31}P NMR spectrum (108 MHz) obtained from the reaction of PPh$_3$, PNP and MVK in CDCl$_3$ after 50 min.

140
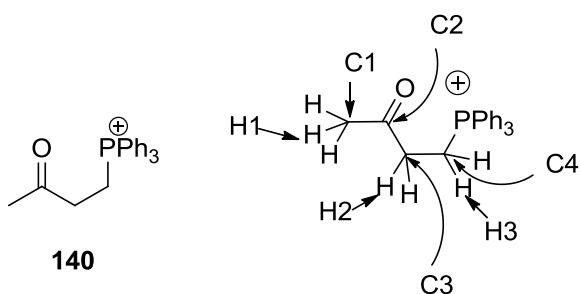
The assignment of intermediate **140** was first achieved by two characteristic protons in ^{1}H NMR spectrum corresponding to H2 and H3 (Figure IV-14). C1 and H1 were also characterized with HMBC and HSQC, C2 with $^3J_{C-P}$ and HMBC, C3 and H3 with HSQC and $^2J_{C-P}$, C4 and H4 with HSQC and $^1J_{C-P}$.

^{1}H NMR (400 MHz, CDCl$_3$): δ 1.95 (3H, s, H1), 2.77-2.84 (2H, m, H2), 3.31-3.38 (2H, m, H3), 7.46-7.57 (15H, m, Ar-H). ^{13}C NMR (100 MHz, CDCl$_3$): δ 16.76 (d, C4, $^1J_{C-P}$ = 55Hz), 29.4 (C1), 35.21 (d, C3, $^2J_{C-P}$ = 3Hz)), 117.0, 117.05, 117.07, 117.86, 130.61, 130.71, 133.21, 133.31, 203. 02 (d, C2, $^3J_{C-P}$ = 12Hz). MS(ESI) (M$^+$) m/z: 333.2. ^{31}P NMR (108 MHz, CDCl$_3$): 25.72.
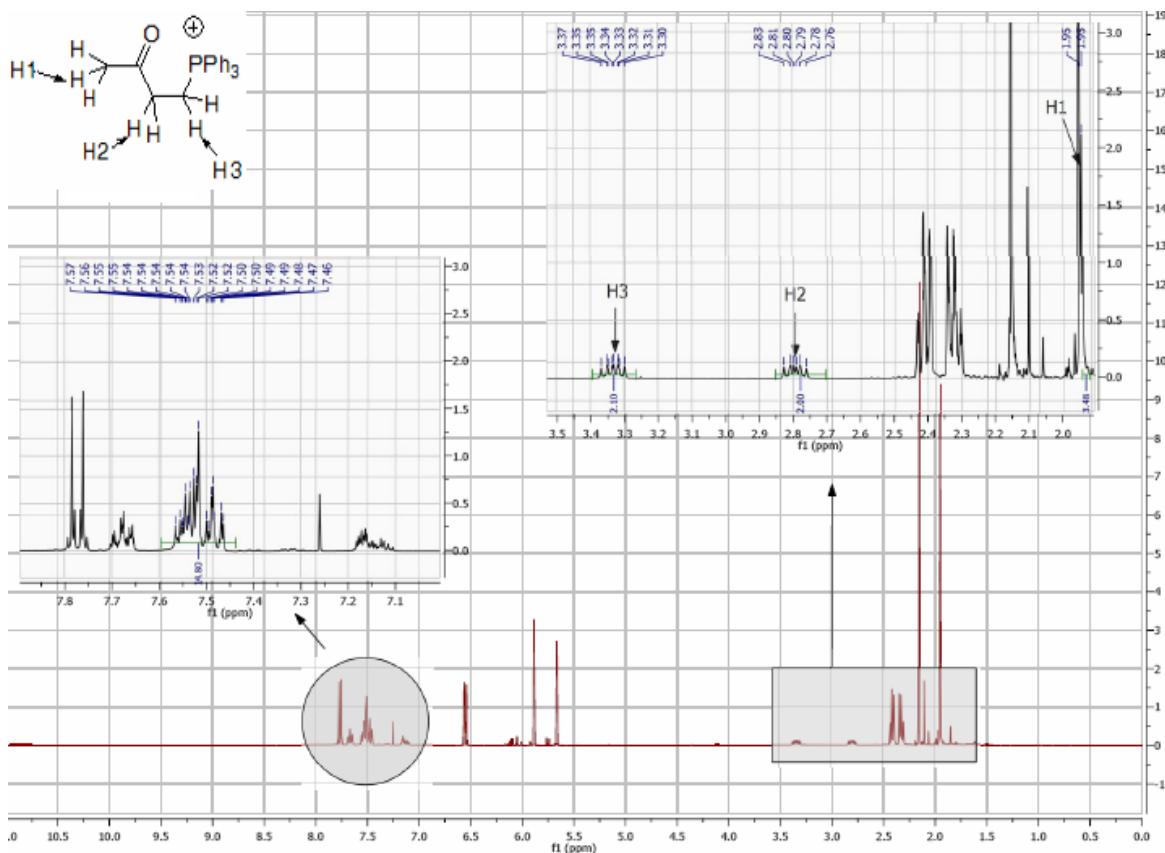
Figure IV-14. ^{1}H NMR (400MHz) of **140** in the reaction of PPh$_3$, PNP and MVK in CDCl$_3$.
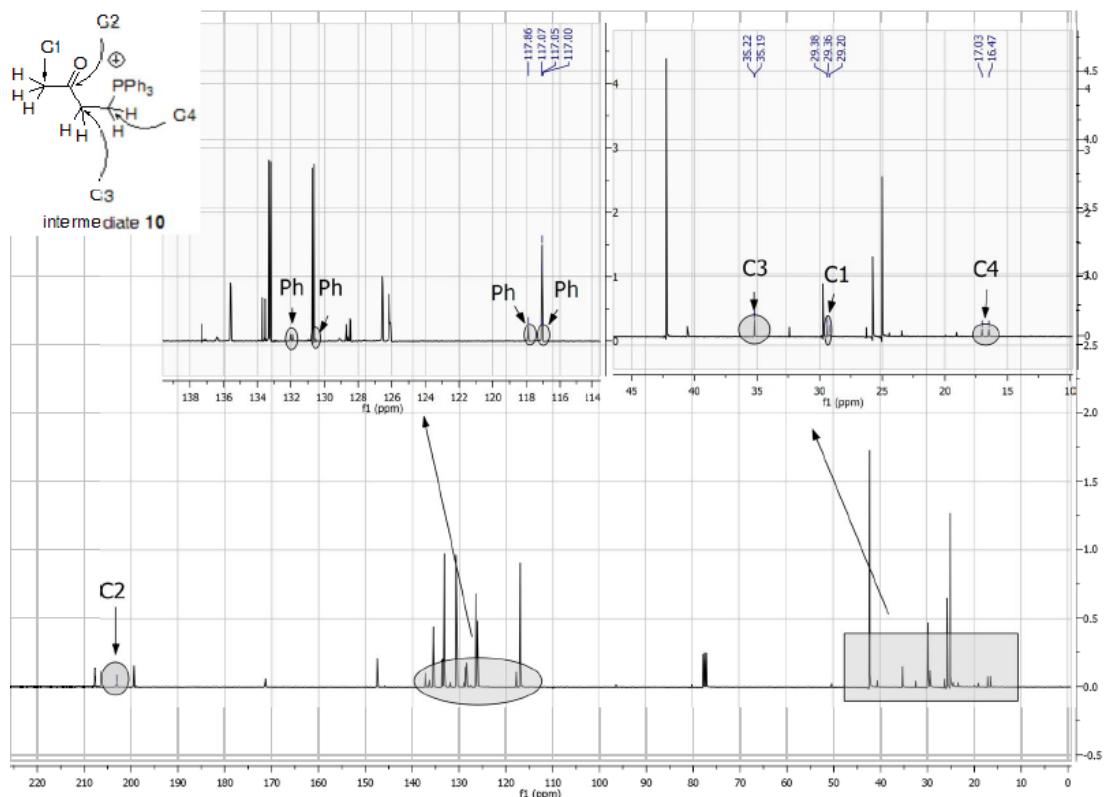
Figure IV-15. ^{13}C NMR (100MHz) of **140** in the reaction of PPh$_3$, PNP and MVK in CDCl$_3$.
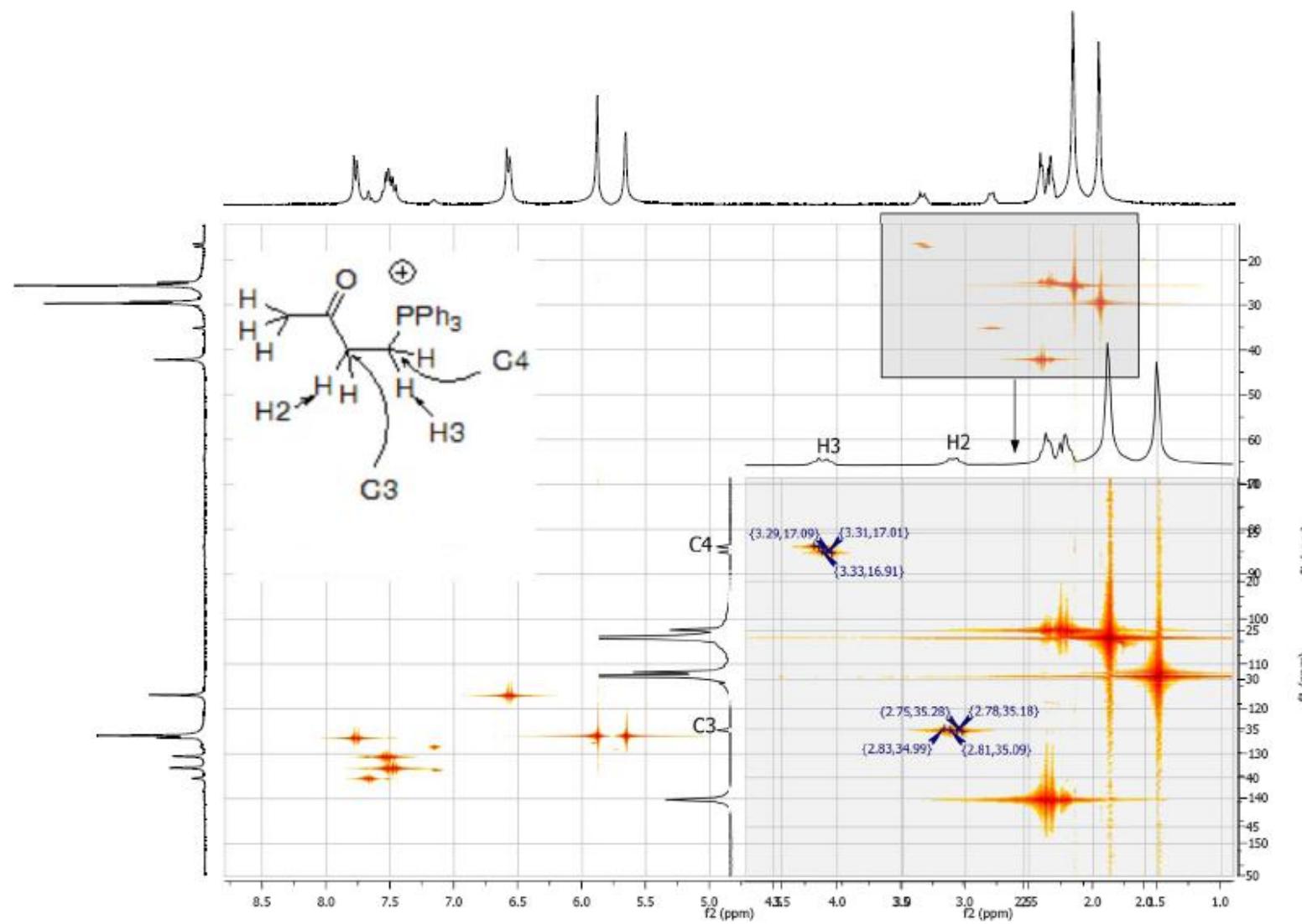
Figure IV-16. **HSQC:** C3 and H2 of **140** were characterized with HSQC and $^2J_{C-P}$, C4 and H3 with HSQC and $^1J_{C-P}$.
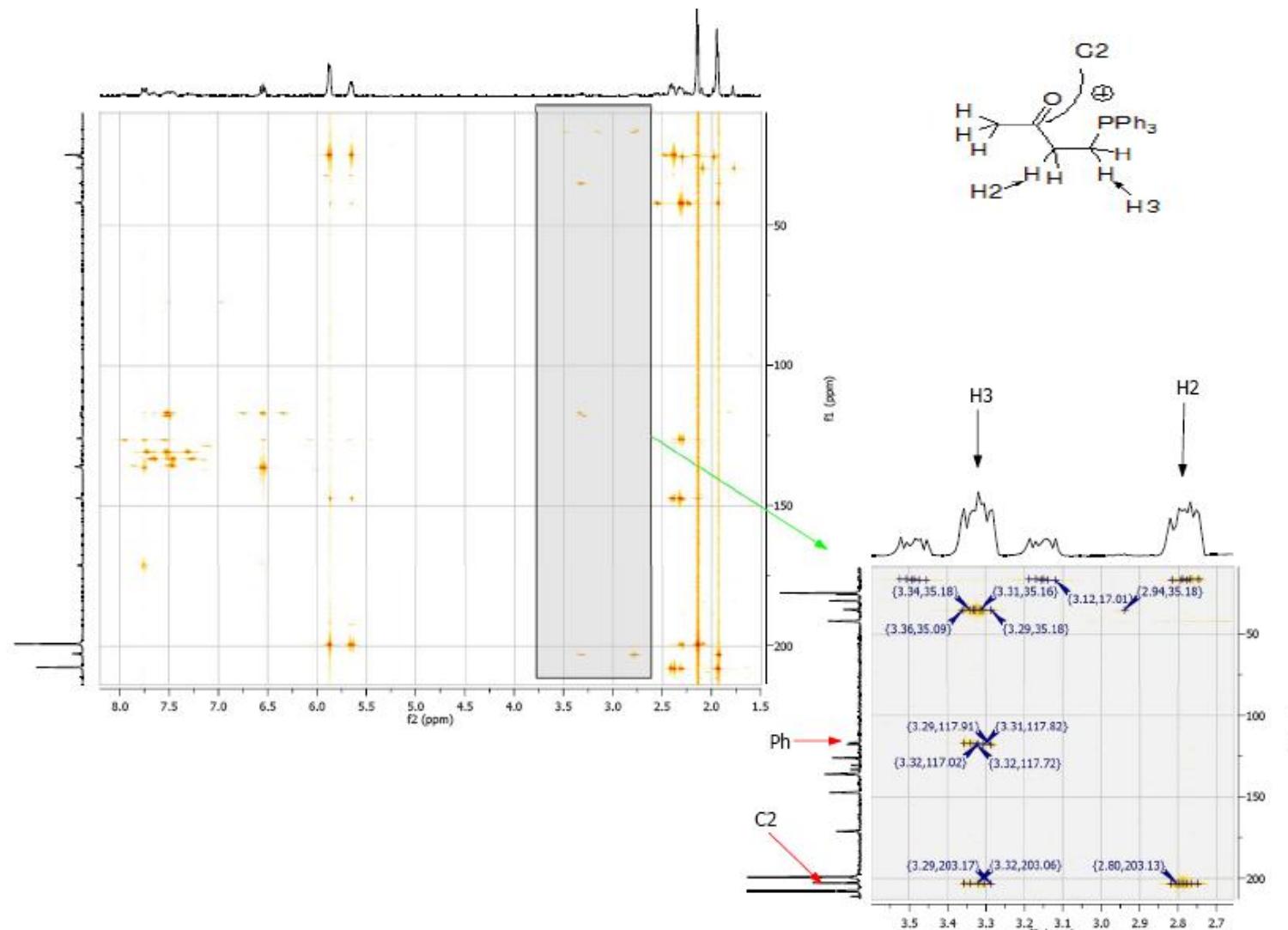
Figure IV-17. **HMBC:** C2 and Ph group of **140** were characterized with HMBC and $^3J_{C-P}$
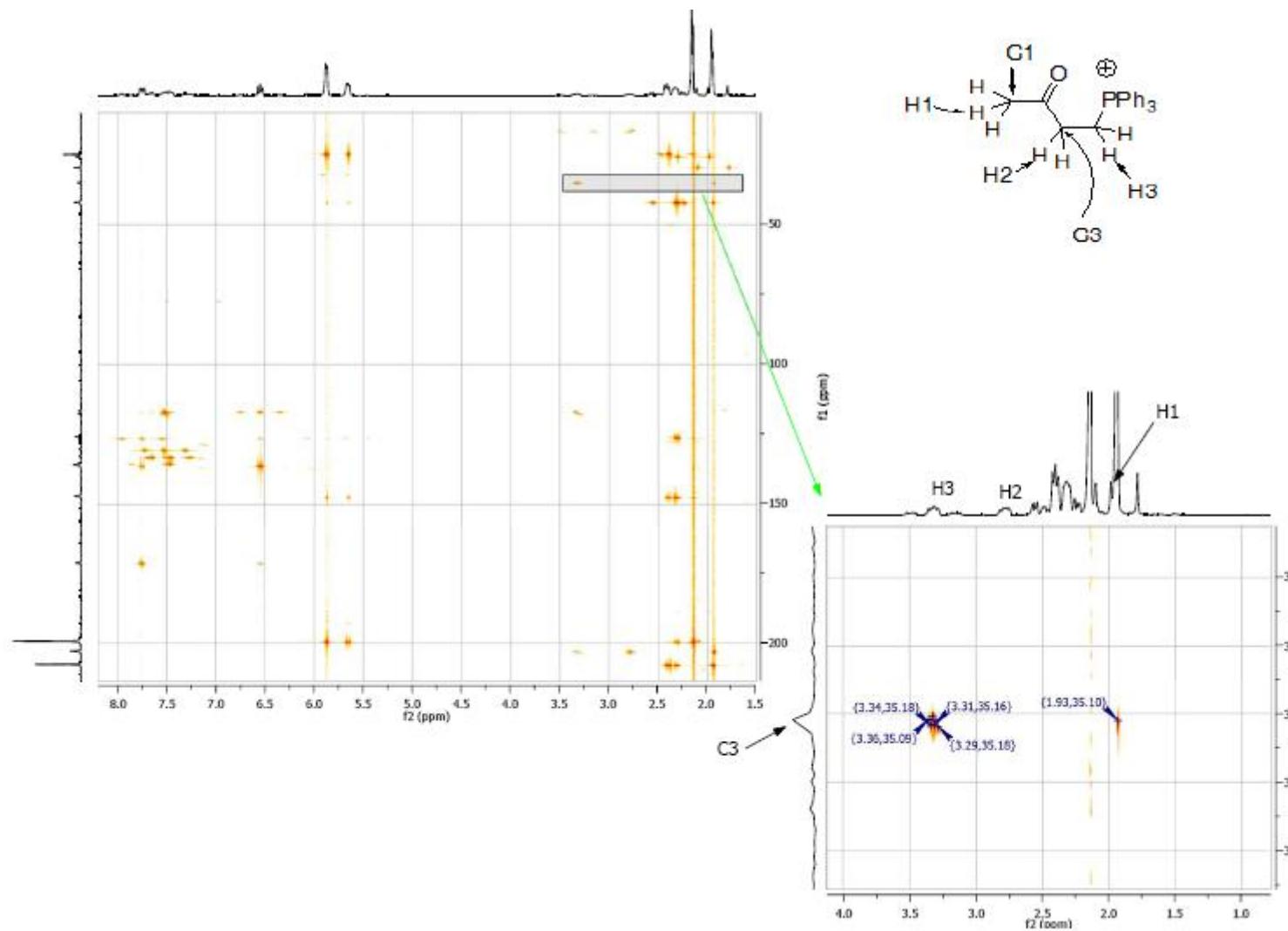
Figure IV-18. **HMBC:** H1 of **140** was characterized with HMBC.
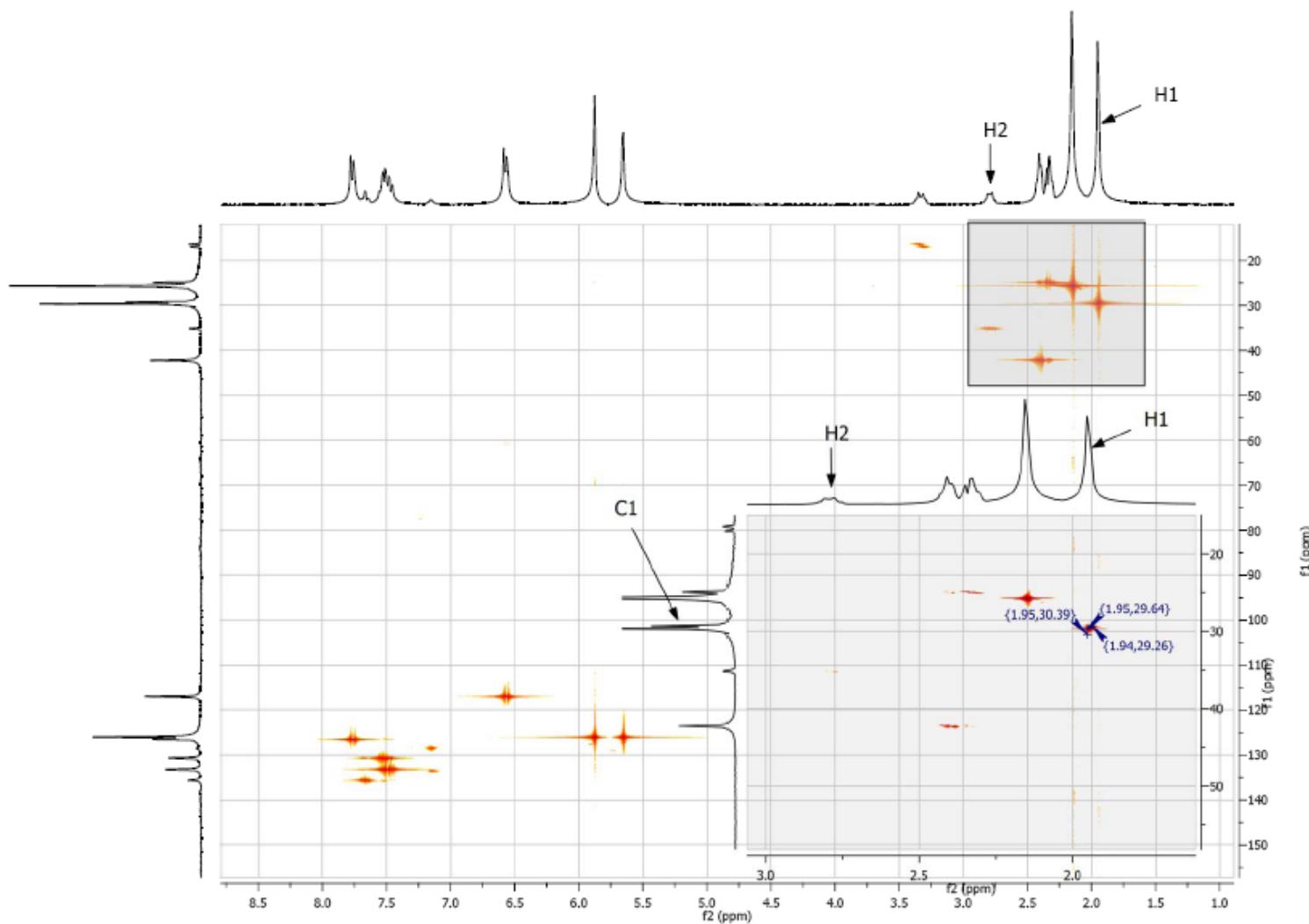
Figure IV-19. **HSQC:** C1 of **140** was characterized with HSQC.
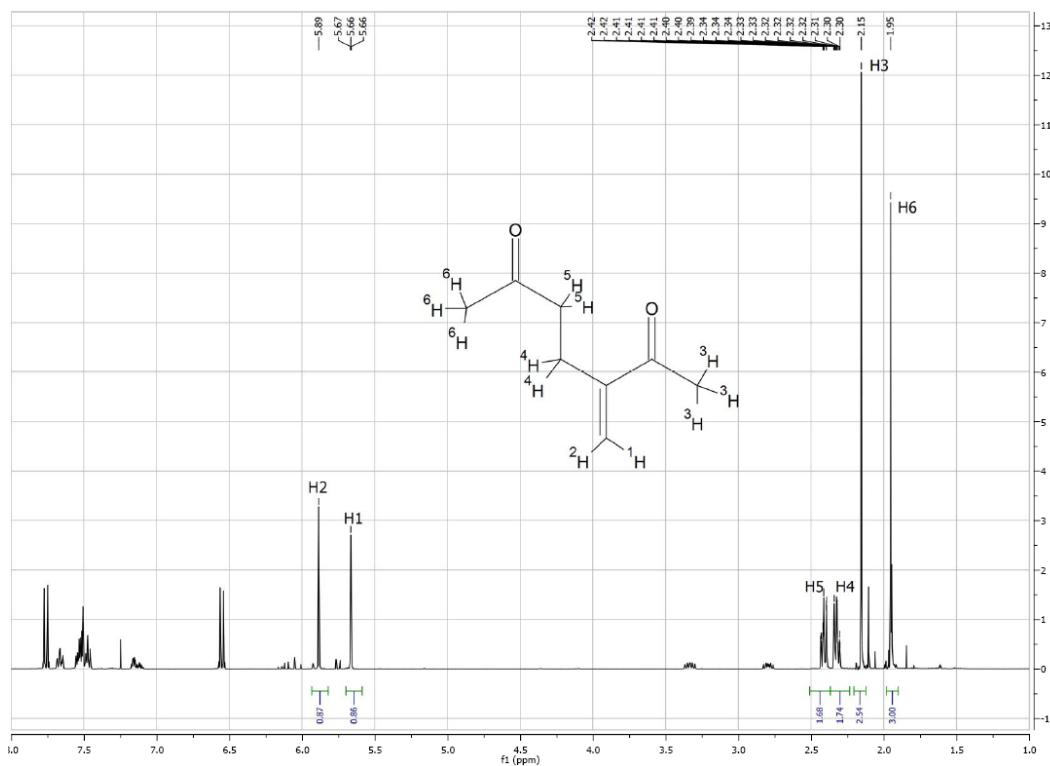
Figure IV-20. ^{1}H NMR of MVK dimer in the reaction of PPh$_3$, MVK and PNP in CDCl$_3$
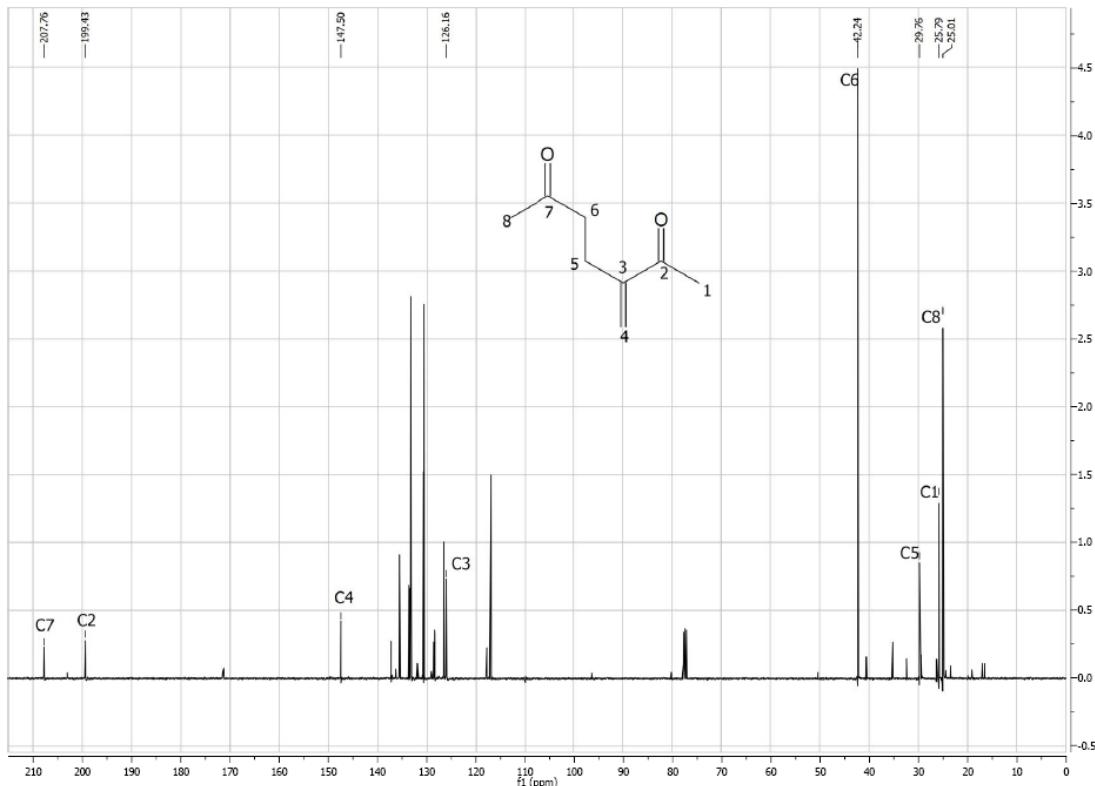
Figure IV-21. ^{13}C NMR of MVK dimer in the reaction of PPh$_3$, MVK and PNP in CDCl$_3$

(c) PPh$_3$, MVK, *p*-chlorobenzaldehyde (CBE) and PNP in CDCl$_3$
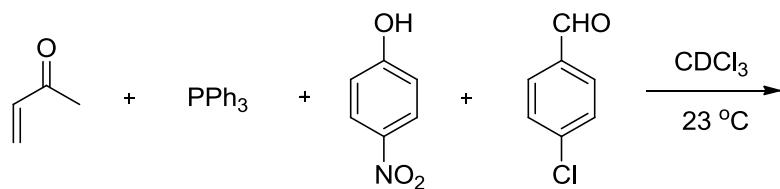
PPh$_3$ (22.3 mg, 0.08 mmol), PNP (17 mg, 0.12 mmol) and *p*-chlorbenzaldehyde (55 mg, 0.4 mmol) and 0.5 mL freshly distilled *d*-chloroform were added to an NMR tube under N$_2$ atmosphere. PNP did not dissolve well, but after MVK (74 µL, 0.8 mmol) was added, PNP dissolved and gave a yellow transparent solution, The ^{31}P NMR showed a peak at -4.47 ppm and another peak at 25.87 ppm.
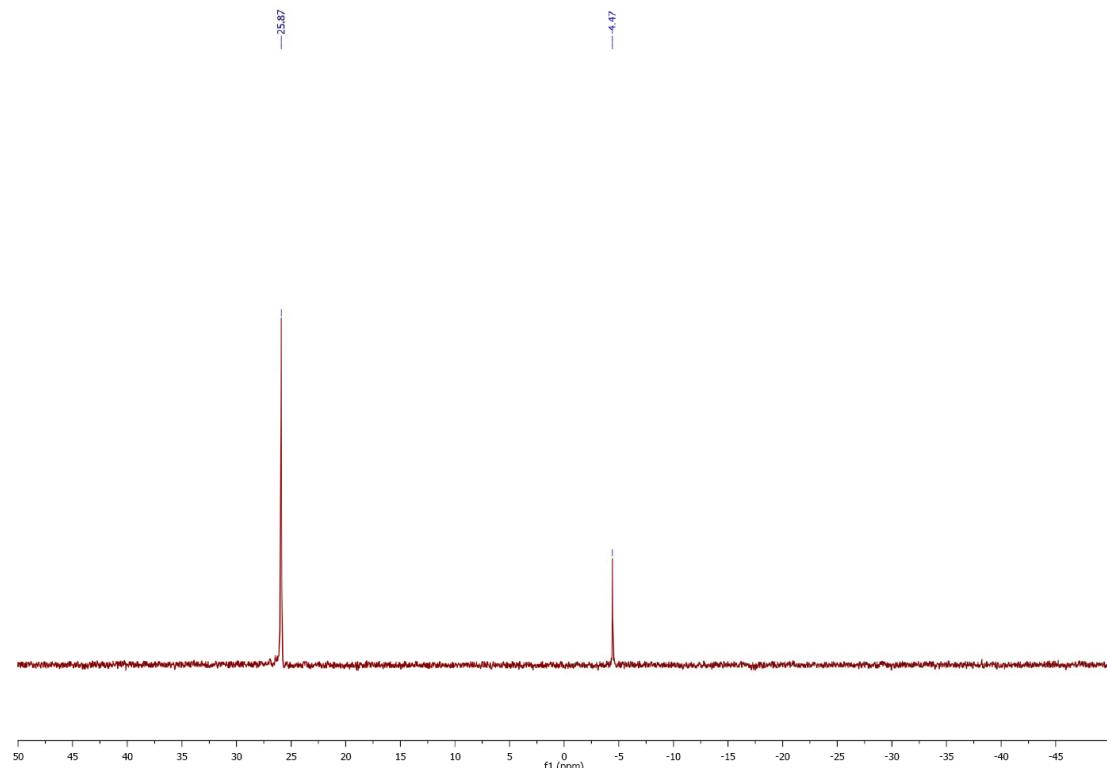
Figure IV-22. ^{31}P NMR spectrum of the reaction of PPh$_3$, MVK, *p*-chlorobenzaldehyde (CBE) and PNP in CDCl$_3$

4.3.1.2 The MS measurement procedure

To a solution of PPh$_3$ (42 mg, 0.16 mmol) and PNP (33 mg, 0.24 mmol) in 2 mL THF, MVK (145 µL, 1.6 mmol)(or EVK(159 µL, 1.6 mmol)) were added under N$_2$ atmosphere. After stirring for 1 hour at room temperature, 100 µL solution was taken, diluted in 1 mL THF and injected to the mass spectrometer (ESI).

(a)

(b)
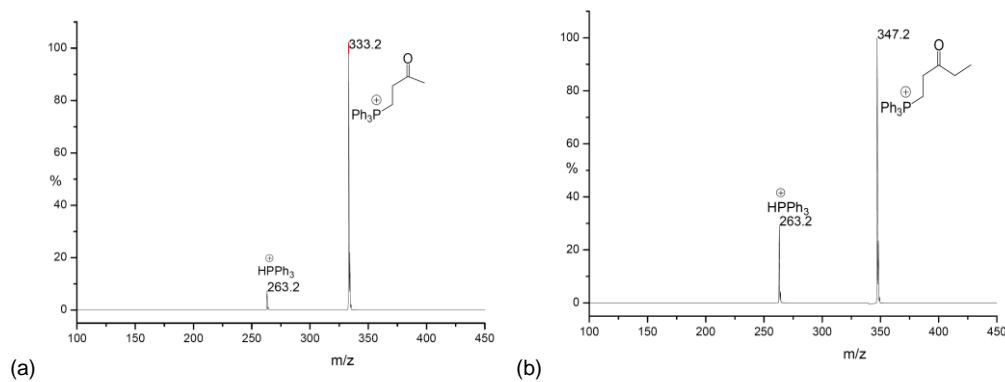
ESI(+)-MS of MVK(a) (or EVK(b)), PNP and PPh$_3$ (molar ratio 10:1.5:1) in THF

(c)

(d)
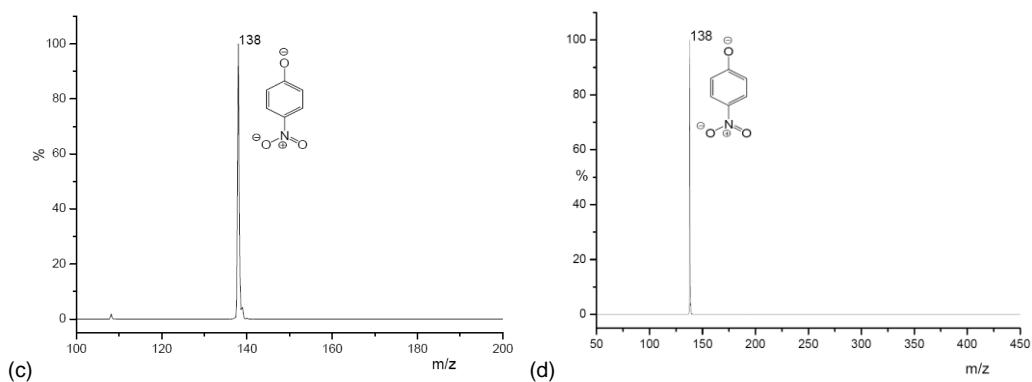
ESI(-)-MS of MVK(c) (or EVK(d)), PNP and PPh$_3$ (molar ratio 10:1.5:1) in THF

(e)

(f)
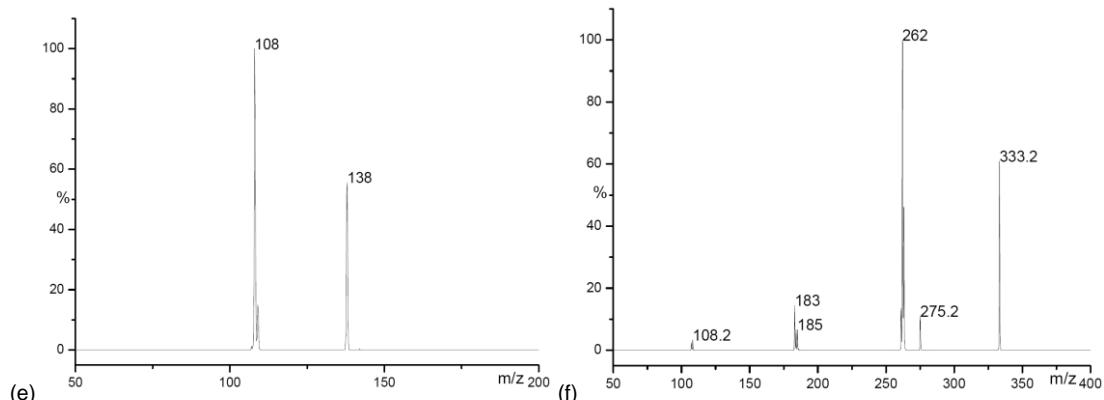
ESI(-)-MS spectrum of the ion of m/z 138(e) and ESI(+)-MS spectrum of the ion of m/z 333.2(f)
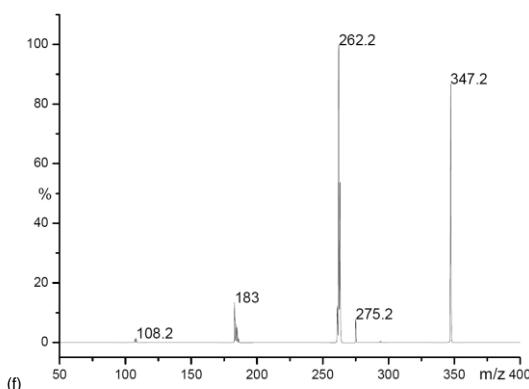
ESI(+)-MS spectrum of the ion of m/z 347.2

4.3.1.3 The synthesis of 140-Br compound

The synthesis of **140**-Br⁻ and **140**-BF$_4$⁻ followed a literature method.[127]

(a)

140-Br⁻
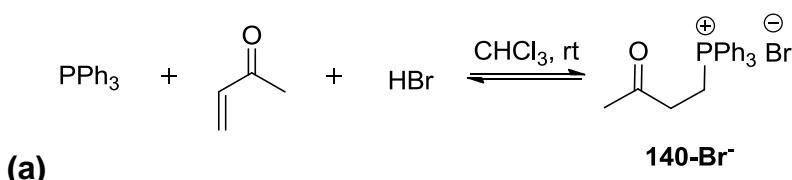
To a stirred solution of PPh$_3$ (2.88 g, 11 mmol), and hydrobromic acid (48 %, 2.4 mL) in 20 mL CHCl$_3$ was added dropwise a solution of MVK (0.7 g, 10 mmol) in 20 mL chloroform. The mixture is stirred at room temperature for 2.5 hours, the chloroform layer is washed with water (4 x 20 mL), dried over sodium sulfate and added dropwise to ether (600 mL), The precipitated salt is filtered, recrystallized from chloroform/ethyl acetate, dried in an exsiccator over phosphorus pentoxide in vacuum to give **140**-Br⁻ as a white salt (1.29 g, yield 27 %). ¹H NMR (200 MHz, CDCl$_3$): δ 2.08 (3H, s), 3.19 (2H, td, J = 16 Hz, J = 7 Hz), 3.96 (2H, td, J = 12 Hz, J = 7 Hz), 7.61-7.84 (15H, m). ³¹P NMR (81 MHz, CDCl$_3$): δ 26.84.

¹H NMR

140
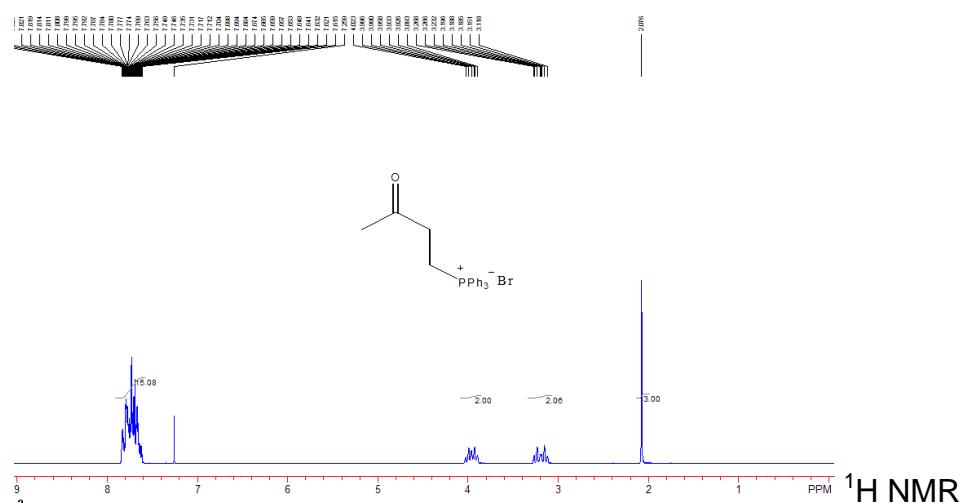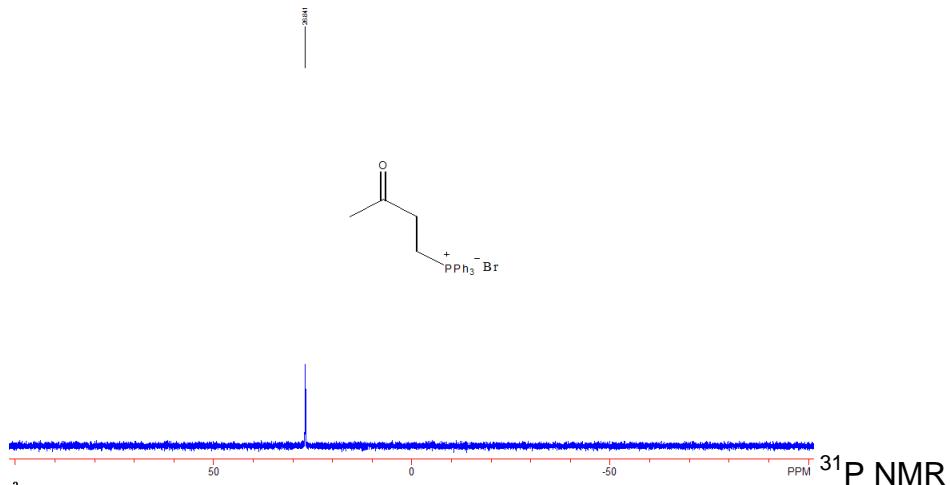
^{31}P NMR

(b)

The synthesis of **140**-BF$_4^-$ follows a similar procedure to that of **140**-Br$^-$.[127b]

White powder, 2.568 g, yield 56 %. ^{1}H NMR (200 MHz, CDCl$_3$): δ 2.09 (3H, s), 3.01 (2H, td, J = 14 Hz, J = 6 Hz), 3.51 (2H, td, J = 12 Hz, J = 6 Hz), 7.62-7.84 (15H, m). ^{31}P NMR (81 MHz, CDCl$_3$): δ 26.36.

^{1}H NMR

^{31}P NMR
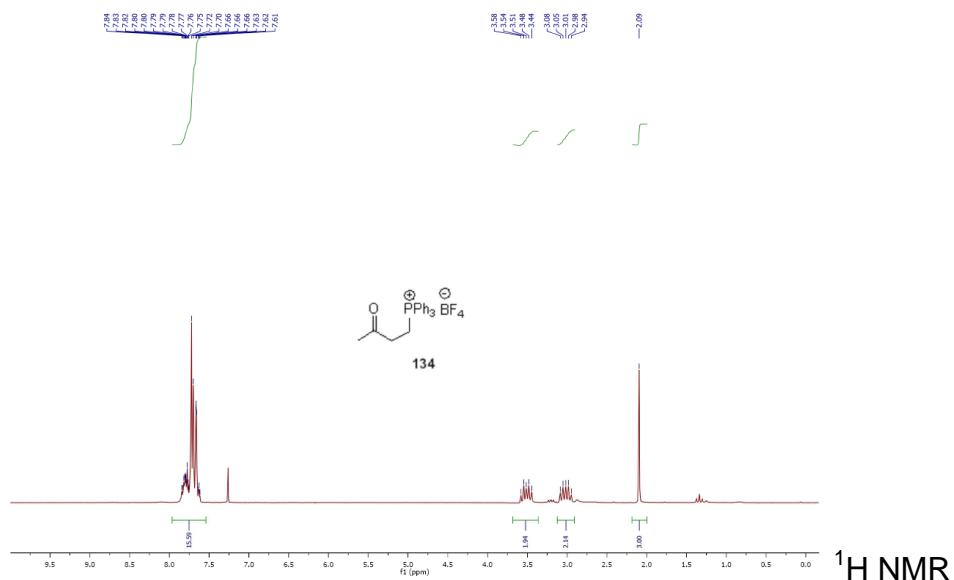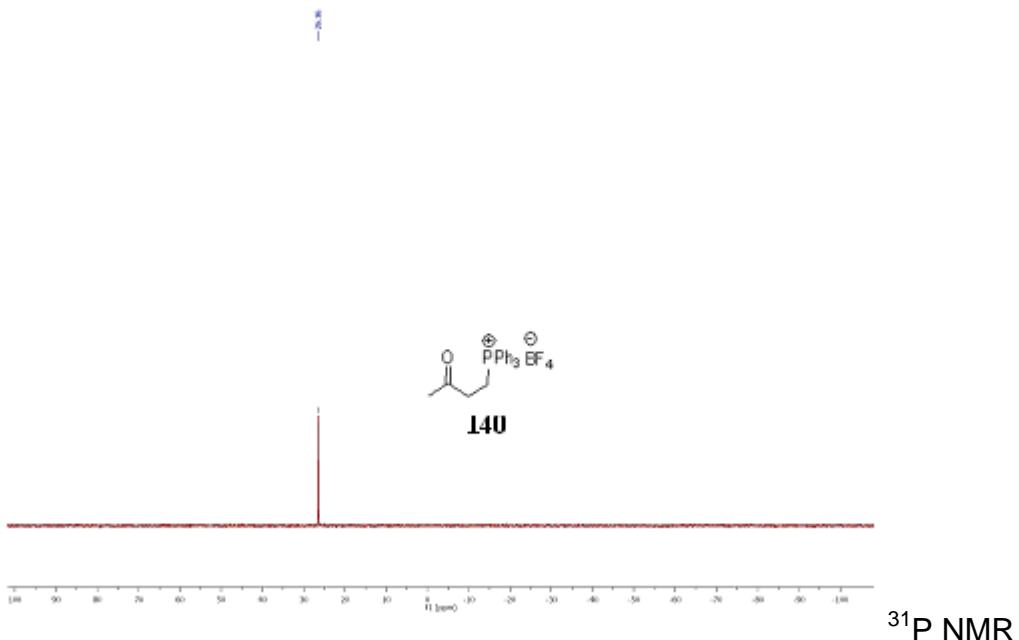
4.3.1.3 Control reaction
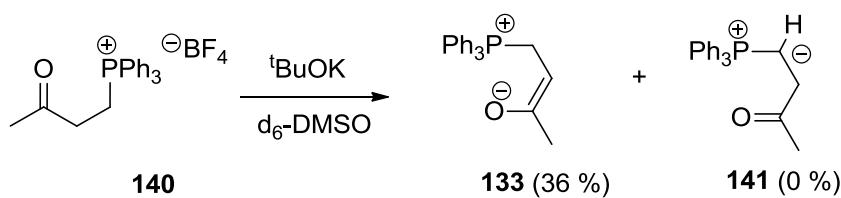
Two stock solutions were prepared in dry calibrated 2 mL flasks; stock solution *A*: 0.083 M in **140** in d_6-DMSO, stock solution *B*: 0.133 M in *t*BuOK in d_6-DMSO. Under nitrogen atmosphere, 0.6 mL of stock solution *A* was injected into a NMR tube to measure the NMR spectrum of starting material. Then 0.3 mL of stock solution *B* was injected to the NMR tube. The sample was submitted to ^{1}H and ^{31}P NMR analysis in order to collect reaction information.

4.3.2 Kinetic studies of the protonation/deprotonation process

(a) Kinetic measurements of the reaction of PPh$_3$, MVK and PNP

Two stock solutions were prepared in dry calibrated 10 mL flasks; stock solution *A*: 0.12 M in PPh$_3$ and 0.006 M in PNP in THF; stock solution *B*: 0.1728 M in MVK in THF. The kinetics of PPh$_3$, MVK and PNP in THF at 20 ^{o}C were followed by UV-Vis spectroscopy, which was collected at stopped-flow spectrophotometer systems. The kinetic run was initiated by mixing equal volumes of stock solutions *A* and *B*.

142

(b) Kinetic measurements of the reaction of PPh₃, ethyl acrylate and PNP

The reaction of PPh₃, ethyl acrylate and PNP was monitored by UV-Vis spectroscopy, which was determined at different time by a J&M TIDAS diode array spectrophotometer connected to a Hellma 661.502-QX quartz Suprasil immersion probe (5 mm light path) by fiber optic cables with standard SMA connectors. The temperature was maintained to 20 $^{\circ}$C by circulating bath cryostats. The reaction was carried out in Schlenk glassware with exclusion of moisture. To this Schlenk glassware was added PPh₃ (3.5 mmol, 917.35 mg), PNP (0.045 mmol, 6.255 mg) in 25 mL THF solution. Ethyl acrylate (12.5 mmol, 1250 mg) was added to initiate this reaction.
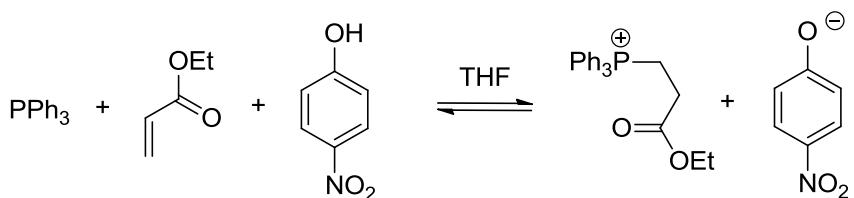
5 APPENDIX

Crystallographic data for BPC1

net formula	$C_{23}H_{24}NOP$
M_r/g mol^{-1}	361.417
crystal size/mm	0.45 × 0.23 × 0.17
T/K	200(2)
radiation	MoKα
diffractometer	'Oxford XCalibur'
crystal system	monoclinic
space group	$P2_1/n$
a/Å	9.0289(3)
b/Å	19.3708(7)
c/Å	11.5454(5)
α/°	90
β/°	91.623(4)
γ/°	90
V/Å^3	2018.45(13)
Z	4
calc. density/g cm^{-3}	1.18934(8)
μ/mm^{-1}	0.147
absorption correction	'multi-scan'
transmission factor range	0.92145–1.00000
refls. measured	12803
R_{int}	0.0351
mean $\sigma(I)/I$	0.0677
θ range	3.88–26.37
observed refls.	2367
x, y (weighting scheme)	0.0587, 0
hydrogen refinement	mixed
refls in refinement	4070
parameters	242
restraints	0
$R(F_{obs})$	0.0404
$R_w(F^2)$	0.1175
S	1.025
shift/error$_{max}$	0.001
max electron density/e Å^{-3}	0.235
min electron density/e Å^{-3}	−0.265

Crystallographic data for BPC10

net formula	$C_{24}H_{26}NOP$
M_r/g mol^{-1}	375.443
crystal size/mm	$0.30 \times 0.20 \times 0.08$
T/K	200(2)
radiation	MoKα
diffractometer	'Oxford XCalibur'
crystal system	monoclinic
space group	$P2_1/n$
a/Å	11.7060(5)
b/Å	8.1893(4)
c/Å	21.5098(12)
α/°	90
β/°	90
γ/°	90
V/Å^3	2062.01(18)
Z	4
calc. density/g cm^{-3}	1.20940(11)
μ/mm^{-1}	0.146
absorption correction	'multi-scan'
transmission factor range	0.85954–1.00000
refls. measured	7037
R_{int}	0.0330
mean $\sigma(I)/I$	0.0965
θ range	3.96–24.50
observed refls.	1852
x, y (weighting scheme)	0.0834, 0
hydrogen refinement	constr
refls in refinement	3381
parameters	248
restraints	0
$R(F_{obs})$	0.0575
$R_w(F^2)$	0.1522
S	0.898
shift/error$_{max}$	0.001
max electron density/e Å^{-3}	1.239
min electron density/e Å^{-3}	−0.251

6   LITERATURE

1 *. Asymmetric Organocatalysis: from Biomimetic Concepts to Applications in Asymmetric Synthesis* (Wiley-VCH, 2005). A. Berkessel, H. Groeger, Eds.

2. K. A. Ahrendt, C. J. Borths, D. W. C. MacMillan, *J. Am. Chem. Soc.* **2000**, *122*, 4243-4244.

3. Reviews on organocatalysis: (a) *Organocatalysis*, B. List, Guest editor, *Chem. Rev.* **2007**, *107*, thematic issue, 5413-5884. (b) P. I. Dalko, L. Moisan, *Angew. Chem. Int. Ed.* **2004**, *43*, 5138-5175. (c) J. Seayad, B. List, *Org. Biomol. Chem.* **2005**, *3*, 719-724. (d) J.-W. Yang, B. List, *Science*, **2006**, *313*, 1584-1586.

4. D. W. C. MacMillan, *Nature*, **2008**, 304-308.

5. (a) W. Steglich, G. Hoefle, *Angew. Chem. Int. Ed.* **1969**, *8*, 981. (b) G. Hoefle, W. Steglich, H. Vorbrüggen, *Angew. Chem.* **1978**, *90*, 602-615. (c) A. Hassner, L. R. Krepski, V. Alexanian, *Tetrahedron* **1978**, *34*, 2069-2076.

6. A. E. J. Nooy, A. C. De Besemer, H. van Bekkum, *Synthesis*, **1996**, 1153.

7. (a) H. Prajecus, *Justus Liebigs Ann. Chem.* **1960**, *634*, 9-22. (b) H. Prajecus, *Justus Liebigs Ann. Chem.* **1960**, *634*, 23-29.

8. Z. G. Hajos, D. R. J. Parrish, *J. Org. Chem.* **1974**, *39*, 1615-1621.

9. U. Eder, G. Sauer, R. Wiechert, *Angew. Chem. Int. Ed. Engl.* **1971**, *10*, 496-497.

10. Y. Tu, Z. Wang, Y. Shi, *J. Am. Chem. Soc.* **1996**, *118*, 9806-9807.

11. S. E. Denmark, Z. Wu, C. Crudden, H. Matsuhashi, *J. Org. Chem.* **1997**, *62*, 8288-8289.

12. D. Yang*,* Y.-C. Yip, M.-W. Tang, M.-K. Wong, J.-H. Zheng, K.-K. Cheung, *J. Am. Chem. Soc.* **1996***, 118,* 491-492*.*

13. M. Sigman, E. N. Jacobsen, *J. Am. Chem. Soc.* **1998**, *120*, 4901–4902.

14. E. J. Corey, M. J. Grogan, *Org. Lett.* **1999**, *1*, 157-160.

15. B. List, R. A. Lerner, C. F. Barbas III, *J. Am. Chem. Soc.* **2000**, *122*, 2395-2396.

16. (a) W. Notz, B. List, *J. Am. Chem. Soc.* **2000**, *122*, 7386-7387. (b) B. List, P. Pojarliev, C. Castello, *Org. Lett.* **2001**, *3*, 573-575. (c) S. Bahmanyar, K. N. Houk, H. J. Martin, B. List, *J. Am. Chem. Soc.* **2003**, *122*, 2475-2479. (d) C. Pidathala, L. Hoang, N. Vignola, B. List, *Angew. Chem. Int. Ed.* **2003**, *42*, 2785-2788.

17. (a) B. List, P. Pojarliev, H. J. Martin, *Org. Lett.* **2001**, *3*, 2423-2425; (b) D.

Enders, A. Seki, *Synlett*, **2002**, 26-28. (c) M. T. Hechavarria Fonseca, B. List, *Angew. Chem. Int. Ed.* **2004**, *43*, 3958–3960.

18. N. Utsumi, H. Zhang, F. Tanaka, C. F. Barbas III, *Angew. Chem.* **2007**, *119*, 1910-1912.

19. (a) B. List, *J. Am. Chem. Soc*, **2002**, *124,* 5656-5657. (b) N. Kumaragurubaran, K. Juhl, W. Zhuang, A. Bøevig, K. A.Jøgensen, *J. Am. Chem. Soc*, **2002**, *124*, 6254-6255. (c) A. Bøevig, K. Juhl, N. Kumaragurubaran, W. Zhuang, K. A. Jøgensen, *Angew. Chem. Int. Ed.* **2002**, *41*, 1790-1792.

20. (*a*) S. P. Brown, M. P. Brochu, C. J. Sinz, D. W. C. MacMillan, *J. Am. Chem. Soc.* **2003**, *125*, 10808-10809. (*b*) G. Zhong, *Angew. Chem. Int. Ed.* **2003**, *42*, 4247-4250. (*c*) Y. Hayashi, J. Yamaguchi, K. Hibino, M. Shoji, *Tetrahedron Lett.* **2003**, *44*, 8293-8296. (*d*) Y.Hayashi, J.Yamaguchi, T. Sumiya, M. Shoji, *Angew. Chem. int. Ed.* **2004**, *43*, 1112-1115; (*e*) A. Bøevig, H. Sund′een, A. C′ordova, *Angew Chem. Int. Ed.* **2004**, *43*, 1109-1112.

21. N. Vignola, B. List, *J. Am. Chem. Soc.* **2004**, 126, 450-451.

22. (a) M. P. Brochu, S. P. Brown, D. W. C. Macmillan, *J. Am. Chem. Soc.* **2004**, *126*, 4108-4109. (b) N. Halland, A. Braunton, S. Bachmann, M. Marigo, K. A. Jøgensen, *J. Am. Chem. Soc.* **2004**, *126*, 4790-4791.

23. G. Lelais, D. W. C. MacMillan, *Aldrichim. Acta.* **2006**, 39, 79-87.

24. (a) W. S. Jen, J. J. M. Wiener, D. W. C. MacMillan, *J. Am.Chem. Soc.* **2000**, *122*, 9874-9875. (b) S. Karlsson, H.-E. Högberg, Tetrahedron, *Asymmetry*, **2002**, *13*, 923-926.

25. (a) N. A. Paras, D. W. C. MacMillan, *J. Am. Chem. Soc.* 2001, **123**, 4370-4371. (b) J. F. Austin, D. W. C. MacMillan, *J. Am. Chem. Soc.* 2002, **124**, 1172-1173. (c) N. A. Paras, D. W. C. MacMillan, *J. Am. Chem. Soc.* 2002, **124**, 7894-7895.

26. (a) A. C. Spivey, S. Arseniyadis, *Angew. Chem. Int. Ed.* **2004**, *43*, 5436-5441. (b) M. R. Heinrich, H. S. Klisa, H. Mayr, H. Zipse, *Angew. Chem. Int. Ed.* **2003**, *42*, 4826-4828. (c) S. Xu, I. Held, B. Kempf, H. Mayr, W. Steglich, H. Zipse, *Chem. Eur. J.* **2006**, *11*, 4751-4757.

27. (a) B. L. Hodous, G. C. Fu, *J. Am. Chem. Soc.* **2002**, *124*, 10006-10007. (b) S. L. Wiskur, G. C. Fu, *J. Am. Chem. Soc.* **2005**, *127*, 6176-6177. (c) C. Schaefer, G. C. Fu, *Angew. Chem. Int. Ed.* **2005**, *44*, 4606-4608. (d) X. Dai, T. Nakai, J. A. C. Romero, G. C. Fu, *Angew. Chem. Int. Ed.* **2007**, *46*, 4367-4369.

28. (a) B. L. Hodus, G. C. Fu, *J. Am. Chem. Soc.* **2002**, *124*, 1518-1579. (b) E. Bappert, P. Mueller, G. C. Fu, *Chem. Commun.* **2006**, 2604-2606.

29. E. C. Lee, K. M. McCauley, G. C. Fu, *Angew. Chem. Int. Ed.* **2007**, *46*, 977-979.

30. T. Ishii, S. Fujioka, Y. Sekiguchi, H. Kotsuki, *J. Am. Chem. Soc.* **2004**, *126*, 9558-9559.

31. Recent review on phase transfer catalysts: T. Hashimoto, K. Maruoka, *Chem. Rev.* **2007**, *107*, 5656-5682.

32. (*a*) M. Koerner, B. Rickborn, *J. Org. Chem.* **1989**, *54*, 6-9. (*b*) M. Koerner, B. Rickborn, *J. Org. Chem.* **1990**, *55*, 2662-2672.

33. K. Tanaka, A. Mori, S. Inoue, *J. Org. Chem.* **1990**, *55*, 181-185.

34. (a) M. S. Iyer, K. M. Gigstad, N. D. Namdev, M. Lipton, *J. Am. Chem. Soc.* **1996**, *118*, 4910-4911. E. J. Corey, M. J. Grogan, *Org. Lett.* **1999**, *1*, 157-160.

35. T. Akiyama, *Chem. Rev.* **2007**, *107*, 5744-5758.

36. (a) A. G. Wenzel, E. N. Jacobsen, *J. Am. Chem. Soc.* **2002**, *124*, 12964-2965. (b) M. S. Sigman, P. Vachal, E. N. Jacobsen, *Angew. Chem.* **2000**, *112*, 1336-1338. (c) G. D. Joly, E. N. Jacobsen, *J. Am. Chem. Soc.* **2004**, *126*, 4102-4103. (d) S. J. Zuend, E. N. Jacobsen, *J. Am. Chem. Soc.* **2009**, *131*, 15358-15374. (e) R. R. Knowles, S. Lin, E. N. Jacobsen*, J. Am. Chem. Soc.* **2010**, *132*, 5030-5032. (f) Y.-Q. Fang, E. N. Jacobsen, *J. Am. Chem. Soc.* **2008**, *130*, 5660-5661.

37. T. Akiyama, J. Itoh, K.Yokota, K. Fuchibe, *Angew. Chem.* **2004**, *116*, 1592-1594.

38. D. Uraguchi, M. Terada, *J. Am. Chem. Soc.* **2004**, *126*, 5356-5357.

39. (a) Q. Kang, Z. Zhao, S.-L. You, *J. Am. Chem. Soc.* **2007**, *129*, 1484-1485. (b) T. Akiyama, H. Morita, J. Itoh, K. Fuchibe, *Org. Lett.* **2005**, *7*, 2583-2585. (c) J. Seayad, A. M. Seayad, B. List, *J. Am. Chem. Soc.* **2006**, *128*, 1086-1087. (d) M. Rueping, E. Sugiono, C. Azap, *Angew. Chem. Int. Ed.* **2006**, *45*, 2617-2619. (e) T. Akiyama, Y. Tamura, J. Itoh, H. Morita, K. Fuchibe, *Synlett* **2006**, 141-143. (f) J. W. Yang, M. T. H. Fonseca, B. List, *Angew. Chem. Int. Ed.* **2004**, *43*, 6660-6662. (g) M. Rueping, E.Sugiono, C. Azap, T. Theissmann, M. Bolte, *Org. Lett.* **2005**, *7*, 3781-3783.

40. P. G. Garcia, F. Lay, P. G. Garcia, C. Rabalakos, B. List, *et al*, *Angew. Chem.*

Int. Ed. **2009**, *48*, 4363-4366.

41. N. Momiyama, Y. Yamamoto, H. Yamamoto, *J. Am. Chem. Soc.* **2007**, *129*, 1190-1195.

42. (a) N. T. McDougal, S. E. Schaus, *J. Am. Chem. Soc.* **2003**, *125*, 12094-12095. (b) N. T. McDougal, W. L. Trevellini, S. A. Rodgen, L. T. Kliman, S. E. Schaus, *Adv. Synth. Catal.* **2004**, *346*, 1231-1240.

43. (a) M. Shibasaki, H. Sasai, T. Arai, *Angew. Chem. Int. Ed.* **1997**, *36*, 1236-1256. (b) M. Shibasaki, N. Yoshikawa, *Chem. Rev.* **2002**, *102*, 2187-2209.

44. (a) M. Sawamura, Y. Ito, *Chem. Rev.* **1992**, *92*, 857-871. (b) H. Steinhagen, G. Helmchen, *Angew. Chem. Int. Ed.* **1996**, *35,* 2339-2342.

45. Y. Wei, M. Shi, *Acc. Chem. Res.* **2010**, *43*, 1005-1018*.*

46. A selection of examples: (a) T. Okino, Y. Hoashi, Y. Takemoto, *J. Am. Chem. Soc.* **2003**, *125*, 12672-12673. (b) Y. Sohtome, Y. Hashimoto, K. Nagasawa, *Adv. Synth. Catal.* **2005**, *347*, 1643-1648. (c) S. B. Tsogoeva, D. A. Yalalov, M. J. Hateley, C. Weckbecker, K. Huthmacher, *Eur. J. Org. Chem.* **2005**, 4995-5000. (d) J. C. Ruble, H. A. Latham, G. C. Fu, *J. Am. Chem. Soc.* **1997**, *119*, 1492-1493. (e) Y. Iwabuchi, M. Nakatani, N. Yokoyama, S. Hatakeyama, *J. Am. Chem. Soc.* **1999**, *121*, 10219-10220.

47. (a) *Comprehensive Organic Synthesis*; B. M. Trost, I. Fleming, Eds; Pergamon: New York, **1991**; Vols. 1-9. (b) *Current Trends in Organic Synthesis*; C. Scolastico, F. Nocotra, Eds; Plenum: New York, **1999**. (c) Special Issue on Catalytic Asymmetric Synthesis. *Acc. Chem. Res.* **2000**, *33*, 323-440. (d) B. M. Trost, *Acc. Chem. Res.* **2002**, *35*, 695-705.

48 . Recent reviews of MBH reaction: (a) D. Basavaiah, A. J. Rao, T. Satyanarayana, *Chem. Rev.* **2003**, *103*, 811-892. (b) D. Basavaiah, K. V. Rao, R. J. Reddy, *Chem. Soc. Rev.* **2007**, *36*, 1581-1588. (c) G. Masson, C. Housseman, J. Zhu, *Angew. Chem. Int. Ed.* **2007**, *46*, 4614-4628. (d) Y.-L. Shi, M. Shi, *Eur. J. Org. Chem.* **2007**, 2905-2916. (e) V. Singh, S. Batra, *Tetrahedron* **2008**, *64*, 4511-4574. (f) V. Declerck, J. Martinez, F. Lamaty, *Chem. Rev.*, **2009**, *109*, 1-48. (g) J. Mansilla, J. M. Saa, *Molecules*, **2010**, *15*, 709-734. (h) D. Basavaiah, B. S. Reddy, S. S. Badsara, *Chem. Rev.*, **2010**, *110*, 5447-5674.

49. K. Morita, Z. Suzuki, H. Hirose, *Bull. Chem. Soc. Jpn.* **1968**, *41*, 2815-2815.

50. A. B. Baylis, M. E. D. Hillman, *Chem. Abstr.* **1972**, *77*, 34174q. *Ger. Offen.* 2155113, **1972**.

51. (a) P. Langer, *Angew. Chem. Int. Ed.* **2000**, *39*, 3049-3052. (b) W. Yin, M. Shi, *Chin. Sci. Bull.* **2010**, *55*, 1699-1711

52. J. S. Hill, N. S. Isaacs, *J. Phys. Org. Chem.* **1990**, *3*, 285-290.

53. (a) H. M. R. Hoffman, J. Rabe, *Angew. Chem. Int. Ed.* **1983**, *22*, 796-797. (b) P. T. Kaye, M. L. Bode, *Tetrahedron Lett.* **1991**, *32*, 5611-5614, (c) Y. Fort, M.-C. Berthe, P. Caubere, *Tetrahedron* **1992**, *48*, 6371-6384.

54. S. E. Drewes, O. L. Njamela, N. D. Emslie, N. Ramesar, J. S. Field, *Synth. Commun.* **1993**, *23*, 2807-2815.

55. (a) L. S. Santos, C. H. Pavam, W. P. Almeida, F. Coelho, M. N. Eberlin, *Angew. Chem. Int. Ed.* **2004**, *43*, 4330-4333. (b) G. W. Amarante, H. M. S. Milagre, B. G. Vaz, B. R. V. Ferreira, M. N. Eberlin, F. Coelho. *J. Org. Chem.* **2009**, *74*, 3031-3037. (c) G. W. Amarante, M Benassi, H. M. S. Milagre, A. A. C. Braga, F. Maseras, M. N. Eberlin, F. Coelho. *Chem. Eur. J.* **2009**, 12460-12469.

56. (a) K. E. Price, S. J. Broadwater, M. H. Jung, D. T. McQuade, *Org. Lett.* **2005**, *7*, 147-150. (b) K. E. Price, S. J. Broadwater, B. J. Walker, D. T. McQuade, *J. Org. Chem.* **2005**, *70*, 3980-3987.

57. V. K. Aggarwal, S. Y. Fulford, G. C. Lloyd-Jones, *Angew. Chem. Int. Ed.* **2005**, 44, 1706-1708.

58. R. Robiette, V. K. Aggarwal, J. N. Harvey, *J. Am. Chem. Soc.* **2007**, *129*, 15513–15525.

59. Selected examples: (a) M. Shi, Y.-H. Liu, *Org. Biomol. Chem.* **2006**, *4*, 1468-1470. (b) K.-S. Park, J. Kim, H. Choo, Y. Chong, *Synlett* **2007**, *3*, 395-398.

60. I. T. Raheem, E. N. Jacobsen, *Adv. Synth. Catal.* **2005**, *347*, 1701-1708.

61. P. Buskens, J. Klankermayer, W. Leitner, *J. Am. Chem. Soc.* **2005**, *127*, 16762-16763.

62. T. Yukawa, B. Seelig, Y. Xu, H, Morimoto, S. Matsunaga, A. Berkessel, M. Shibasaki, *J. Am. Chem. Soc.* **2010**, *132*, 11988-11992.

63. C. Yu, B. Liu, L. Hu, *J. Org. Chem.* **2001**, *66*, 5413-5418.

64. P. Ribiere, N. Yadav-Bhatnagar, J. Martinez, F. Lamaty, *QSAR Comb. Sci.* **2004**, *23*, 911

65. (a) T. Kataoka, T. Iwama, S. I. Tsujiyama, *Chem. Commun.* **1998**, 197-199. (b) T. Kataoka, T. Iwama, S. I. Tsujiyama, T. Iwamura, S. I. Watanabe, *Tetrahedron* **1998**, *54*, 11813-11824. (c) E. L. Myers, J. G. de Vries, V. K. Aggarwal, *Angew. Chem. Int. Ed.* **2007**, 46, 1893-1896.

66. D. Basavaiah, B. Sreenivasulu, A. J. Rao, *J. Org. Chem.*, **2003**, *68*, 5983-5991.

67. F. Coelho, W. P. Almeida, D. Veronese, C. R. Mateus, E. C. S. Lopes, R. C. Rossi, G. P. C. Silveira, C. H. Pavam, *Tetrahedron* **2002**, *58*, 7437-7447.

68. V. K. Aggarwal, I. Emme, S. Y. Fulford, *J. Org. Chem.* **2003**, *68*, 692-700.

69. M. Shi, J.-K. Jiang, C.-Q. Li, *Tetrahedron Lett.* **2002**, *43*, 127-130.

70. (a) N. E.Leadbeater, C. Van der Pol, *J. Chem. Soc., Perkin Trans. 1* **2001**, 2831-2835. (b) R. S.Grainger, N. E. Leadbeater, A. M. Pamies, *Catal. Commun.* **2002**, *3*, 449-452.

71. V. K. Aggarwal, A. Mereu, *Chem. Commun.* **1999**, 2311-2312.

72. (a) S. Luo, B. Zhang, J. He, A. Janczuk, P. G. Wang, J. P. Cheng, *Tetrahedron Lett.* **2002**, *43*, 7369-7371. (b) R. Gatri, M. M. El Gaied, *Tetrahedron Lett.* **2002**, *43*, 7835-7836.

73. (a) F. Rezgui, M. M. El Gaied, *Tetrahedron Lett.* **1998**, *39*, 5965-5966. (b) K. Y. Lee, J. H. Gong, J. N. Kim, *Bull. Korean Chem. Soc.* **2002**, *23*, 659-660.

74. M. Baida, S. Kobayashi, F. Brotzel, U. Schmidhammer, E. Riedle, H. Mayr, *Angew. Chem. Int. Ed.* **2007**, 46, 6176-6179.

75. Y. M. A. Yamada, S. Ikegami, *Tetrahedron Lett.* **2000**, *41*, 2165-2169.

76. M. Shi, Y.-M. Xu, *Tetrahedron: Asymmetry* **2002**, *13*, 1195-1200.

77. M. R. Netherton, G. C. Fu, *Org. Lett.* **2001**, *3*, 4295-4298.

78. Z. He, X. Tang, Y. Chen, Z. He, *Adv. Synth. Catal.* **2006**, *348*, 413-417.

79. (a) V. K. Aggarwal, G. J. Tarver, R. McCague, *Chem. Commun.* **1996**, 2713-2714. (b) V. K. Aggarwal, A. Mereu, G. J. Tarver, R. McCague, *J. Org. Chem.* **1998**, *63*, 7183-7189.

80. M. Kawamura, S. Kobayashi, *Tetrahedron Lett.* **1999**, *40*, 1539-1542.

81. Y. Sotohme, A. Tanatani, Y. Hashimoto, K. Nagasawa, *Tetrahedron Lett.* **2004**, *45*, 5589-5592.

82. M. Shi, Y.-M. Xu, *Angew. Chem. Int. Ed.* **2002**, 41, 4507-4510.

83 (a) M. Shi, L.-H. Chen, *Chem. Commun.* **2003**, *1310*-1311. (b) M. Shi, L.-H. Chen, C.-Q. Li, *J. Am. Chem. Soc.* **2005**, *127*, 3790-3800.

84. Z.-Y. Lei, X.-G, Liu, M. Shi, M. Zhao, *Tetrahedron: Asymmetry* **2008**, *19*, 2058-2062.

85. Y.-H. Liu, L.-H. Chen, M. Shi, *Adv. Synth. Catal.* **2006**, *348*, 973-979.

86. Y.-L. Shi, M, Shi. *Adv. Synth. Catal.* **2007**, *349*, 2129-2135.

87. Y.-H. Liu, M. Shi, *Adv. Synth. Catal.* **2008**, *350*, 122-128.

88. K. Matsui, S. Takizawa, H. Sasai, *J. Am. Chem. Soc.* **2005**, 127, 3680-3681.

89. K. Matsui, S. Takizawa, H. Sasai, *Synlett* **2006**, 761-765.

90. (a) J.-M. Garnier, C. Anstiss, F. Liu, *Adv. Synth. Catal.* **2009**, *351*, 331-338. (b) J.-M. Garnier, F. Liu, *Org. Biomol. Chem.* **2009**, *7*, 1272-1275.

91. K. Ito, K. Nishida, T. Gotauda, *Tetrahedron Lett.* **2007**, *48*, 6147-6149.

92. K. Yuan, L. Zhang, H.-L. Song, Y. Hu, X.-Y. Wu, *Tetrahedron Lett.* 2008, *49*, 6262–6264.

93. R. Gausepohl, P. Buskens, J. Kleinen, A. Bruckmann, C. W. Lehmann, J. Klankermayer, W. Leitner. *Angew. Chem. Int. Ed.* **2006**, *45*, 3689-3692.

94. (a) Y. Wei, T. Singer, H. Mayr, G. N. Sastry, H. Zipse, *J. Comp. Chem.* **2008**, *29*, 291-297. (b) Y. Wei, G. N. Sastry, H. Zipse, *J. Am. Chem. Soc.* **2008**, *130*, 3473-3477. (c) Y. Wei, G. N. Sastry, H. Zipse, *Org. Lett.* **2008**, *10*, 5413–5417.

95. For review, see: (a) G. Hoefl, W. Steglich, H. Vorbrueggen, *Angew. Chem. Int. Ed.* **1978**, *90*, 569-583. (b) E. Vedjes, M. Jure. *Angew. Chem. Int. Ed.* **2005**, *44*, 3974-4001. (c) R. P. Wurz, *Chem. Rev.* **2007**, *107*, 5570-5595.

96 . (a) L. M. Litvinenko, A. I. Kirichenko, *Dokl. Chem.* **1967**, 763-766. (b) *Dokl.Akad. Nauk SSSR Ser. Khim.* **1967**, *176*, 97-100.

97. J. Habermann, S. V. Ley, J. S. Scott, *J. Chem. Soc. Perkin Trans. 1*, **1999**, 1253-1255.

98. S. K. Chaudary, O. Hernandez, *Tetrahedron Lett.* **1979**, 99-102.

99. (a) Y. M. Shen, W. L. Duan, M. Shi, *Adv. Synth. Catal.* **2003**, *345*, 337-340. (b) Y. M. Shen, W. L. Duan, M. Shi, *Eur. J. Org. Chem.* **2004**, 3080-3089. (c) R. A. Shiels,; C. W. Jones, *J. Mol. Catal. A: Chem.* **2007**, *261*, 160-166. (d) D. J. Darensbourg, *Chem. Rev.* **2007**, *107*, 2388-2410. (e) G. W. Coates, D. R. Moore, *Angew. Chem. Int. Ed.* **2004**, *43*, 6618-6639. (f) W. L. Dai, S. L. Luo, S. F. Yin, C. T. Au, *Applied. Catalysis: General* **2009**, *366*, 2-12.

100. (a) T. A. Duffey, S. A. Shaw, E. Vedejs, *J. Am. Chem. Soc.* **2009**, *131*, 14-15. (b) De C. Kanta, E. G. Klauber, D. Seidel, *J. Am. Chem. Soc.* **2009**, *131*,

17060-17061. (c) O. Gleeson, R. Tekoriute, Y. K. Gun´ko, S. J. Connon, *Chem. Eur. J.* **2009**, *15*, 5669-5673. (d) T. A. Duffey, J. A. MacKay, E. J. Vedejs, *J. Org. Chem.* **2010**, *75*, 4674-4685.

101. (a) A. C. Spivey, A. Maddaford, A. Redgrave, *Org. Prep. Proced. Int.* **2000**, *32*, 331-365. (b) S. France, D. J. Guerin, S. J. Miller, T. Lectka, *Chem. Rev.* **2003**, *103*, 2985-3012.

102. V. Gold, E. G.Jefferson, *J. Chem. Soc.* **1953**, 1409-1415.

103. L. I. Bondarenko, A. I. Kirichenko, L. M. Litvinenko, I. N. Dmitrenko, V. D. Kobets, *J. Org. Chem. USSR (Engl. Transl.)* **1981**, 2310-2316; *Zh. Org. Khim.* **1981**, *17*, 2588-2594.

104. (a) I. Held, S. Xu, H. Zipse, *Synthesis* **2007**, 1185-1196. (b) I. Held, E. Larionov, C. Bozler, F. Wagner, H. Zipse, *Synthesis* **2009**, 2267-2277. (c) I. Held, P. von den Hoff, D. S. Stephenson, H. Zipse, *Adv. Synth. Catal.* **2008**, *350*, 1891-1900.

105. (a) PDLB3, 4, 5, 6 were prepared by Jowita Humin, see: Jowita Humin, Master thesis, **2010**. (b) PDLB 8, 9, 11, 12 were prepared by Evgeny Larionov, see: Evgeny Larionov, Ph. D thesis **2011**. (c) DEAP was prepared by Raman Tandon, see: Raman Tandon, Ph. D thesis **2013**. (d) PDLB 7, 13, 14 were synthesized by Dr. Valerio D'Elia.

106. F. G. Bordwell, *Acc. Chem. Res.* **1988**, 456-463.

107. P. T. Anastas, J. C. Warner, *Green Chemistry: Theory and Practice,* Oxford University Press, New York **1998**, 30.

108. (a) F. Cozzi, *Adv. Synth. Catal.* **2006**, *348*, 1367-1390. (b) *Recoverable and Recyclable Catalysts*, John Wiley & sons, **2009**, M. Benaglia, (Editor).

109. (a) S. Shinkai, H. Tsuji, Y. Hara, O. Manabe, *Bull. Chem. Soc. Jpn.* **1981**, *54*, 631-632. (b) J. Yoshida, J. Hashimoto, N. Kawabata, *Bull. Chem. Soc. Jpn.* **1981**, *54*, 309-310. (c) F. M. Menger, D. J. Mccann, *J. Org. Chem.* **1985**, *50*, *3928*-3930. (d) A. Deratani, G. D. Darling, D. Horak, J. M. J. Frechet, *Macromolecules* **1987**, *20*, 767-772. (e) F. Guendouz, R. Jacquier, J. Verducci, *Tetrahedron* **1988**, *44*, 7095-7108.

110. H.-T. Chen, S. Huh, J. W. Wiench, M. Pruski, V. S.-Y. Lin, *J. Am. Chem. Soc.* **2005**, *127*, 13305-13311.

111. C. O'Dalaigh, S. A. Corr, Y. Gun´ko, S. J. Connon, *Angew. Chem. Int. Ed.* **2007**, *46*, 4329-4332.

112. K. E. Price, B. P. Mason, A. R. Bogdan, S. J. Broadwater, J. L. Steinbacher, D. T. McQuade, *J. Am. Chem. Soc.* **2006**, *128*, 10376-10377.

113. A. Corma, H. Garcia, A. Leyva, *Chem. Commun.* **2003**, 2806-2807.

114. (a) E. Vedejs, S. T. Diver, *J. Am. Chem. Soc.* **1993**, *115*, 3358-3359. (b) E. Vedejs, J. A. MacKay, *Org. Lett.* **2001**, *3*, 535-536. (c) E. Vedejs, O. Daugulis, L. A. Harper, J. A. MacKay, D. R. Powell, *J. Org. Chem.* **2003**, *68*, 5020-5027. (d) J. A. MacKay, E. Vedejs, *J. Org. Chem.* **2006**, *71*, 498-503.

115. For a review see: C. E. Aroyan, A. Dermenci, S. J. Miller, *Tetrahedron* *2009*, *65*, 4069–4084.

116. I. C. Stewart, R. G. Bergman, F. D. Toste, *J. Am. Chem. Soc.* **2003**, *125,* 8696-8697.

117. C. Lindner, B. Maryasin, F. Richter, H. Zipse, *J. Phys. Org. Chem.* **2010**, 2010, 23, 1036-1042.

118. (a) U. Mayer, V. Gutmann, W. Gerger, *Monatsh. Chem.* **1975**, *106*, 1235-1257. (b) V. Gutmann, *Electrochem. Acta* **1976**, *21*, 661-670. (c) V. Gutmann, *Coord. Chem. Rev.*, **1976**, *18,* 225–255.

119. H. Kropt, M.R. Yazdanbachsch *Tetrahedron* **1974**, 30, 3455-3459.

120. (a) S. J. Zuend, E. N. Jacobsen, *J. Am. Chem. Soc.* **2009**, *131*, 15358-15374. (b) K. Koehler, W. Sandstrom, E. H. Cordes, *J. Am. Chem. Soc.* **1964**, *86*, 2413-2419.

121. σ_p is obtained from C. Hansch, A. Leo, R. W. Taft, *Chem. Rev.* **1991**, 165-195.

122. O. Herd, A. Hessler, M. Hingst, M. Tepper, O. Stelzer, *J. Organomet. Chem.*, **1996**, 522, 69-76.

123. Raman Tandon, Master Thesis **2009**.

124. E. Wiedemann, Y.-H. Liu, H. Zipse, unpublished results.

125. (a) H. Mayr, B. Kempf, A. R. Ofial, *Acc. Chem. Res.* **2003**, *36*, 66-77. (b) T. B. Phan, M. Breugst, H. Mayr, *Angew. Chem. Int. Ed.* **2006**, *45*, 3869-3874.

126. B. E. Love, P. S. Raje, T. C. Williams II, *Synlett.* **1994**, 493-495.

127 (a) H. J. Cristau, J. P. Vors, H. Christol, *Synthesis*, **1979**, 538-541. (b) H. J. Cristau, B. Chabaud, H. Christol, *J. Org. Chem.* **1984**, 2023-2025.

Curriculum Vitae

Name: YingHao Liu

Date of Birth: Aug. 31, 1980   **Town of Birth**: Yantai, P. R. China

Nationality: Chinese   **Marital status**: Married, one child

Education:

2007. 10 - 2011. 1, Ph. D, Department of Chemistry, University of Munich, Munich, Germany. Prof. Dr. **Hendrik Zipse** group

2004. 8 - 2007. 7, Research assistant, in Shanghai Institute of Organic Chemistry, Chinese Academy of Sciences, Shanghai, China. Prof. **Min Shi** group

2002.9 - 2004. 7, Master of science, Nanjing University of Science & Technology, Nanjing, China. Prof. **Yuejun Zhang** group.

1998. 9 - 2002. 7, Bachelor of science, Nanjing University of Science & Technology, Nanjing, China. Prof. **Yuejun Zhang** group.

Publications:

1. Min Shi,* Shi-Cong Cui and ***Ying-Hao Liu***. Mannich-type Reaction of (1-Methoxy-2-methylpropenyloxy)trimethylsilane with Arylaldehydes and Aromatic Amines Catalyzed by Perfluorinated Rare Earth Metal Salts in Fluorous Phase. *Tetrahedron* **2005**, *61*, 4965-4970.

2. ***Ying-Hao Liu,*** Lian-Hui Chen and Min Shi*. "Asymmetric Aza-Morita-Baylis Hillman Reaction of *N*-Sulfonated Imines with Activated Olefins Catalyzed by Chiral Phosphine Lewis Bases Bearing Multiple Phenol Groups." *Advanced Synthesis & Catalysis* **2006,** *348*, 973-979.

3. Min Shi* and ***Ying-Hao Liu***. "Traditional Morita-Baylis-Hillman Reaction of Aldehydes with Methyl Vinyl Ketone Co-Catalyzed by Triphenylphosphine and Nitrophenol." *Organic & Biomolecular Chemistry* **2006**, *4*, 1468-1470.

4. Yong-Hua Yang, *Ying-Hao Liu* and Min Shi*. "Reactions of Cyclopropyl Aryl Ketones with Ketoacetic Acids Catalyzed by $C_8F_{17}SO_3H$ in Fluorous Phase." *Organic & Biomolecular Chemistry* **2006,** *4*, 4131-4134.

5. Min Shi,* *Ying-Hao Liu* and Lian-Hui Chen. "Asymmetric Catalysis of Morita-Baylis-Hillman Reactions by Chiral Phosphine Lewis Bases Bearing Multiple Phenol Groups." *Chirality* **2007**, 19, 124-128.

6. *Ying-Hao Liu* and Min Shi*. "Dendritic chiral phosphine Lewis bases catalyzed asymmetric aza-Morita-Baylis-Hillman reaction of N-sulfonated imines with activated olefins." *Advanced Synthesis & Catalysis* **2008,** 350, 122-128.

7. Valerio D'elia, *Yinghao Liu*, and Hendrik Zipse*. "Immobilized DMAP-Derivatives Rivaling Homogeneous DMAP." *Eur. J. Org. Chem.* accepted.

8. *Yinghao Liu* and Hendrik Zipse*. "Bifunctional Catalysis in the aza-Morita-Baylis- Hillman Reaction." prepared.

9. *Yinghao Liu*, Evgeny Larionov, Valerio D'elia, Raman Tandon and Hendrik Zipse*. "Pyridine-derived Lewis base-catalyzed aza-Morita-Baylis-Hillman reaction." in preparation.

10. *Yinghao Liu*, Boris Maryasin and Hendrik Zipse*. "Protonation/Deproton-ation Equilibria in the Morita-Baylis-Hillman Reaction." prepared

11. Christoph Lindner, *Yinghao Liu*, and Hendrik Zipse*. "The Reactivity of Selected Phosphanes." in preparation.